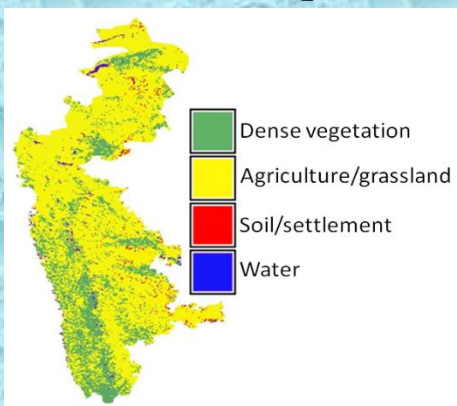
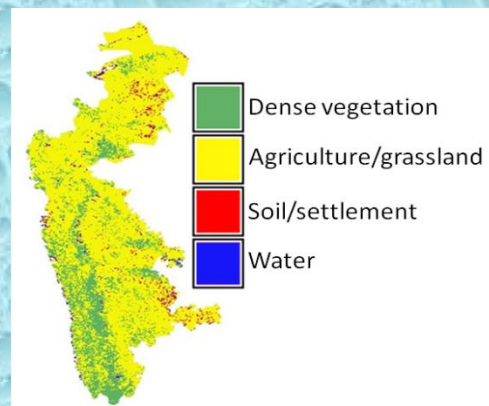


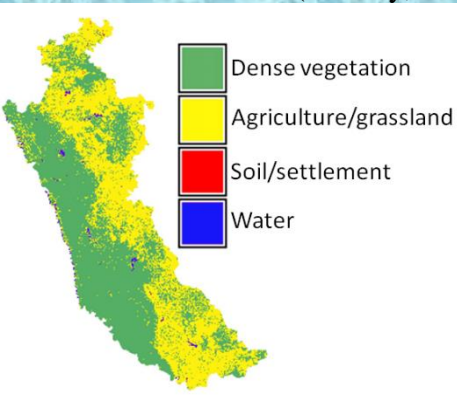
Time-series MODIS NDVI based Vegetation Change Analysis with Land Surface Temperature and Rainfall in Western Ghats, India



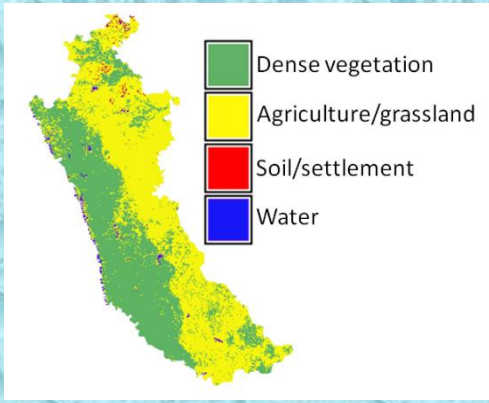
Northern Western Ghats (January, 2003)



Northern Western Ghats (December, 2012)



Central Western Ghats (January, 2003)

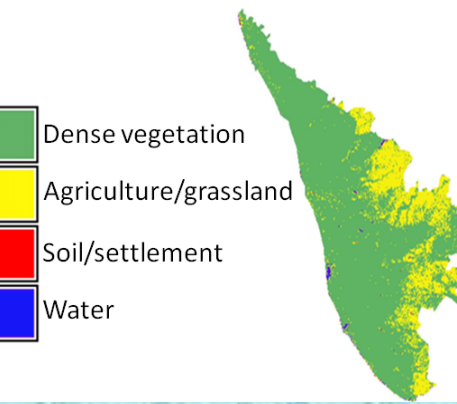


Central Western Ghats (December, 2012)

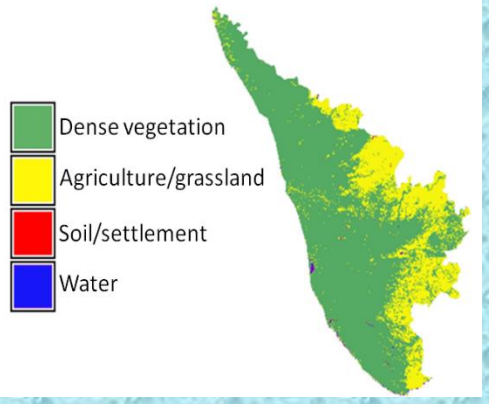
T. V. Ramachandra

Uttam Kumar

Anindita Dasgupta



Southern Western Ghats (January, 2003)



Southern Western Ghats (December, 2012)

ENVIS Technical Report 100

April 2016

Energy & Wetlands Research Group [CES TE15]

Centre for Ecological Sciences,

Indian Institute of Science,

Bangalore - 560012, INDIA



Web: <http://ces.iisc.ernet.in/energy/>, <http://ces.iisc.ernet.in/biodiversity>

Email: cestvr@ces.iisc.ernet.in, energy@ces.iisc.ernet.in

Time-series MODIS NDVI based Vegetation Change Analysis with Land Surface Temperature and Rainfall in Western Ghats, India

T. V. Ramachandra

Uttam Kumar

Anindita Dasgupta

Citation: Ramachandra T V, Uttam Kumar and Anindita Dasgupta, 2016, Time-series MODIS NDVI based Vegetation Change Analysis with Land Surface Temperature and Rainfall in Western Ghats, India, ENVIS Technical Report 100, Sahyadri Conservation Series 53, Energy & Wetlands Research Group, CES, Indian Institute of Science, Bangalore 560012.

Financial Assistance

NRDMS Division, The Ministry of Science & Technology (DST), Government of India

The Ministry of Environment, forests and Climate Change, Government of India

Indian Institute of Science



ENVIS Technical Report 100

April 2016

**Energy & Wetlands Research Group,
Centre for Ecological Sciences, TE 15
New Bioscience Building, Third Floor, E Wing
[Near D-Gate] Indian Institute of Science**

Bangalore 560012, India

<http://ces.iisc.ernet.in/energy>
<http://ces.iisc.ernet.in/biodiversity>

Email: cestvr@ces.iisc.ernet.in,
energy@ces.iisc.ernet.in
sahyadri@ces.iisc.ernet.in

Time-series MODIS NDVI based Vegetation Change Analysis with Land Surface Temperature and Rainfall in Western Ghats, India

T. V. Ramachandra

Uttam Kumar

Anindita Dasgupta

Citation: Ramachandra T V, Uttam Kumar and Anindita Dasgupta, 2016, Time-series MODIS NDVI based Vegetation Change Analysis with Land Surface Temperature and Rainfall in Western Ghats, India, ENVIS Technical Report 100, Sahyadri Conservation Series 53, Energy & Wetlands Research Group, CES, Indian Institute of Science, Bangalore 560012.

Financial Assistance

NRDMS Division, The Ministry of Science & Technology (DST), Government of India

The Ministry of Environment, forests and Climate Change, Government of India

Indian Institute of Science

The study revealed that dense forest area (intact contiguous forests) in the northern, central and southern Western Ghats has considerably decreased by 2.84%, 4.38% and 5.77%, and agricultural/grassland has increased by 2.23%, 4.32% and 5.85%. The trends in rainfall time-series data reveal a decreasing trend in the rainfall pattern from 2013 towards 2020 in northern, central and southern Western Ghats, revealing the likely grave situation threatening water and food security in peninsular India with the increasing trends of deforestation in the ecologically vital Western Ghats.

Web URL: https://www.researchgate.net/profile/T_V_Ramachandra/publications

<http://ces.iisc.ernet.in/energy>, <http://ces.iisc.ernet.in/biodiversity/>

Time-series MODIS NDVI based Vegetation Change Analysis with Land Surface Temperature and Rainfall in Western Ghats, India

Abstract

Land cover (LC) changes are one of the important factors altering the landscape structure affecting ecosystem goods and services. Landscape status assessments through well-established spatial metrics help in monitoring ecosystem trends. Incorporating two-date or sometime lower-frequency-multi-date images based change detection using Landsat or IRS LISS-III/IV data have limited performance for applications in ecologically rich and biologically complex systems. In this context, MODIS based temporal data have wide applicability in providing cost-effective means to develop LC details over large geographic regions. This study explored the use of 250 m multi-temporal (2003–2012) MODIS NDVI 16-day composite data, MODIS LST (land surface temperature) data and monthly rainfall data obtained from Department of Economics and Statistics (Government of Karnataka), Indian Water Portal and NOAA to study vegetation changes and corresponding impact on local temperature along with the rainfall pattern analysis in one of the hottest biodiversity hotspots of the world – the Western Ghats of India.

The study revealed that dense forest area (intact contiguous forests) in the northern, central and southern Western Ghats has considerably decreased by 2.84%, 4.38% and 5.77%, and agricultural/grassland has increased by 2.23%, 4.32% and 5.85%. There is a marginal increase in settlement/open area with the decrease in the spatial extent of water bodies in all the three studied regions. The coefficient of correlation of the different season NDVI of dense vegetation revealed various responses to changing LST and precipitation. NDVI trends were found correlated with the regional climatic variables in 10 years. Monthly NDVI exhibited significant correlations with monthly mean temperature and monthly precipitation during the study period. The trends in rainfall time-series data were analysed using statistical methods and modelled using autoregressive integrated moving average (ARIMA) which indicated a decreasing trend in the rainfall pattern over forest and agricultural/grassland areas from 2013 towards 2020 in northern, central and southern Western Ghats, revealing the likely grave situation threatening water and food security in peninsular India with the increasing trends of deforestation in the ecologically vital Western Ghats.

Keywords: Vegetation, MODIS, climate change, NDVI, LST, rainfall, modelling, Western Ghats, India

Contents

Abstract.....	1
List of tables.....	7
1. Introduction.....	9
2. Objective.....	13
3. Study area and data	14
4. Methods.....	16
5. Results.....	18
5.1 Time-series MODIS NDVI based LC change analysis from 2003 to 2012	19
5.2 Time-series NDVI analysis of different LC classes.....	29
5.3 Decadal climatic parameters influencing NDVI: temperature variation and rainfall pattern analysis in Western Ghats from 2003 to 2012	39
5.4 Relationship of NDVI of dense vegetation with climatic variables in Western Ghats	61
5.5 Spatial patterns of seasonal NDVI trend: changes in NDVI (of dense vegetation) and the turning point.....	76
6. Is there a varying trend in rainfall pattern as a result of climate change/variability in Western Ghats?	91
7. Discussion.....	106
8. Conclusions.....	112
References.....	113
Appendix 1.....	121
Appendix 2.....	138
Appendix 3.....	150

List of figures

Figure 1: Western Ghats, India including major ecological regions (northern, central and southern Western Ghats).....	15
Figure 2: Flowchart of the overall method.....	18
Figure 3: A small part of the study area (a) and (b) as seen in Google Earth in 2003 and 2012; (c) NDVI of the same region in January, 2003 and December, 2012.	19
Figure 4: Boxplots for dense vegetation, agriculture/grassland, soil/settlement and water for the year January, 2003 and December, 2012 for northern Western Ghats (X-axis: Month, Y-axis: NDVI values).....	20
Figure 5: LC maps of northern, central and southern Western Ghats of January, 2003 and December, 2012.	21
Figure 6: Percentage change (monthly) in dense vegetation and agriculture/grassland in northern Western Ghats from 2003 to 2012.	24
Figure 7: Percentage change (monthly) in dense vegetation and agriculture/grassland in central Western Ghats from 2003 to 2012.	25
Figure 8: Percentage change (monthly) in dense vegetation and agriculture/grassland in southern Western Ghats from 2003 to 2012.	25
Figure 9: Annual change from one LC class to other LC classes in northern Western Ghats between 2003 to 2012 obtained from MODIS NDVI. The base image (background) is 250 m black and white version of MODIS NDVI of January, 2003. Colour palate in the middle represents changes in that year.....	26
Figure 10: Annual change from one LC class to other LC classes in central Western Ghats between 2003 to 2012 obtained from MODIS NDVI. The base image (background) is 250 m black and white version of MODIS NDVI of January, 2003. Colour palate in the middle represents changes in that year.....	27
Figure 11: Annual change from one LC class to other LC classes in southern Western Ghats between 2003 to 2012 obtained from MODIS NDVI. The base image (background) is 250 m black and white version of MODIS NDVI of January, 2003. Colour palate in the middle represents changes in that year.....	27
Figure 12: Boxplots for dense vegetation, agriculture/grassland, soil/settlement and water for the year 2003 and 2012 for northern Western Ghats (X-axis: Month, Y-axis: NDVI values).	30
Figure 13: Boxplots for dense vegetation, agriculture/grassland, soil/settlement and water for the year 2003 and 2012 for central Western Ghats (X-axis: Month, Y-axis: NDVI values).	31
Figure 14: Boxplots for dense vegetation, agriculture/grassland, soil/settlement and water for the year 2003 and 2012 for southern Western Ghats (X-axis: Month, Y-axis: NDVI values).	32

Figure 15: Monthly minimum, mean and maximum NDVI values for dense vegetation for the northern, central and southern Western Ghats (top, middle and bottom graphs in the figure)	34
Figure 16: Temporal mean NDVI profiles for the major phenological endmembers corresponding to the 3 (northern, central and southern) climatic regions of Western Ghats (Note: X-axis: Mean NDVI values, Y-axis: Month-Year).....	35
Figure 17: Boxplot of monthly NDVI changes of dense forest for monsoon season (June, August and September) in Western Ghats from 2003 to 2012.....	36
Figure 18: Summary trend maps of NDVI changes in Western Ghats from 2003 to 2012 calculated from monthly (January and December) NDVI time-series.....	38
Figure 19: Sample monthly temperature maps (in °C) for 2003 and 2012 for northern Western Ghats. Images of June and August had lot of pixels with cloud cover, so these images have many no data values (white in colour). (Note: July temperature map was not computed due to presence of cloud in the data.).....	40
Figure 20: Monthly temperature maps (in °C) for 2003 and 2012 for central Western Ghats. Images of June and August had lot of pixels with cloud cover, so these images have many no data values (white in colour). (Note: July temperature map was not computed due to presence of cloud in the data.)	42
Figure 21: Monthly temperature maps (in °C) for 2003 and 2012 for southern Western Ghats. Images of June and August had lot of pixels with cloud cover, so these images have many no data values (white in colour). (Note: July temperature map was not computed due to presence of cloud in the data.)	43
Figure 22: Monthly minimum, mean and maximum temperature (in °C) of the three regions (top - northern, middle - central and bottom - southern Western Ghats). [X-axis: temperature (in °C), Y-axis: Month-Year].	44
Figure 23: Mean monthly temperature \pm standard deviation (in °C) for northern, central and southern Western Ghats (top - northern, middle - central and bottom - southern Western Ghats).	45
Figure 24: Monthly rainfall maps (in mm) for 2003 and 2012 for northern Western Ghats.	47
Figure 25: Monthly rainfall maps (in mm) for 2003 and 2012 for central Western Ghats.	48
Figure 26: Monthly rainfall maps (in mm) for 2003 and 2012 for southern Western Ghats.	50
Figure 27: Total annual rainfall (in mm) for northern Western Ghats from 2003 to 2012 with rain gauge stations overlaid.....	51
Figure 28: Total annual rainfall (in mm) for central Western Ghats from 2003 to 2012 with rain gauge stations overlaid.....	52
Figure 29: Total annual rainfall (in mm) for southern Western Ghats from 2003 to 2012 with rain gauge stations overlaid.....	53
Figure 30: Mean monthly temperature (Y-axis in °C) and monthly rainfall (secondary Y-axis in mm) for northern Western Ghats.....	54

Figure 31: Mean monthly temperature (Y-axis in °C) and monthly rainfall (secondary Y-axis in mm) for central Western Ghats.	54
Figure 32: Mean monthly temperature (Y-axis in °C) and monthly rainfall (secondary Y-axis in mm) for southern Western Ghats.	55
Figure 33: Changes in monthly NDVI and climatic variables from 2003 to 2012. 10-years mean monthly NDVI, 10-years mean monthly temperature (in °C), and 10-years mean monthly rainfall (in mm) for northern, central and southern Western Ghats.	59
Figure 34: Spatial distribution of pattern in dense vegetation and LST through PCA in northern Western Ghats. Red polygonal shapes highlight past and current status of dense vegetation and the corresponding LST through PC's in those areas.	60
Figure 35: Regression between NDVI and climatic variables (LST and rainfall) in northern (top row), central (middle row) and southern Western Ghats (bottom row).....	61
Figure 36: Correlations between 10-years (2003 to 2012) mean monthly NDVI, LST and rainfall for northern, central and southern Western Ghats.	62
Figure 37: Pixel to pixel correlation maps between NDVI and LST for northern Western Ghats.	63
Figure 38: Pixel to pixel correlation maps between NDVI and rainfall for northern Western Ghats...	64
Figure 39: Pixel to pixel correlation maps between LST and rainfall for northern Western Ghats.....	65
Figure 40: Pixel to pixel correlation maps between NDVI and LST for central Western Ghats.	66
Figure 41: Pixel to pixel correlation maps between NDVI and rainfall for central Western Ghats.	67
Figure 42: Pixel to pixel correlation maps between LST and rainfall for central Western Ghats.	68
Figure 43: Pixel to pixel correlation maps between NDVI and LST for southern Western Ghats.	69
Figure 44: Pixel to pixel correlation maps between NDVI and rainfall for southern Western Ghats...	70
Figure 45: Pixel to pixel correlation maps between LST and rainfall for southern Western Ghats.	71
Figure 46: Trends in summer, monsoon and winter of mean forest NDVI, mean temperature and total rainfall for northern Western Ghats.	77
Figure 47: Seasonal trends in summer, monsoon and winter of mean forest NDVI, mean temperature and total rainfall for northern, central and southern Western Ghats.	78
Figure 48: Standard anomalies in seasonal mean forest NDVI, seasonal mean temperature and seasonal total rainfall for northern Western Ghats (a-summer, b-monsoon, c-winter); central Western Ghats (d-summer, e-monsoon, f-winter), and for southern Western Ghats (g-summer, h-monsoon, i-winter).	79
Figure 49: Seasonal variations of forest NDVI, LST and rainfall in summer (March to May), monsoon (June to October) and winter (November to February) in northern Western Ghats.....	81

Figure 50: Seasonal variations of forest NDVI, LST and rainfall in summer (March to May), monsoon (June to October) and winter (November to February) in central Western Ghats.....	82
Figure 51: Seasonal variations of forest NDVI, LST and rainfall in summer (March to May), monsoon (June to October) and winter (November to February) in southern Western Ghats.....	84
Figure 52: Spatial distribution of trends (rate of change) in summer and winter season for forest NDVI (yr^{-1}), LST ($^{\circ}\text{C yr}^{-1}$) and rainfall (mm yr^{-1})	87
Figure 53: Pixel to pixel correlation between forest NDVI, LST and rainfall for summer, monsoon and winter season for northern Western Ghats.....	89
Figure 54: Pixel to pixel correlation between forest NDVI, LST and rainfall for summer, monsoon and winter season for central Western Ghats.....	90
Figure 55: Pixel to pixel correlation between forest NDVI, LST and rainfall for summer, monsoon and winter season for southern Western Ghats.....	91
Figure 56: CUSUM plots using observed monthly total rainfall for Mumbai and Goa (January, 2003 to December, 2012).....	94
Figure 57: CUSUM plots using observed monthly total rainfall for Honavar and Udupi (January, 2003 to December, 2012).....	94
Figure 58: CUSUM plots using observed monthly total rainfall for Kozhikode and Thiruvananthapuram (January, 2003 to December, 2012).....	95
Figure 59: Rainfall time-series plots over dense forest cover.....	100
Figure 60: Decomposition of time-series – observed, trend, seasonal and random components over dense forest cover.	101
Figure 61: Time-series forecast plots of rainfall over forest cover for the northern, central and southern Western Ghats.	102
Figure 62: Rainfall time-series plots over agriculture/grassland land cover.....	103
Figure 63: Decomposition of time-series – observed, trend, seasonal and random components of rainfall in agriculture/grassland land cover.....	104
Figure 64: Time-series forecast plots of rainfall in agriculture/grassland areas for the northern, central and southern Western Ghats.	105

List of tables

Table 1: LC change statistics of northern Western Ghats from 2003 to 2012 based on NDVI classification	22
Table 2: LC change statistics of central Western Ghats from 2003 to 2012 based on NDVI classification	22
Table 3: LC change statistics of southern Western Ghats from 2003 to 2012 based on NDVI classification	23
Table 4: Annual conversion from dense vegetation to other LC classes, and from other LC classes to agricultural/grassland in the three regions of Western Ghats.	28
Table 5: LC change statistics of Western Ghats from 2003 to 2012 based on NDVI differencing	38
Table 6: Mean (μ) \pm standard deviation (σ) of NDVI, LST and rainfall for forest and agriculture/grassland class for northern Western Ghats.....	55
Table 7: Mean (μ) \pm standard deviation (σ) of NDVI, LST and rainfall for forest and agriculture/grassland class for central Western Ghats	56
Table 8: Mean (μ) \pm standard deviation (σ) of NDVI, LST and rainfall for forest and agriculture/grassland class for southern Western Ghats	57
Table 9: Image to image Pearson product-moment correlation coefficient (CC or r) between monthly NDVI of forest and agriculture/grassland class with LST and rainfall for northern Western Ghats	73
Table 10: Image to image Pearson product-moment correlation coefficient (CC or r) between monthly NDVI of forest and agriculture/grassland class with LST and rainfall for central Western Ghats.....	74
Table 11: Image to image Pearson product-moment correlation coefficient (CC or r) between monthly NDVI of forest and agriculture/grassland class with LST and rainfall for southern Western Ghats	75
Table 12: Turning point (TP) for forest NDVI, LST and rainfall for three different season for northern Western Ghats	81
Table 13: Turning point (TP) for forest NDVI, LST and rainfall for three different season for central Western Ghats	83
Table 14: Turning point (TP) for forest NDVI, LST and rainfall for three different season for southern Western Ghats	83
Table 15: CC (p -value < 0.01) between forest NDVI-LST and forest NDVI-rainfall for the TP years for summer, monsoon and winter for the three regions of the Western Ghats	86
Table 16: Rate of change of forest NDVI, LST and rainfall for summer and winter season.....	86
Table 17: Results of step change analysis using rank sum method	95
Table 18: Trend analysis using Mann-Kendall method	96

Table 19: Decadal changes in area of LC in Western Ghats.....	107
Table 20: Decadal changes in LST in Western Ghats.....	108
Table 21: Decadal changes in rainfall in Western Ghats	108

1. Introduction

The structure of the landscape is undergoing transformation either naturally or due to anthropogenic activities. Land cover (LC) changes aggravated with the enhanced anthropogenic activities to meet the growing demand of burgeoning population has led to alterations in the regional climate. LC changes refer to human modification of the Earth's terrestrial surface for food and other essentials. Terrestrial ecosystems are permanently changing at a variety of spatial and temporal scales due to natural and/or anthropogenic causes. Changes in LC induced by any of these agents (either human and/or natural processes) play a major role in global as well as regional scale patterns, which in turn influence weather and climate. The key links between LC with weather and climate include the exchange of greenhouse gases (water vapour, carbon dioxide, methane and nitrous oxide) and sensible heat between the land surface and the atmosphere, the radiation (both solar and long wave) balance of the land surface, and the roughness of the land surface and its uptake of momentum from the atmosphere (Loveland et al., 2003). The current rate of LC changes has increased drastically with wider extent and intensity, driving unprecedented changes in ecosystems and environmental processes at regional and global scales. Extensive clearing of forests for unplanned developmental activities and management practices have encouraged the concentration of human populations, accompanied by the intensification of agriculture in the biologically productive lands and the abandonment of unproductive lands, threatening the sustainability of land resources. Mismanagement of land resources is linked to potentially negative consequences. LC changes encompass the greatest environmental concern today, including climate change, biodiversity loss, global warming, ground water depletion, and the pollution of water, soil and air (Ellis and Pontius, 2010). Moreover, local alterations in LC can have global consequences, requiring local and regional solutions with cooperation of the stakeholders in land management at all scales. Monitoring the locations and distributions of LC change and curtailing its negative consequences while sustaining the production of essential resources and resilience of degraded ecosystem is a major challenge for management, policy decision makers and economic planners and is important for establishing links between policy decisions, regulatory actions and subsequent land use activities (Lunetta et al., 2006).

Ideally, frequently updated data of environmental status, trends, are essential for understanding ecosystem processes and modeling. However, currently available LC datasets for large geographic regions are produced on an intermittent basis and are often outdated with the current pace of change. A scientific investigation to understand the cause and consequences of LC change across a range of spatial and temporal scales is now possible with the availability of temporal remote sensing (RS) data with advancements in geoinformatics and modeling techniques, together with the field based scientific methods. The knowledge of spatial and temporal distributions of vegetation are fundamental to many aspects of environmental science, time-series global change detection for evolving appropriate strategies for sustainable management of natural resources. Acquisitions of data

remotely through space borne sensors have offered means of measuring vegetation properties at regional to global scales over the last two decades. Phenological changes during the growing season can be studied by examining the spectral signature changes in the RS data. Time-series remotely sensed data acquired in different spectral bands aid in LC change detection analysis. They provide a powerful tool to learn from past events, monitor current conditions (Orr et al., 2004), and prepare for future change. However, spectral-based change detection techniques (classification) have limited performance in biologically complex ecosystems due to phenology-induced errors (Lunetta et al., 2002a, b). Other factors that limit the application of post-classification change detection techniques include cost, consistency, and error propagation (Singh, 1989).

On the other hand, ecosystem-specific regeneration rates are an important consideration for determining the required frequency of data collections to minimize errors. As part of the natural processes associated with vegetation dynamics, plants undergo intra-annual cycles (phenology). Earlier researches have focused on monitoring changes in vegetation growth due to its important role in regulating terrestrial carbon cycle and the climate system. During different stages of vegetation growth, plant structures and associated pigment assemblages can vary significantly. Changes in vegetation productivity are a primary regulator of the variation in terrestrial net carbon update (Zhao and Running, 2010). Further, changes in vegetation productivity alter biophysical land surface properties and the amount and nature of the energy transfer to the atmosphere, which ultimately changes the local or regional climate (Jackson et al., 2008). Hence, increased attention has been paid to the dynamic rules of vegetation growth and its response to climate change at regional, continental and global scales in the past several decades (Zhang et al., 2013). Ability to identify vegetation classes using remote sensor systems is due to wavelength-specific foliar reflectance (0.76–0.90 μm), pigment absorptions (0.45–0.69 μm), and foliar moisture content (1.55–1.75 μm). Vegetation type appear significantly different at various stages during intra-annual growth cycles (Lunetta et al., 2006) enabling the analysis of seasonal variations. Comparison of current vegetation data records with historic long-term averages have been used to support ecosystem monitoring (Orr et al., 2004). Long term analysis of the vegetation changes over wet, normal and dry years is a vital requirement to closely look into vegetation response to climatic changes. Based on these, numerous pre-classification change detection approaches have been developed and refined to provide optimal performance over the greatest possible range of ecosystem conditions. These semi-automated digital data processing approaches include image-based composite analysis (Weismiller et al., 1997) and principal components analysis (PCA) (Byrne et al., 1980; Lillesand and Keifer, 1972; Richards, 1984).

Vegetation indices are commonly applied data transformation technique (Crist, 1985; Jensen, 2005) where the vegetation signal is boosted and the information becomes more useful when two or more bands are combined into a vegetation index (VI). VI can then be used as surrogate measures of vegetation activity. A widely used VI to separate vegetation from non-vegetative classes is NDVI (Normalised Difference Vegetation Index). NDVI is dependent on the spectral relationships of vegetation in the red and near-infrared (NIR) part of the spectrum. Due to vegetation pigment absorption (chlorophyll, proto-chlorophyll), the

reflected red energy decreases, while the reflected NIR energy increases as a result of the strong scattering processes of healthy leaves within the canopy. NDVI can provide a useful index of vegetation variability on seasonal and inter-annual time-scales, and that long-term monitoring of NDVI elucidates relationships between inter-annual fluctuations of vegetation and climate. NDVI theoretically takes values ranging from -1.0 to +1.0. Positive NDVI values (NIR>RED) indicate green, vegetated surfaces, and higher values indicate vegetation with good canopy density. The red portion of the spectrum decreases as solar radiation is absorbed, largely by chlorophyll, whereas reflectance of the NIR portion is caused by leaf mesophyll structure (Kremer and Running, 1993). Negative or zero NDVI values indicate non-vegetated surfaces such as water, ice, and snow.

NDVI have been directly used as a surrogate of plant photosynthetic activity and helps in detecting the biotic responses to climate change (Zhou et al., 2001). This has been effectively used in vegetation dynamics monitoring and to study the vegetation responses to climatic changes at different scales during the past few years and have been a useful tool to couple climate and vegetation distribution and performance at large spatial and temporal scales (Pettorelli et al., 2005). Satellite-derived seasonal greenness/NDVI data have the potential to provide temporal indicators of the onset, end, peak and duration of vegetation greenness as well as the rate of growth, senescence and periodicity of photosynthetic activity (Reed et al., 1994; Yang et al., 1998). Past studies have demonstrated the potential of using NDVI to study vegetation dynamics (Townshend and Justice, 1986; Verhoef et al., 1996), illustrating the value of using high temporal resolution imageries to monitor changes in wetland vegetation (Elvidge et al., 1998) and document the importance of image temporal frequency for accurately detecting forest changes in the southeastern United States (Lunetta et al., 2004). Lyon et al. (1998) reported that NDVI was the best performing VI (vegetation index) for detecting LC changes in the ecologically complex vegetation communities in Chiapas, Mexico. Consistent NDVI time-series are paramount in monitoring ecological resources that are being altered by climate and human impacts (Willem et al., 2006). However, Lunetta et al., (2002a, b) determined that image differencing methods such as two-date NDVI differencing and Multiband Image Differencing (MID) do not perform well in a biologically complex vegetation community in North Carolina. There is also an expanding need for continuous data streams to support the development of spatially distributed landscape process models that would incorporate higher frequency simulations (time steps).

Earlier the time-series data analyses have largely focused on the use of coarse-resolution ($\geq 1 \text{ km}^2$) AVHRR (Advance Very High Resolution Radiometer) data to document LC and analyse vegetation phenology and dynamics (Justice et al., 1985; Townshend and Justice, 1986; Justice et al., 1991; Loveland et al., 1991). Availability of MODIS data having a 250 m spatial resolution in the red and NIR channels provides opportunity to map phenology at a much finer scale than AVHRR data. With the advent of MODIS NDVI 250 m data, time-series data analysis have been adapted for many applications even though their utility are occasionally limited by the availability of high-quality (e.g., cloud-free) data (Jin and Sader, 2005). Since 2000, NDVI data derived from the Terra/MODIS satellite sensors are being regularly used because they provide higher spatial resolution, enhanced atmospheric

corrections and more precise geo-registration. Time-series NDVI are shown to capture essential features of seasonal and inter-annual vegetation variability and have been used to extract numerical observations related to vegetation dynamics (Pettorelli et al., 2005; Tucker and Sellers, 1986). Researchers have incorporated a number of processing techniques including weighted regression smoothing (Li and Kafatos, 2000), Fourier and wavelet transformation filtering (Sakamoto et al., 2005), weighted least squares (Reed, 2006) and wavelet feature extraction (Bruce et al., 2006) to deal with the data quality issues.

Spectral VI with its impact on local temperature and rainfall can be used to investigate and understand the interactions between vegetation dynamics and landscape ecosystems, monitor the effects of deforestation, investigate climate change and carbon sequestration, assess natural resources, agricultural production and food, aid in land management and sustainability to support ecosystem monitoring (Myneni et al., 1997; Nemani et al., 2003; Orr et al., 2004; Seelan et al., 2003; Yang et al., 1998). Specifically, vegetation changes and their relationships with temperature has been the subject of interest. The relationship between different LC types with LST (land surface temperature) revealed that NDVI and LST generally tend to show strong correlation (Ramachandra et al., 2008; Mao et al., 2012). In many cases, higher the NDVI, lower is the LST and vice versa. NDVI in conjunction with LST have been used for many different studies, such as, to derive the spatial extent of the LC change effect (Gunawardhana and Kazama, 2012), to estimate moisture content in forest fire (Chuvieco et al., 2004), to estimate land surface emissivities over agricultural areas (Jiménez-Muñoz et al., 2006), to estimate extent of vegetation types (Raynolds et al., 2008), to predict crop grain yield (Balaghi et al., 2008), to assess vegetation change and their response to climate change (Zhang et al., 2013), drought assessment (Karnieli et al., 2009), etc.

Vegetation vigor and productivity are related to hydrological variables, hence rainfall data serves as a surrogate measure of these factors at the landscape scale (Groeneveld and Baugh, 2007; Wang et al., 2003). NDVI is strongly coupled to rainfall fluctuations with index values generally increasing with rainfall (Tucker et al., 1991). This close coupling makes it possible to employ NDVI as a proxy for the land surface response to rainfall variation. The positive trend in NDVI is thereby taken as a response to an overall increase in precipitation (Hickler et al., 2005; Nicholson et al., 1990), although, there have been various theories for the rainfall variability such as influence by global sea surface temperature (Caminade and Terray, 2010), large scale changes in LC and land-atmosphere interaction (Hulme 2001; Nicholson, 2000). Whether the climate impact or human activities are dominating rainfall variability or not, the greening trend is a subject of debate and ongoing research (Huber et al., 2011). In one of the studies by Seaquist et al., (2008) NDVI was first regressed on satellite-measured precipitation data and then the NDVI residual time-series was searched for significant trends for the period 1982–2003. The trends in the residuals depict thereby that part of the measured NDVI was not explained by precipitation. Yet, Herrmann et al., (2005) used all the months of the year, including the long dry season in their study which introduced noise and skewness in the data distribution. NDVI residual time-series, originating from regressing NDVI on rainfall have also been used for identifying significant long-term trends in vegetation greenness induced by other factors than water availability (Huber et al., 2011).

2. Objective

NDVI, temperature and rainfall are critical in understanding the interactions between terrestrial ecosystems and climate system in an eco-sensitive region. The inter-annual variations in vegetation cover is one of the main drivers of climate changes (Piao et al., 2006; Zhou et al., 2001; Schimel et al., 2001). Investigations of the correlation between NDVI and climate factors (Zhang et al., 2013) aid in understanding the causes that bring changes in the terrestrial ecosystem carbon cycle and shed light on the mechanisms controlling the response of terrestrial carbon storage to climate variability (Braswell et al., 1997; Potter and Brooks, 1998). During the past two decades, numerous studies have attempted the relationships between NDVI and climate factors in different geographic regions and ecosystems. However, the mechanisms of the response of vegetation to climate change are still not clear (Wang et al., 2003). Most of these studies have related NDVI with climate factors during the growing season or examined their spatial changes (Schultz and Halpert, 1995; Yang et al., 1997; Potter and Brooks, 1998; Suzuki et al., 2000). Some studies have focused on the relationships between change in NDVI and climate variables in different seasons to described their spatial patterns (Jobbagy et al., 2002; Piao et al., 2003, 2004; Wang et al., 2003; Zhou et al., 2003). However, there are no studies focusing on long time sequence of NDVI with the climatic parameters in the Western Ghats region in India. This region constitute one of the 34 global biodiversity hotspots having exceptional levels of plant endemism and serious levels of habitat loss (Conservation International, 2005), therefore, the study of vegetation change and relationship between NDVI and climatic parameters in this area is of significance.

Here, datasets of the satellite-derived NDVI and climatic factors are combined to analyse spatio-temporal patterns of vegetation growth. The aim is to assess NDVI based vegetation changes and their response to climatic factors or climate change parameters from 2003 to 2012 in Western Ghats, India. The primary purpose of this study is to identify the extent and location of vegetation changes occurred in Western Ghats region during the past 10 years. Understanding the impact of climate changes on vegetation growth in this region is critical because this region is among the most fragile ecosystems. First, we analysed changes in NDVI and its relationship with climatic factors such as temperature and precipitation data and then we explored the variation trends in NDVI to gain further insights into the contribution of different seasons to NDVI.

The objectives of this study are:

1. To construct a long-term NDVI, LST and rainfall time-series datasets covering 2003–2012 by integrating MODIS NDVI, MODIS LST and rainfall data from monitoring stations.
2. To understand the LC change, temperature variation and rainfall pattern in Western Ghats during 10 years (from 2003 to 2012).
3. To explore the inter-annual variation in growth of dense vegetation from 2003 to 2012.

4. Present an analysis of the trends of vegetation (forest and agricultural) and climatic variables (temperature and precipitation) using the constructed NDVI and climate data sets, and investigate their relationship in different months and seasons during 2003–2012.
5. Make a comparison about the correlation of NDVI–temperature and NDVI–precipitation, and model the precipitation pattern in vegetation areas.

Results of this study would provide an example for further studies by integrating NDVI data from different sources to monitor long time-sequence NDVI change, and provide extended NDVI dataset as driving data for estimating long series net primary productivity (NPP) of vegetation.

3. Study area and data

The research was conducted over 160,000 km² of Western Ghats of the Indian peninsula (figure 1). The rugged range of hills stretching for about 1600 km along the west coast from south of Gujarat state to the end of the peninsula (8–21° N and 73–78° E), is interrupted only by a 30 km break in Kerala, the Palghat Gap (Radhakrishna, 2001) in India. The hill ranges of the Western Ghats extend along the west coast of India from river Tapti in the north to the southern tip of India. Western Ghats have an average height of 900 m amsl with several cliffs rising over 1000 m. The Nilgiri Plateau to the north and Anamalais to the south of the Palghat Gap exceed 2000 m in many places. Towards the eastern side, the Ghats merge with the Deccan Plateau which gradually slopes towards the Bay of Bengal. Their positioning makes Western Ghats biologically rich and biogeographically unique – a veritable treasure house of biodiversity. Hundreds of rivers originate from several mountains and run their westward courses towards the Arabian Sea. Only three major rivers, joined by many of their tributaries flow eastward, longer distances, towards the Bay of Bengal (Dikshit, 2001; Radhakrishna, 2001). The Western Ghat's rivers are very critical resources for peninsular India's drinking water, irrigation and electricity (Chandran et al., 2010).

The study area includes 3 diverse eco-regions or climatic zone types as shown in figure 1. The complex geography, wide variations in annual rainfall from 1000–6000 mm, and altitudinal decrease in temperature coupled with anthropogenic factors have produced a variety of vegetation types in the Western Ghats. Tropical evergreen forest is the natural climax vegetation of western slopes, which intercept the south-west monsoon winds. Towards the rain-shadow region, eastwards vegetation changes rapidly from semi-evergreen to moist deciduous and dry deciduous kinds, the last one being characteristic of the semi-arid Deccan region as well. All these types of natural vegetation degrade rapidly in places of high human impact in the form of tree felling, fire and pastoralism, producing scrub, savanna and grassland. Lower temperature, especially in altitudes exceeding 1500 m, has produced a unique mosaic of montane 'shola' evergreen forests alternating with rolling grasslands, mainly in the Nilgiris and the Anamalais (Pascal, 1988).

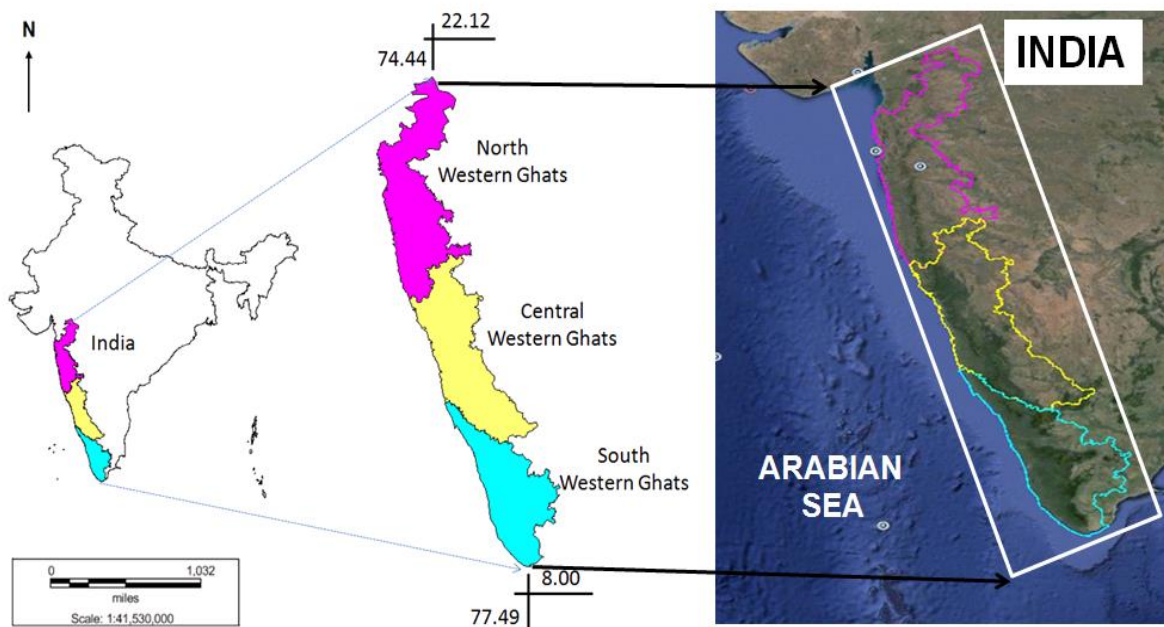


Figure 1: Western Ghats, India including major ecological regions (northern, central and southern Western Ghats).

Following data from various sources were used in this study:

1. MODIS (Moderate Resolution Imaging Spectroradiometer) NDVI 16-day composite grid data L3 product in Sinusoidal projection (MOD13Q1) with 250 m spatial resolution having 4800 rows x 4800 columns in HDF format were downloaded from January 2003 to December 2012 (10 years) from NASA Earth Observing System (EOS) data gateway (<http://reverb.echo.nasa.gov/reverb/>).

MODIS is a key instrument aboard the Terra and Aqua satellites, which view the entire Earth's surface every 1–2 days and acquire data in 36 discrete spectral bands ranging in wavelengths from 0.4 mm to 14.4 mm. These data have improved our understanding of global dynamics and processes occurring on land, oceans, and in the lower atmosphere (Ren et al., 2008). MODIS have the advantage of higher spatial and spectral resolutions compared to NOAA (National Oceanic and Atmospheric Administration)/AVHRR, and higher spectral and temporal resolution compared to SPOT (systeme probatoire d'observation de la terre) or TM (Thematic Mapper) multi-spectral data. Since MODIS data are acquired in narrow spectrum, the impact of water vapor absorption in the NIR band is minimized, the red band data is more sensitive to chlorophyll, and therefore the quality of NDVI data is better (Gitelson et al., 1997; Huete et al., 2002; Kaufman and Tanre', 1996; van Leeuwen et al., 1999). Therefore, MODIS NDVI has been extensively used in crop mapping (Xiao et al., 2005), vegetation phenology (Beck et al., 2006), vegetation classification (Wardlow et al., 2007), and land use/land cover change (Lunetta et al., 2006), etc.

It is to be noted that the NDVI data pertaining to July was dominated by cloud presence for all the years (this is peak monsoon month/season in tropical region), hence July data have been discarded from analysis.

2. MODIS LST level-3 data (MOD11A2 L3) with 1200 rows x 1200 columns at 1 km spatial resolution available every 8 days were downloaded from January 2003 to December 2012 (10 years) from NASA Earth Observing System (EOS) data gateway (reverb.echo.nasa.gov/reverb/). This global LST and Emissivity MODIS 8-day product are composed from the daily 1-kilometer LST product (MOD11A1) and stored on a 1-km Sinusoidal grid as the average values of clear-sky LSTs. It is to be noted that the LST data pertaining to July was full of cloud for all the years (due to monsoon season in tropical region), hence July data have been discarded from analysis.
3. Monthly rainfall data of Indian cities (falling in Western Ghats region) were downloaded from India Water Portal (<http://www.indiawaterportal.org/metdata>), National Climate Data Center, NOAA (<http://gis.ncdc.noaa.gov/map/viewer>) and directorate of Economics and Statistics, Government of Karnataka (<http://des.kar.nic.in>).
4. Ground truth data were collected through a hand held pre calibrated GPS.
5. Google Earth (<http://earth.google.com>) and Bhuvan (<http://bhuvan.nrsc.gov.in>) data were used in exploratory data analysis, validation and supervised classification of the LC in the study area.
6. Survey of India (SOI) Topographical maps of 1:250000 and 1:50000 scale (<http://www.surveyofindia.gov.in>) for generating base layers (road and drainage network, administrative boundaries, etc.).

Spatial analyses were carried out in Linux based free and open source software GRASS – Geographic Resources Analysis Support System (<http://wgbis.ces.iisc.ernet.in/grass>) and R statistical package (<http://www.r-project.org>).

4. Methods

The steps involved are listed below and shown in figure 2.

- 1) **Creation of base layers:** Base layers like district boundary, district with taluk and village boundaries, road network, drainage network, mapping of water bodies, etc. were generated from SOI topographic maps of scale 1:250000 and 1:50000.
- 2) **Geo-referencing of MODIS NDVI data:** MODIS NDVI data were geo-corrected with known ground control points (GCP's), projected to Polyconic (latitude-longitude

coordinate system) with Evrst 56 datum, and resampled to 250 m × 250 m grid cell, multilayer image stack followed by masking and cropping of the study area.

- 3) **Geo-referencing of MODIS LST data:** MODIS LST data were geo-corrected with known GCP's and projected to Polyconic system, Evrst 56 datum, followed by masking and cropping of the study area. These 1 km bands were resampled to 250 m using nearest neighbourhood technique to be consistent with MODIS NDVI bands.
- 4) **Computation of LST from MODIS LST bands:** MODIS Land Surface Temperature/Emissivity (LST/E) data with 1 km spatial resolution with a data type of 16-bit unsigned integer were multiplied by a scale factor of 0.02 (<http://lpdaac.usgs.gov/modis/dataproducts.asp#mod11>). The corresponding temperatures for all data were converted to degree Celsius (°C).
- 5) **Generation of rainfall maps:** Interpolation of rainfall data points were performed by *krigging* to obtain rainfall raster maps at 250 m spatial resolution so as to maintain consistency of spatial resolutions between datasets.
- 6) **NDVI thresholding:** NDVI data were thresholded empirically with field data to segregate NDVI values into four LC classes – dense vegetation, agricultural/farmland/grassland, settlement/barren land/soil and water bodies through training data, boxplot, Google Earth and field knowledge.
- 7) **Validation of classified maps:** The LC maps obtained by thresholding NDVI maps were validated using test data collected from ground and other sources discussed later.
- 8) **LC Change detection:** LC change detection was performed by comparing the LC area per class during 10 years.
- 9) **Seasonal pattern/trend analysis:** NDVI, LST and rainfall data of vegetation class (forest and agricultural) were analysed to understand their variations in different seasons (summer, monsoon and winter) during 10 years.
- 10) **Statistical analysis:** Relationship between time-series NDVI, LST and rainfall data were analysed using statistical methods.
- 11) **Trend analysis and modelling:** The rainfall patterns in forest and agriculture/grassland areas were modelled and forecasted using autoregressive integrated moving average (ARIMA).

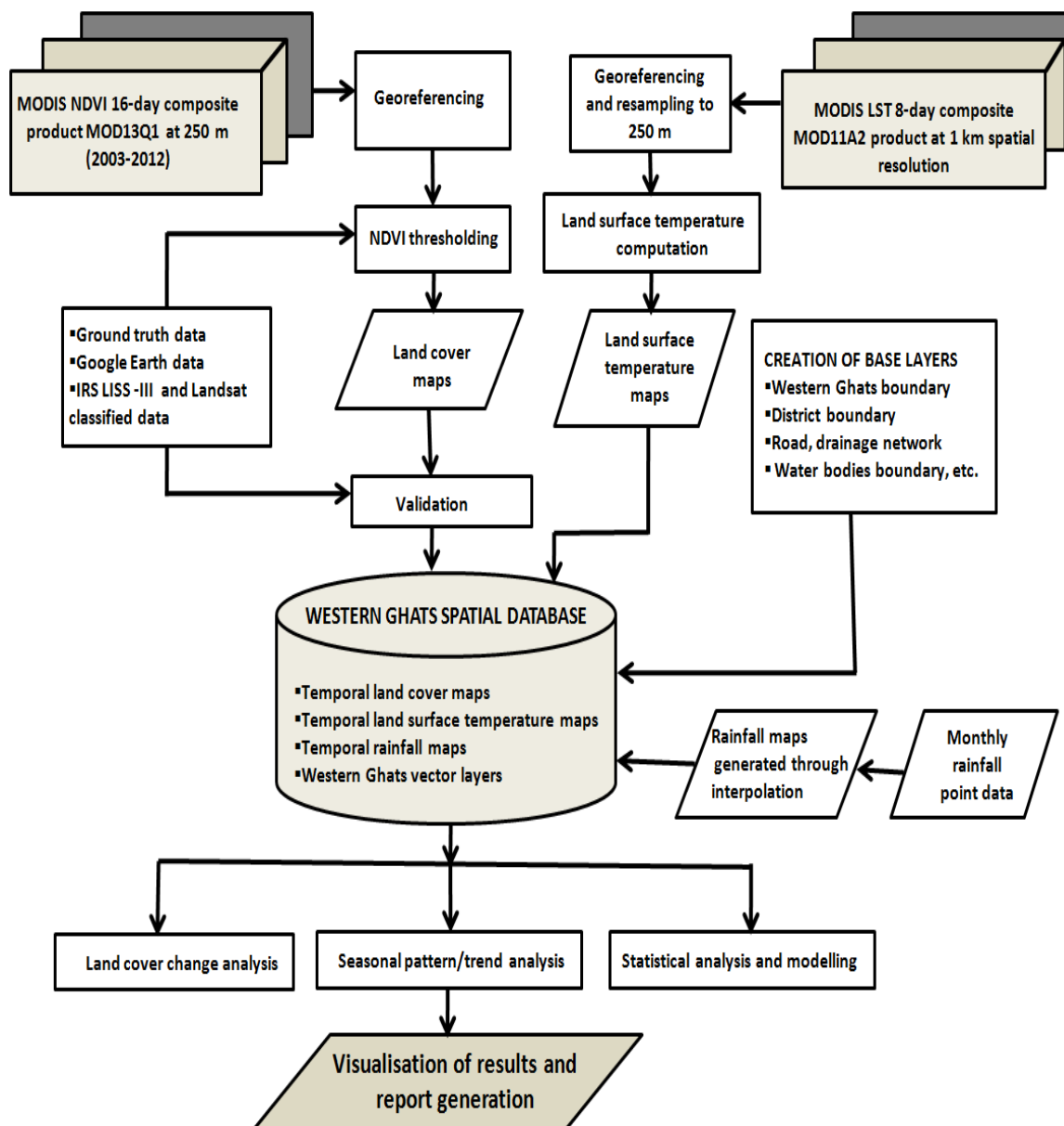


Figure 2: Flowchart of the overall method.

5. Results

MODIS NDVI and LST data were used to generate monthly NDVI and monthly temperature maps. Detail documentation of MODIS NDVI compositing process and Quality Assessment Science Data Sets (QASDS) is available at NASA's MODIS web site (MODIS, 1999). MODIS LST products user's guide documents data generation, data attributes and quality assurance details. LST maps were calibrated and validated from past data records collected by NOAA (<http://gis.ncdc.noaa.gov/map/viewer>). Monthly rainfall raster maps were obtained by interpolation of point data and the values were validated using rain gauge stations located at several sites in the study area. A small part of the study area as seen in Google Earth

(<http://earth.google.com>) in 2003 is given in figure 3 (a) and in 2012 is given in figure 3 (b) respectively, and figure 3 (c) shows NDVI of January, 2003 and December, 2012 corresponding to the region shown in figure 3 (a) and (b).

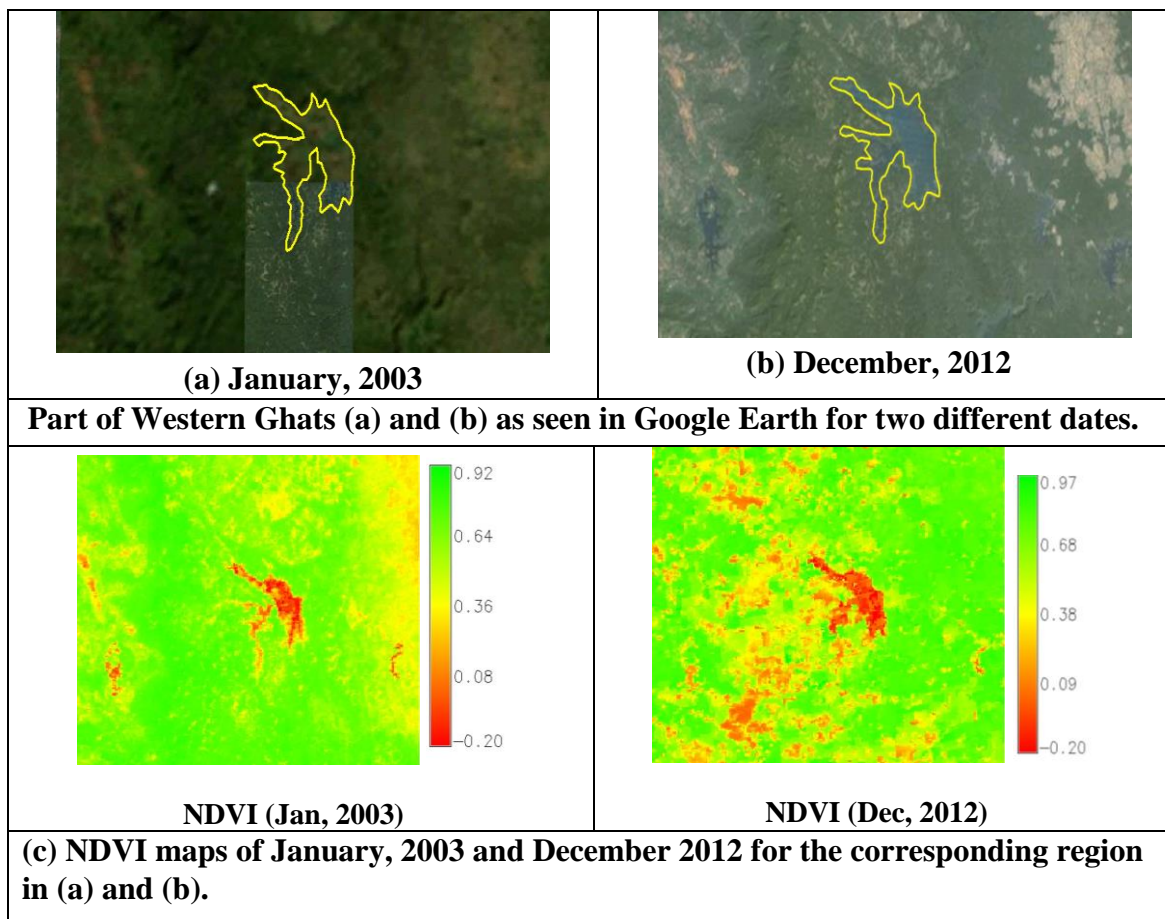


Figure 3: A small part of the study area (a) and (b) as seen in Google Earth in 2003 and 2012; (c) NDVI of the same region in January, 2003 and December, 2012.

5.1 Time-series MODIS NDVI based LC change analysis from 2003 to 2012

MODIS NDVI time-series and reference data were used for multi-temporal LC analysis and validation. Monthly NDVI values for each 250 m grid cell within the study area (during 2003–2012) were identified that exhibited greater than specified threshold values known as “NDVI class separation threshold” and were labeled as separate LC classes. Boxplots were generated to understand the variability and to visualize the separation of classes through their statistical properties such as median and inter-quartile range for each class. The ambiguities in separation between two different LC classes due to seasonal differences were resolved by adjusting the NDVI class separation threshold and expert knowledge. Figure 4 shows variations (boxplots) for the four LC classes – dense vegetation, agriculture/grassland, soil/settlement and water for January, 2003 and December, 2012 respectively for northern Western Ghats.

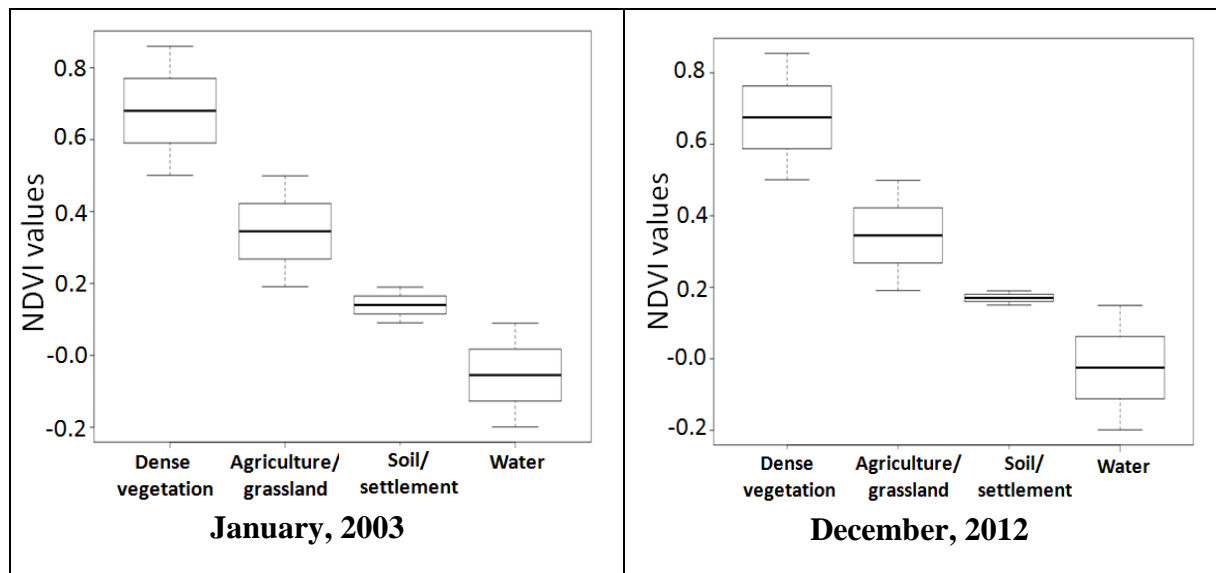


Figure 4: Boxplots for dense vegetation, agriculture/grassland, soil/settlement and water for the year January, 2003 and December, 2012 for northern Western Ghats (X-axis: Month, Y-axis: NDVI values).

Boxplots helped in visualizing the separability of LC classes through NDVI. Their inter-quartile range and whiskers aided in assessing the overlapping regions between classes which further helped in adjusting the NDVI thresholds for different LC classes, for each month and different years. The boxplots show that LC classes were separable and NDVI thresholding was successful in delineating the LC classes from multi-temporal NDVI images. Similarly, the four LC classes were also separated for central and southern Western Ghats based on monthly NDVI thresholding from 2003 to 2012 that have not been shown here. The LC maps were validated in various ways –

- i) by overlaying test data obtained using GPS and field survey.
- ii) by comparison with limited number of temporal high resolution classified images (Landsat ETM+ available in public domain and IRS LISS III/IV images procured from NRSC – National Remote Sensing Centre, Hyderabad, India).
- iii) by visual inspection/expert knowledge, and
- iv) by comparing each of the LC classes with Google Earth historical images (<http://earth.google.com>) through visual checks.

However, the error matrices have not been shown here because of the large spatial and temporal nature of the data. The producer's accuracies ranged from 67 to 81%, user's accuracies ranged from 69 to 84% and overall accuracies ranged between 65 to 80.5%. Figure 5 shows sample LC maps of January 2003 and December 2012 for northern, central and southern Western Ghats and table 1–3 depicts the LC class statistics. Figure 6–8 shows

time-series graph for the LC change (dense vegetation and agriculture) for northern, central and southern Western Ghats.

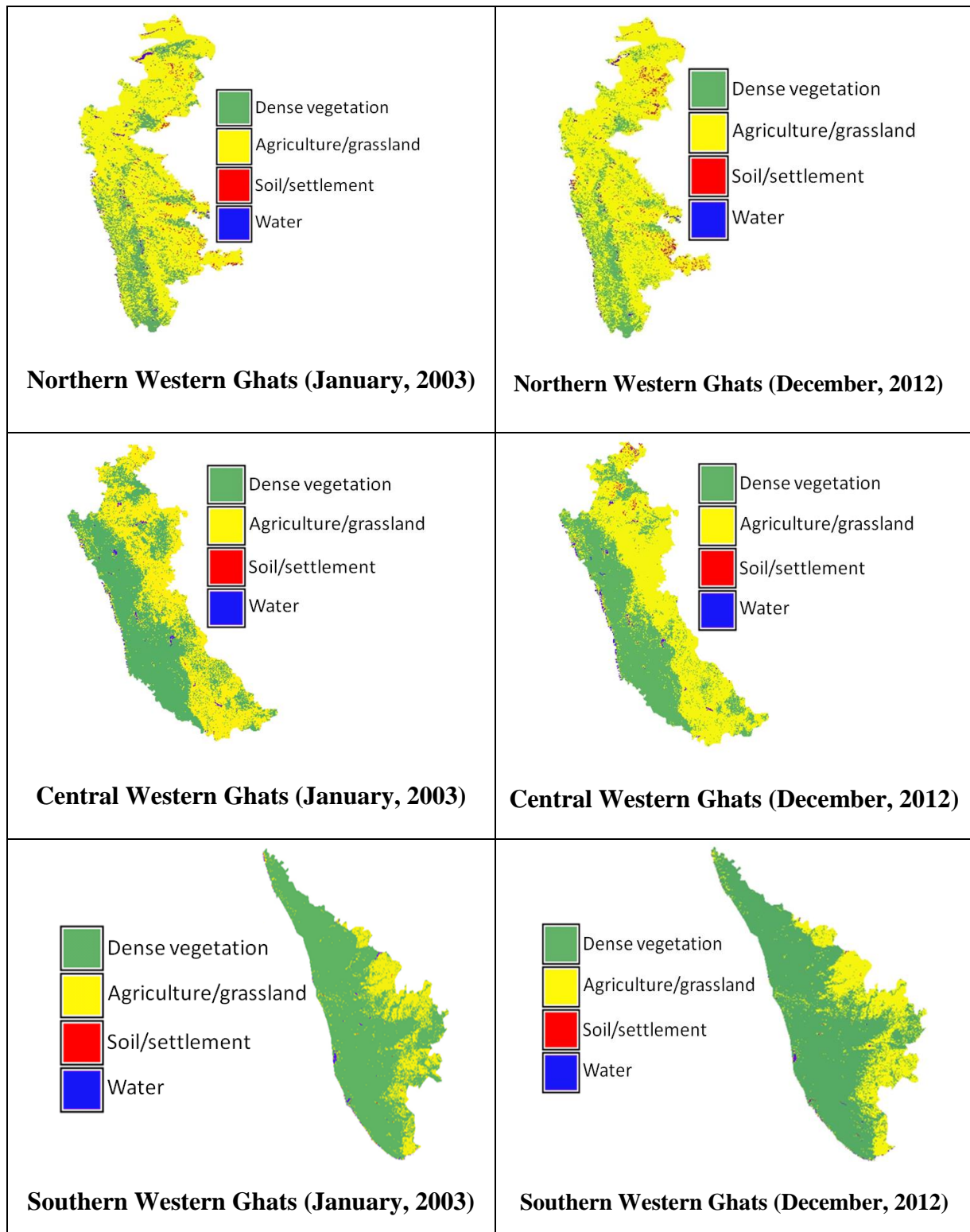


Figure 5: LC maps of northern, central and southern Western Ghats of January, 2003 and December, 2012.

Table 1: LC change statistics of northern Western Ghats from 2003 to 2012 based on NDVI classification

Month-Year	Dense Vegetation		Agriculture/grassland		Soil/settlement		Water	
	ha	%	ha	%	ha	%	ha	%
Jan-03	2340719	23.64	7315449	73.88	108282.6	1.09	138085.2	1.39
Jan-04	2276359	22.99	7356046	74.29	128151	1.29	142058.9	1.43
Jan-05	2233782	22.56	7404565	74.78	131131.2	1.32	133118.1	1.34
Jan-06	2196157	22.18	7434270	75.08	126164.1	1.27	146032.5	1.47
Jan-07	2177344	21.99	7421201	74.95	166894.3	1.68	137091.8	1.38
Jan-08	2164373	21.86	7448133	75.22	177821.9	1.79	116230	1.17
Jan-09	2146649	21.68	7420408	74.94	168881.1	1.7	166894.3	1.68
Jan-10	2133974	21.55	7505563	75.80	147025.9	1.48	115236.6	1.16
Jan-11	2119023	21.40	7478828	75.53	177821.9	1.79	137091.8	1.38
Jan-12	2106053	21.27	7509524	75.84	169874.5	1.71	117223.4	1.18
Dec-12	2059516	20.80	7536259	76.11	182789	1.84	123183.9	1.24

Table 2: LC change statistics of central Western Ghats from 2003 to 2012 based on NDVI classification

Month-Year	Dense Vegetation		Agriculture/grassland		Soil/settlement		Water	
	ha	%	ha	%	ha	%	ha	%
Jan-03	5073131	53.39	4331023	45.58	4751	0.05	93119.6	0.98
Jan-04	5031322	52.95	4368081	45.97	6651.4	0.07	95970.2	1.01
Jan-05	4981957	52.43	4402288	46.33	17103.6	0.18	95970.2	1.01
Jan-06	4956754	52.17	4435545	46.68	17103.6	0.18	95020	1
Jan-07	4940102	51.99	4471653	47.06	9502	0.1	76966.2	0.81
Jan-08	4876439	51.32	4502059	47.38	27555.8	0.29	86468.2	0.91
Jan-09	4851733	51.06	4550520	47.89	20904.4	0.22	78866.6	0.83
Jan-10	4834630	50.88	4564773	48.04	19004	0.2	85518	0.9
Jan-11	4806175	50.58	4598980	48.4	19954.2	0.21	76966.2	0.81
Jan-12	4709168	49.56	4684498	49.3	33257	0.35	73165.4	0.77
Dec-12	4656546	49.01	4741510	49.9	49410.4	0.52	56061.8	0.59

Table 3: LC change statistics of southern Western Ghats from 2003 to 2012 based on NDVI classification

Month-Year	Dense Vegetation		Agriculture/grassland		Soil/settlement		Water	
	ha	%	ha	%	ha	%	ha	%
Jan-03	5897318	78.78	1538333	20.55	7485.81	0.1	42669.09	0.57
Jan-04	5839677	78.01	1593728	21.29	7485.81	0.1	44914.84	0.6
Jan-05	5755243	76.88	1636397	21.86	6737.23	0.09	44914.84	0.6
Jan-06	5664509	75.67	1721735	23	6737.23	0.09	44914.84	0.6
Jan-07	5621840	75.1	1811565	24.2	6737.23	0.09	45663.42	0.61
Jan-08	5564948	74.34	1867709	24.95	6737.23	0.09	45663.42	0.61
Jan-09	5541742	74.03	1893909	25.3	4491.48	0.06	45663.42	0.61
Jan-10	5531262	73.89	1908881	25.5	8982.97	0.12	36680.45	0.49
Jan-11	5508056	73.58	1923104	25.69	5988.64	0.08	48657.74	0.65
Jan-12	5483353	73.25	1951550	26.07	5240.06	0.07	45663.42	0.61
Dec-12	5465387	73.01	1976253	26.4	8982.97	0.12	35183.29	0.47

Sometimes, it was difficult to segregate dense vegetation from agriculture/grassland by identifying an exact NDVI threshold, and exposed soil covered with grass created confusion between soil and grassland. Table 1–3 shows that forest area have decreased by ~3% in northern, by ~4.4% in central and by 5.7% in southern Western Ghats. Agriculture/grasslands have increased by 2.23% in northern, by 4.3% in central and 5.8% in southern region respectively. Soil/settlement have increased marginally and the spatial extent of water bodies have decreased in all the three regions of Western Ghats. Figure 6–8 show percentage change in the estimate of dense vegetation and agriculture/grassland in northern, central and southern Western Ghats from 2003 to 2012. Northern and central Western Ghats shows very similar trends. Dense vegetation/forest area increases in September–October–November and decreases in January–February. This season (August–September–October) corresponds from mid to end of the monsoon that brings heavy showers from Arabian Sea. Due to this rain, entire Ghat region is full of thick vegetation. Agriculture/grassland area is maximum in August–September and December–January and minimum in April–May in both northern and central Western Ghats. However, southern Western Ghats shows a slightly different pattern with peak dense vegetation between October through June and lowest in August and September. Agriculture crops occupy maximum spatial extent between August to December and show valleys in the time-series graph between April to June.

The valleys in the three graphs (figure 6 to 8) for all the three climatic/ecological regions for agriculture correspond to April to June when there is no water and the farmlands are generally fallow. The farmers wait for the monsoon in July/August to sow the crops. Crops mature and are ready for harvesting in December/January indicating peak in the graphs with maximum area under this class (agriculture). These crops are popularly known as kharif crops

or monsoon crops (July to October) and rabi crops (October to March). Southern Western Ghats receives the first rainfall of monsoon season in the country every year and therefore agriculture/grassland areas show an early increasing trend in this region. It is to be noted that the data for July month was not available (due to the presence of clouds), therefore the graph suddenly dips down in this month for all the years. Figure 6–8 brings a very important conclusion, i.e. the total dense green area in northern and central Western Ghats are between 20–80% of all the LC classes while dense vegetation constitute around 60–95% of the southern Western Ghats throughout the years of study (2003–2012).

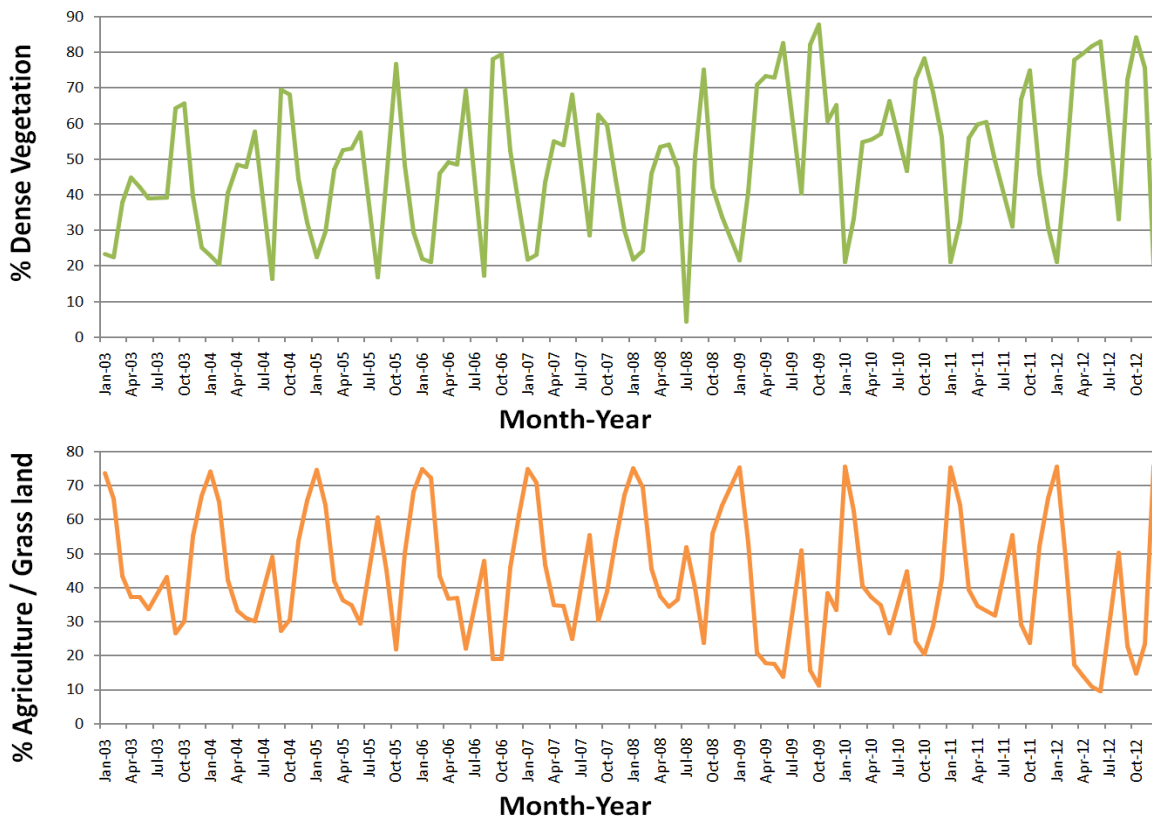


Figure 6: Percentage change (monthly) in dense vegetation and agriculture/grassland in northern Western Ghats from 2003 to 2012.

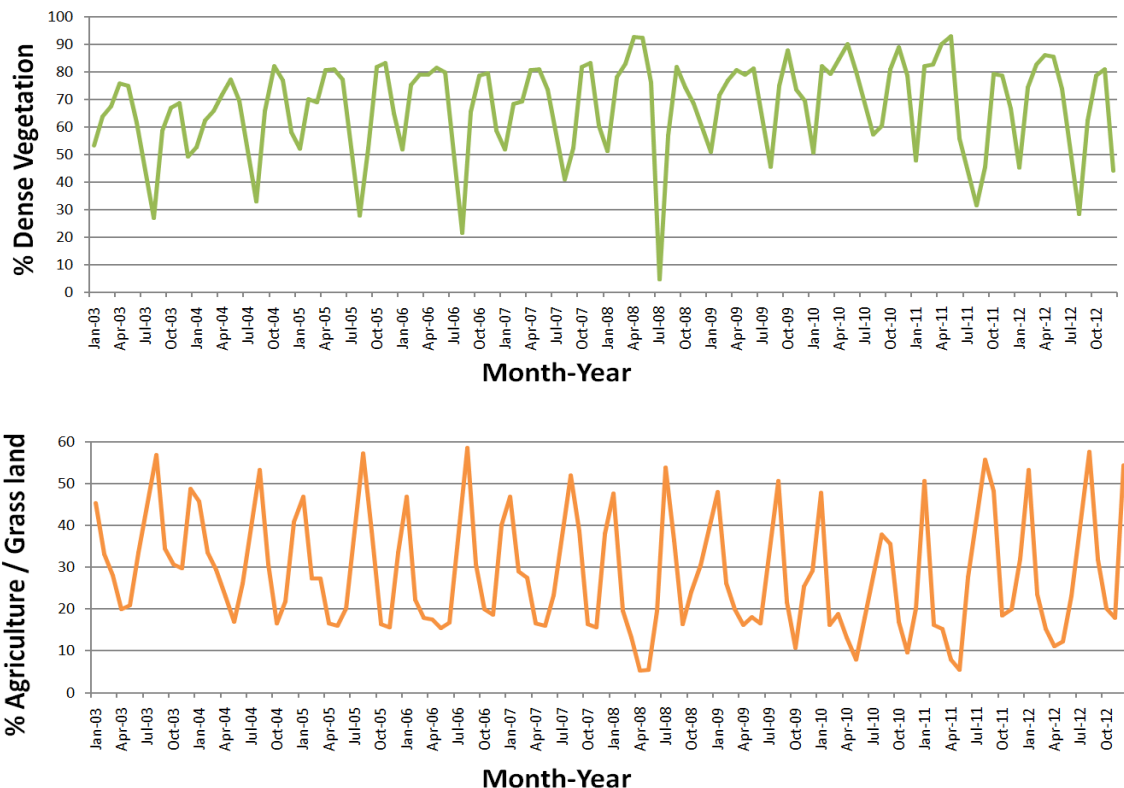


Figure 7: Percentage change (monthly) in dense vegetation and agriculture/grassland in central Western Ghats from 2003 to 2012.

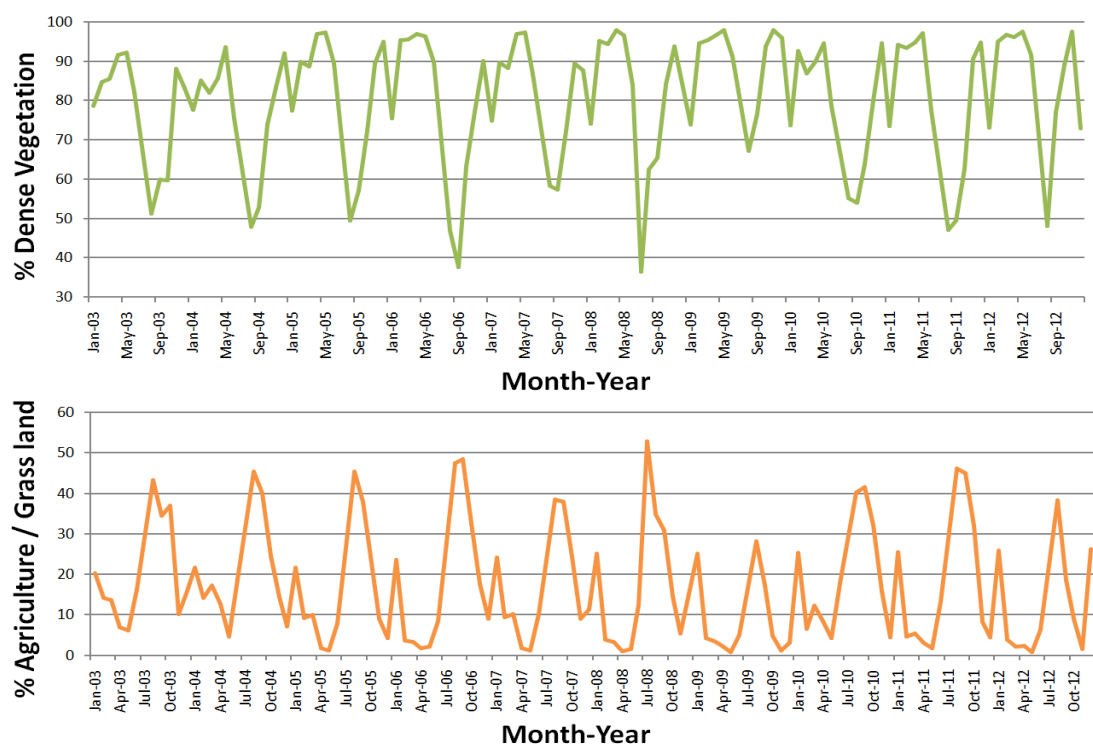


Figure 8: Percentage change (monthly) in dense vegetation and agriculture/grassland in southern Western Ghats from 2003 to 2012.

Figure 9–11 show changes in dense vegetation/forest (left figure) and agriculture/grassland (right figure) to other LC classes. The changes are represented by different colours for a year. For example, in figure 9, yellow in the legend shows areas that have been converted from dense vegetation to either agriculture or grassland or soil/settlement or water in 2003 (in the left figure). Whereas red pixels in the right figure shows areas that have been converted from either dense vegetation, or soil/settlement or other classes to agriculture/grassland in 2004. Similarly, figures 10 and 11 reflect the changes in central and southern Western Ghats. Table 4 shows area converted from dense vegetation to other three classes, and from other three classes to agriculture/grassland in the three regions of Western Ghats. It indicates the area (in ha) that have changed from dense vegetation class to other LC classes (agriculture, soil or water) from January, 2003 to December, 2003 and then for each subsequent year (2004 to 2012). It may be noted that the total area belonging to dense vegetation class is decreasing every year indicating "forest loss" although there might be pixels belonging to other three classes that would also have changed to dense vegetation class at other pixel locations but may be present in low numbers (counts) in the entire image. Minus sign indicates loss in overall forest area every year. The remaining part of the table shows annual conversion from other classes (dense vegetation, soil/settlement and water) to agriculture/grassland indicated by positive sign. It signifies that overall, agricultural area is increasing at the cost of other three LC classes.

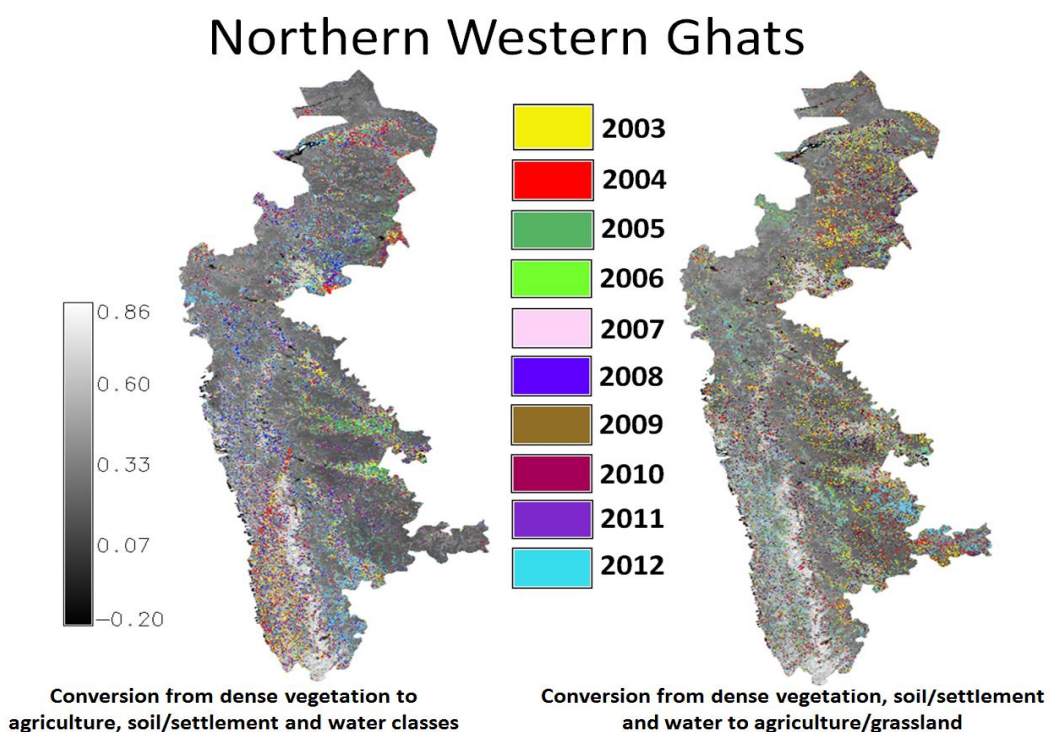


Figure 9: Annual change from one LC class to other LC classes in northern Western Ghats between 2003 to 2012 obtained from MODIS NDVI. The base image (background) is 250 m black and white version of MODIS NDVI of January, 2003. Colour palate in the middle represents changes in that year.

Central Western Ghats

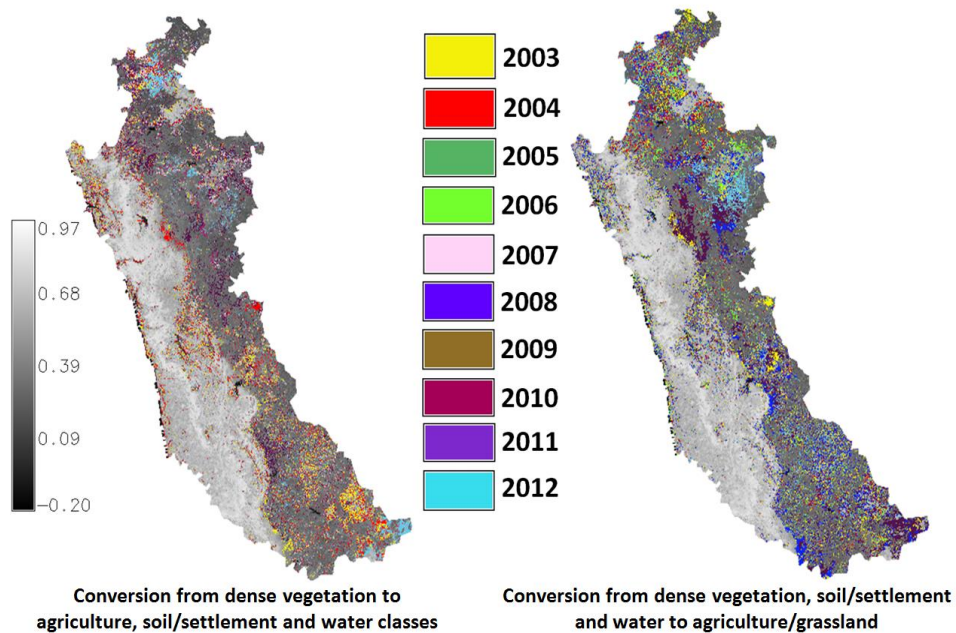


Figure 10: Annual change from one LC class to other LC classes in central Western Ghats between 2003 to 2012 obtained from MODIS NDVI. The base image (background) is 250 m black and white version of MODIS NDVI of January, 2003. Colour palate in the middle represents changes in that year.

Southern Western Ghats

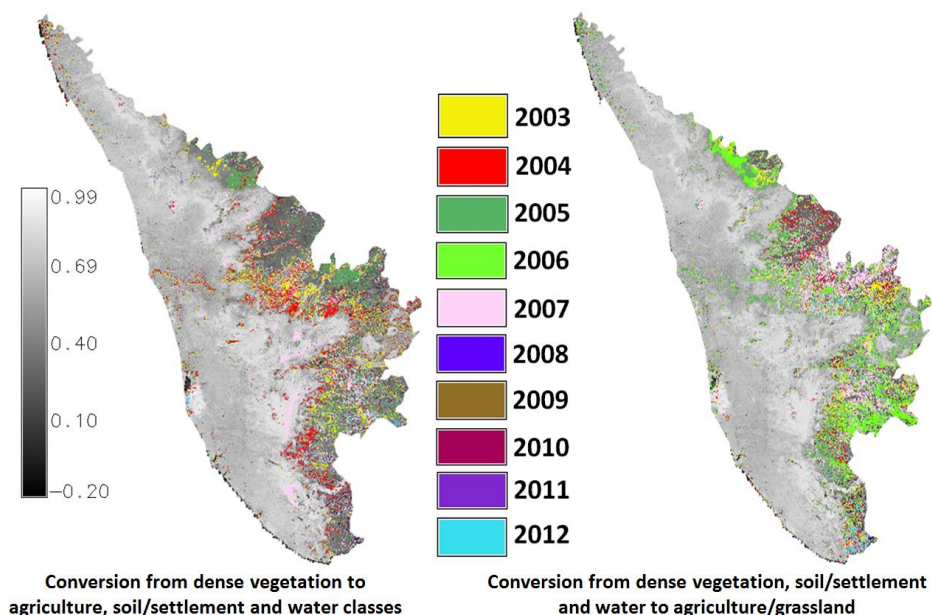


Figure 11: Annual change from one LC class to other LC classes in southern Western Ghats between 2003 to 2012 obtained from MODIS NDVI. The base image (background) is 250 m black and white version of MODIS NDVI of January, 2003. Colour palate in the middle represents changes in that year.

Table 4: Annual conversion from dense vegetation to other LC classes, and from other LC classes to agricultural/grassland in the three regions of Western Ghats.

Annual conversion from dense vegetation to other classes (agriculture/grassland, soil/settlement and water)			
From year – To year	Northern Western Ghats (area in ha)	Central Western Ghats (area in ha)	Southern Western Ghats (area in ha)
January, 2003 – January, 2004	-64360	-41809	-57641
January, 2004 – January, 2005	-42577	-49365	-84435
January, 2005 – January, 2006	-37625	-25203	-90733
January, 2006 – January, 2007	-18813	-16652	-42669
January, 2007 – January, 2008	-12971	-63663	-56892
January, 2008 – January, 2009	-17724	-24706	-23206
January, 2009 – January, 2010	-12675	-17103	-10480
January, 2010 – January, 2011	-14951	-28455	-23206
January, 2011 – January, 2012	-12970	-97007	-24703
January, 2012 – December, 2012	-46537	-52622	-17966
Annual conversion from other classes (dense vegetation, soil/settlement and water) to agriculture/grassland			
January, 2003 – January, 2004	+40597	+37058	+55395
January, 2004 – January, 2005	+48519	+34207	+42669
January, 2005 – January, 2006	+29705	+33257	+85338
January, 2006 – January, 2007	+13069	+36108	+89830
January, 2007 – January, 2008	+26932	+30406	+56144
January, 2008 – January, 2009	+27725	+48460	+26200
January, 2009 – January, 2010	+85155	+14253	+14972
January, 2010 – January, 2011	+26735	+34207	+14223
January, 2011 – January, 2012	+30696	+85518	+28446
January, 2012 – December, 2012	+26735	+57012	+24703

5.2 Time-series NDVI analysis of different LC classes

Figure 12–14 shows monthly boxplots for dense vegetation, agriculture/grassland, soil/settlement and water for the year 2003 and 2012 for northern, central and southern Western Ghats (X-axis: Month, Y-axis: NDVI values). In general, median of all the boxplots of dense vegetation class (figure 12 and 13 for 2003 and 2012) is different for northern and central Western Ghats. However, the locations of median are closer for a few consecutive months (for example, February–March, September–October) in southern Western Ghats and their trends (figure 14) for 2003 and 2012 are alike with overlapping inter-quartile range. For all the three regions of Western Ghats, median NDVI is low during March to June, which corresponds to the summer season and the leaves have either dried or fallen. In September–November, median NDVI is higher compared to other months; this is also evident from the graphs in figure 6, 7 and 8 showing percentage change in dense vegetation from 2003 to 2012 and from monthly minimum, maximum and mean NDVI values for dense vegetation for northern, central and southern Western Ghats in figure 15.

Agriculture shows a similar trend like dense vegetation; they have different medians for all the months, yet the median follows similar trend across the months in a year in northern and central Western Ghats (see figure 12 and 13). April–May–June have lowest median when the crops are being sown at the beginning of monsoon with smallest box and inter-quartile range and highest median in September to November which is the time before harvesting of crops (matured/grownup state). This observation is also supported by the change in LC statistics in figure 6 and 7.

Southern Western Ghats presents a slightly different picture with a dissimilar trend as that of other two regions, although they follow a similar yearly trend across months in 2003 and 2012 which are multimodal and non-sinusoidal (figure 15) with overlapping inter-quartile ranges (see figure 14). The peak season for agricultural crops is August to December and have lowest median in March–April–May. This may indicate early summer and early onset of monsoon in this region. LC change statistics in figure 8 further corroborates this trend.

Soil/settlements have minimum NDVI in May/June (summer) and have maximum NDVI (towards positive) in November–January. For southern Western Ghats, minimum NDVI for soil occurs in May and maximum occurs during August to December, earlier than northern and central regions. Water bodies exhibit least NDVI from April to June as they are either dry or have less water and have maximum NDVI in August (monsoon) with plenty of rain water in rivers/streams, water accumulated in lakes and sometimes covered with macrophytes.

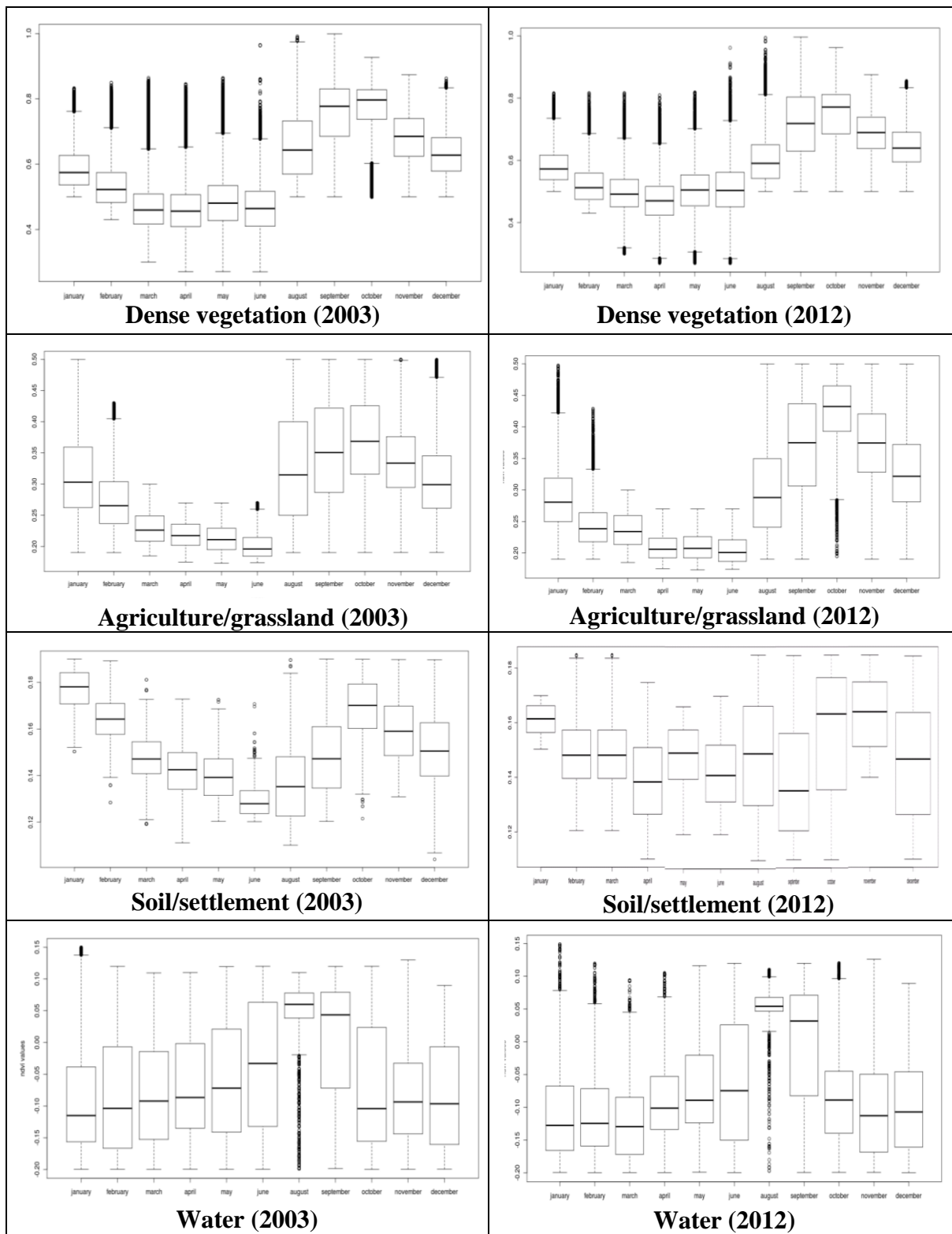


Figure 12: Boxplots for dense vegetation, agriculture/grassland, soil/settlement and water for the year 2003 and 2012 for northern Western Ghats (X-axis: Month, Y-axis: NDVI values).

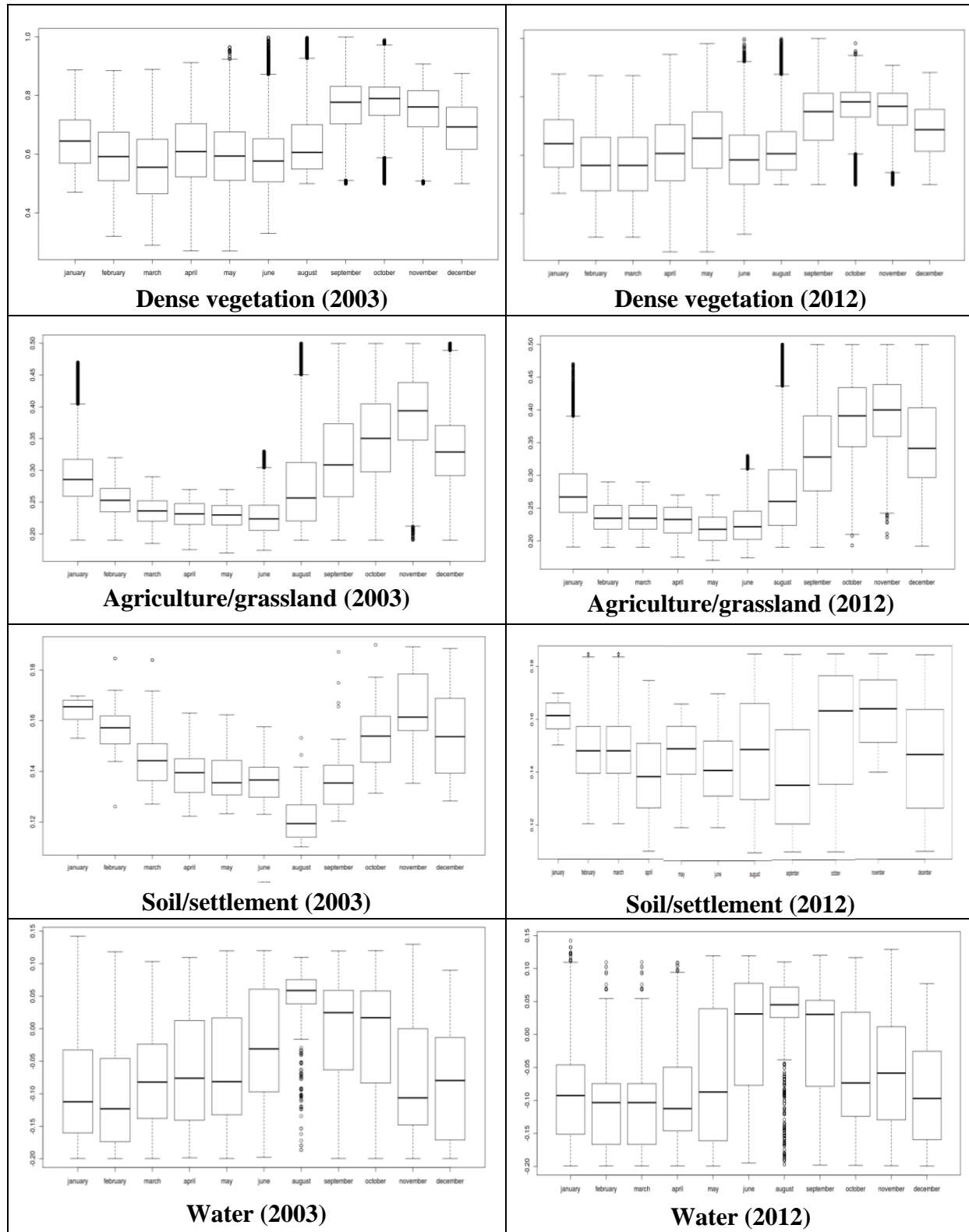


Figure 13: Boxplots for dense vegetation, agriculture/grassland, soil/settlement and water for the year 2003 and 2012 for central Western Ghats (X-axis: Month, Y-axis: NDVI values).

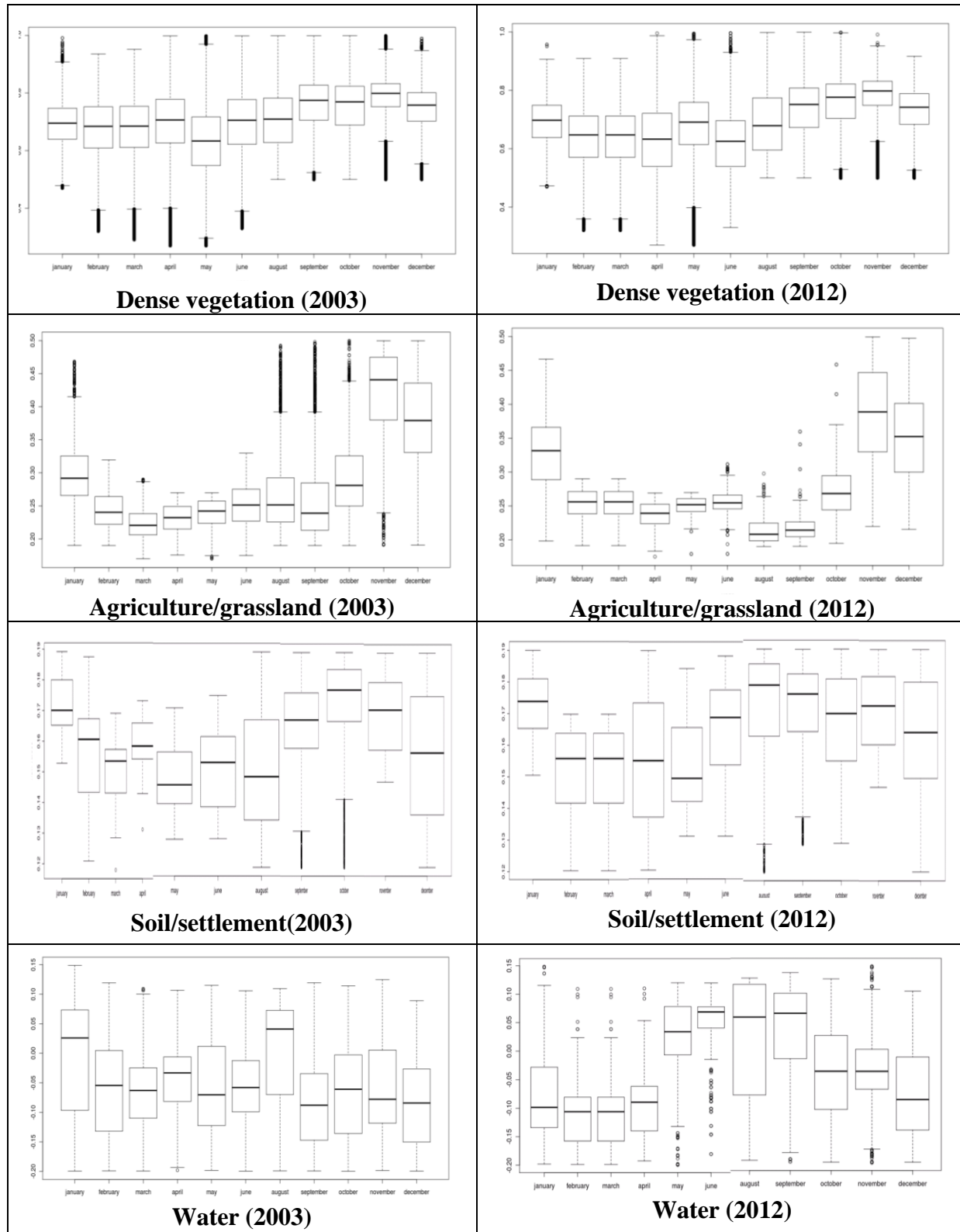


Figure 14: Boxplots for dense vegetation, agriculture/grassland, soil/settlement and water for the year 2003 and 2012 for southern Western Ghats (X-axis: Month, Y-axis: NDVI values).

Statistical analysis showed that the above boxplots are not exactly symmetrical about median, hence sample mean does not coincide with sample median. Therefore median does not necessarily represent the trend of LC classes for further analysis, so we explore the utility of minimum-mean-maximum time-series NDVI values of dense vegetation and subsequently study the different LC classes using mean NDVI.

Figure 15 depicts monthly minimum, mean and maximum NDVI time-series values for dense vegetation for the northern, central and southern Western Ghats (top, middle and bottom graphs) from 2003 to 2012. The trend line almost shows a sinusoidal wave pattern with peak NDVI values in August–February and valley in April–June in northern and central Western Ghats. Southern Western Ghats shows a slightly different pattern with maximum NDVI depicted by high peak (close to +1 NDVI values) most of the months in a year. It shows high mean NDVI between September–January and low NDVI values between March to June (in summer months) every year.

A comparison of NDVI values with the spatial extent graphs in figure 6–8 reveal that northern and central Western Ghats show maximum spatial extent under dense vegetation in September–November whereas peak NDVI is present from August to January. The peak NDVI may also be contributed from the agricultural crops which are in their growing stage in September and in matured stage in December. They are harvested in December/January, bringing down the spatial extent in January–February while the reflectance from dense green forest may still exhibit high NDVI values till February.

In southern Western Ghats, spatial extent of dense vegetation is maximum during October to June while the peak NDVI reflectance is from September to January. This indicates that forest and agricultural crops (that also include coconut, rubber, coffee plantation, etc.) mature during September to January exhibiting high mean NDVI, while the geographical extent of combined forest and agricultural crops remain high through October to June. One reason for this could be that, the contribution from vegetation and agricultural crops to high reflectance in NIR band could be least after harvesting (in February), thereby decreasing the overall mean NDVI. On the other hand, agriculture crops have a low geographical extent among green vegetation and the southern Western Ghats is mostly dominated by dense mixed vegetation. So, even though the mean NDVI forms a valley after harvesting (in February), the overall dense vegetation continue to show higher spatial extent till June across years. This phenomenon is observed as a repeated cycle every year during the course of this study. It also indicates that during the growth stage of the plants in September to January, it is difficult to separate the dense agricultural crops from dense vegetation by means of NDVI and high spectral resolution sensors with higher number of spectral bands such as Hyper-spectral data may be required for further classification of different vegetation types. From the above discussion and also reported by Lunetta et al., (2006), we see that minimum and maximum NDVI values mainly aid in separation of LC classes. Therefore mean NDVI values of different LC classes (Aguilar et al., 2012; Mao et al., 2012; Raynolds et al., 2008) are explored further in analyzing the behaviour of different LC classes.

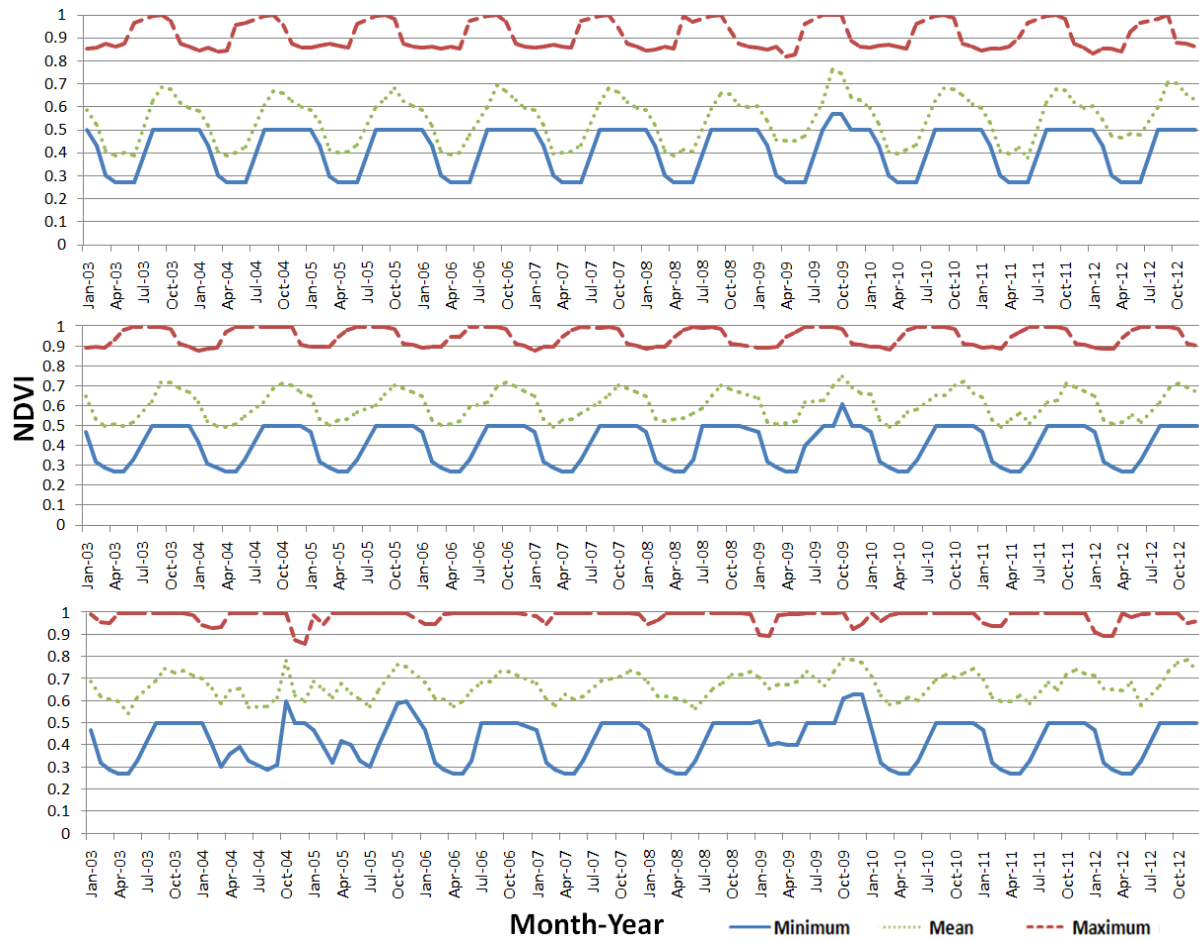


Figure 15: Monthly minimum, mean and maximum NDVI values for dense vegetation for the northern, central and southern Western Ghats (top, middle and bottom graphs in the figure).

Figure 16 shows temporal mean NDVI profiles for the major end members (dense vegetation, agriculture/grassland, soil/settlement and water bodies) corresponding to the 3 (northern, central and southern) climatic regions of Western Ghats.

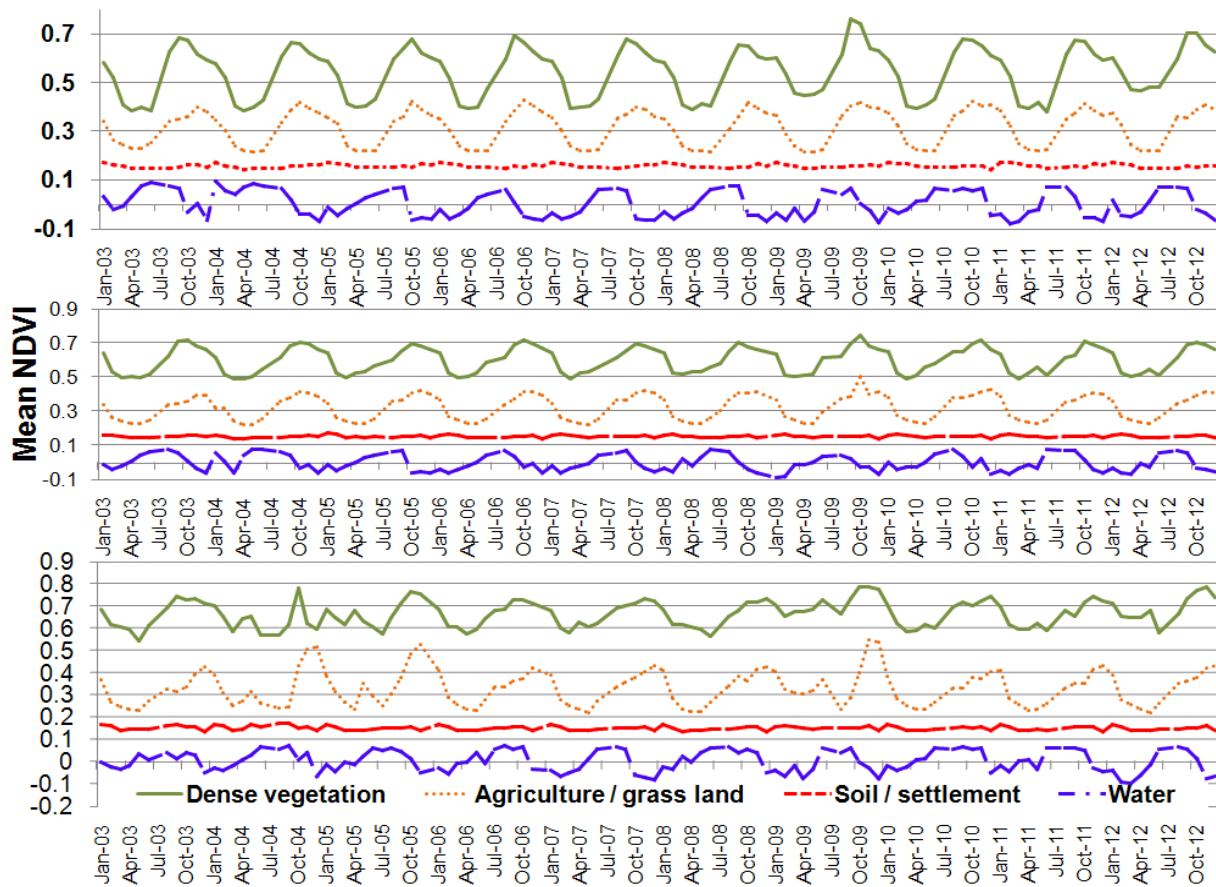


Figure 16: Temporal mean NDVI profiles for the major end members corresponding to the 3 (northern, central and southern) climatic regions of Western Ghats (Note: X-axis: Mean NDVI values, Y-axis: Month-Year).

Figure 16 indicates that mean NDVI of dense vegetation and agriculture follow similar patterns in northern and central Western Ghats with peak in monsoon (September–October–November) and valleys in summer (April–May) respectively. Bare soil/settlement have almost constant mean NDVI and have low NDVI values close to 0. Southern Western Ghats shows similar trend like northern and central Western Ghats, however the peaks and valleys are not uniform for dense forest/vegetation and tend to rise during October each year (see figure 16). NDVI values for water tend to increase whenever there is a peak in vegetation across the months and year (in monsoon season) in all the three regions of Western Ghats.

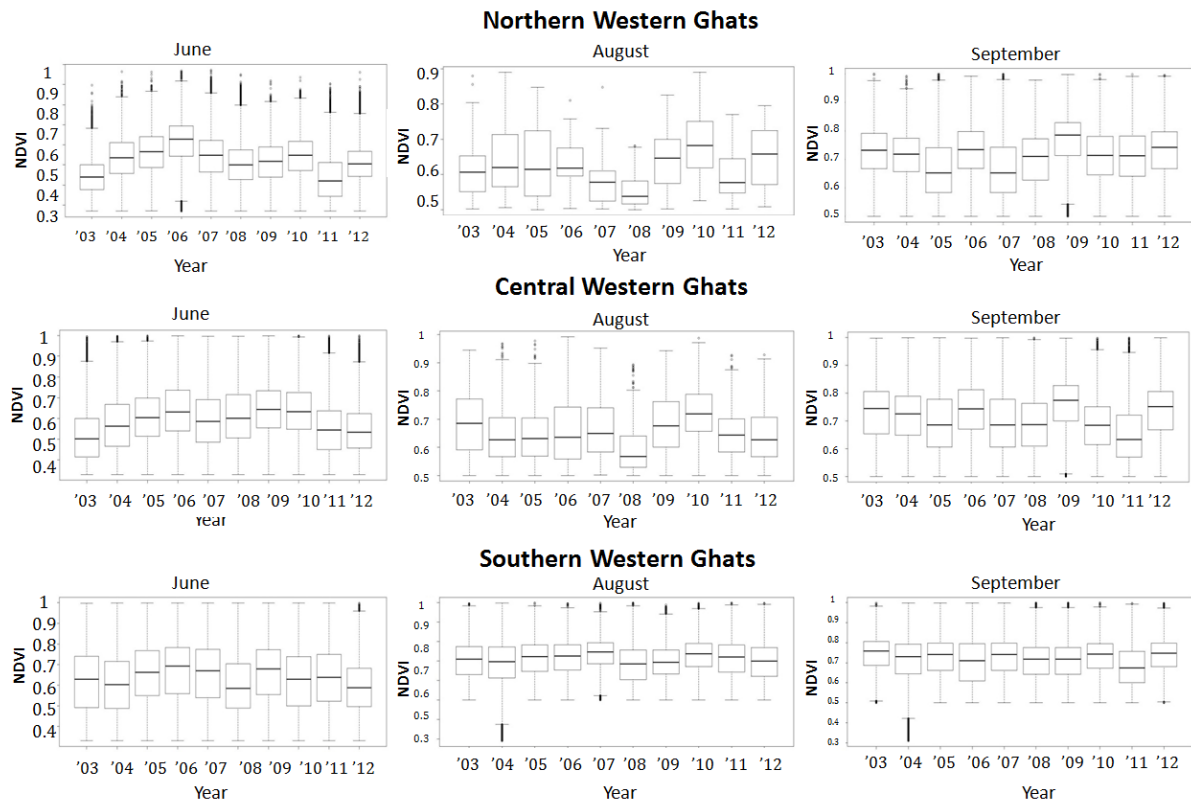


Figure 17: Boxplot of monthly NDVI changes of dense forest for monsoon season (June, August and September) in Western Ghats from 2003 to 2012.

Figure 17 is the boxplot of NDVI changes for forest class in June, August and September (monsoon season) for northern, central and southern Western Ghats from 2003 to 2012. It is shown that the median of the boxplot follow a somewhat sinusoidal pattern in each month in northern and central Western Ghats from 2003 to 2012. For southern Western Ghats, the pattern in the median has less deviation across the years. The noticeable points here are:

- i.) In northern Western Ghats, 2005, 2006, and 2010 shows higher median values (ranging approximately from 0.5 to 0.7) compared to 2003 and 2011 that have the lesser NDVI inter-quartile range for June (median is ~0.5).
- ii.) For central Western Ghats, 2003–4 and 2011–12 show lesser median in the month of June than in the middle years.
- iii.) In central Western Ghats, 2008 has least median (~0.5–0.55) for August for both northern and central Western Ghats indicating lesser vegetation; the reason for this may be attributed to the climatic and physical factors. The median in September is generally higher in the year 2006, 2009 and 2012 than other two months (June and August) in both the regions showing more greenery than other years.
- iv.) Particularly, southern Western Ghats shows higher NDVI values for all three months for all the years (2003 to 2012) compared to northern and central Western Ghats indicating more greenery and this trend is static. For all the other months (except monsoon season), the records show static patterns.

Figure 18 shows summary trend maps of NDVI changes in northern, central and southern Western Ghats from 2003 to 2012 calculated from monthly NDVI time-series. It is to be noted that the NDVI differencing values can range from +2 to -2 for the difference image. For example, Map1 and Map 2 can have NDVI value range from +1 to -1. Extreme changes in NDVI can result from pixels subtracting -1 from +1 (i.e. +1 - (-1)) which is +2 where the actual change is negative and decreasing value from +1 to -1, so should be shown as -2. The difference pixel can also result from subtracting +1 from -1 (i.e. -1 - (1)) which is -2 where the actual change is positive and increasing from -1 to +1, so should be shown as +2. Therefore, the difference values are multiplied by -1 to show the actual magnitude and direction of the change in differences.

Figure 18 indicates different pattern for northern, central and southern regions. Major changes from 2003 to 2012 have taken place in the 0.0 to 0.1 (grey) and 0 to -0.3 (pink) followed by 0.1 to 0.2 (green) in northern Western Ghats. In central and southern regions, major changes have taken between 0 to -0.3 (pink) followed by 0 to 0.1 (grey) with a marginal change between 0.1 to 0.2 (green). Table 5 shows the LC change statistics in Western Ghats based on NDVI differencing. NDVI difference ranges with large change are highlighted in shaded rows corresponding to graphs in figure 18.

Table 5: LC change statistics of Western Ghats from 2003 to 2012 based on NDVI differencing

Northern Western Ghats			Central Western Ghats			Southern Western Ghats		
NDVI differencing range	Area		NDVI differencing range	Area		NDVI differencing range	Area	
	ha	%		ha	%		ha	%
-0.76 - -0.3	14740	0.16	-0.80 - -0.3	15249	0.17	-1.8 - -0.3	16545	0.24
-0.3-0.0	2272093	25.1	-0.3-0.0	6804193	77.1	-0.3-0.0	4426429	64.31
0.0-0.10	5671090	62.64	0.0-0.10	1864756	21.13	0.0-0.10	2206011	32.05
0.10-0.20	1038850	11.47	0.10-0.20	119077	1.35	0.10-0.20	188560	2.74
0.20-0.40	55858	0.62	0.20-0.40	19707	0.22	0.20-0.40	37274	0.54
0.40-0.84	1180	0.01	0.40-0.80	1994	0.02	0.40-1	8273	0.12
Total	9053811	100		8824976	100		6883092	100

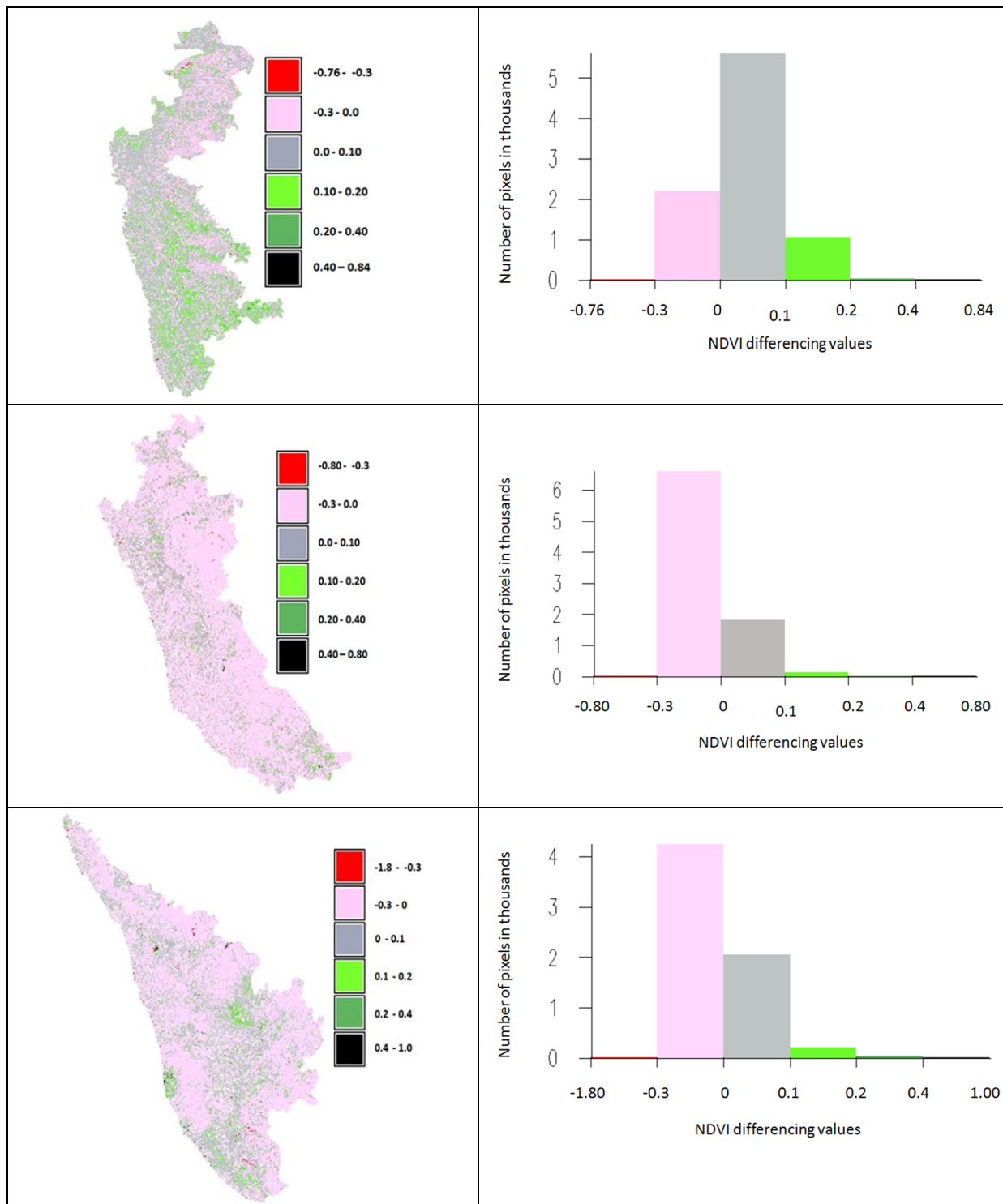
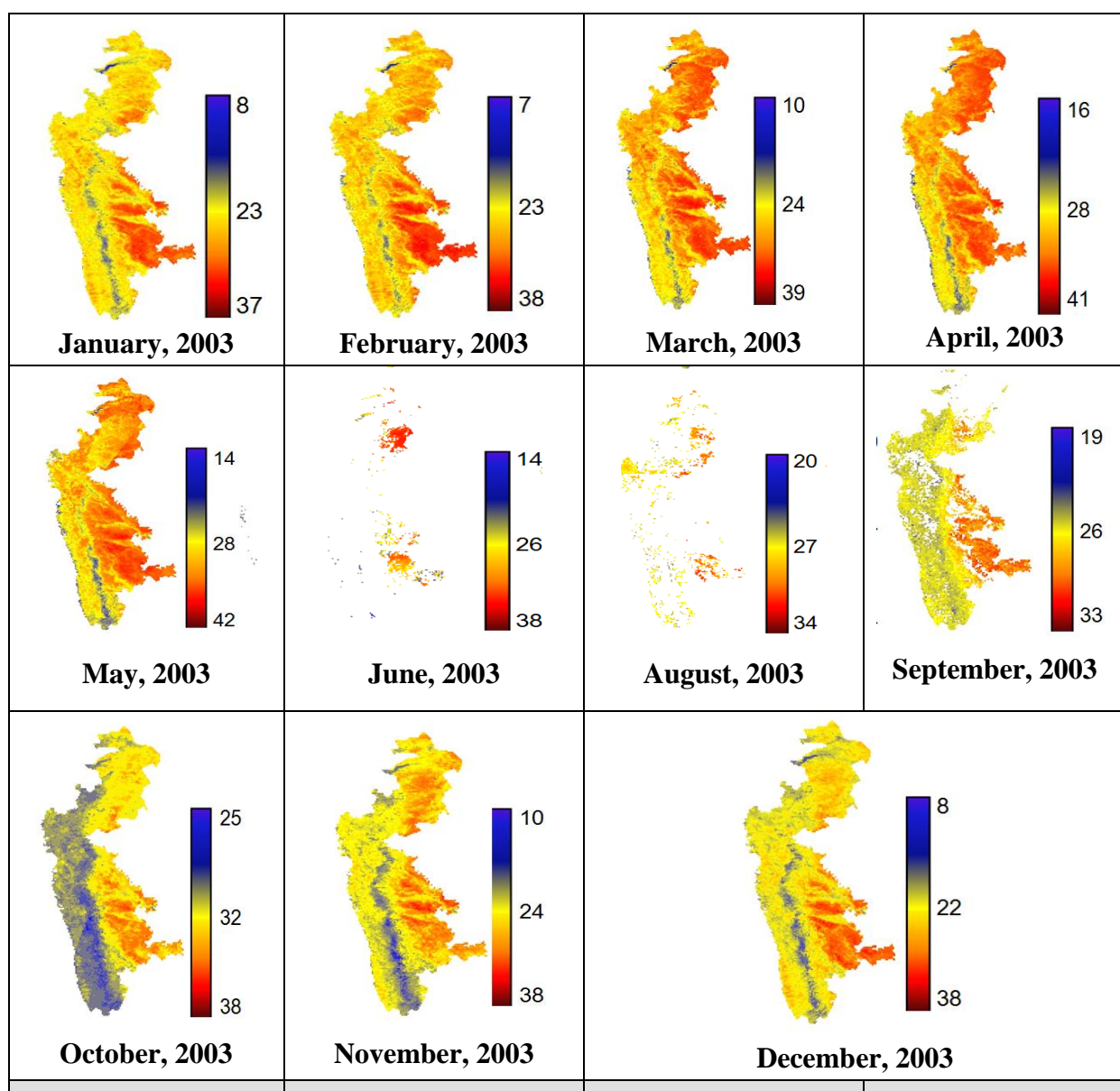


Figure 18: Summary trend maps of NDVI changes in Western Ghats from 2003 to 2012 calculated from monthly (January and December) NDVI time-series.

5.3 Decadal climatic parameters influencing NDVI: temperature variation and rainfall pattern analysis in Western Ghats from 2003 to 2012

Many research results show that changes in vegetation are seriously influenced by temperature and precipitation. For example, Li et al. (2002) observed that a significant correlation exist between NDVI and eco-climatic parameters, and that NDVI growing degree days correlation was stronger than NDVI–rainfall correlation. These studies presented reasonable and reliable conclusions regarding NDVI changes and the relationship between vegetation NDVI and climatic parameters.

Figure 19–21 shows sample temperature maps (in °C) computed for northern, central and southern Western Ghats from January to December 2003 and 2012. Figure 22 shows minimum, mean and maximum temperature of the three regions.



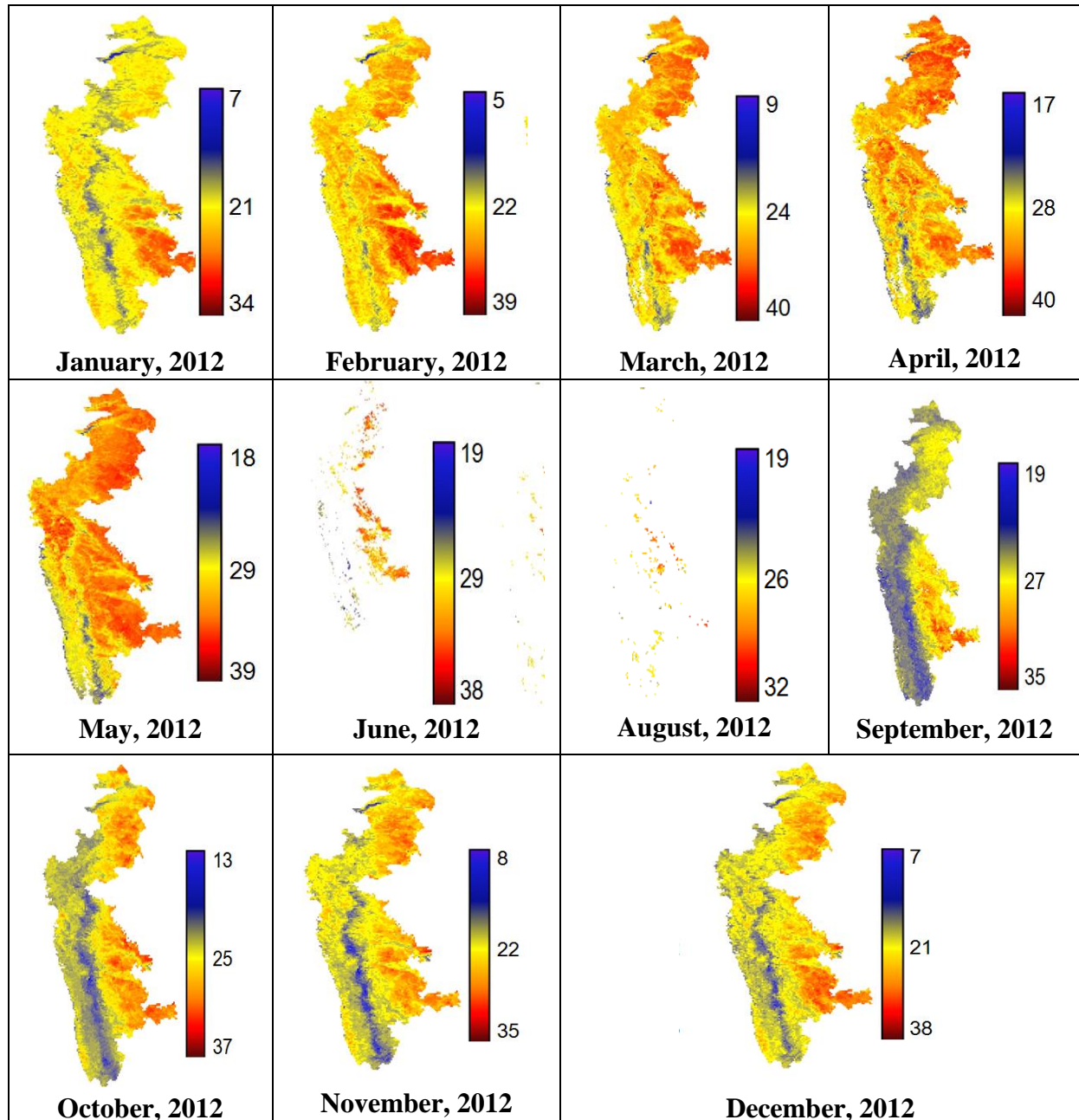
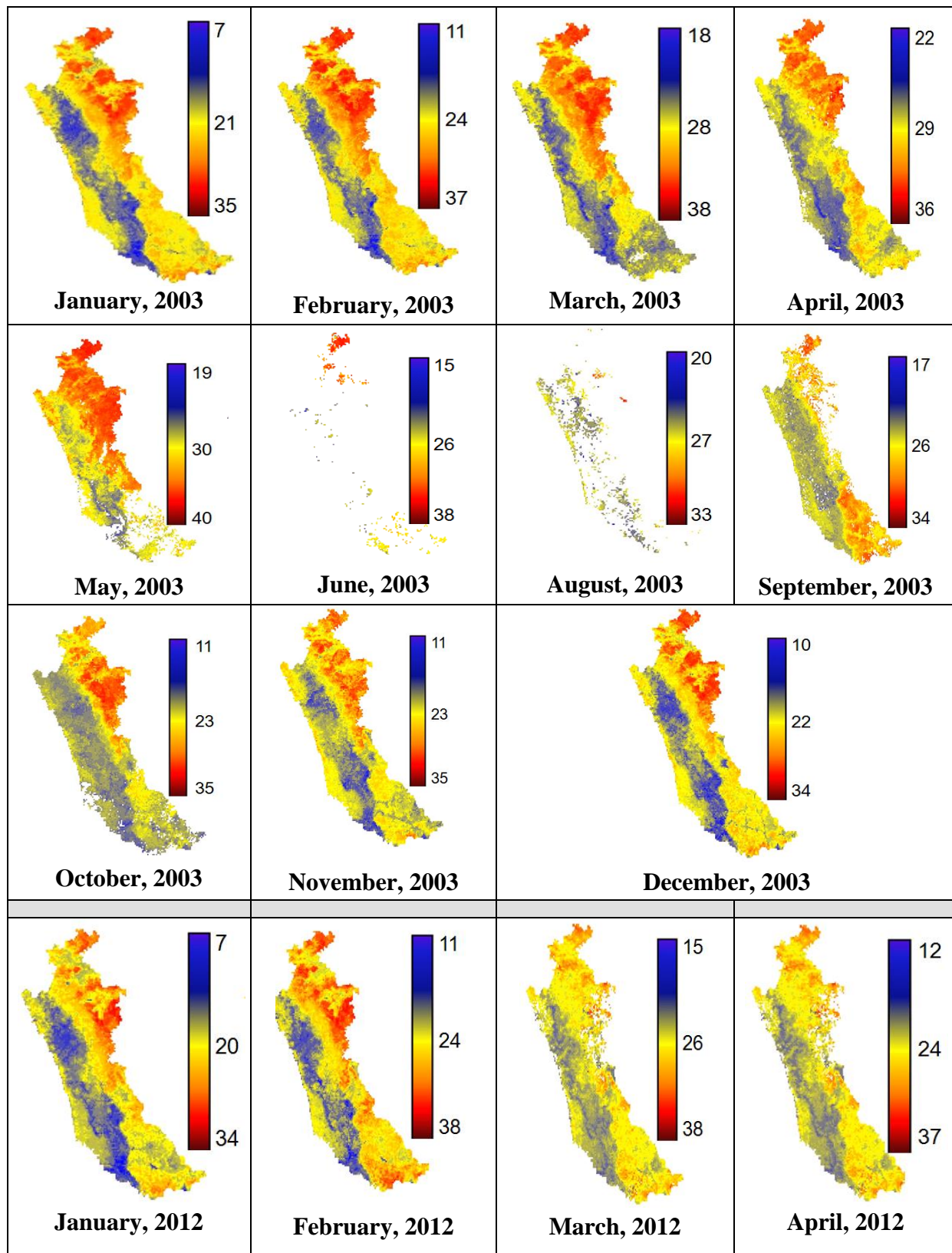


Figure 19: Sample monthly temperature maps (in °C) for 2003 and 2012 for northern Western Ghats. Images of June and August had lot of pixels with cloud cover, so these images have many no data values (white in colour). (Note: July temperature map was not computed due to presence of cloud in the data.)



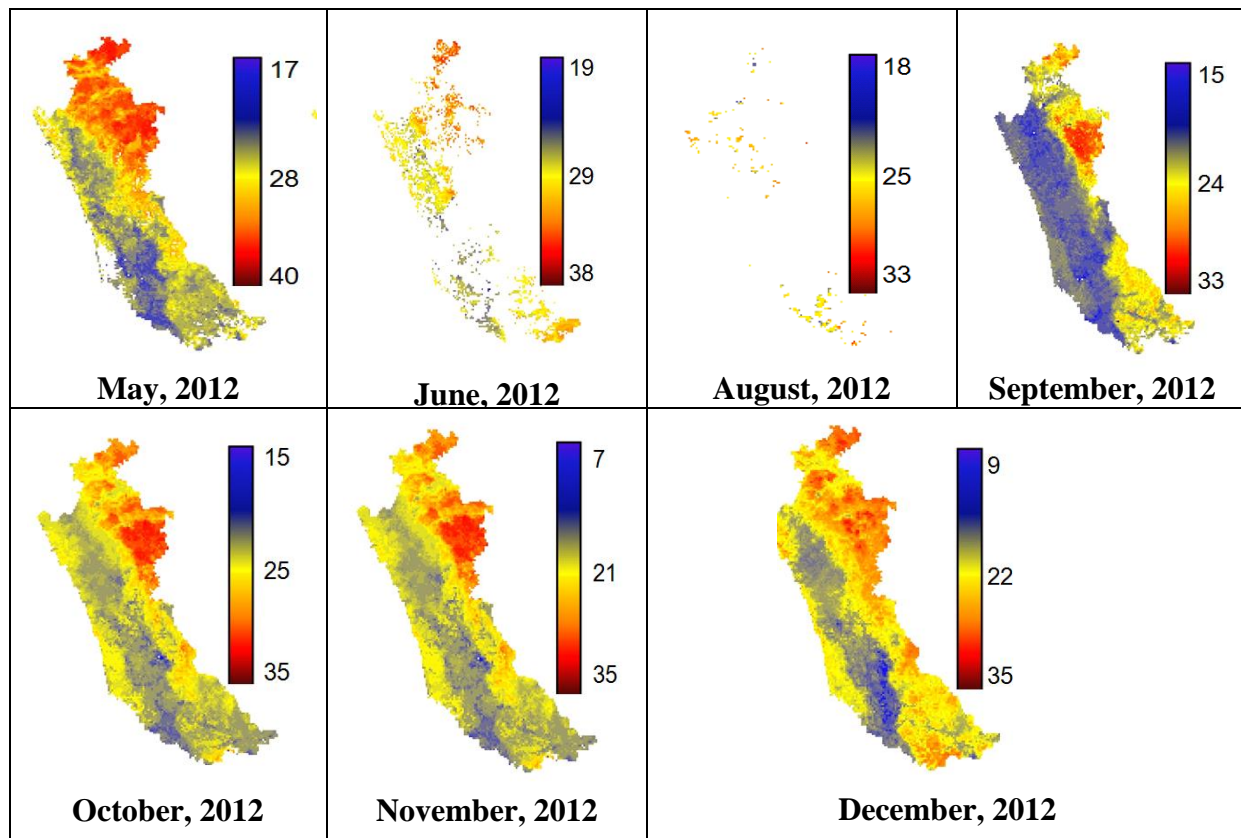
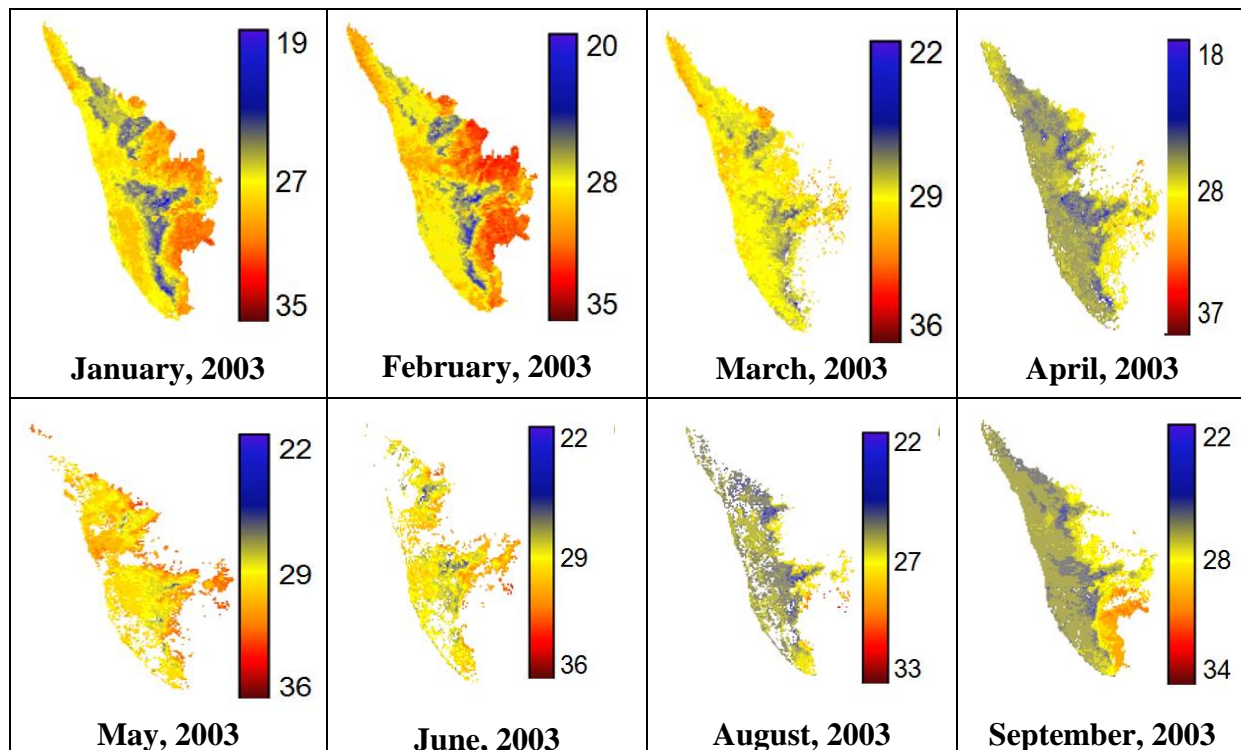


Figure 20: Monthly temperature maps (in °C) for 2003 and 2012 for central Western Ghats. Images of June and August had lot of pixels with cloud cover, so these images have many no data values (white in colour). (Note: July temperature map was not computed due to presence of cloud in the data.)



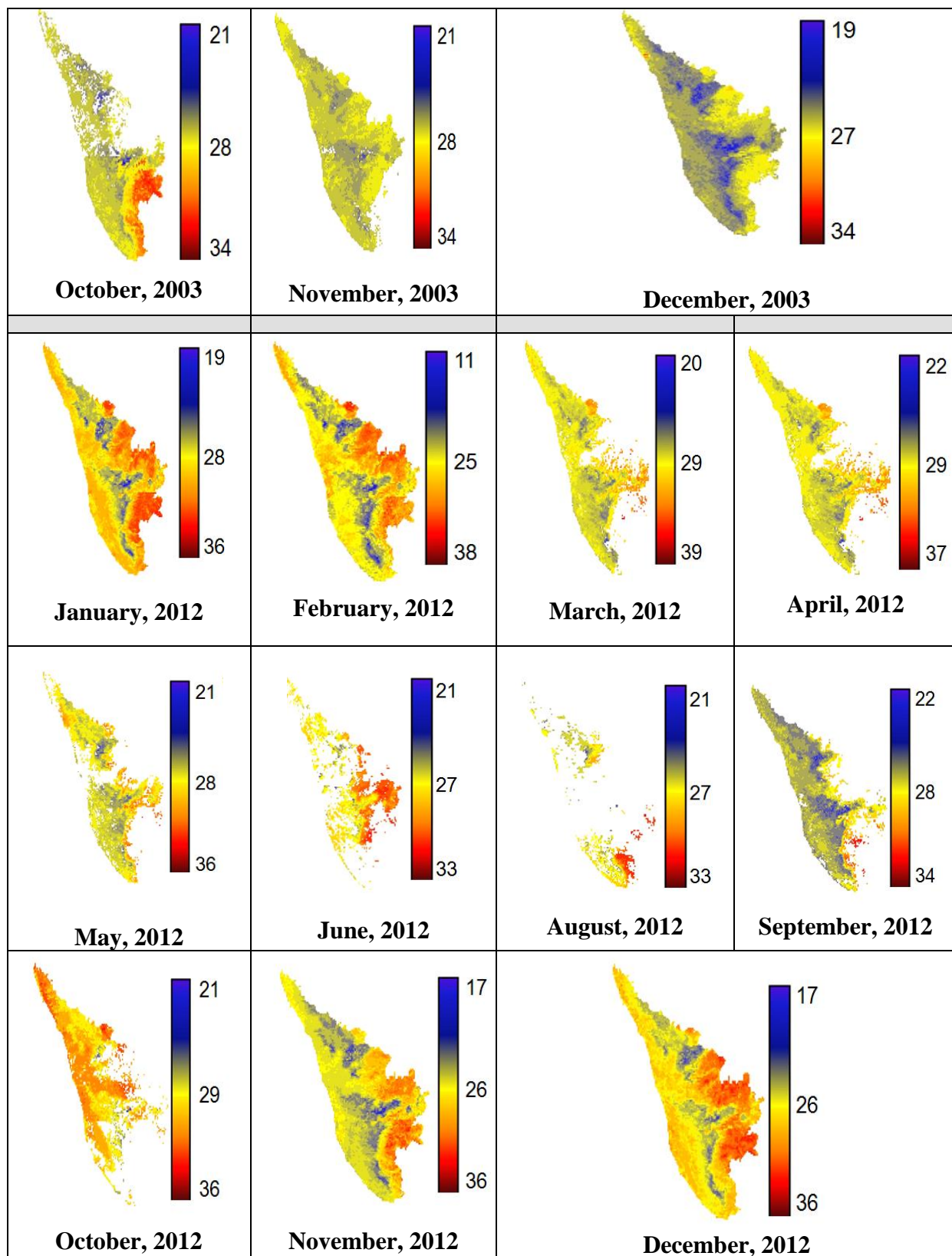


Figure 21: Monthly temperature maps (in °C) for 2003 and 2012 for southern Western Ghats. Images of June and August had lot of pixels with cloud cover, so these images have many no data values (white in colour). (Note: July temperature map was not computed due to presence of cloud in the data.)

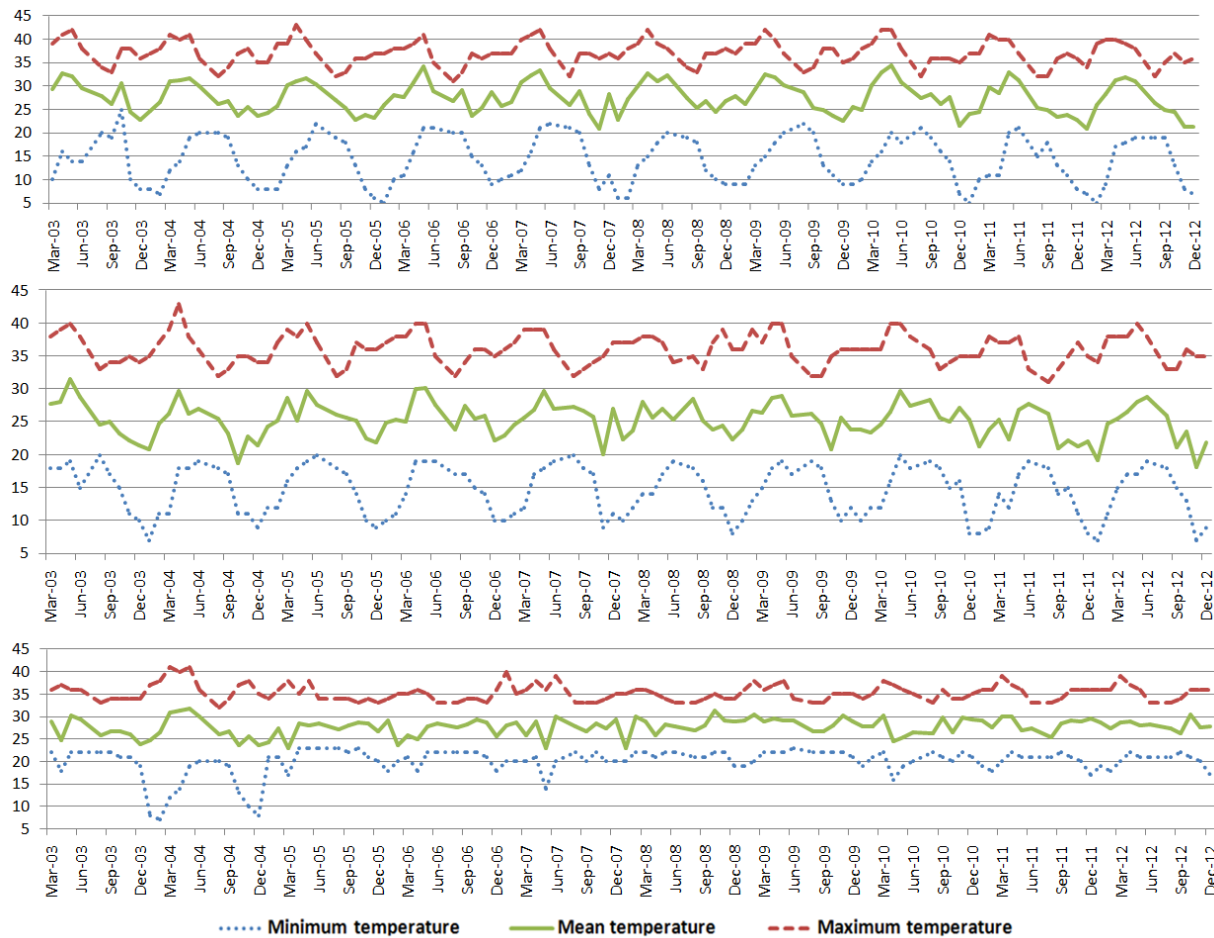


Figure 22: Monthly minimum, mean and maximum temperature (in $^{\circ}\text{C}$) of the three regions (top - northern, middle - central and bottom - southern Western Ghats). [X-axis: Month-Year, Y-axis: temperature (in $^{\circ}\text{C}$)].

Figure 22 shows that minimum, mean and maximum temperature, which almost follow a wave like pattern with peak summer temperature (14–42 $^{\circ}\text{C}$) in April–May–June every year and lowest winter temperature (7–38 $^{\circ}\text{C}$) in December–January (shown in blue dotted line) in northern and central Western Ghats. Southern Western Ghats shows a slightly different pattern with maximum variance in temperature in December–January months and highest temperature in summer (March–April–May) each year. There is not much variability between summer (11–39 $^{\circ}\text{C}$) and winter temperatures ranges (8–35 $^{\circ}\text{C}$). Figure 23 shows mean monthly temperature \pm standard deviation graph further highlighting the temperature variation trend.

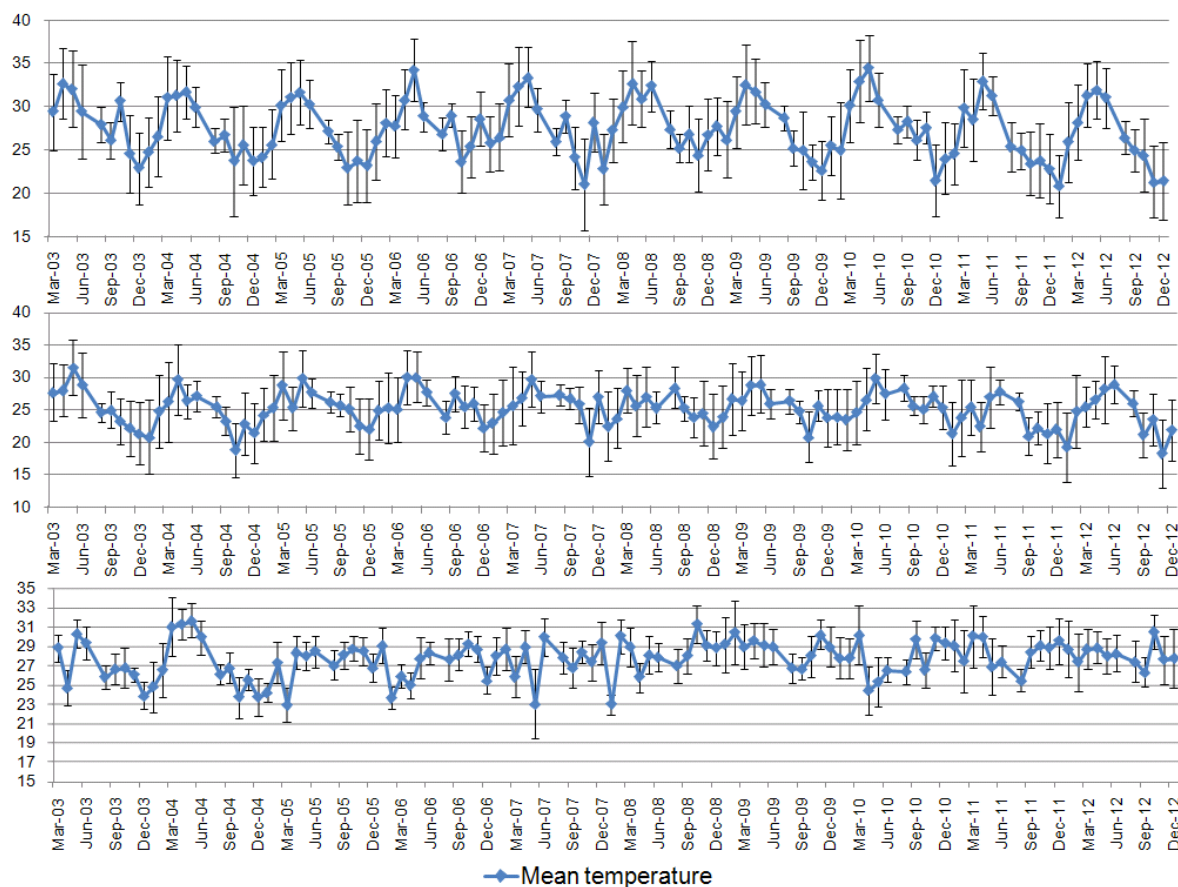
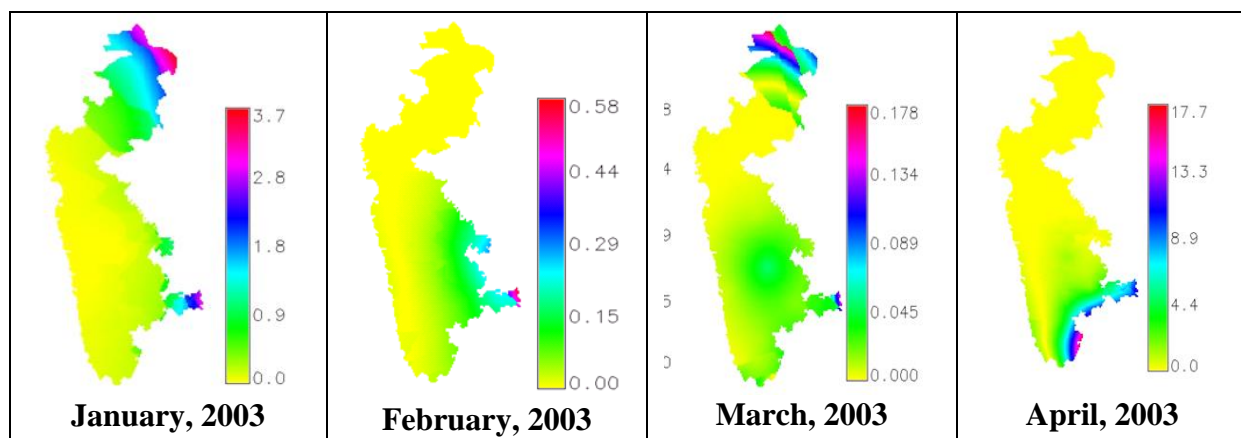
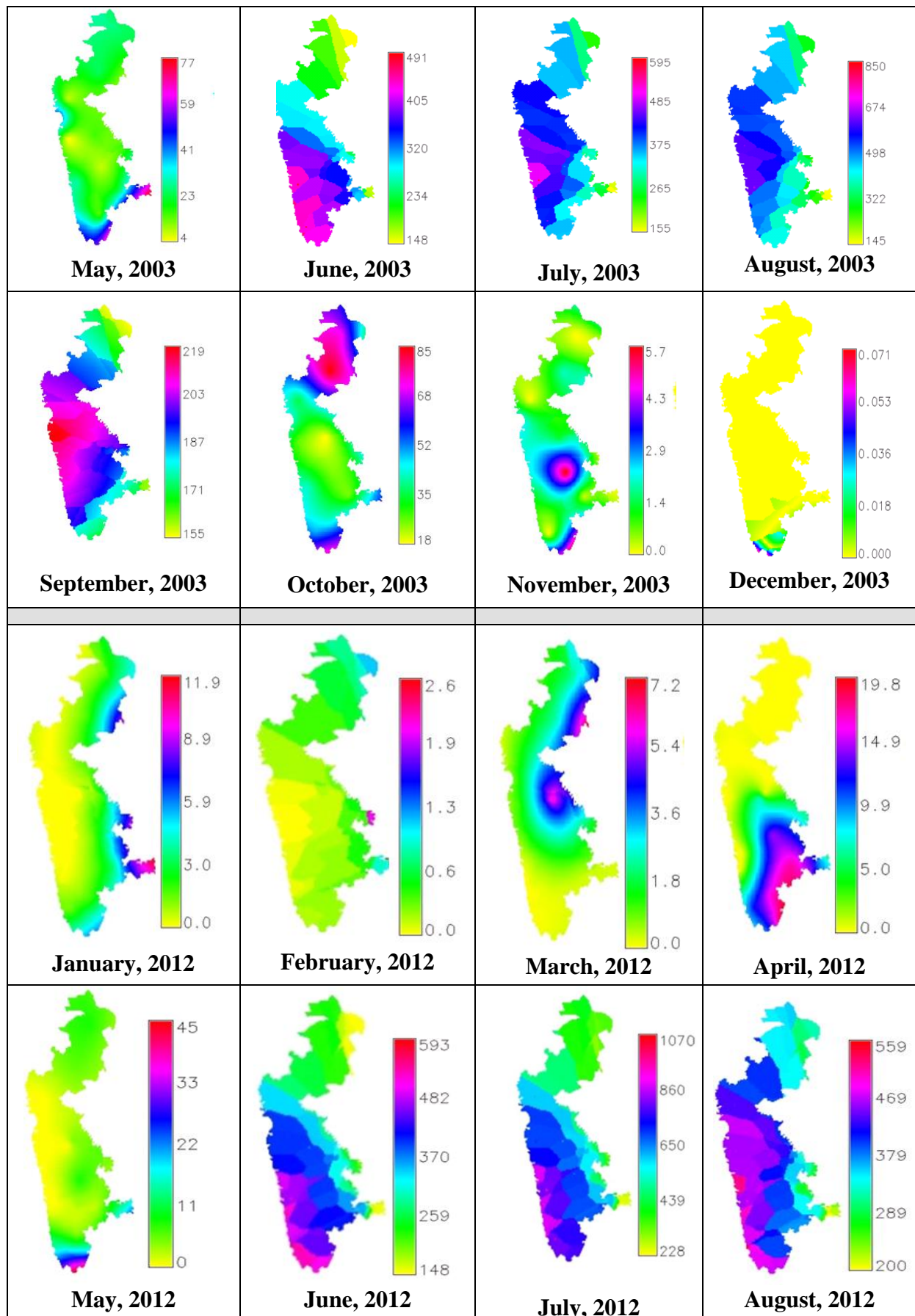


Figure 23: Mean monthly temperature \pm standard deviation (in $^{\circ}\text{C}$) for northern, central and southern Western Ghats (top - northern, middle - central and bottom - southern Western Ghats) X-axis: Month-Year, Y-axis: temperature (in $^{\circ}\text{C}$)

Figure 24–26 shows sample rainfall maps (in mm) for northern, central and southern Western Ghats from January to December 2003 and 2012.





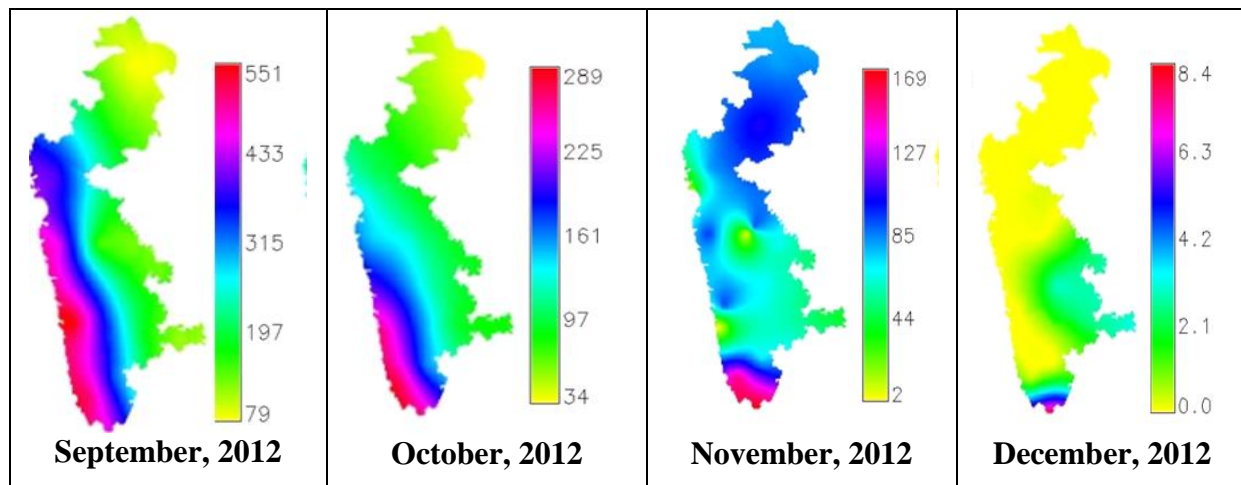
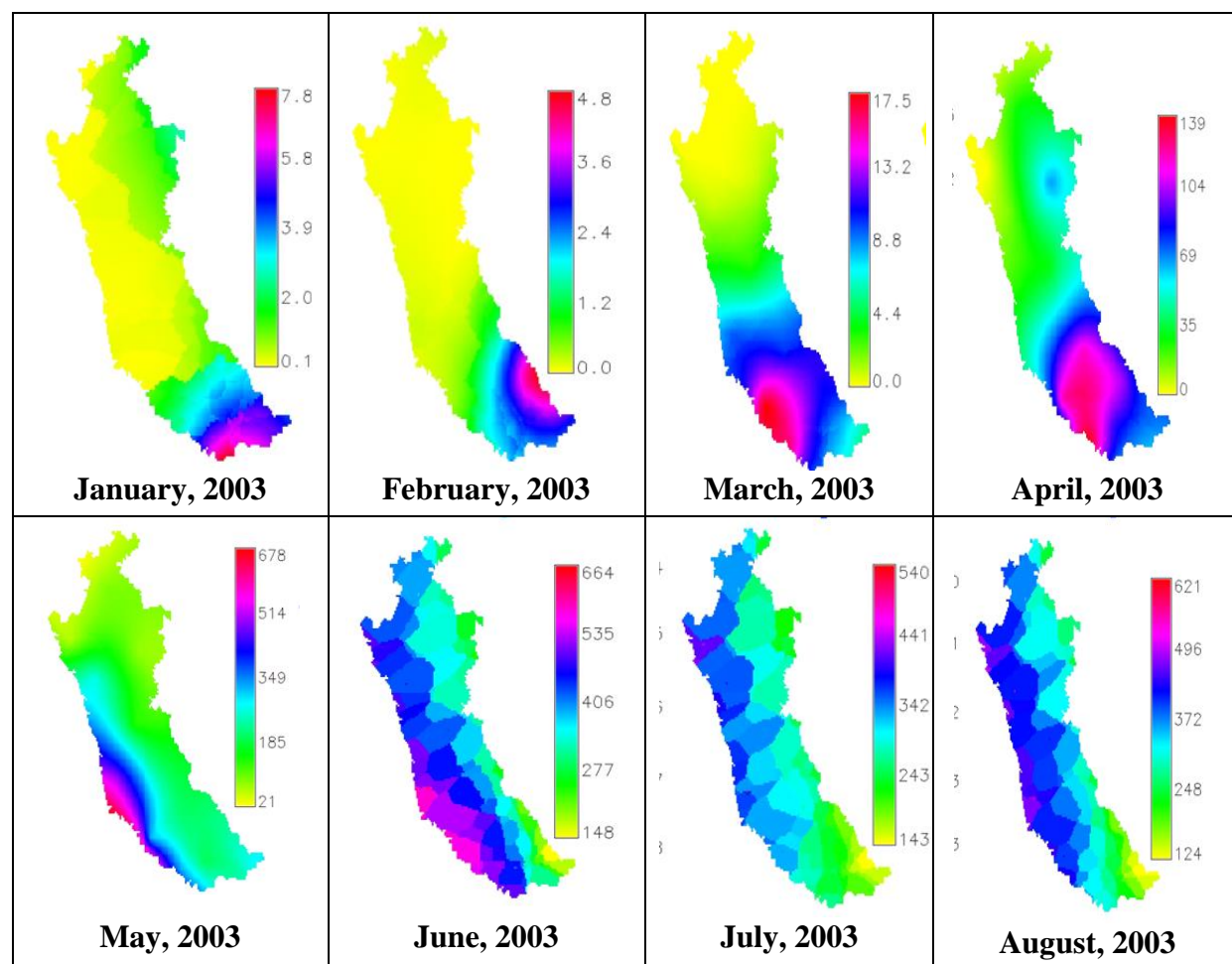


Figure 24: Monthly rainfall maps (in mm) for 2003 and 2012 for northern Western Ghats.



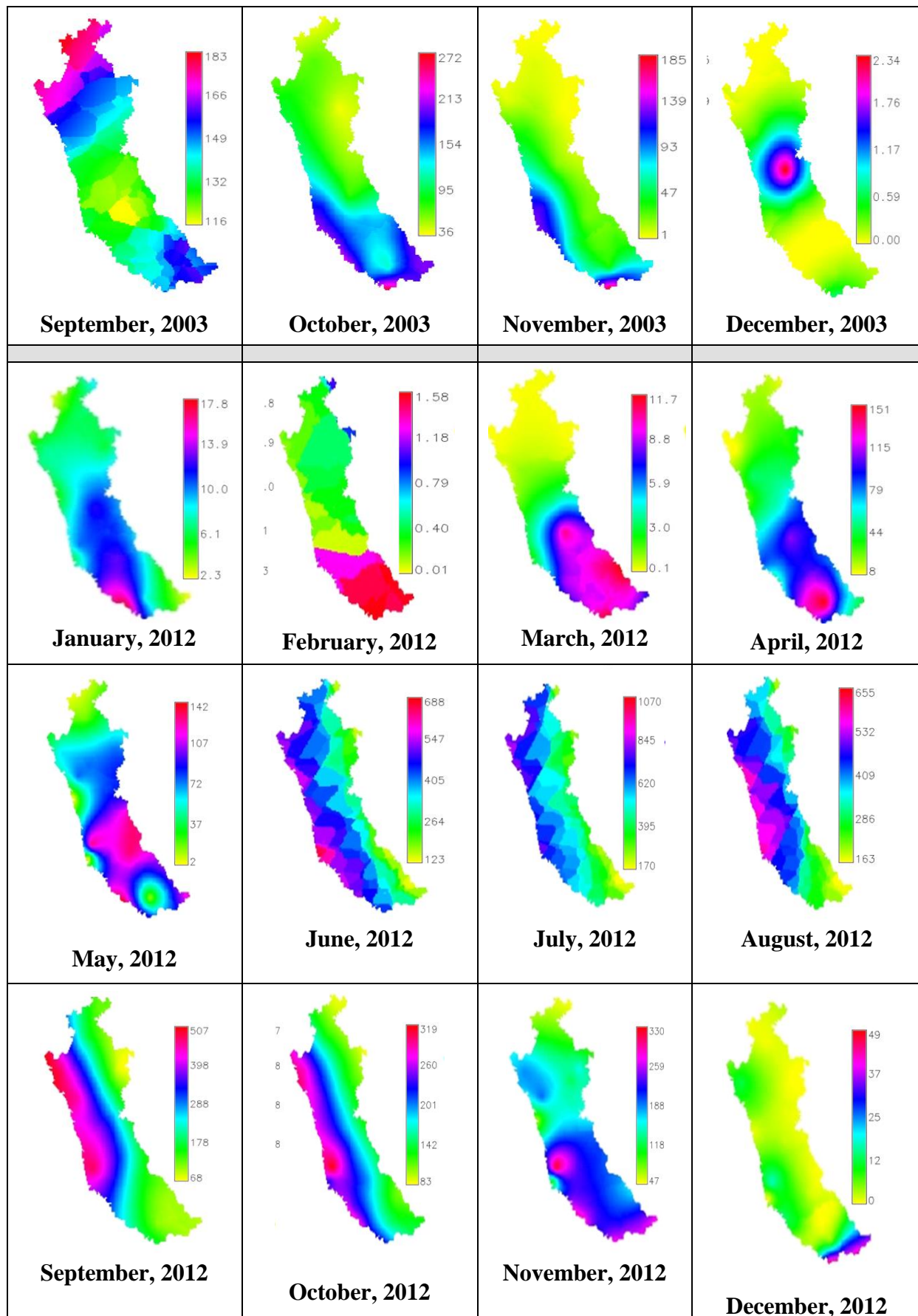
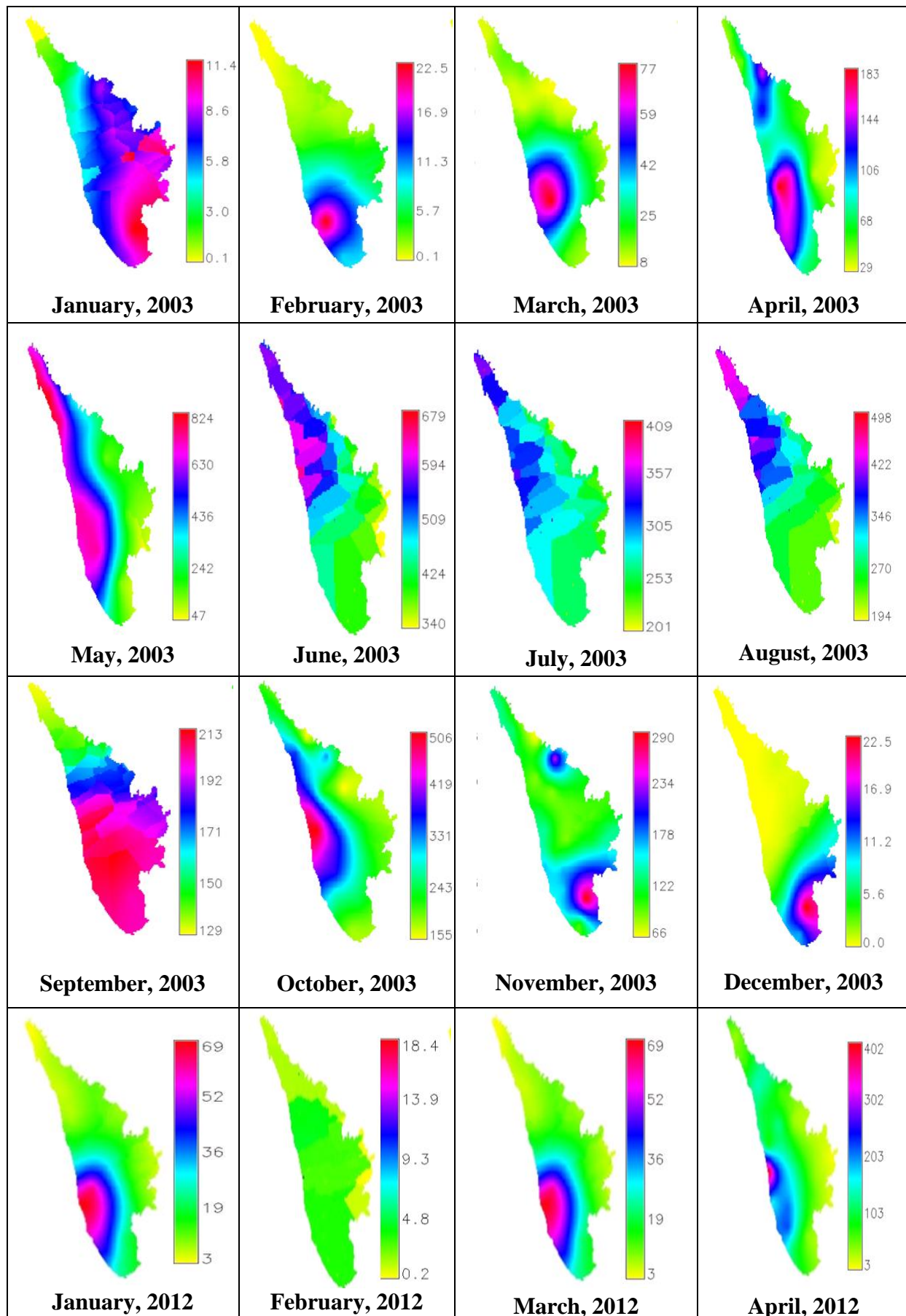


Figure 25: Monthly rainfall maps (in mm) for 2003 and 2012 for central Western Ghats.



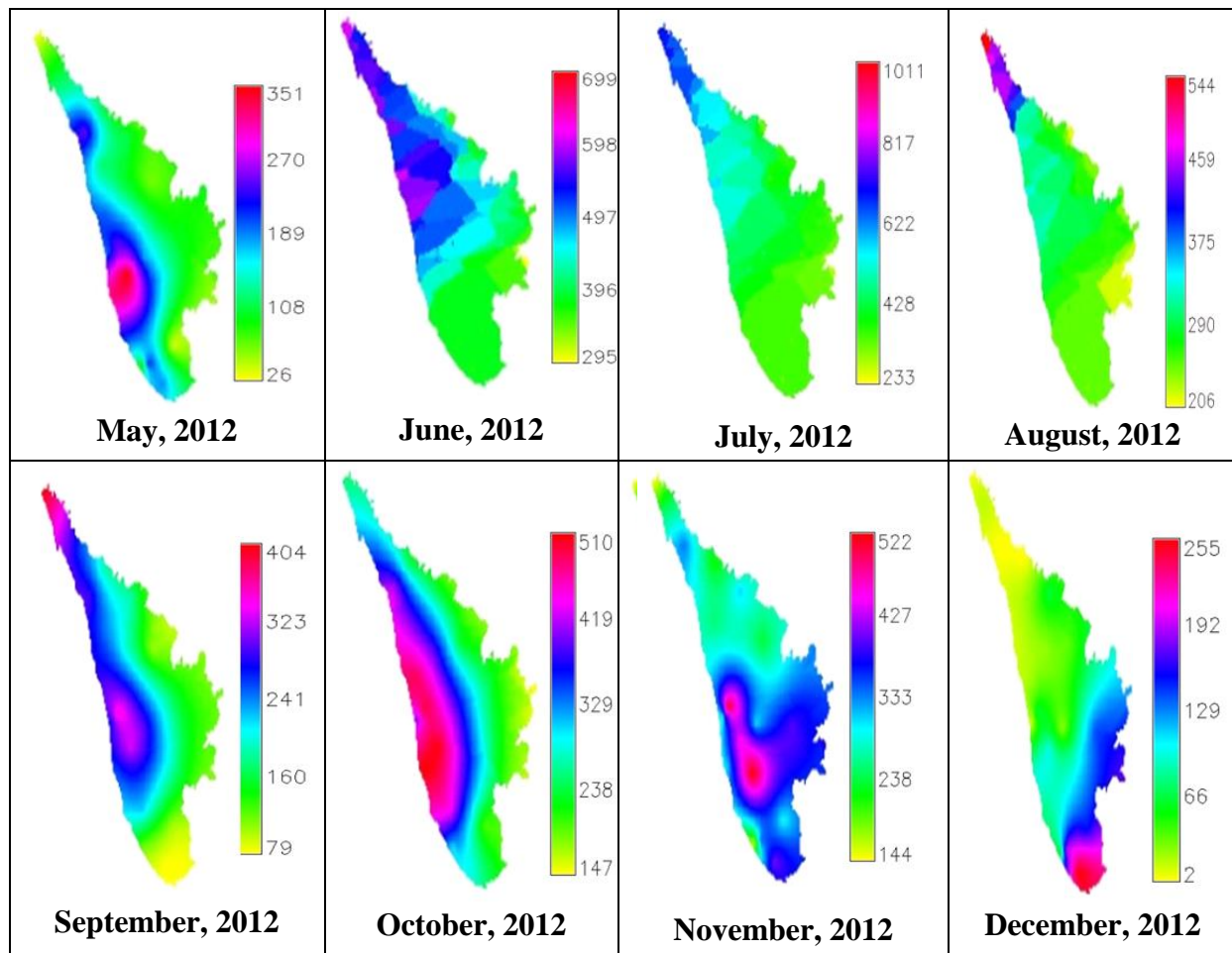


Figure 26: Monthly rainfall maps (in mm) for 2003 and 2012 for southern Western Ghats.

Figure 27–29 shows total annual rainfall for the three regions. It is evident from the figures that the coastal areas receive highest rainfall and its intensity decreases towards the eastern side in the central and southern Western Ghats. The areas that receive lesser rainfall (called the rain shadow area) are often plains where agriculture is practiced. The rain fed areas have undulating terrain with mix of evergreen to semi-evergreen forest that regulates the regional temperatures between 22 to 32 °C. In southern Western Ghats, plantation is practiced in the hilly areas.

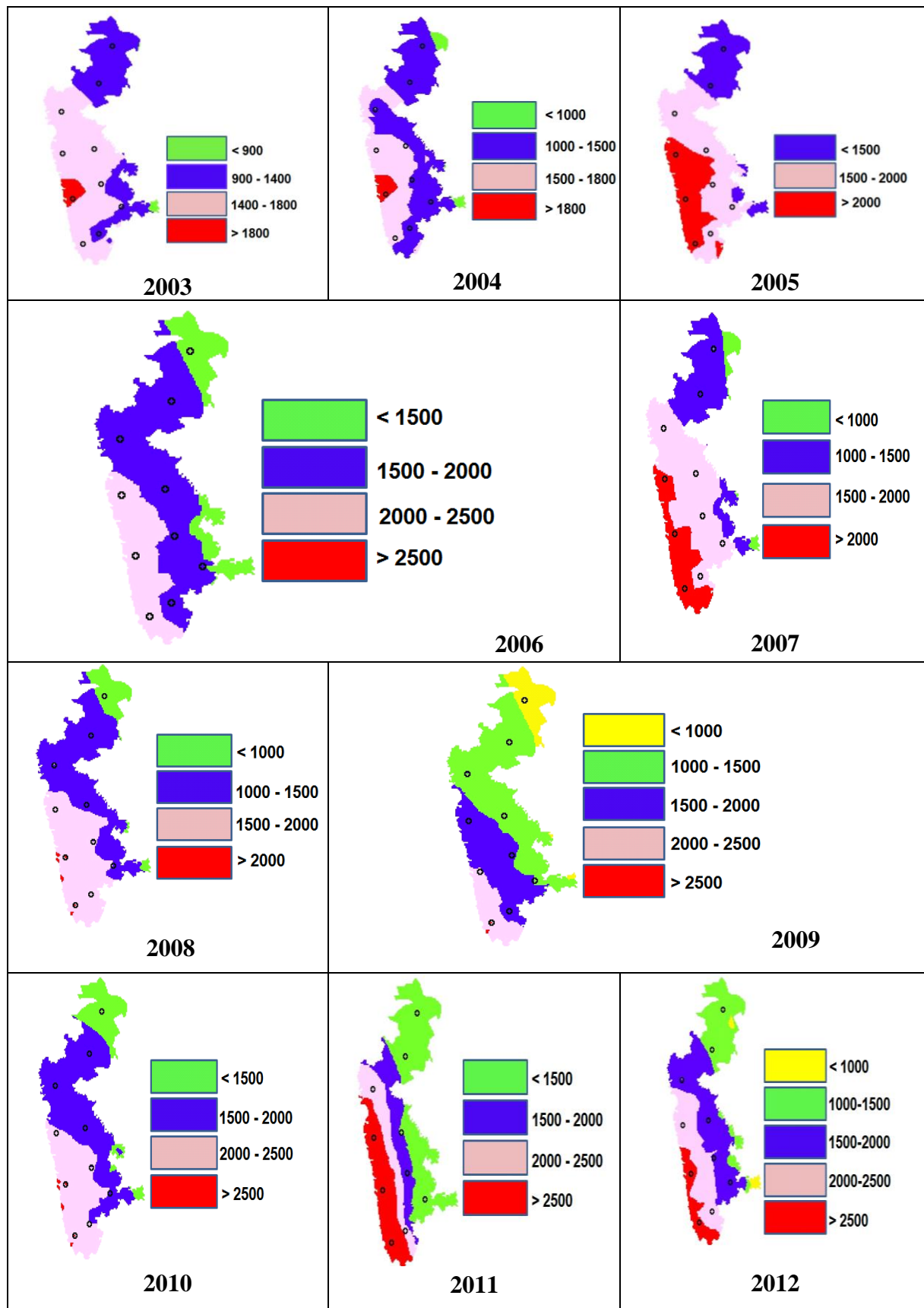


Figure 27: Total annual rainfall (in mm) for northern Western Ghats from 2003 to 2012 with rain gauge stations overlaid.

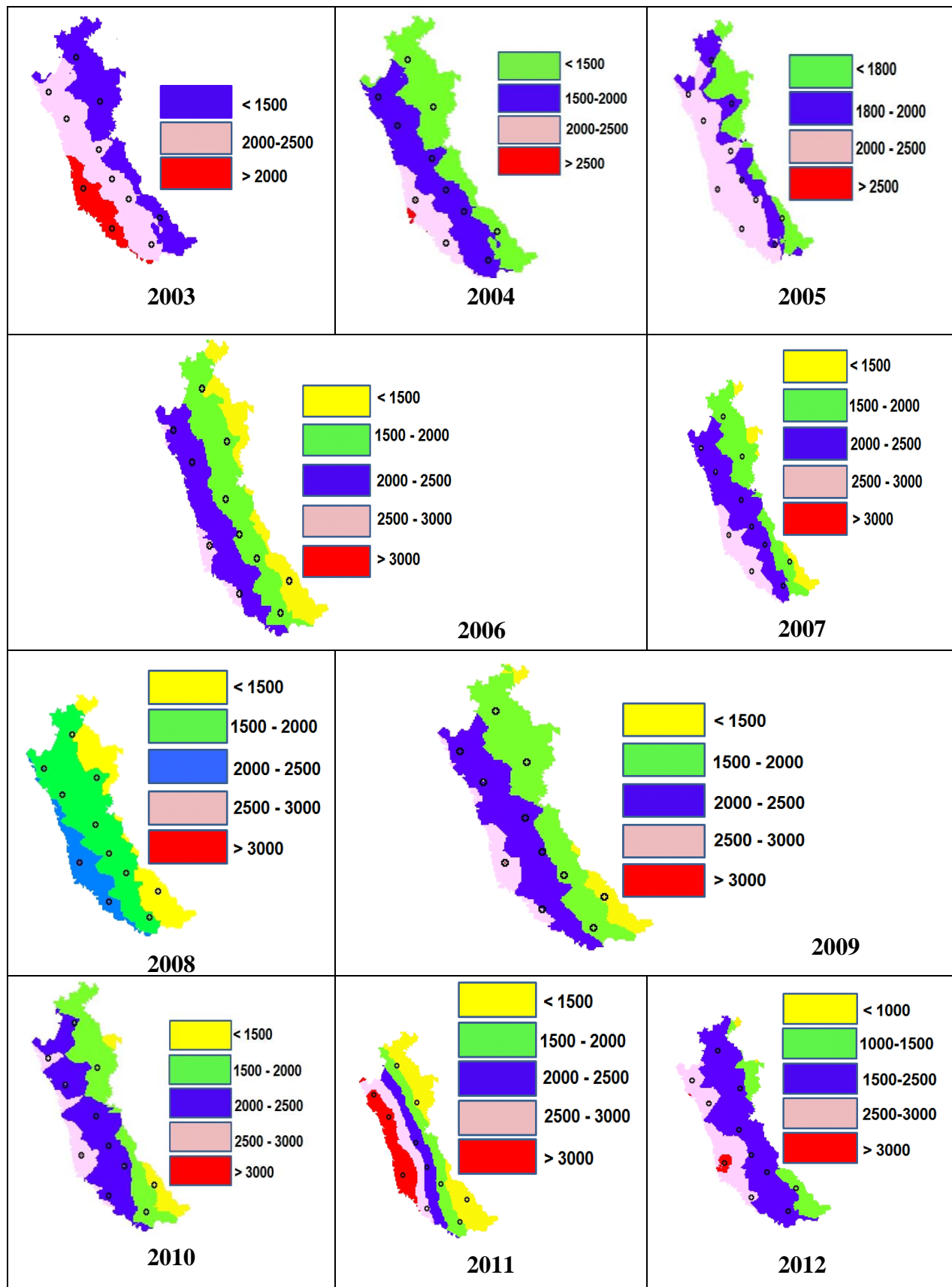


Figure 28: Total annual rainfall (in mm) for central Western Ghats from 2003 to 2012 with rain gauge stations overlaid.

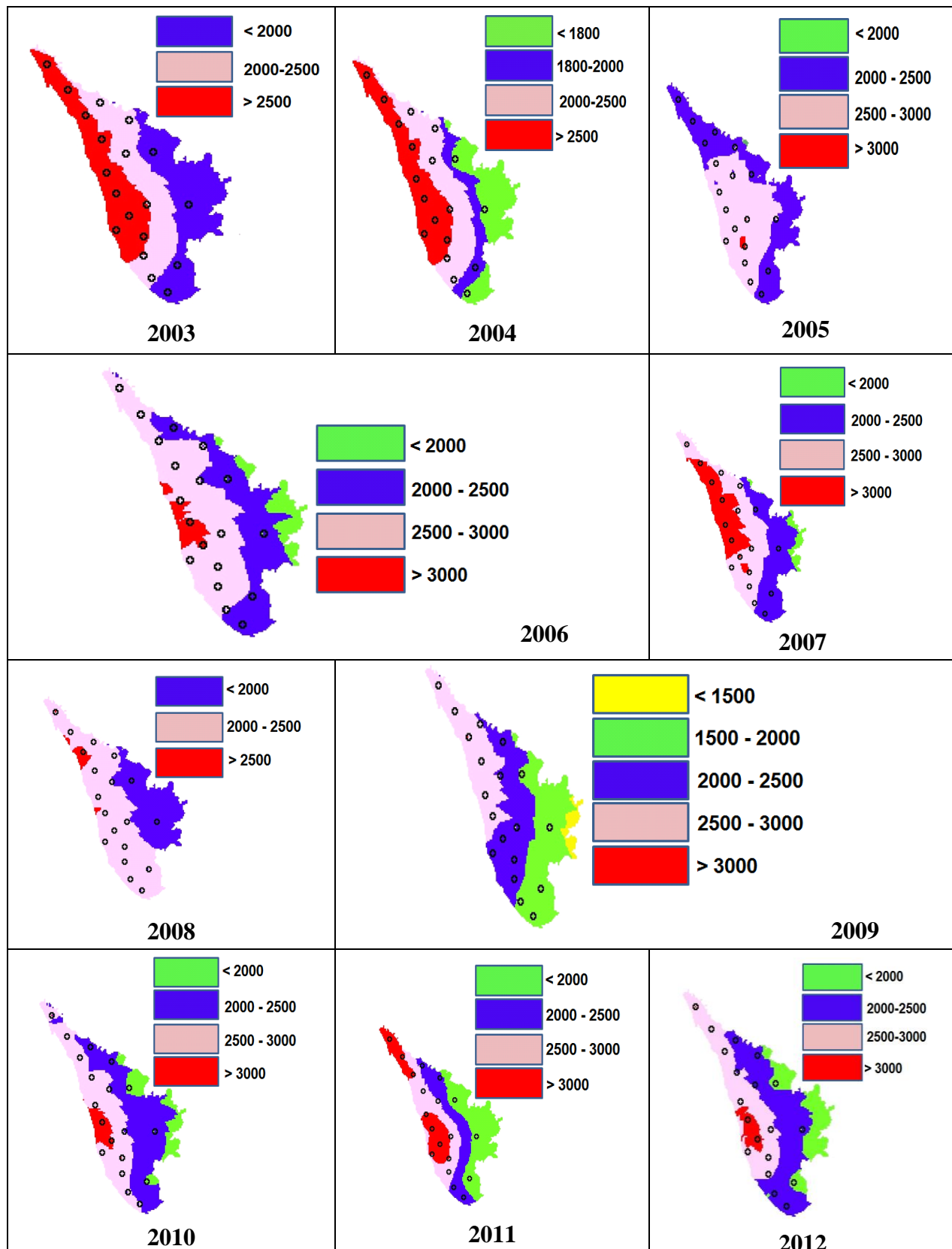


Figure 29: Total annual rainfall (in mm) for southern Western Ghats from 2003 to 2012 with rain gauge stations overlaid.

Figure 30–32 shows mean monthly temperature (Y-axis in °C) and monthly rainfall (secondary Y-axis in mm) for northern, central and southern Western Ghats respectively. Table 6–8 details monthly mean (μ) \pm standard deviation (σ) of NDVI, LST and rainfall for forest and agriculture/grassland (2003 and 2012) for northern, central and southern Western Ghats with missing data indicated with "--". Appendix 1 details mean NDVI, LST and rainfall for all the months and year for both the classes. Northern and central Western Ghats typically experience high rainfall (~ 450 to 500 mm) during June to September each year with 2009 receiving lowest rainfall among all the years as seen in figure 30 and 31. The mean temperature almost follows a cyclic pattern (with higher standard deviation), and extreme summer temperatures in April–May with minimum and maximum temperature between 20 to 35 °C in northern Western Ghats and 18 to 30 °C in central Western Ghats. Southern Western Ghats has early onset of the monsoon with highest rainfall in June every year and hottest days during April to May with lower temperature variations across the year (23° to 30° C) as shown in figure 32.

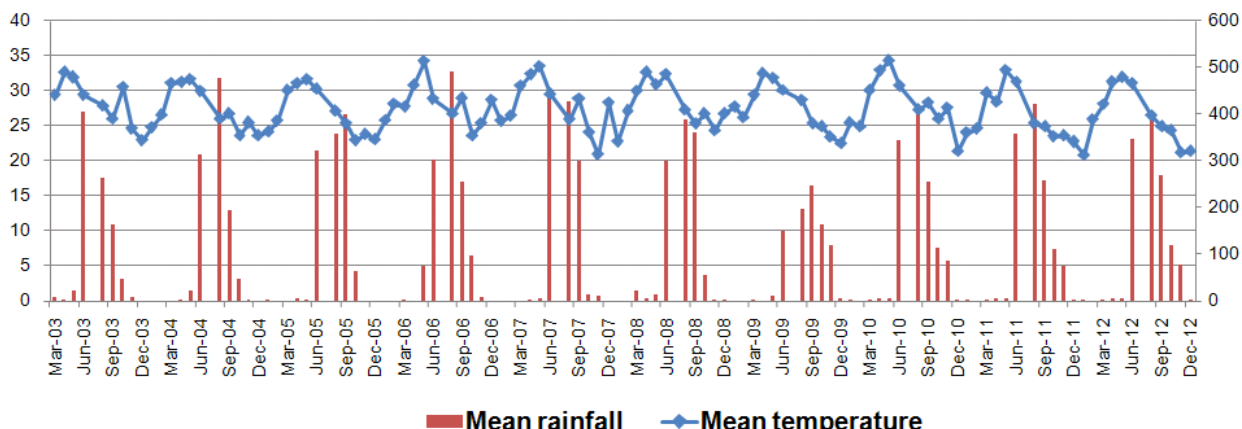


Figure 30: Mean monthly temperature (Y-axis in °C) and monthly rainfall (secondary Y-axis in mm) for northern Western Ghats.

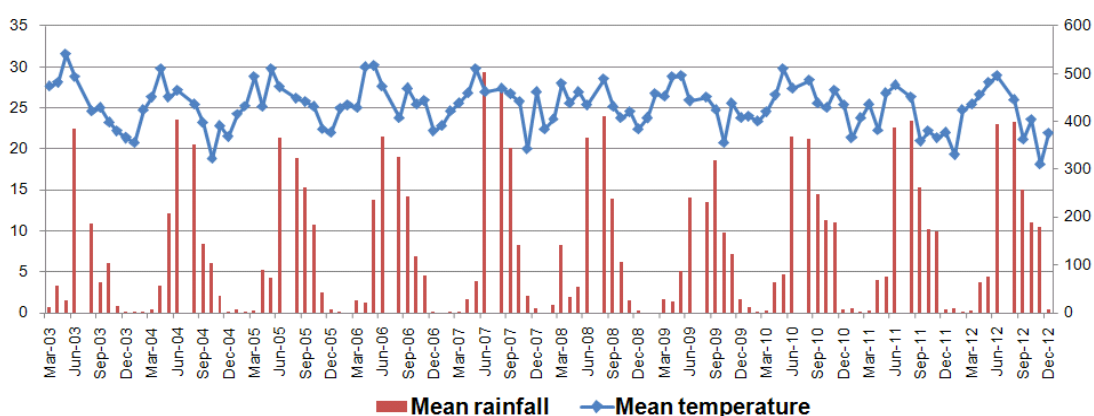


Figure 31: Mean monthly temperature (Y-axis in °C) and monthly rainfall (secondary Y-axis in mm) for central Western Ghats.

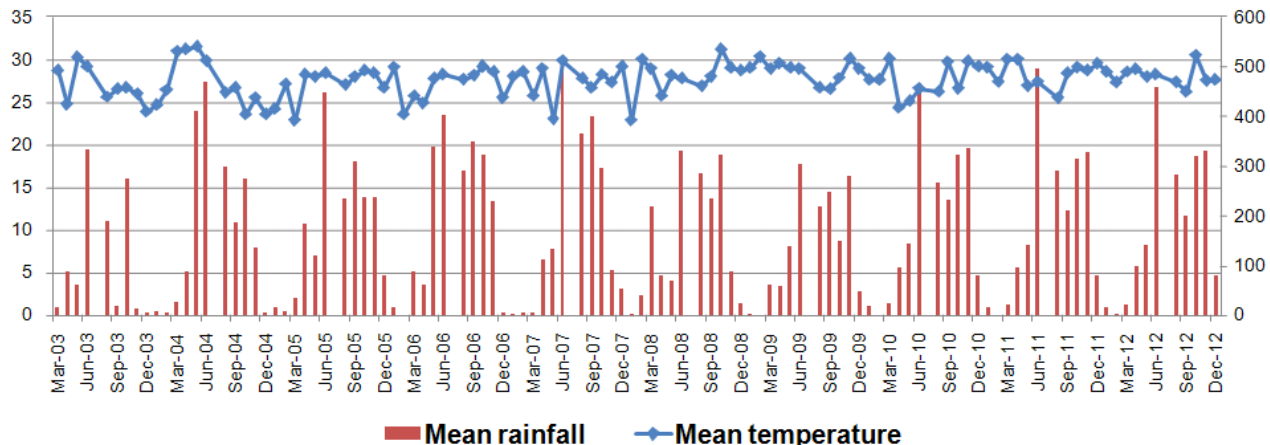


Figure 32: Mean monthly temperature (Y-axis in °C) and monthly rainfall (secondary Y-axis in mm) for southern Western Ghats.

Table 6: Mean (μ) \pm standard deviation (σ) of NDVI, LST and rainfall for forest and agriculture/grassland class for northern Western Ghats

Month, Year	NDVI ($\mu \pm \sigma$)	LST ($\mu \pm \sigma$)	rainfall ($\mu \pm \sigma$)	Month, Year	NDVI ($\mu \pm \sigma$)	LST ($\mu \pm \sigma$)	rainfall ($\mu \pm \sigma$)
Forest							
Jan, 2003	0.59 \pm 0.07	21 \pm 4	0.23 \pm 0.41	Jan, 2012	0.58 \pm 0.06	18.18 \pm 2	1.5 \pm 2
Feb, 2003	0.52 \pm 0.08	22 \pm 3	0.03 \pm 0.04	Feb, 2012	0.52 \pm 0.07	22.07 \pm 3	0.3 \pm 0
Mar, 2003	0.41 \pm 0.09	25.96 \pm 3.3	7.02 \pm 0.78	Mar, 2012	0.42 \pm 0.09	25.93 \pm 3	1.6 \pm 1
Apr, 2003	0.39 \pm 0.10	29.95 \pm 4	1.18 \pm 2.47	Apr, 2012	0.40 \pm 0.1	29.45 \pm 3	5.7 \pm 6
May, 2003	0.4 \pm 0.11	29.02 \pm 4	17.74 \pm 8	May, 2012	0.41 \pm 0.1	30.17 \pm 3	5.3 \pm 7
Jun, 2003	0.4 \pm 0.1	23.31 \pm 5	444 \pm 145	Jun, 2012	0.41 \pm 0.1	28.33 \pm 3	391.0 \pm 84
Aug, 2003	0.63 \pm 0.09	27.50 \pm 2	266 \pm 72	Aug, 2012	0.60 \pm 0.07	25.66 \pm 1	421.8 \pm 48
Sep, 2003	0.69 \pm 0.10	25.27 \pm 1	169 \pm 35	Sep, 2012	0.67 \pm 0.09	24.35 \pm 2	284.2 \pm 135
Oct, 2003	0.68 \pm 0.1	29.43 \pm 2	46.42 \pm 17	Oct, 2012	0.68 \pm 0.09	22.93 \pm 3	127.8 \pm 60
Nov, 2003	0.62 \pm 0.1	23 \pm 3	6.09 \pm 2.65	Nov, 2012	0.63 \pm 0.08	19.37 \pm 2	78.0 \pm 26
Dec, 2003	0.6 \pm 0.1	19.56 \pm 2.83	0.00 \pm 0.01	Dec, 2012	0.61 \pm 0.09	18.14 \pm 3	0.9 \pm 1

Agriculture/grassland							
Jan, 2003	0.34 ± 0.08	22 ± 3	0.51 ± 0.74	Jan, 2012	0.35 ± 0.1	21.43 ± 3	2 ± 2.09
Feb, 2003	0.3 ± 0.07	23 ± 4	0.03 ± 0.06	Feb, 2012	0.31 ± 0.1	26.76 ± 4	0.35 ± 0.3
Mar, 2003	0.24 ± 0.03	30.77 ± 3	7.35 ± 0.94	Mar, 2012	0.24	30.26 ± 3	2.22 ± 1
Apr, 2003	0.22 ± 0.03	34.56 ± 3	0.61 ± 1.79	Apr, 2012	0.22	33.5 ± 3	3.61 ± 5.5
May, 2003	0.22 ± 0.03	33.75 ± 3	24.81 ± 9.9	May, 2012	0.22	33.9 ± 2	4.74 ± 3
Jun, 2003	0.22	30.06 ± 5.5	402 ± 109	Jun, 2012	0.22	31.96 ± 3	295.3 ± 83
Aug, 2003	0.37 ± 0.09	27.95 ± 2.1	260 ± 66.6	Aug, 2012	0.34 ± 0.1	26.67 ± 2	398.7 ± 56
Sep, 2003	0.37 ± 0.09	27.31 ± 2	160 ± 31	Sep, 2012	0.37 ± 0.1	26.14 ± 3	231 ± 114
Oct, 2003	0.37 ± 0.09	32.78 ± 1.5	43.67 ± 21	Oct, 2012	0.41 ± 0.1	29.4 ± 3	87.95 ± 35
Nov, 2003	0.37 ± 0.08	26.5 ± 3.5	7.18 ± 2.20	Nov, 2012	0.39 ± 0.1	23.78 ± 3	76.16 ± 19
Dec, 2003	0.36 ± 0.08	23.54 ± 3.6	0	Dec, 2012	0.37 ± 0.1	23.08 ± 4	0.70 ± 1

Table 7: Mean (μ) ± standard deviation (σ) of NDVI, LST and rainfall for forest and agriculture/grassland class for central Western Ghats

Month, Year	NDVI ($\mu \pm \sigma$)	LST ($\mu \pm \sigma$)	rainfall ($\mu \pm \sigma$)	Month, Year	NDVI ($\mu \pm \sigma$)	LST ($\mu \pm \sigma$)	rainfall ($\mu \pm \sigma$)
Forest							
Jan, 2003	0.65 ± 0.11	17 ± 4	0.81 ± 1.26	Jan, 2012	0.65 ± 0.1	15.9 ± 4	9.21 ± 2.7
Feb, 2003	0.53 ± 0.15	22 ± 5	0.66 ± 1.04	Feb, 2012	0.53 ± 0.2	22.8 ± 5	0.66 ± 0.6
Mar, 2003	0.50 ± 0.16	25.81 ± 3.4	10.74 ± 1	Mar, 2012	0.51 ± 0.2	24.98 ± 3	4.83 ± 4
Apr, 2003	0.51 ± 0.17	26.78 ± 3.4	58.4 ± 37	Apr, 2012	0.52 ± 0.2	26.15 ± 3	66 ± 34
May, 2003	0.50 ± 0.16	29.92 ± 4	25.67 ± 7	May, 2012	0.55 ± 0.2	26.86 ± 4	78 ± 31
Jun, 2003	0.52 ± 0.12	25.76 ± 2.9	459 ± 308	Jun, 2012	0.52 ± 0.1	28 ± 2.4	407 ± 107
Aug, 2003	0.62 ± 0.1	24.48 ± 1.1	209 ± 115	Aug, 2012	0.62 ± 0.1	26 ± 1.9	429 ± 87
Sep, 2003	0.72 ± 0.11	23.9 ± 1.98	67.87 ± 20	Sep, 2012	0.69 ± 0.1	19.9 ± 2	286 ± 110

Oct, 2003	0.72 ± 0.11	21.5 ± 1.85	112 ± 46.7	Oct, 2012	0.71 ± 0.1	22 ± 2.88	201 ± 52
Nov, 2003	0.69 ± 0.11	20 ± 5	16.7 ± 10.3	Nov, 2012	0.69 ± 0.1	17.99 ± 5	189 ± 48
Dec, 2003	0.67 ± 0.1	18.23 ± 3.6	0.43 ± 0.49	Dec, 2012	0.67 ± 0.1	19.8 ± 4	6.86 ± 7
Agriculture/grassland							
Jan, 2003	0.34 ± 0.07	24 ± 4	1.67 ± 1.76	Jan, 2012	0.36	23 ± 3.9	8.27 ± 2.4
Feb, 2003	0.27 ± 0.03	29 ± 4	0.84 ± 1.22	Feb, 2012	0.27	31 ± 3.4	0.67 ± 0.5
Mar, 2003	0.25 ± 0.03	31.5 ± 3.78	11.13 ± 1.1	Mar, 2012	0.25	28 ± 2.7	3.2 ± 3.92
Apr, 2003	0.23 ± 0.02	31.86 ± 3	51.83 ± 27	Apr, 2012	0.24	29.5 ± 37	51.5 ± 33
May, 2003	0.23 ± 0.03	36 ± 2	22.7 ± 6.18	May, 2012	0.23	35.47 ± 3	59.1 ± 26
Jun, 2003	0.26 ± 0.04	30 ± 4.9	243 ± 167	Jun, 2012	0.26	31 ± 3.1	343 ± 97
Aug, 2003	0.34 ± 0.09	24.51 ± 1.2	179 ± 100	Aug, 2012	0.35 ± 0.1	25.9 ± 2	376 ± 108
Sep, 2003	0.35 ± 0.09	27.29 ± 2.6	51 ± 20	Sep, 2012	0.37 ± 0.1	23 ± 3.9	195 ± 115
Oct, 2003	0.36 ± 0.08	26.88 ± 3.5	85.26 ± 49	Oct, 2012	0.4 ± 0.07	28 ± 4.7	135 ± 35
Nov, 2003	0.4 ± 0.07	26 ± 3.29	7.08 ± 7.08	Nov, 2012	0.42 ± 0.1	24.6 ± 4	138.9 ± 51
Dec, 2003	0.38 ± 0.07	24 ± 3.57	0.39 ± 0.5	Dec, 2012	0.4 ± 0.06	25.5 ± 3	4.1 ± 6.85

Table 8: Mean (μ) \pm standard deviation (σ) of NDVI, LST and rainfall for forest and agriculture/grassland class for southern Western Ghats

Month, Year	NDVI ($\mu \pm \sigma$)	LST ($\mu \pm \sigma$)	rainfall ($\mu \pm \sigma$)	Month, Year	NDVI ($\mu \pm \sigma$)	LST ($\mu \pm \sigma$)	rainfall ($\mu \pm \sigma$)
Forest							
Jan, 2003	0.69 ± 0.1	27 ± 2	6.6 ± 2.53	Jan, 2012	0.69 ± 0.1	28.2 ± 2.7	16.6 ± 11
Feb, 2003	0.62 ± 0.16	28 ± 3	6.66 ± 5.35	Feb, 2012	0.61 ± 0.2	27.16 ± 3	2.88 ± 1
Mar, 2003	0.61 ± 0.17	29 ± 1.37	14.9 ± 1.56	Mar, 2012	0.6 ± 0.15	28.8 ± 2	22 ± 16.7
Apr, 2003	0.6 ± 0.18	24.7 ± 1.8	91.3 ± 35	Apr, 2012	0.56 ± 0.2	28.9 ± 1.6	101 ± 63
May, 2003	0.55 ± 0.15	30.38 ± 1.4	64.69 ± 38	May, 2012	0.59 ± 0.2	27 ± 3	140 ± 68

Jun, 2003	0.62 ± 0.16	29.3 ± 1.6	336 ± 159	Jun, 2012	0.56 ± 0.1	28.3 ± 1.9	463.1 ± 7
Aug, 2003	0.69 ± 0.1	25.73 ± 1	189.7 ± 73	Aug, 2012	0.68 ± 0.1	26.6 ± 1.2	293 ± 55
Sep, 2003	0.75 ± 0.1	25.96 ± 0.8	21.64 ± 22	Sep, 2012	0.72 ± 0.1	26.1 ± 1.1	232 ± 67
Oct, 2003	0.73 ± 0.1	26 ± 1	300 ± 82	Oct, 2012	0.73 ± 0.1	30.6 ± 1.5	354 ± 94
Nov, 2003	0.74 ± 0.1	26 ± 0.7	13.05 ± 5.7	Nov, 2012	0.74 ± 0.1	27.3 ± 2.3	333 ± 61
Dec, 2003	0.7 ± 0.1	23.6 ± 1.3	4.07 ± 5.27	Dec, 2012	0.72 ± 0.1	27.1 ± 2.6	75 ± 58.6
Agriculture/grassland							
Jan, 2003	0.37 ± 0.06	30 ± 2	8.67 ± 1.64	Jan, 2012	0.41 ± 0.1	32.1 ± 1.8	13.6 ± 11
Feb, 2003	0.27 ± 0.03	32 ± 1	5.04 ± 3.54	Feb, 2012	0.29	31.43 ± 2	2.5 ± 1.1
Mar, 2003	0.25 ± 0.03	30.34 ± 1.2	15.31 ± 0.6	Mar, 2012	0.26	27.15 ± 2	22.4 ± 16
Apr, 2003	0.24 ± 0.02	27.42 ± 2.9	55.36 ± 23	Apr, 2012	0.24	29.74 ± 3	57.7 ± 46
May, 2003	0.23 ± 0.03	29.45 ± 1.9	44.93 ± 24	May, 2012	0.23	35 ± 2	6 ± 3
Jun, 2003	0.28 ± 0.04	29.74 ± 2.7	333.9 ± 80	Jun, 2012	0.28	28.67 ± 2	431 ± 64
Aug, 2003	0.33 ± 0.09	26.06 ± 1.7	191.6 ± 47	Aug, 2012	0.33 ± 0.1	28.8 ± 2.6	273 ± 48
Sep, 2003	0.32 ± 0.09	28.25 ± 1.7	12.23 ± 8.5	Sep, 2012	0.33 ± 0.1	27.5 ± 2.4	157 ± 56
Oct, 2003	0.34 ± 0.08	28.6 ± 2.61	238 ± 63.2	Oct, 2012	0.35 ± 0.1	30.5 ± 2.2	265 ± 75
Nov, 2003	0.4 ± 0.08	26.25 ± 0.9	10.6 ± 2.35	Nov, 2012	0.43 ± 0.1	30.5 ± 2.1	332 ± 46
Dec, 2003	0.43 ± 0.06	25.53 ± 1	6.98 ± 6.56	Dec, 2012	0.43 ± 0.1	31.79 ± 2	95.8 ± 48

In general, lower NDVI values are observed during March to June and higher NDVI values are seen during August to January/February for all the years for both dense vegetation and agriculture. The variability between summer and winter mean temperatures is not high. June to September/October have maximum rainfall in both forest and agricultural areas in northern Western Ghats. 2012 witnessed higher rainfall even in October–November. In central Western Ghats, the observations are similar to that of northern region, however NDVI values for green vegetation is higher, the minimum–maximum temperature range is lower i.e. the regions is cooler and the area witnesses higher rainfall compared to northern Western Ghats. Southern Western Ghats exhibit higher NDVI values throughout the year for dense vegetation

(> 0.55) with maximum NDVI reaching 0.79. Overall, forest and agricultural class exhibit high NDVI other than during the month of February to June. The mean temperature variation is very small (~ 23 to ~ 35 °C) throughout the year and rainfall is more during April to October/November.

The scale of the monthly NDVI changes over time is a key sign of the contribution of vegetation presence activity in different months to total yearly vegetation growth. Figure 33 shows change in monthly NDVI and climatic variables from 2003 to 2012. The mean monthly NDVI reached maximum values during August to November. From March to June, the mean monthly NDVI was low as also observed in figure 15 and 16. The highest mean monthly NDVI value was 0.68 during August in northern Western Ghats, 0.71 in central region and 0.74 in November in southern region as shown in figure 33.

The NDVI patterns were coupled with the climatic variables. Monthly LST showed a contrasting pattern to NDVI (figure 33). When NDVI is low, during March to June, the LST is high, 31 °C in May in northern region and 28 °C in central. However, mean monthly LST in southern Western Ghats ranged between 25 °C to 30 °C throughout the year with highest LST recorded in March and November (28 °C) as in figure 33. Rainfall follows a similar pattern as that of NDVI in northern region with a high of 375.5 mm in August, a high of 390 mm in central region in June, and 420.5 mm in southern Western Ghats in June as well (see figure 33).

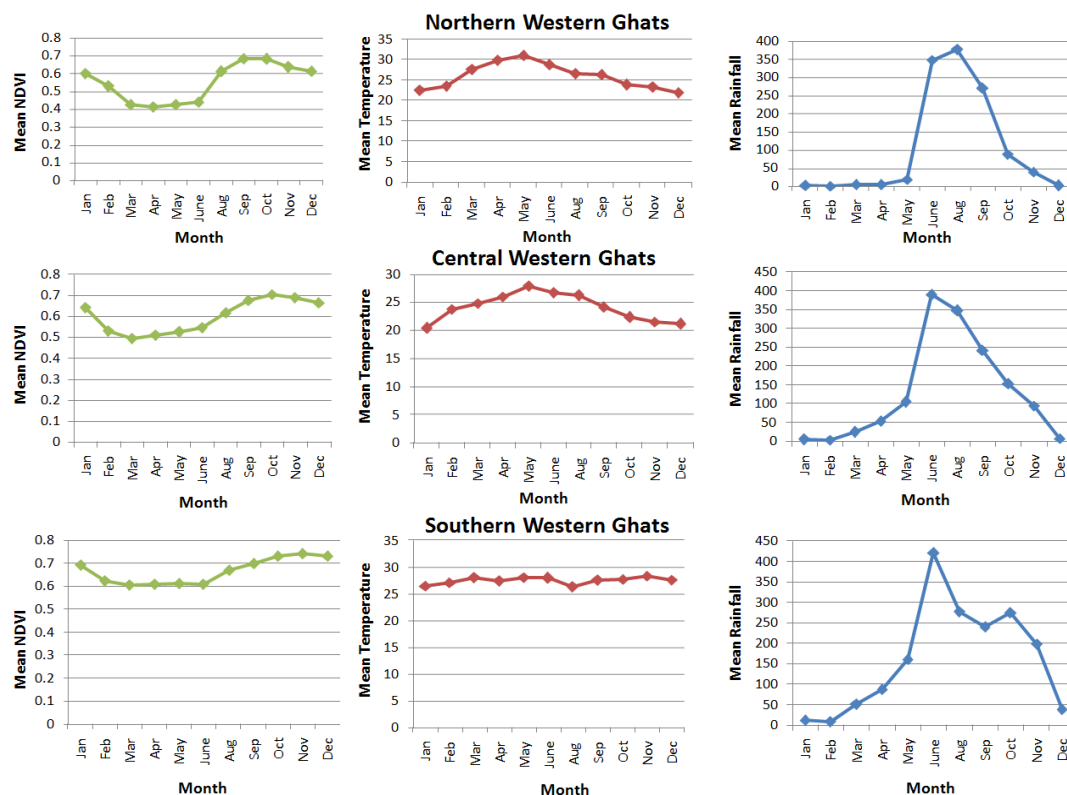


Figure 33: Changes in monthly NDVI and climatic variables from 2003 to 2012. 10-years mean monthly NDVI, 10-years mean monthly temperature (in °C), and 10-years mean monthly rainfall (in mm) for northern, central and southern Western Ghats.

Principal component analysis (PCA) was carried out on the 12-months NDVI, LST and rainfall images for all the years. PCA transform multidimensional image data into a new, uncorrelated co-ordinate system or vector space. The purpose of this process is to compress all the information contained in an original n – band data set into fewer than n “new bands” or components. The new components are then used in lieu of the original data and are effective tool for change detection (Fung and LeDrew, 1987; Macleod and Congalton, 1998; Michener and Houhoulis, 1997). Major components of respective images corresponding to two time periods can determine changes.

Figure 34 shows PC1 and PC2 of 2003 and 2012 of NDVI and LST highlighting major changes in the LC pattern. The red oval shapes in southern region and circles in northern region show the status of dense vegetation during 2003 to 2012 as also highlighted in the corresponding LC maps. The major dense forest area (inside the oval shape) is highlighted in PC2 of NDVI of 2003 and 2012. PC1 of LST highlighted the temperature variations and it was found that the low and high LST pixels were clearly separable. The corresponding temperature in dense vegetation was low (~ 30 °C) in summer (March to May) and was as high as 42 °C in settlement/open dry soil areas in 2003. Similarly, PC1 of LST of 2012 highlighted lower LST (30 °C) in forest areas in summer while settlement areas exhibited high LST (40 °C). PCA of rainfall did not show any distinct pattern. Similar analysis was carried out for the central and southern Western Ghats, which revealed likewise observations for which the results are not displayed here.

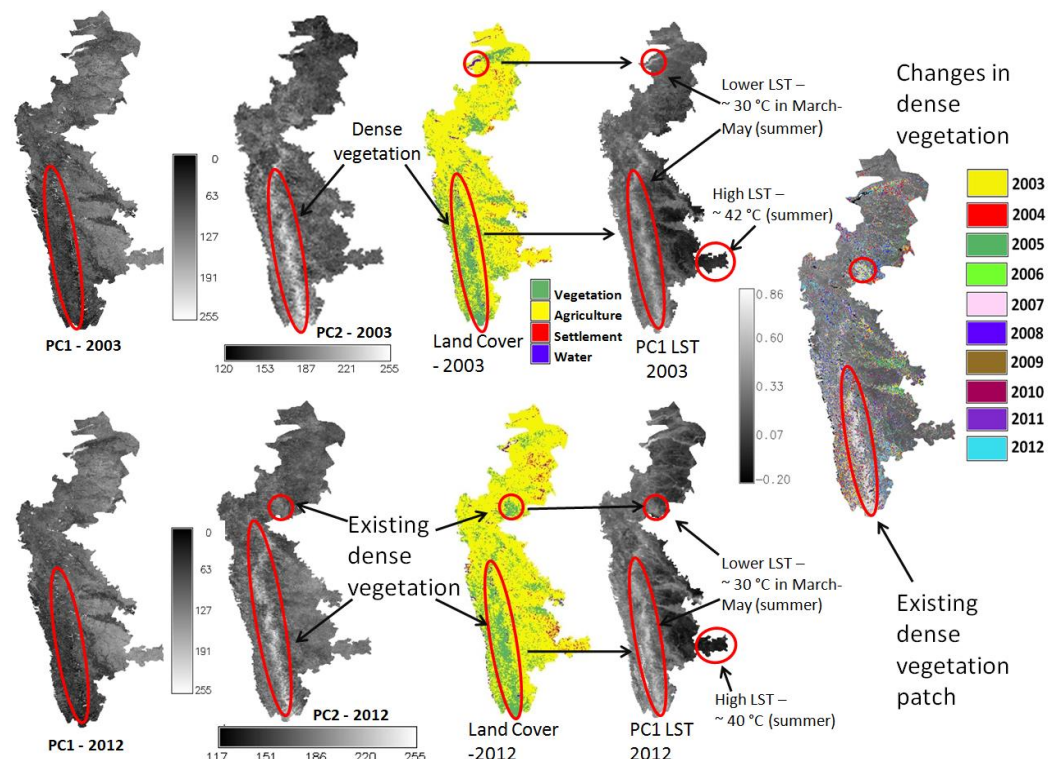


Figure 34: Spatial distribution of pattern in dense vegetation and LST through PCA in northern Western Ghats. Red polygonal shapes highlight past and current status of dense vegetation and the corresponding LST through PC's in those areas.

5.4 Relationship of NDVI of dense vegetation with climatic variables in Western Ghats

To analyse the effects of regional climatic changes on monthly NDVI of dense vegetation, Pearson product-moment correlation between NDVI–LST, NDVI–rainfall and LST–rainfall were explored. Monthly mean NDVI, LST and rainfall data were subject to regression analysis to understand their behaviour as shown in figure 35.

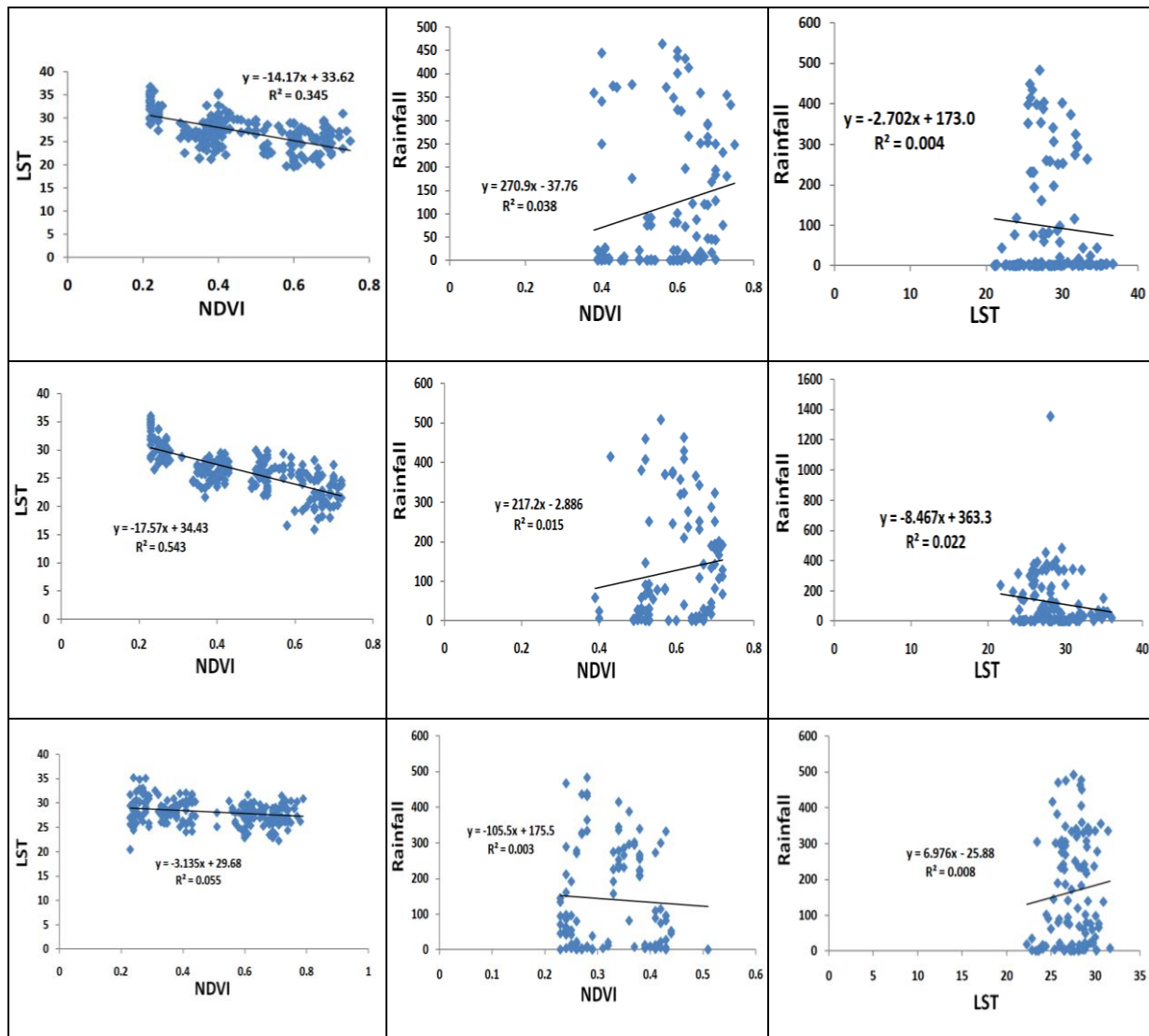


Figure 35: Regression between NDVI and climatic variables (LST and rainfall) in northern (top row), central (middle row) and southern Western Ghats (bottom row).

The trend line between data points of NDVI and LST had a negative slope indicating a negative correlation with $R^2 = 0.35$ for northern and 0.54 for central Western Ghats. For southern Western Ghats, the trend line had almost no slope indicating a weak negative or positive correlation. Precipitation is the most important source of soil moisture and NDVI values are also closely linked with precipitation. NDVI and rainfall had positive slope for northern and central region ($R^2 = 0.038$ and 0.015) and a slightly negative slope for southern Western Ghats with lesser R^2 value (0.003). LST and rainfall had negative slope for northern

and central Western Ghats with low R^2 values (0.004 and 0.022) indicating a negative relationship between these variables whereas the southern Western Ghats data showed a positive correlation with low R^2 value (0.008) for the best fit line.

Figure 36 shows correlation between monthly NDVI and climatic variables. In the northern region, a negative correlation is observed between NDVI–LST and NDVI–rainfall during December to May and a positive correlation is seen between June to November (5% level). In the central Western Ghats, a positive correlation between NDVI–LST is seen in January, March, May and from September to December while other months have negative correlation. Rainfall has positive correlation with NDVI in all months except from April to September. Southern Western Ghats shows a crisscross pattern between NDVI–LST–rainfall and is complicated. From February to June, when rainfall increases, LST decreases. LST shows positive correlation from November to January.

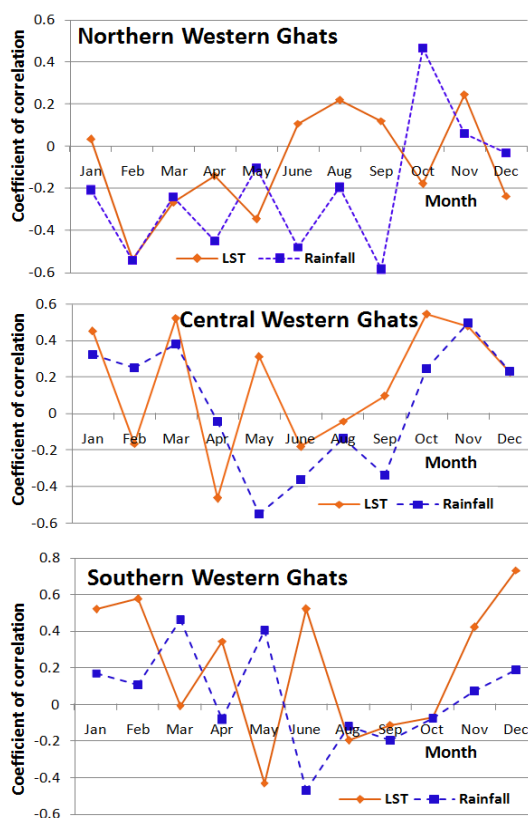


Figure 36: Correlations between 10-years (2003 to 2012) mean monthly NDVI, LST and rainfall for northern, central and southern Western Ghats.

These trends gave an overall idea of the expected relationship between vegetation and climatic variables and motivated us to explore these covariates on a pixel by pixel basis for each year to enhance visualisation of the spatial patterns and on an image to image basis for better numerical description with the time-series monthly data as discussed below. Figure 37–45 shows pixel to pixel correlation maps between NDVI, LST and rainfall for the northern, central and southern Western Ghats from 2003 to 2012.

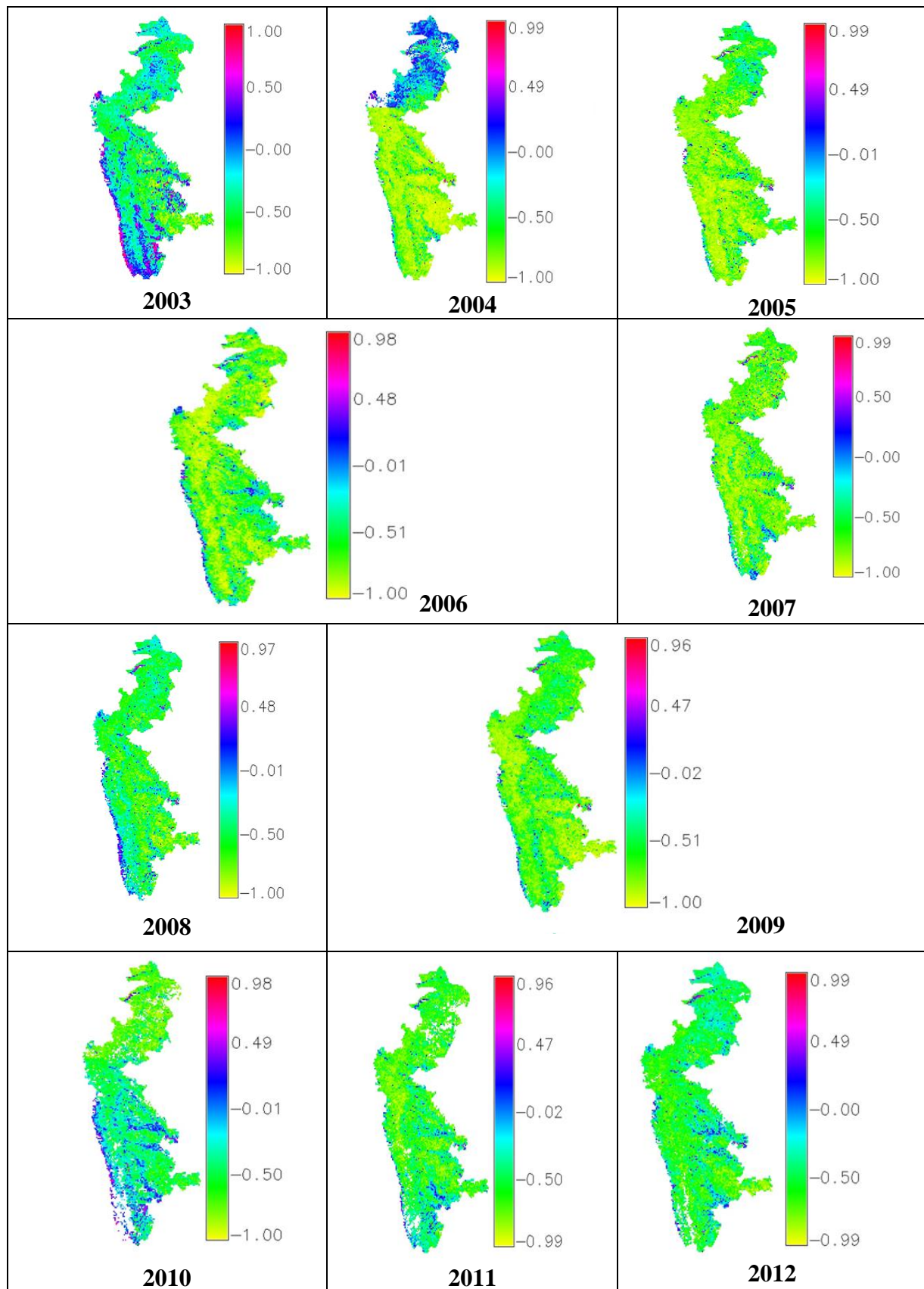


Figure 37: Pixel to pixel correlation maps between NDVI and LST for northern Western Ghats.

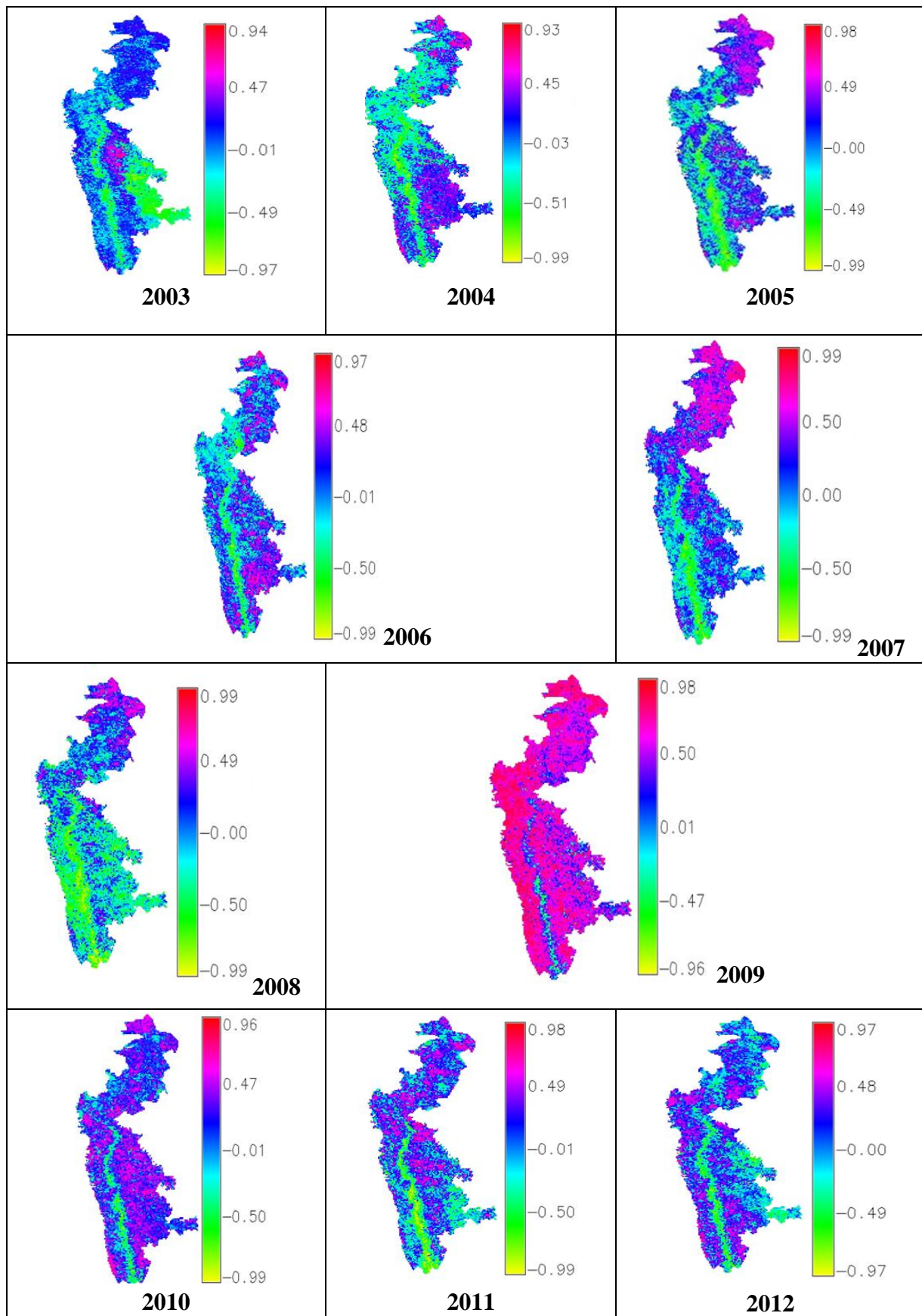


Figure 38: Pixel to pixel correlation maps between NDVI and rainfall for northern Western Ghats.

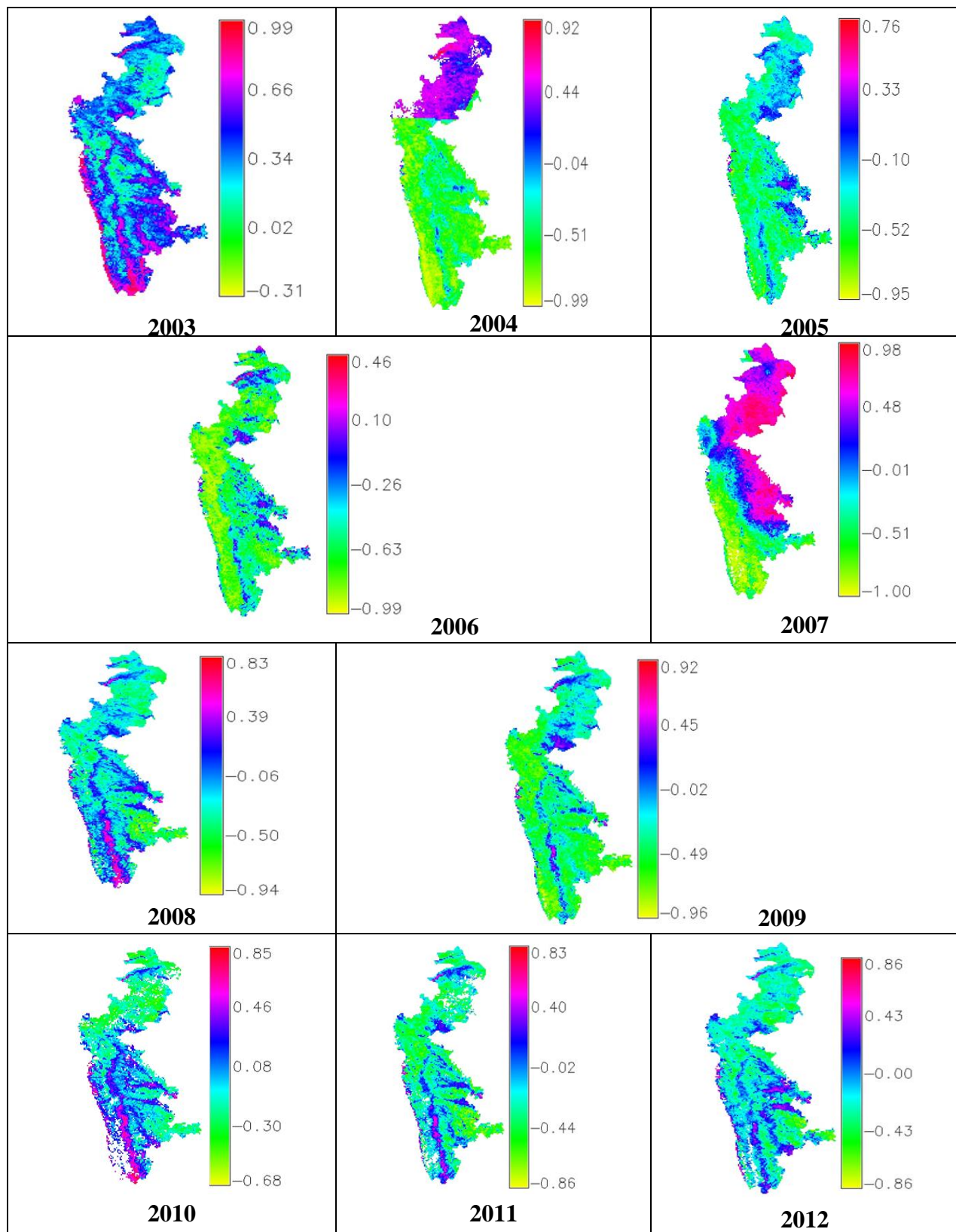


Figure 39: Pixel to pixel correlation maps between LST and rainfall for northern Western Ghats.

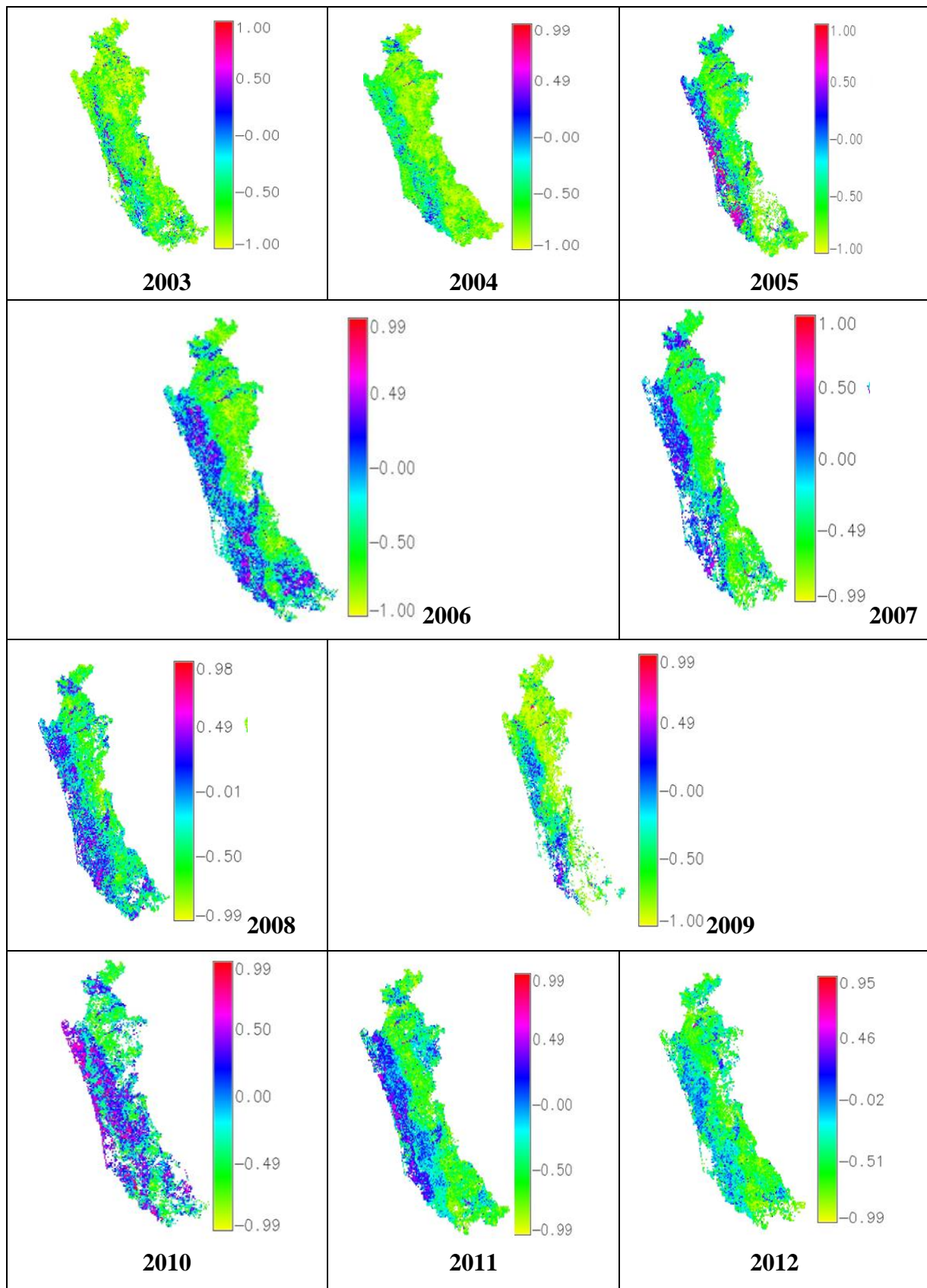


Figure 40: Pixel to pixel correlation maps between NDVI and LST for central Western Ghats.

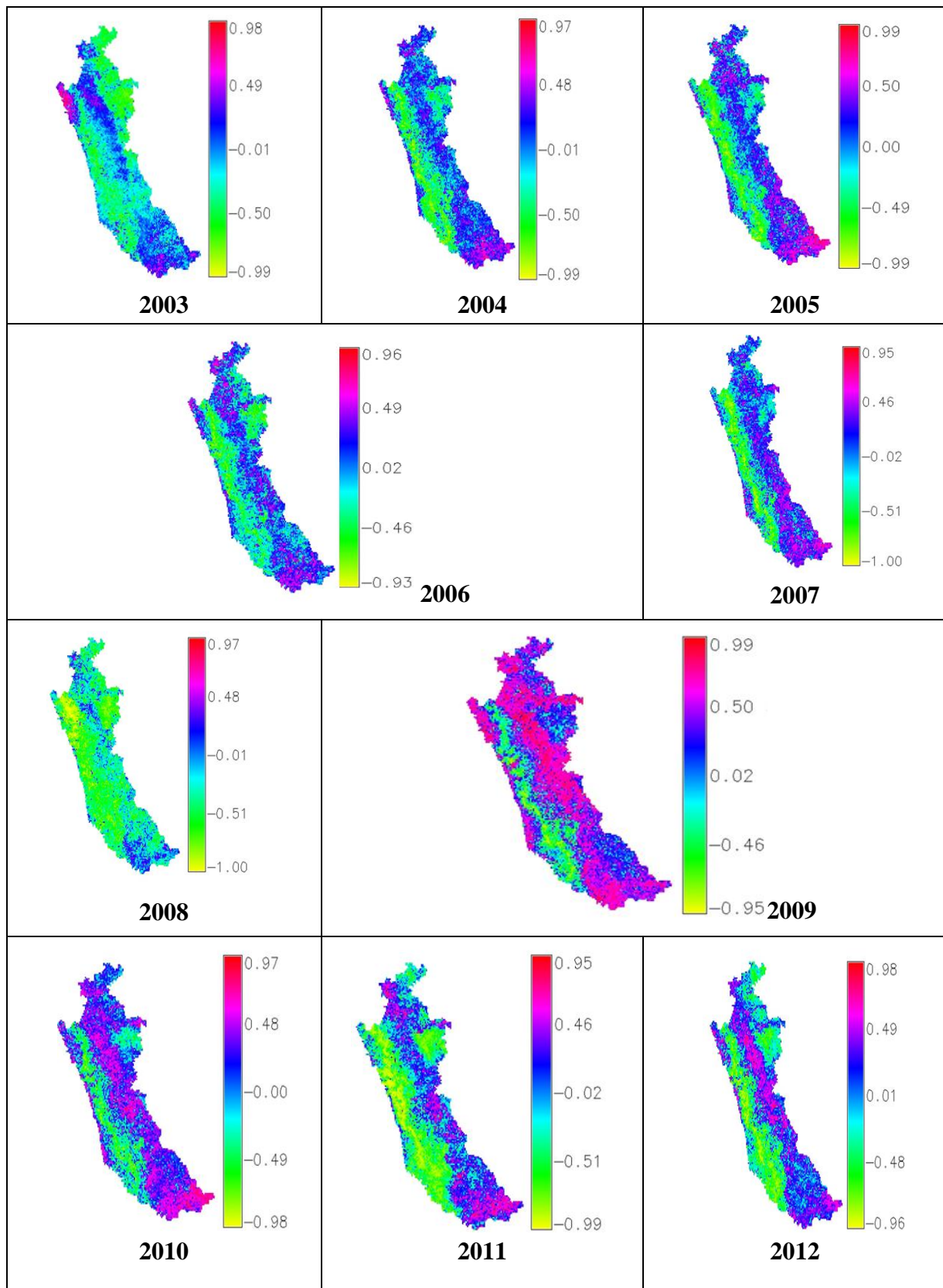


Figure 41: Pixel to pixel correlation maps between NDVI and rainfall for central Western Ghats.

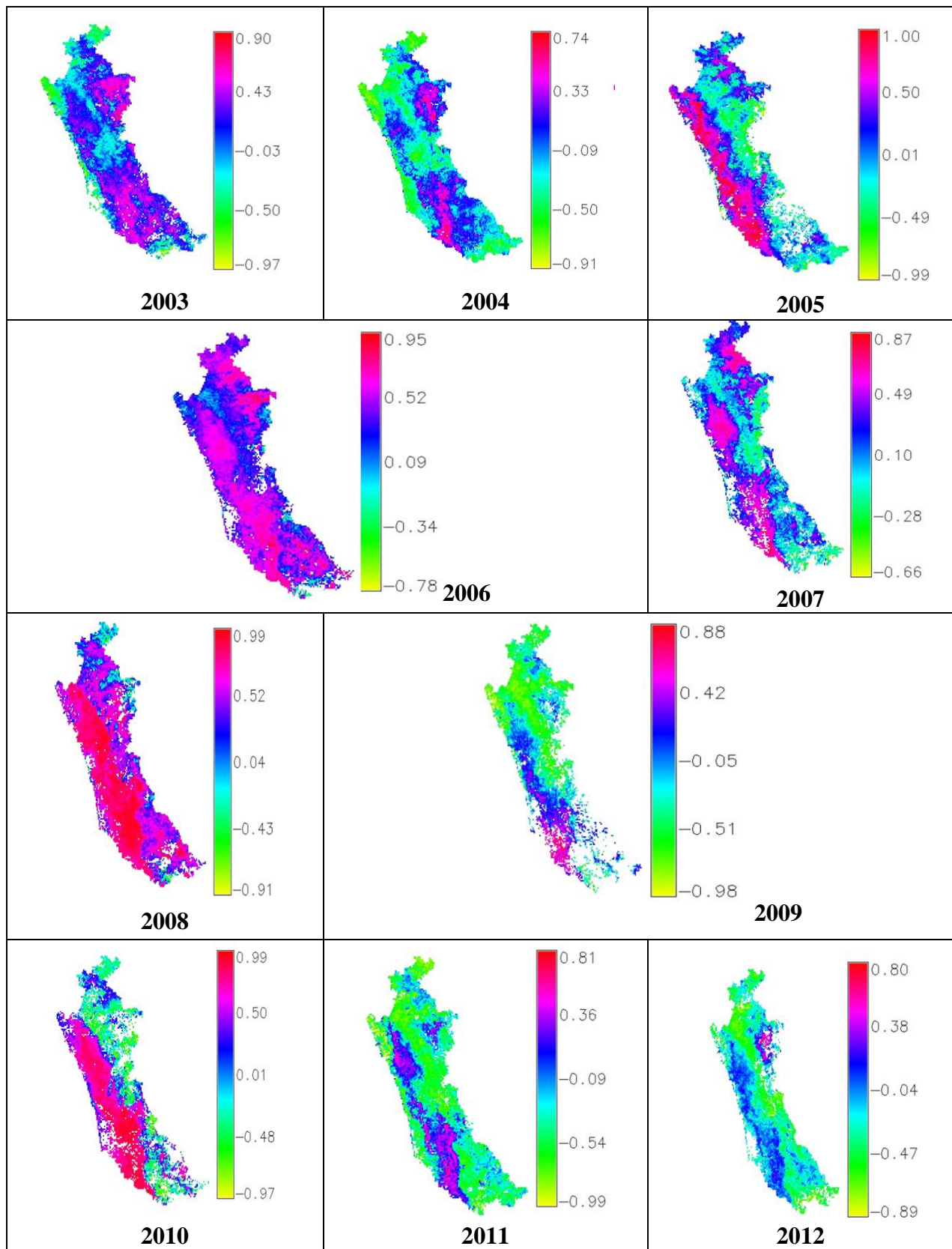


Figure 42: Pixel to pixel correlation maps between LST and rainfall for central Western Ghats.

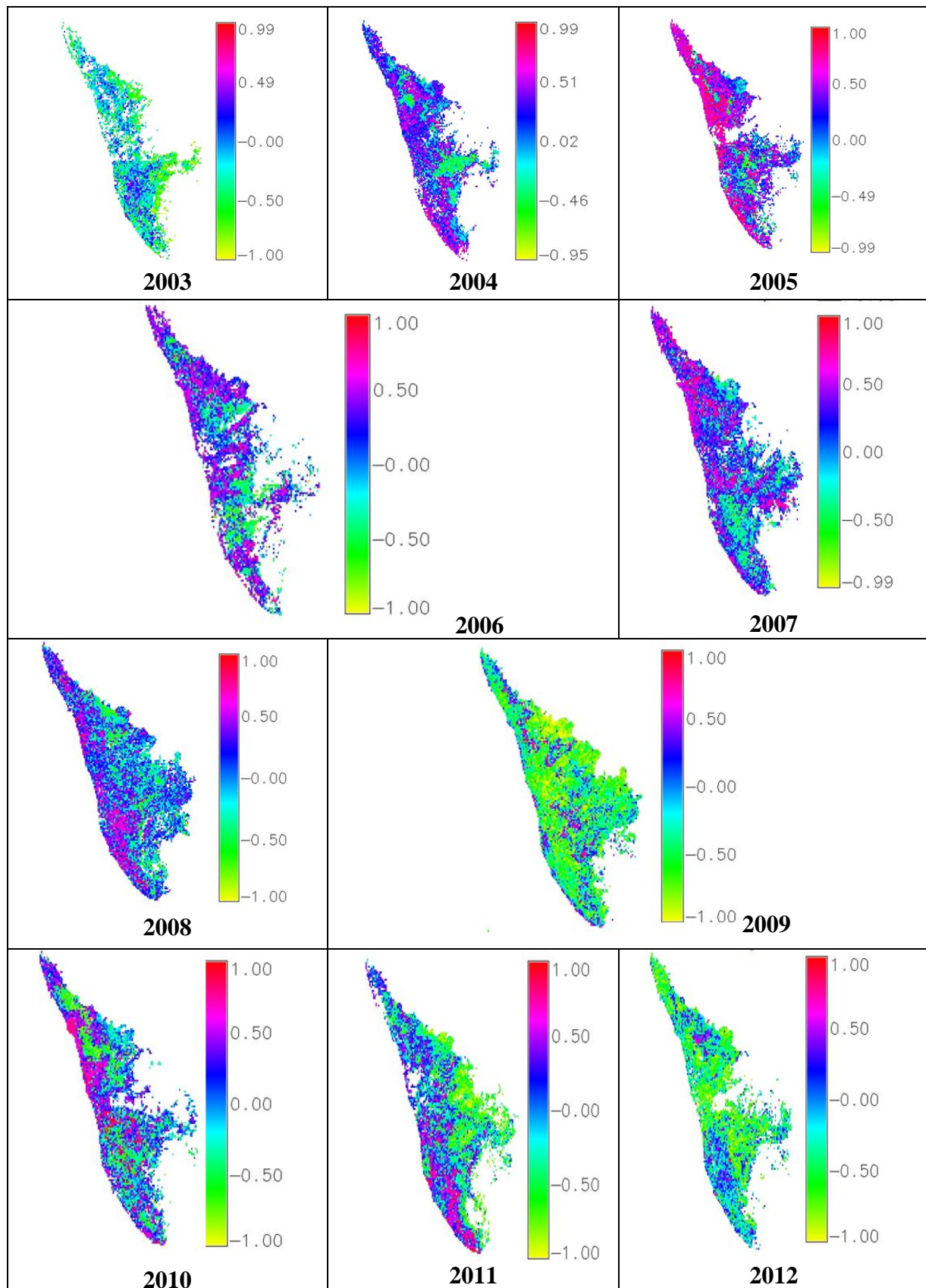


Figure 43: Pixel to pixel correlation maps between NDVI and LST for southern Western Ghats.

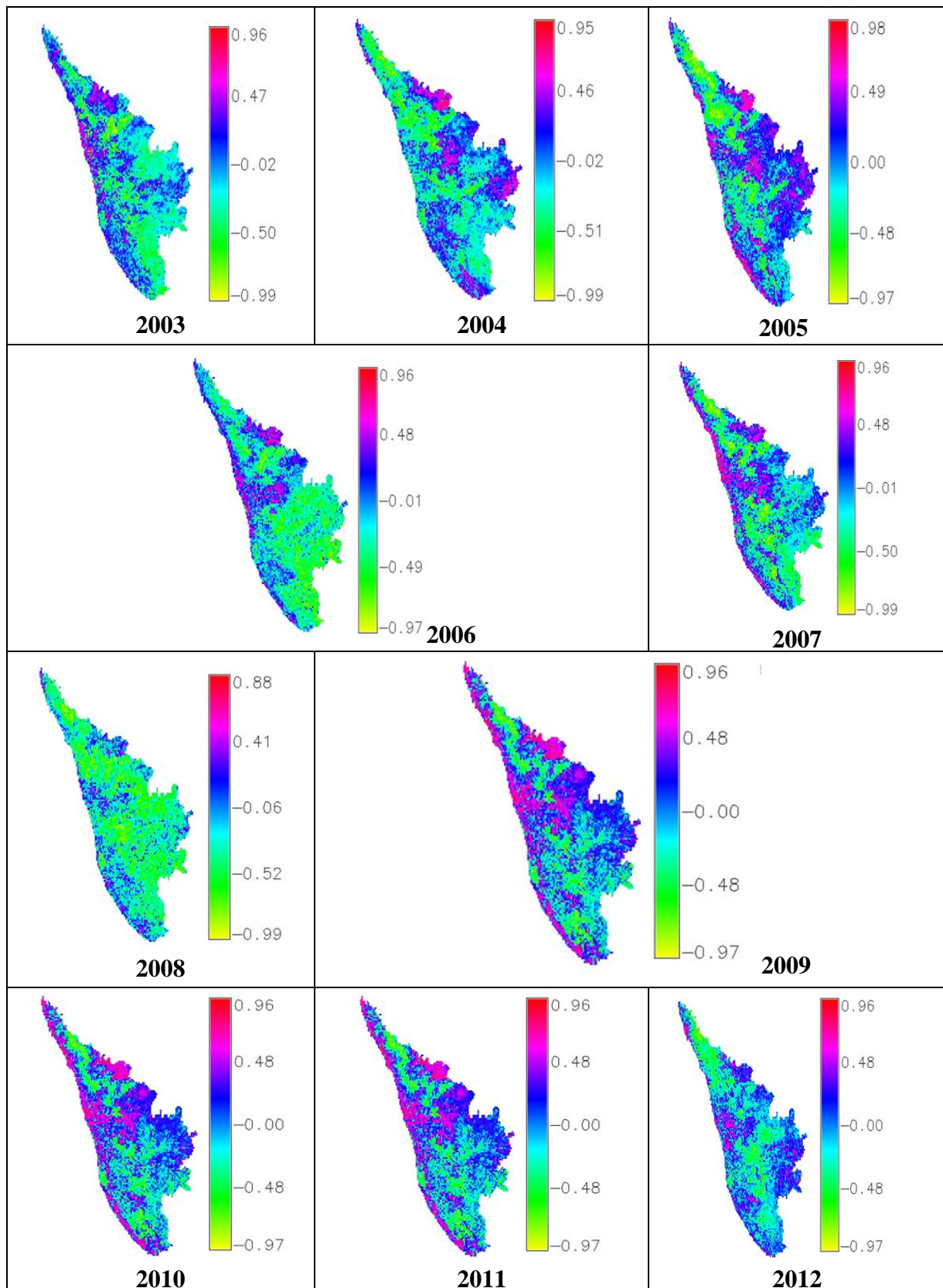


Figure 44: Pixel to pixel correlation maps between NDVI and rainfall for southern Western Ghats.

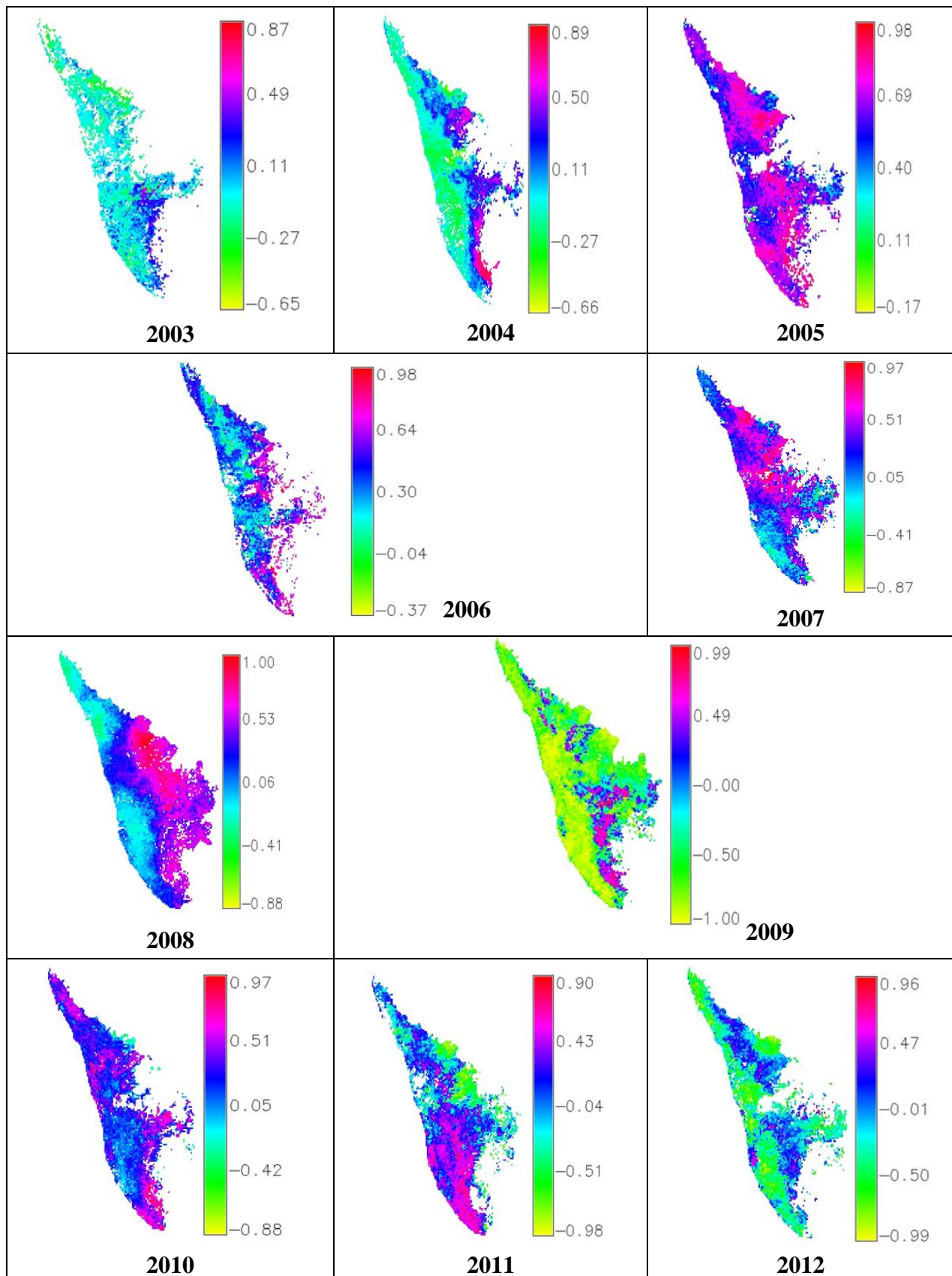


Figure 45: Pixel to pixel correlation maps between LST and rainfall for southern Western Ghats.

NDVI and LST were negatively correlated (at 99% confidence interval) in most areas during 2003 to 2012 in northern and central Western Ghats (figure 37 and 40) reestablishing that vegetation and dense forest decrease surface temperature. Northern Western Ghats showed minimum positive correlation value of 0.96 in 2009 and 2011 and a minimum negative correlation of -0.99 in 2011–2012 and central Western Ghats had minimum positive correlation value of 0.95 in 2012 and a minimum negative correlation of -0.99 in 2007, 2008, and 2010–12. However, a similar observation was not noticed in southern Western Ghats (figure 43) where weak negative to strong positive correlation was found during 2004–2008 and 2010 suggesting the possible effects of temperature on NDVI in most parts of the region (with a maximum positive correlation value of 0.99 in 2003-4 and a minimum negative correlation of -0.95 in 2004). The positive correlation may have been caused due to high temperature even with dense vegetation as this region has equatorial climatic influence which enhances photosynthesis and respiration for plant growth (Mao et al., 2012). In contrast, 2003, 2009, 2011–12 showed negative correlation.

Rainfall is the most important source of soil moisture; NDVI was closely linked with rainfall. Most areas showed weak negative to strong positive correlation (figure 38) between NDVI and rainfall during 2003–2012; the year 2009 exhibited very high correlation in the entire region. This reaffirmed that forest tend to bring rainfall in tropical region. The minimum positive and negative correlation was 0.93 in 2004 and -0.96 in 2009. A strip of area stretched from the center to the southernmost part of the image representing water body on the ground (with negative NDVI values) showed negative correlation whereas LST and rainfall showed positive correlation in this area. For the central Western Ghats, from 2003 to 2008, weak negative to positive correlation was found in most of the region except southern most part, where correlation was strongly positive. From 2009 to 2012, weak negative to strong positive correlation was observed stretching from the center to eastern most part of the region from north to south (figure 41) with a minimum positive correlation of 0.95 in 2007 and 2011 and a minimum negative correlation of -0.93 in 2006. In southern Western Ghats, 2003 to 2008 exhibited stronger negative to weak positive correlation whereas, the trend changed to weak negative to stronger positive correlation from 2009–12 (figure 44) with a minimum positive correlation of 0.88 in 2008 and minimum negative correlation of -0.97 during 2005–6 and 2009–12.

Increasing temperature enhances the intensity of transpiration, and decreasing precipitation reduces the available moisture for plants (Yang et al., 2009). The relationship between LST and rainfall in the northern Western Ghats had many variations for each year. Only data of 2003 showed positive relationship whereas 2004 and 2007 depicted positive correlation in northern part and negative correlation in southern half of the region (2004 data seems to have image anomaly). All other years showed negative to weak positive correlation with a minimum positive correlation value of 0.46 in 2006 and a minimum negative correlation value of -0.31 in 2003 in the region with weak positive correlation mainly corresponding to water bodies (figure 39). Data of central Western Ghats showed both weak negative to strong positive correlation for the year 2003–5, 2007, 2009, 2011–12. The remaining years show stronger positive correlation. The minimum positive correlation was 0.74 in 2004 to a

minimum of -0.66 in 2007 (figure 42). Southern Western Ghats region showed weak negative to positive correlation in the year 2003–4 and strong negative correlation in 2009 and 2012. Stronger positive correlation exist for the year 2005–8, 2010–11 with a minimum positive correlation of 0.87 in 2003 and a minimum negative correlation of -0.17 in 2005 (figure 45).

To further understand the relationship between NDVI and climatic variables, image to image correlation coefficient (CC or r) values between monthly NDVI of forest with LST and rainfall, and monthly NDVI of agriculture/grassland class with LST and rainfall for northern, central and southern Western Ghats were computed. Table 9–11 shows monthly correlation values of 2003 and 2012 for forest and agriculture class. For other years, correlation tables are provided in Appendix 2. Correlation between monthly LST and rainfall were not computed as they did not reveal any information in previous analysis and their pattern were not clear. Missing data have been shown with "--". The analysis reconfirmed the negative correlation between NDVI and LST in northern and central Western Ghats and negative to weak positive correlation in southern Western Ghats. Most months showed weak negative to strong positive correlation between NDVI and rainfall during 2003–2012 in northern and central Western Ghats. Southern Western Ghats exhibited stronger negative to weak positive correlation between 2003 to 2008 and weak negative to stronger positive correlation from 2009–12 between NDVI and rainfall further corroborating the pixel to pixel analysis. In northern and central region, at the beginning of the summer months, most of the trees (apart from the evergreen forest) have limited vegetation growth, hence strong negative correlation implies increased temperature in those areas and less precipitation. The situation prevails until monsoon arrives at the end of summer season.

Table 9: Image to image Pearson product-moment correlation coefficient (CC or r) between monthly NDVI of forest and agriculture/grassland class with LST and rainfall for northern Western Ghats

Month, Year	CC (r) (NDVI-LST)	CC (r) (NDVI-rainfall)	Month, Year	CC (r) (NDVI-LST)	CC (r) (NDVI-rainfall)
Forest					
Jan, 2003	--	-0.09	Jan, 2012	-0.41	-0.16
Feb, 2003	--	-0.06	Feb, 2012	-0.54	-0.13
Mar, 2003	-0.65	0.06	Mar, 2012	-0.66	-0.15
Apr, 2003	-0.65	0.3	Apr, 2012	-0.73	0.26
May, 2003	-0.63	-0.19	May, 2012	-0.74	0.28
Jun, 2003	-0.43	-0.12	Jun, 2012	-0.24	0.18
Aug, 2003	-0.17	0.09	Aug, 2012	-0.1	0.08
Sep. 2003	-0.36	-0.05	Sep. 2012	-0.28	0.24
Oct, 2003	-0.73	-0.19	Oct, 2012	-0.65	0.44
Nov, 2003	-0.5	-0.13	Nov, 2012	-0.60	0.08

Dec, 2003	-0.42	0.17	Dec, 2012	-0.41	0.09
Agriculture/grassland					
Jan, 2003	--	-0.21	Jan, 2012	-0.47	-0.26
Feb, 2003	--	-0.14	Feb, 2012	-0.5	-0.21
Mar, 2003	-0.41	-0.23	Mar, 2012	-0.34	-0.16
Apr, 2003	-0.38	-0.05	Apr, 2012	-0.23	-0.14
May, 2003	-0.31	-0.15	May, 2012	-0.26	-0.18
Jun, 2003	-0.18	0.27	Jun, 2012	-0.16	0.15
Aug, 2003	-0.1	-0.03	Aug, 2012	-0.22	0.17
Sep. 2003	-0.39	0.33	Sep. 2012	-0.16	0.08
Oct, 2003	-0.55	0.38	Oct, 2012	-0.22	0.01
Nov, 2003	-0.67	-0.26	Nov, 2012	-0.49	-0.1
Dec, 2003	-0.55	0.11	Dec, 2012	-0.54	-0.1

Table 10: Image to image Pearson product-moment correlation coefficient (CC or r) between monthly NDVI of forest and agriculture/grassland class with LST and rainfall for central Western Ghats

Month, Year	CC (r) (NDVI-LST)	CC (r) (NDVI-rainfall)	Month, Year	CC (r) (NDVI-LST)	CC (r) (NDVI-rainfall)
Forest					
Jan, 2003	--	-0.24	Jan, 2012	-0.24	0.0
Feb, 2003	--	-0.31	Feb, 2012	-0.21	0.07
Mar, 2003	-0.7	-0.2	Mar, 2012	-0.26	0.27
Apr, 2003	-0.78	-0.06	Apr, 2012	-0.29	0.29
May, 2003	-0.75	-0.15	May, 2012	-0.07	0.38
Jun, 2003	-0.29	0.26	Jun, 2012	-0.10	0
Aug, 2003	-0.07	0.16	Aug, 2012	-0.4	-0.03
Sep. 2003	-0.55	0.24	Sep. 2012	-0.05	-0.04
Oct, 2003	-0.60	-0.05	Oct, 2012	0.02	-0.11
Nov, 2003	-0.65	0.27	Nov, 2012	-0.34	0.36
Dec, 2003	-0.61	0.05	Dec, 2012	-0.42	0.20
Agriculture/grassland					
Jan, 2003	--	0.04	Jan, 2012	-0.44	0.1
Feb, 2003	--	0.13	Feb, 2012	-0.27	0.2

Mar, 2003	-0.21	0.18	Mar, 2012	-0.24	0.3
Apr, 2003	-0.21	0.26	Apr, 2012	-0.21	0.3
May, 2003	-0.17	-0.01	May, 2012	-0.15	0.4
Jun, 2003	-0.45	0.23	Jun, 2012	-0.26	0.16
Aug, 2003	-0.06	0.12	Aug, 2012	0.08	0.06
Sep. 2003	-0.08	-0.08	Sep. 2012	-0.2	0.04
Oct, 2003	-0.48	0.37	Oct, 2012	-0.4	0.21
Nov, 2003	-0.39	0.35	Nov, 2012	-0.31	0.32
Dec, 2003	-0.41	0.03	Dec, 2012	-0.3	0.1

Table 11: Image to image Pearson product-moment correlation coefficient (CC or r) between monthly NDVI of forest and agriculture/grassland class with LST and rainfall for southern Western Ghats

Month, Year	CC (r) (NDVI-LST)	CC (r) (NDVI-rainfall)	Month, Year	CC (r) (NDVI-LST)	CC (r) (NDVI-rainfall)
Forest					
Jan, 2003	--	-0.06	Jan, 2012	-0.58	0.16
Feb, 2003	--	0.17	Feb, 2012	-0.68	0.2
Mar, 2003	-0.42	-0.06	Mar, 2012	-0.58	0.15
Apr, 2003	-0.66	-0.55	Apr, 2012	-0.47	0.5
May, 2003	-0.19	0.41	May, 2012	-0.17	0.33
Jun, 2003	-0.28	-0.09	Jun, 2012	-0.43	0.23
Aug, 2003	-0.18	-0.07	Aug, 2012	-0.18	0.00
Sep. 2003	-0.38	0.11	Sep. 2012	-0.32	0.19
Oct, 2003	-0.24	0.22	Oct, 2012	-0.05	0.24
Nov, 2003	-0.42	0.16	Nov, 2012	-0.73	-0.04
Dec, 2003	-0.58	-0.13	Dec, 2012	-0.62	-0.21
Agriculture/grassland					
Jan, 2003	--	0.13	Jan, 2012	0.00	0.00
Feb, 2003	--	-0.25	Feb, 2012	0.00	0.03
Mar, 2003	-0.08	0.17	Mar, 2012	0.24	-0.09
Apr, 2003	0.00	-0.02	Apr, 2012	0.32	0.28
May, 2003	0.19	-0.15	May, 2012	0.13	0.24
Jun, 2003	0.23	0.1	Jun, 2012	0.37	-0.16

Aug, 2003	0.07	0.04	Aug, 2012	0.41	0.15
Sep. 2003	-0.43	0.06	Sep. 2012	0.15	0.26
Oct, 2003	-0.36	0.11	Oct, 2012	0.22	0.08
Nov, 2003	0.33	0.01	Nov, 2012	0.26	-0.05
Dec, 2003	-0.11	-0.02	Dec, 2012	-0.11	0.1

Through long-term data analysis, trends in ecological indicators can also be assessed (Orr et al., 2004). The ultimate goal of the time-series analysis of the historical biophysical data is to improve our forecasting capability and make inferences about climate and drought conditions while improving critical vegetation mapping capabilities associated with critical needs such as production estimates, habitat assessments, etc.

5.5 Spatial patterns of seasonal NDVI trend: changes in NDVI (of dense vegetation) and the turning point

It is critical to understand the responses of dense vegetation growth to environmental change and to get a better understanding of the interactions between terrestrial ecosystem and climatic parameters.

The magnitude of the seasonal NDVI and its change over time are important indicators of the contribution of vegetation activity in different seasons to total annual plant growth (Piao et al., 2003). Western Ghats is characterised by three main seasons namely, summer (which spans from March to May), monsoon (June to October), and winter (November to February). Seasonal NDVI for summer, monsoon and winter were computed that is the average monthly composite NDVI for the three seasons. To detect the variation trends in NDVI with climatic variables (LST and rainfall) for each season (Zhang et al., 2013), a least-square regression was applied as follows:

$$y = \alpha + bt + \varepsilon$$

where y represents yearly NDVI or a climate variable, t is the year, a and b are fitted variables (a is the intercept and b is the slope), and ε is the residual error.

In this context, a piecewise regression through brute force iterative approach to detect the potential turning points (TPs) of the NDVI, LST and rainfall time-series data was used. Piece wise regression have been successfully used to evaluate the variation trends in community ecology (Swift and Hannon, 2010; Sun et al., 2011; Wang et al., 2011), NDVI and climate over time (Sun et al., 2011; Wang et al., 2011), because it effectively detects TPs in noisy time-series data. A piecewise linear regression with one TP was applied (a p -value < 0.01 was considered significant) to time-series data of NDVI, LST and rainfall from 2003 to 2012 as follows:

$$y = \begin{cases} \beta_0 + \beta_1 t + \varepsilon, & t \leq \alpha \\ \beta_0 + \beta_1 t + \beta_2(t - \alpha) + \varepsilon, & t > \alpha \end{cases}$$

Where y is yearly NDVI, t is the year, α is the estimate TP of the time-series, β_0 , β_1 , and β_2 are the regression coefficients, ε is the residual random error. Figure 46 shows the seasonal time-series graph of mean NDVI, mean LST and total rainfall. A similar cyclic pattern is also observed in central and southern Western Ghats except the range of values for NDVI, LST and rainfall.

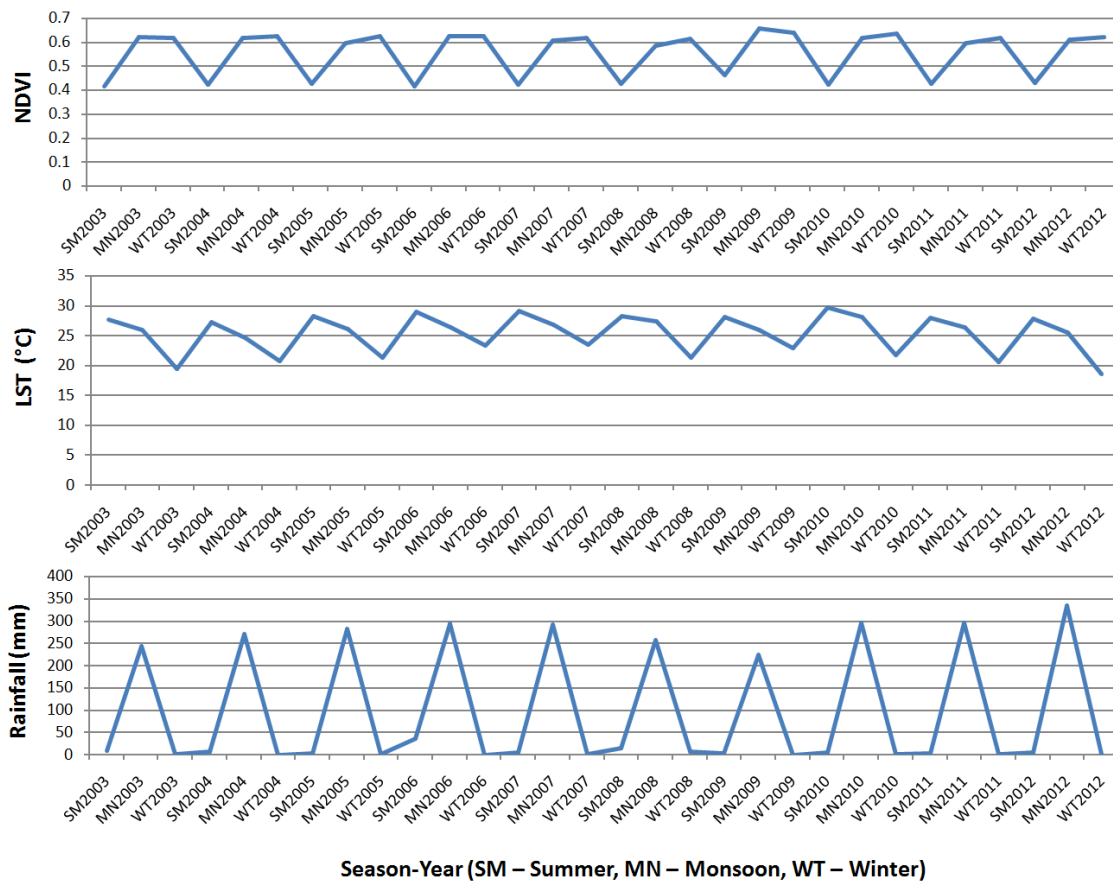


Figure 46: Trends in summer, monsoon and winter of mean forest NDVI, mean temperature and total rainfall for northern Western Ghats.

However, the patterns in figure 46 does not reveal the seasonal variations and thus figure 47 gives a detailed descriptive picture of the three variables for the 10-year interval. It is evident that NDVI values are higher in monsoon and winter compared to summer in all three regions. The summer mean temperature is higher followed by monsoon and winter in northern and central regions whereas the pattern in southern region is irregular. Rainfall has been always higher in monsoon season in all the three regions.

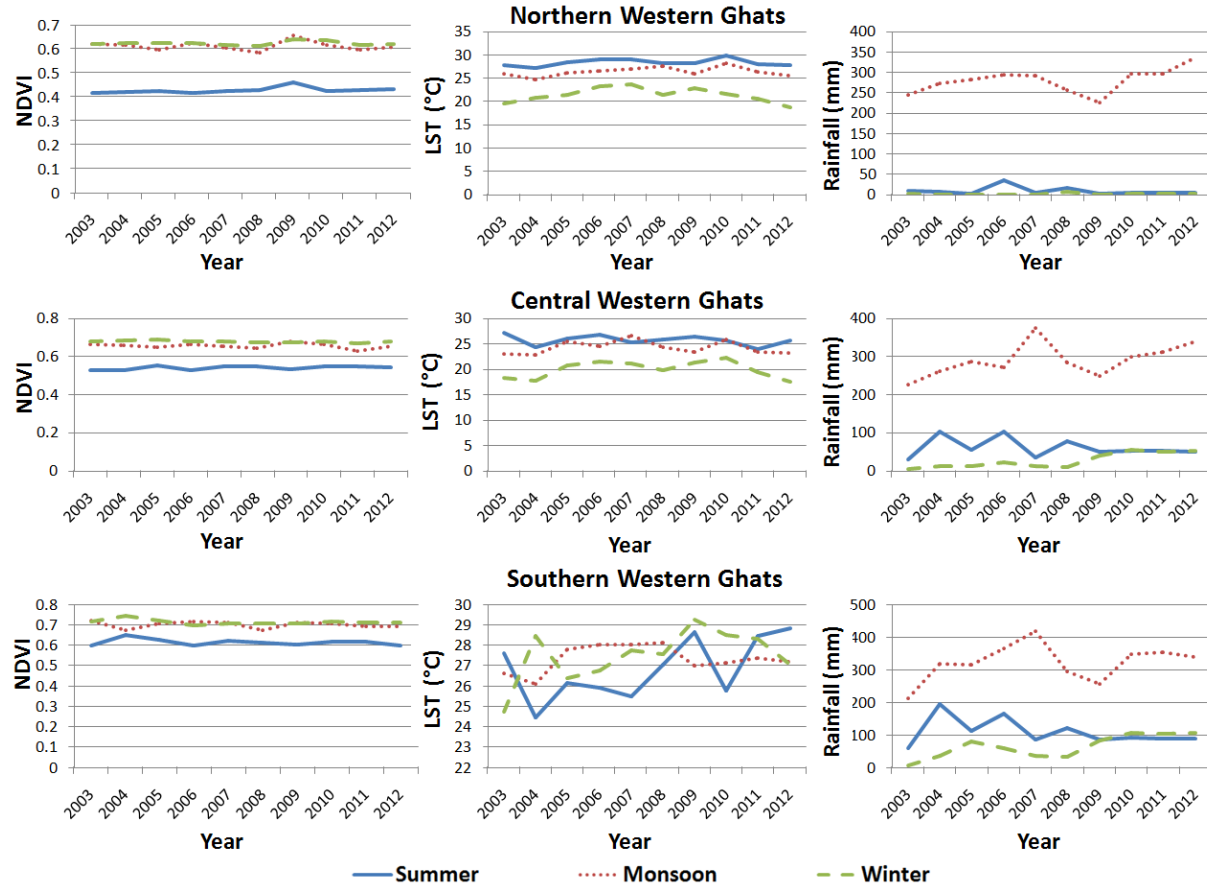


Figure 47: Seasonal trends in summer, monsoon and winter of mean forest NDVI, mean temperature and total rainfall for northern, central and southern Western Ghats.

Figure 48 shows time-series seasonal (summer, monsoon and winter) graphs of the trend in the climatic parameters (seasonal mean NDVI, seasonal mean LST and seasonal total rainfall) of forest for northern, central and southern Western Ghats respectively. X-axis is the standardised anomalies and Y-axis represents the year. A standard anomaly is a measure of the distance between data value and its mean. It removes influence of location and spread of data and is easier to discern normal versus unusual values with $\mu=0$ and $\sigma=1$.

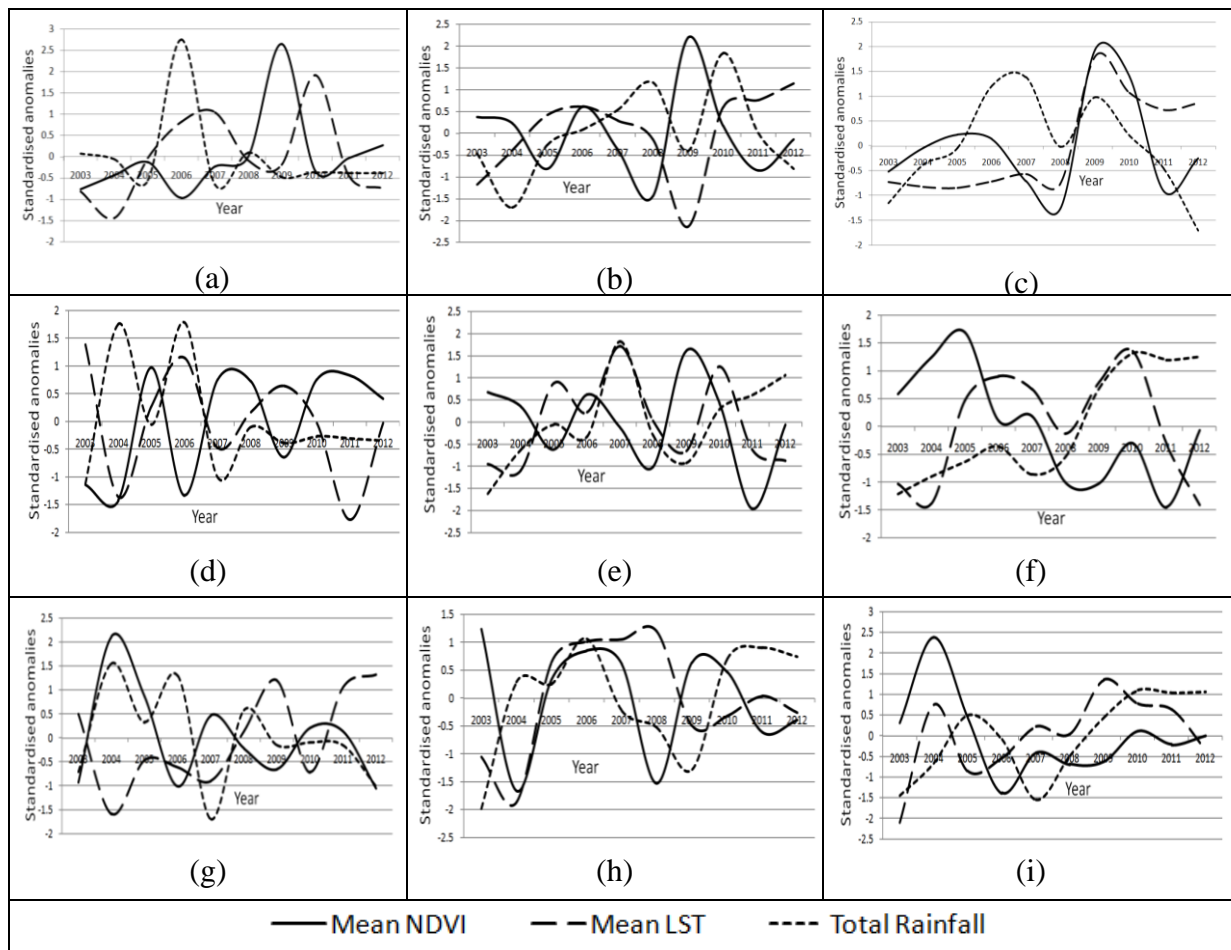


Figure 48: Standard anomalies in seasonal mean forest NDVI, seasonal mean temperature and seasonal total rainfall for northern Western Ghats (a-summer, b-monsoon, c-winter); central Western Ghats (d-summer, e-monsoon, f-winter), and for southern Western Ghats (g-summer, h-monsoon, i-winter).

The combined influence on NDVI is evident from the variation curves. In northern Western Ghats, mean of seasonal mean NDVI of forest from 2003 to 2012 was relatively lower in summer (0.43) compared to monsoon (0.61) and winter (0.63). It is clear from figure 48 (a) that seasonal mean NDVI was higher in 2009 compared to other years in summer. The mean of 10–years mean summer temperature was higher (28.36°C) and descended to 26.39°C in monsoon and around $21.4 \pm 1.6^{\circ}\text{C}$ in winter as found from the seasonal data of 2003–2012. Seasonal total rainfall was higher in 2006 in northern Western Ghats in summer (figure 48 (a)). It was found that Goa (which lies in northern Western Ghats) had an abnormally very high rainfall in May, 2006 (350 mm) which inherently increased the summer rainfall. To recall, major rain gauge stations were used in interpolation to obtain rainfall maps. NDVI, LST had an overall increasing trend and rainfall had a decreasing trend (figure 48 (a)). When LST and rainfall were high, NDVI was low (2006) and vice versa (in 2009) as shown in figure 48 (a), which also happens to be the TP of NDVI in summer (see table 12). During monsoon (figure 48 (b)), mean of total seasonal rainfall during 10 years was 1077 (± 129.43)

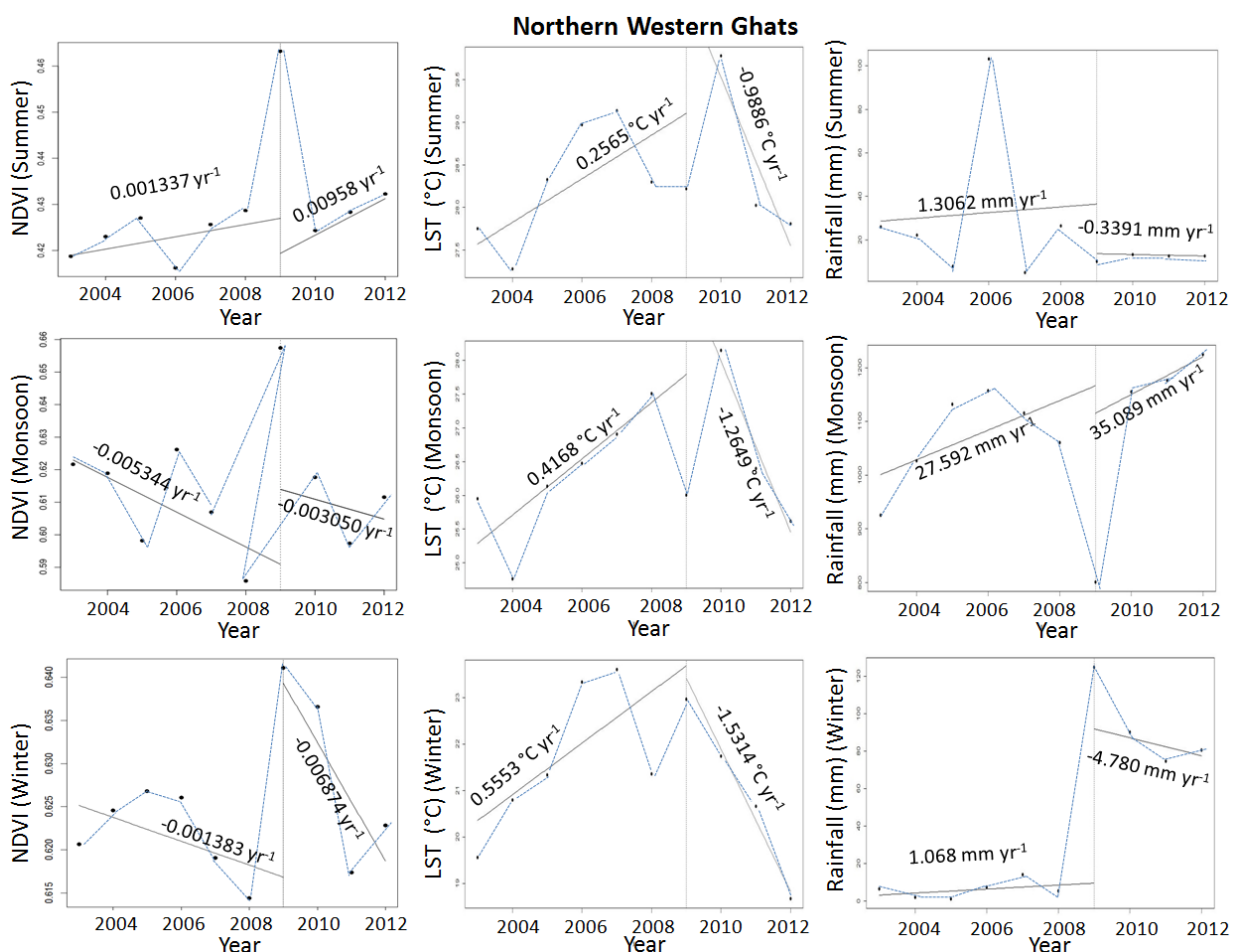
mm. NDVI, LST and rainfall had increasing trend, however in 2009, when LST and rainfall showed decreasing trends (figure 48 (b)), NDVI was maximum in the 10 years duration which is also the TP of NDVI in monsoon (table 12). During winter, mean of total seasonal rainfall from 2003 to 2012 was 40.60 (\pm 46.67) mm, which is higher compared to summer season because the area receives northeast rainfall in November (figure 48 (c)). Overall, in this region, NDVI and LST showed increasing trend and rainfall exhibited a decreasing trend.

In central Western Ghats, the situation was similar to that of northern Western Ghats. Mean of seasonal mean NDVI of 10 years increased from 0.54 to 0.66 to 0.68 during summer to monsoon to winter and mean of seasonal mean LST recorded was 25.68 °C in summer, 24.21 °C in monsoon and 19.94 °C in winter. Mean of total seasonal rainfall of 10 years was highest in monsoon (1132 ± 176 mm). The NDVI values and rainfall were relatively higher and LST was lower when compared to northern Western Ghats. Overall, seasonal mean NDVI of summer followed a sinusoidal pattern with peak in 2005, 2007 and 2010 and trough (lower amplitude value) in 2004, 2006 and 2009 as shown in figure 48 (d). Seasonal mean LST also followed sinusoidal pattern with peak in 2003, 2006 and 2009 and trough in 2004, 2007 and 2011 (figure 48 (d)). Seasonal total rainfall in summer was at its peak in 2004 and 2006 and had a decreasing trend thereafter. In 2006, when LST and rainfall were maximum, NDVI had low value (figure 48 (d)). Summers were dry with almost lesser and static rainfall from 2008, however, LST showed a regular pattern. In monsoon, mean NDVI had peak in 2009 with upward trend, mean LST and total seasonal rainfall had increasing trend with peak in 2007 (figure 48 (e)). The area had more greenery due to higher temperature and rainfall, therefore it is a growing season. In winter, mean NDVI and mean LST had a decreasing trend (figure 48 (f)). LST had peak in 2006, 2009–2010, i.e., they had warm winter with decreasing rainfall.

Southern Western Ghats showed higher mean (with lesser deviation) in summer NDVI (0.62), monsoon NDVI (0.70) and winter NDVI (0.71) from 2003 to 2012 compared to northern and central Western Ghats. It clearly reveals that southern Western Ghats have higher photosynthesis and more evergreen/semi-evergreen forest than both northern and central Western Ghats. Summer, monsoon and winter mean temperatures were higher with higher total rainfall in all the seasons. Summer temperatures have increased and NDVI and rainfall trends have decreased during 2003–2012, with peak NDVI and rainfall in 2004 (figure 48 (g)). In monsoon, NDVI shows a cyclic pattern with decreasing trend and increasing rainfall in 2006, and 2010–2012 (figure 48 (h)). In winter, NDVI had a decreasing trend with increasing LST, and increasing rainfall (because of northeast monsoon), the pattern of which was static for the last 3 years as shown in figure 48 (i)). Table 12–14 gives the TP for NDVI, LST and rainfall for the three seasons in the three regions of Western Ghats determined from piece wise regression. It is to be noted that the TP is not same for all the three climatic parameters and the seasons. Inter-seasonal variation of NDVI and climatic parameters are shown in figure 49–51. The TPs are indicated with a vertical line in each graph. Overall variation trend in NDVI–LST and NDVI–rainfall within the three regions were calculated to see if those could conceal significant changes in short periods.

Table 12: Turning point (TP) for forest NDVI, LST and rainfall for three different season for northern Western Ghats

TP (northern Western Ghats)			
Parameter → Season ↓	NDVI	LST	Rainfall
Summer	2009	2010	2007
Monsoon	2009	2010	2009
Winter	2009	2007	2009

**Figure 49: Seasonal variations of forest NDVI, LST and rainfall in summer (March to May), monsoon (June to October) and winter (November to February) in northern Western Ghats.**

At the regional scale, the TP's between 2003 to 2012 based on MODIS NDVI occurred in different years in summer, monsoon and winter season as listed in table 12. However, as NDVI showed a TP of 2009 in all three seasons, we assume a constant TP of 2009 in northern Western Ghats to make an easier interpretation of the relationships between different

climatic parameters. A statistically significant increasing trend in NDVI was observed in summer (0.0013 yr^{-1} , $R^2=0.94$, $p\text{-value}=0.003$) from 2003 to 2009 and 2009 to 2012 (0.0096 yr^{-1} , $R^2=0.92$, $p\text{-value}<0.005$). In monsoon, a decreasing trend (-0.005 yr^{-1} , $R^2=0.74$, $p\text{-value}=0.09$), and in winter a similar drift (-0.0013 yr^{-1} , $R^2=0.75$, $p\text{-value}=0.09$ from 2003 to 2009 and -0.007 yr^{-1} between 2009 to 2012, $R^2=0.71$, $p\text{-value}=0.13$) was observed.

For LST, an initial increasing and then a sudden decreasing trend was observed in summer ($0.26 \text{ }^{\circ}\text{C yr}^{-1}$, $R^2=0.62$, $p\text{-value}=0.22$), a slow increasing rate of $0.42 \text{ }^{\circ}\text{C yr}^{-1}$ was seen in monsoon ($R^2=0.62$, $p\text{-value}=0.22$), and $0.56 \text{ }^{\circ}\text{C yr}^{-1}$ was witnessed in winter ($R^2=0.80$, $p\text{-value}=0.05$) as shown in figure 49.

The rainfall trend tends to increase (1.31 mm yr^{-1} , $R^2=0.56$, $p\text{-value}=0.31$) in summer. The TP graph also shows an increasing trend between 2003 to 2009 (27.6 mm yr^{-1} , $R^2=0.84$, $p\text{-value}=0.07$) and 2009 to 2012 (35.09 mm yr^{-1} , $R^2=0.85$, $p\text{-value}=0.03$) in monsoon. The trend in winter was almost a static line between 2003 to 2009 and a slightly decreasing trend (-4.78 mm yr^{-1} , $R^2=0.99$, $p\text{-value}=0.00002$).

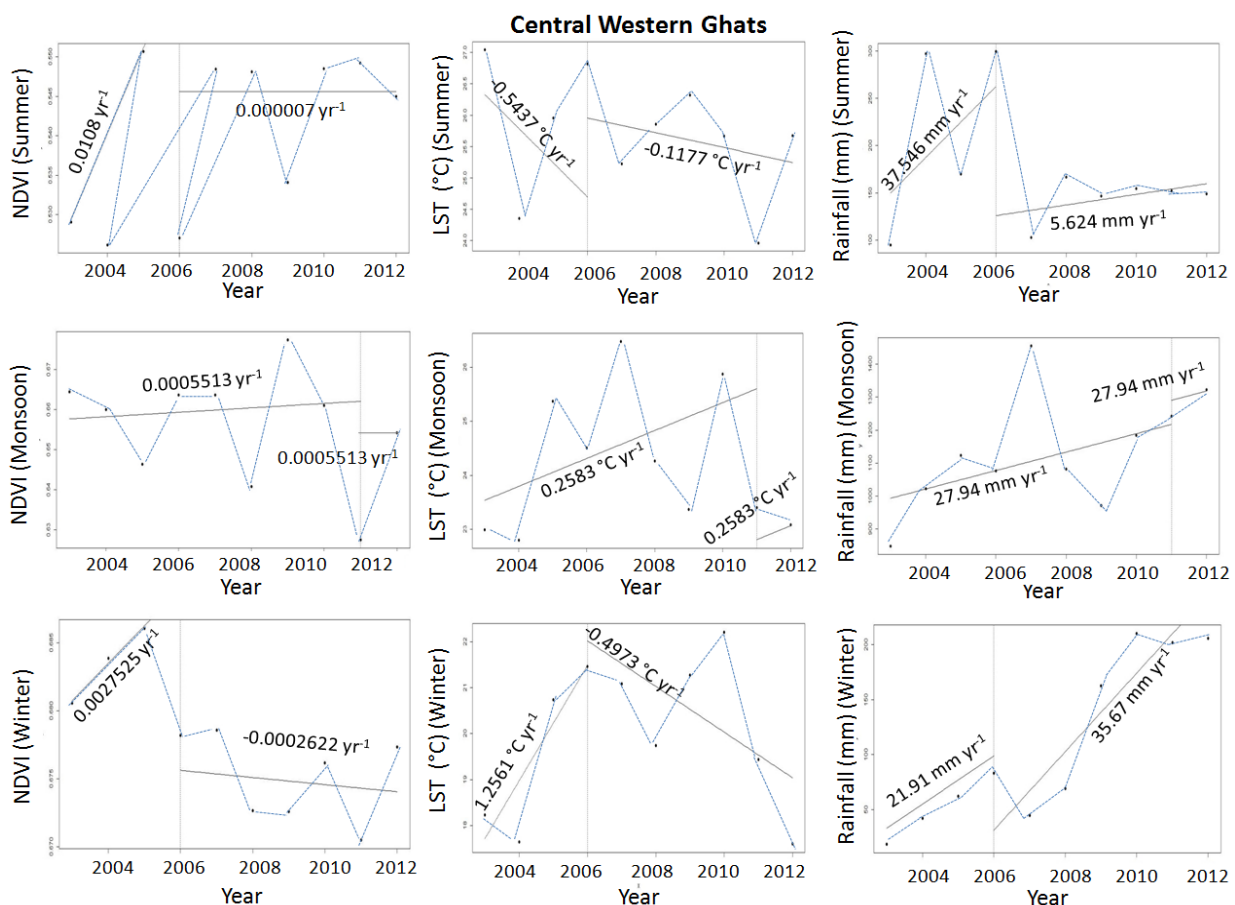


Figure 50: Seasonal variations of forest NDVI, LST and rainfall in summer (March to May), monsoon (June to October) and winter (November to February) in central Western Ghats.

Table 13: Turning point (TP) for forest NDVI, LST and rainfall for three different season for central Western Ghats

TP (central Western Ghats)			
Parameter → Season ↓	NDVI	LST	Rainfall
Summer	2006	2006	2006
Monsoon	2011	2011	2011
Winter	2006	2006	2006

NDVI TP spatially averaged over the central region with marginally increasing trend (0.01 yr^{-1} , $R^2=0.68$, $p\text{-value}=0.15$) in summer in 2006. The variation in monsoon (TP=2011) was static and winter experienced an increasing trend once again (TP=2006) with (0.002 yr^{-1} , $R^2=0.78$, $p\text{-value}=0.07$).

LST had a steep decreasing trend between 2003 to 2006 ($-0.54 \text{ }^{\circ}\text{C yr}^{-1}$, $R^2=0.59$, $p\text{-value}=0.27$) and a marginal slope between 2006 and 2012. On the other hand, LST showed steep increase in 2011 in monsoon ($0.26 \text{ }^{\circ}\text{C yr}^{-1}$, $R^2=0.56$, $p\text{-value}=0.31$) and an increasing and decreasing trend in winter with TP =2006 ($0.5 \text{ }^{\circ}\text{C yr}^{-1}$, $R^2=0.69$, $p\text{-value}=0.05$).

Rainfall showed a high increasing trend in summer with TP=2006 (37.55 mm yr^{-1} , $R^2=0.60$, $p\text{-value}=0.26$). It also showed an increasing trend throughout monsoon (27.94 mm yr^{-1} , $R^2=0.85$, $p\text{-value}=0.02$) and a steep increasing trend in winter before and after 2006 (35.67 mm yr^{-1} , $R^2=0.97$, $p\text{-value}<0.0005$).

Table 14: Turning point (TP) for forest NDVI, LST and rainfall for three different season for southern Western Ghats

TP (southern Western Ghats)			
Parameter → Season ↓	NDVI	LST	Rainfall
Summer	2005	2005	2005
Monsoon	2005	2005	2005
Winter	2005	2005	2005

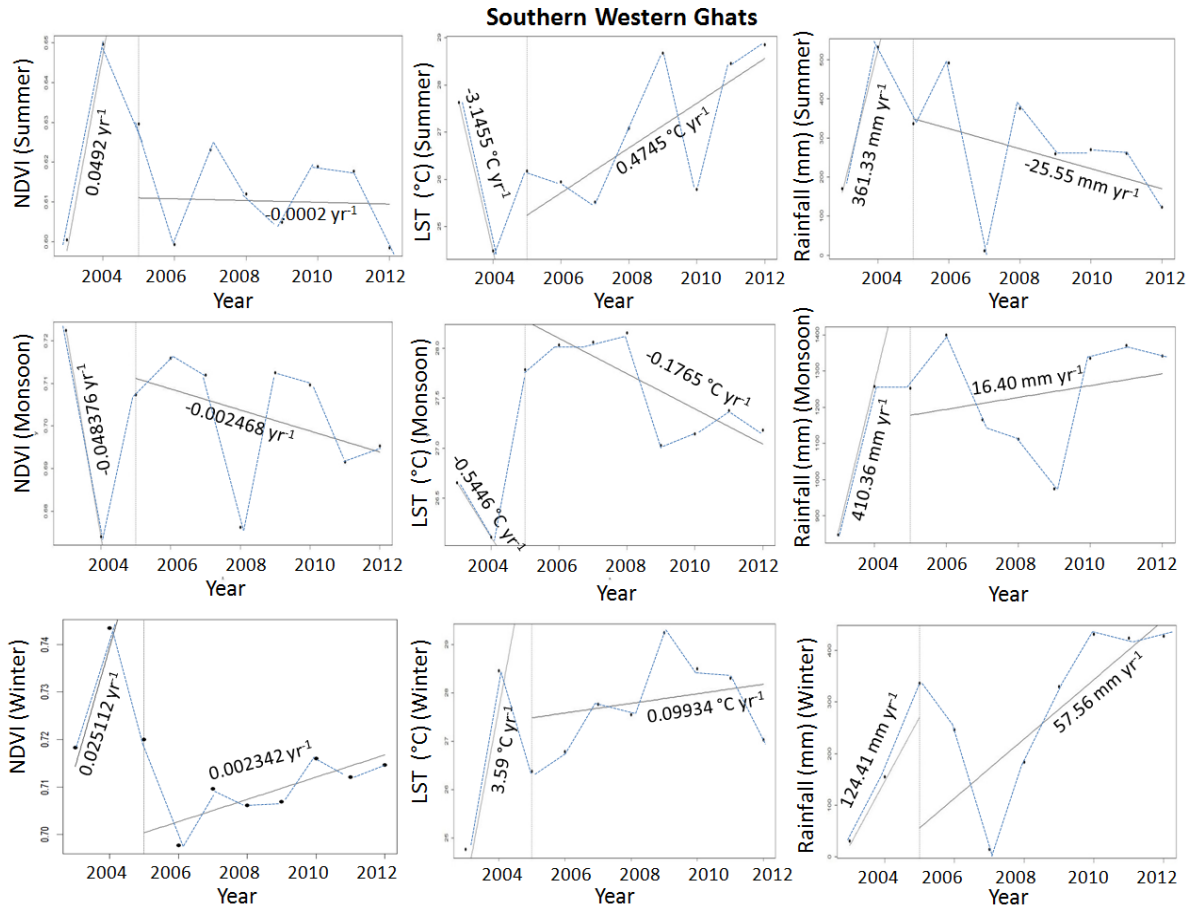


Figure 51: Seasonal variations of forest NDVI, LST and rainfall in summer (March to May), monsoon (June to October) and winter (November to February) in southern Western Ghats.

NDVI in summer in southern Western Ghats showed an increasing trend (0.05 yr^{-1} , $R^2=0.75$, $p\text{-value}=0.09$) and a steep decreasing trend in monsoon (-0.05 yr^{-1} , $R^2=0.56$, $p\text{-value}=0.31$), followed by a steep increment in winter (0.03 yr^{-1} , $R^2=0.68$, $p\text{-value}=0.16$).

LST showed a decreasing trend in summer ($-3.15 \text{ }^{\circ}\text{C yr}^{-1}$, $R^2=0.66$, $p\text{-value}=0.08$) and increasing trend ($0.48 \text{ }^{\circ}\text{C yr}^{-1}$, $R^2=0.64$, $p\text{-value}=0.04$) after TP in 2005. In contrary, it showed a continuous decreasing pattern ($-0.55 \text{ }^{\circ}\text{C yr}^{-1}$, $R^2=0.85$, $p\text{-value}=0.03$) and an increasing trend in winter before the TP ($3.59 \text{ }^{\circ}\text{C yr}^{-1}$, $R^2=0.72$, $p\text{-value}=0.11$).

Rainfall showed an increasing trend before TP in 2005 ($361.33 \text{ mm yr}^{-1}$, $R^2=0.84$, $p\text{-value}=0.005$) and a slightly decreasing pattern ($-25.55 \text{ mm yr}^{-1}$, $R^2=0.44$, $p\text{-value}=0.30$) in summer. In monsoon, it showed an increasing trend both before and after the TP ($410.36 \text{ mm yr}^{-1}$, $R^2=0.57$, $p\text{-value}=0.01$; 16.40 mm yr^{-1} , $R^2=0.72$, $p\text{-value}=0.11$) and a similar increasing trend in winter (57.56 mm yr^{-1} , $R^2=0.87$, $p\text{-value}=0.02$).

The response of NDVI, LST and rainfall to climate change: Changes in vegetation productivity is mainly determined by climate change (Angert et al., 2005; Piao et al., 2006). Previous studies have shown that temperature changes at the beginning and end of growing

season have large effects on vegetation growth. In our study, we found weak negative correlation between NDVI and LST in northern and central Western Ghats (see table 15) with a strong negative correlation during 2006–2012 in central region in summer. A strong negative correlation was also observed in southern Western Ghats, i.e. when temperature has increased in summer, a slowed plant growth is observed in all the regions. A negative correlation is also observed between NDVI–rainfall in northern and central Western Ghats, however, southern region showed strong positive correlation during 2003–2005 and a negative correlation during 2005–2012. Rainfall causes more clouds to appear and then reduces incident radiation. Limited incident radiation hinders photosynthesis which is essential for vegetation growth (Song and Ma, 2008).

Table 15: CC (*p*-value < 0.01) between forest NDVI-LST and forest NDVI-rainfall for the TP years for summer, monsoon and winter for the three regions of the Western Ghats

		Northern Western Ghats			Central Western Ghats			Southern Western Ghats		
TP→		2003–2012	2003–2009	2009–2012	2003–2012	2003–2006	2006–2012	2003–2012	2003–2005	2005–2012
Summer	NDVI-LST	-0.12	-0.04	-0.34	-0.34	0.04	-0.76	-0.7	-0.99	-0.49
	NDVI-rainfall	-0.41	-0.44	-0.99	-0.54	-0.39	-0.76	0.35	0.99	-0.49
TP→		2003–2012	2003–2009	2009–2012	2003–2012	2003–2011	2011–2012	2003–2012	2003–2005	2005–2012
Monsoon	NDVI-LST	-0.3	-0.47	-0.15	-0.10	-0.11	-1	0.14	0.52	-0.16
	NDVI-rainfall	-0.64	-0.7	-0.94	-0.45	-0.48	1	-0.29	-0.75	0.05
TP→		2003–2012	2003–2009	2009–2012	2003–2012	2003–2006	2006–2012	2003–2012	2003–2005	2005–2012
Winter	NDVI-LST	0.32	0.31	0.78	-0.20	-0.21	0.17	0.05	0.93	-0.07
	NDVI-rainfall	0.62	0.83	0.87	-0.60	-0.16	-0.33	-0.12	-0.05	0.44

During monsoon, negative relationship between vegetation and temperature was keenly observed in northern and central Western Ghats and a weak positive correlation in southern Western Ghats. Vegetation also had a negative correlation with rainfall in all the three regions. Vegetation was more negatively correlated with rainfall than with temperature.

In winter season, northern and southern Western Ghats experienced a positive correlation between vegetation and temperature and a weak negative correlation was found in central region. Rainfall was strongly positively correlated with vegetation in northern region and negatively correlated in central and southern Western Ghats. Thus whether temperature and rainfall were the main climate factors affecting vegetation productivity varied with region, season and TP. In southern Western Ghats, NDVI were alternatively regulated by temperature and rainfall in different seasons (see table 15, southern Western Ghats column). However, monsoon and winter NDVI was more correlated with temperature than with rainfall, with similar results been reported by Mao et al., (2012). The overall decline in vegetation may be attributed to decreasing rainfall and low soil temperature that do not provide suitable environment for growth of vegetation.

Although the trends in seasonal NDVI were complicated and exhibited variations, a high degree of spatial heterogeneity on per-pixel analysis was found. Figure 52 shows spatial patters of the summer and winter seasons NDVI trend for dense vegetation class and table 16 gives the numerical description of the rate of change. Monsoon trend images were not generated as the data had presence of cloud.

Table 16: Rate of change of forest NDVI, LST and rainfall for summer and winter season

Northern Western Ghats								
NDVI (yr ⁻¹)			LST (°C yr ⁻¹)			rainfall (mm yr ⁻¹)		
Rate of change	ha	%	Rate of change	ha	%	Rate of change	ha	%
Summer								
-0.034 – 0	545690	21.17	-0.071 – 0	381750.23	81.98	-4.7 – 0	2394457	93.26
0 – 0.031	2032031	78.83	0 – 0.067	83902.52	18.02	0 – 1.2	173056	6.74
Winter								
-0.020 – 0	120106.98	18.58	-1.28 – 0	735611.38	97.92	8 – 20	389266	13.19
0 – 0.022	526321.77	81.42	0 – 0.92	15593.07	2.08	20 – 37	2562328	86.81
Central Western Ghats								
NDVI (yr ⁻¹)			LST (°C yr ⁻¹)			rainfall (mm yr ⁻¹)		
Rate of change	ha	%	Rate of change	ha	%	Rate of change	ha	%
Summer								
-0.034 – 0	458812	27.72	-0.82 – 0	1604316	88.98	5.2 – 10	138067.26	19.66
0 – 0.051	1196283	72.28	0 – 0.41	198623	11.02	10 – 21.2	564167.96	80.34
Winter								
-0.022 – 0	427804	16.15	-0.74 – 0	2223262	72.66	-35 – -10	4323886	97.64
0 – 0.032	2221605	83.85	0 – 0.76	836761	27.34	-10 – -6	104338	2.36
Southern Western Ghats								

NDVI (yr^{-1})			LST ($^{\circ}\text{C yr}^{-1}$)			rainfall (mm yr^{-1})		
Rate of change	ha	%	Rate of change	ha	%	Rate of change	ha	%
Summer								
-0.045 – 0	1282187	31.79	-0.04 – 0	473.76	0.06	-26 – 0	4067942	86.73
0 – 0.046	2750969	68.21	0 – 0.51	754192.03	99.94	0 – 9	622483	13.27
Winter								
-0.029 – 0	737212	30.62	-0.25 – 0	20790	1.95	18 – 30	882285	31.8
0 – 0.028	1670660	69.38	0 – 0.51	1046397	98.05	30 – 74	1892024	68.2

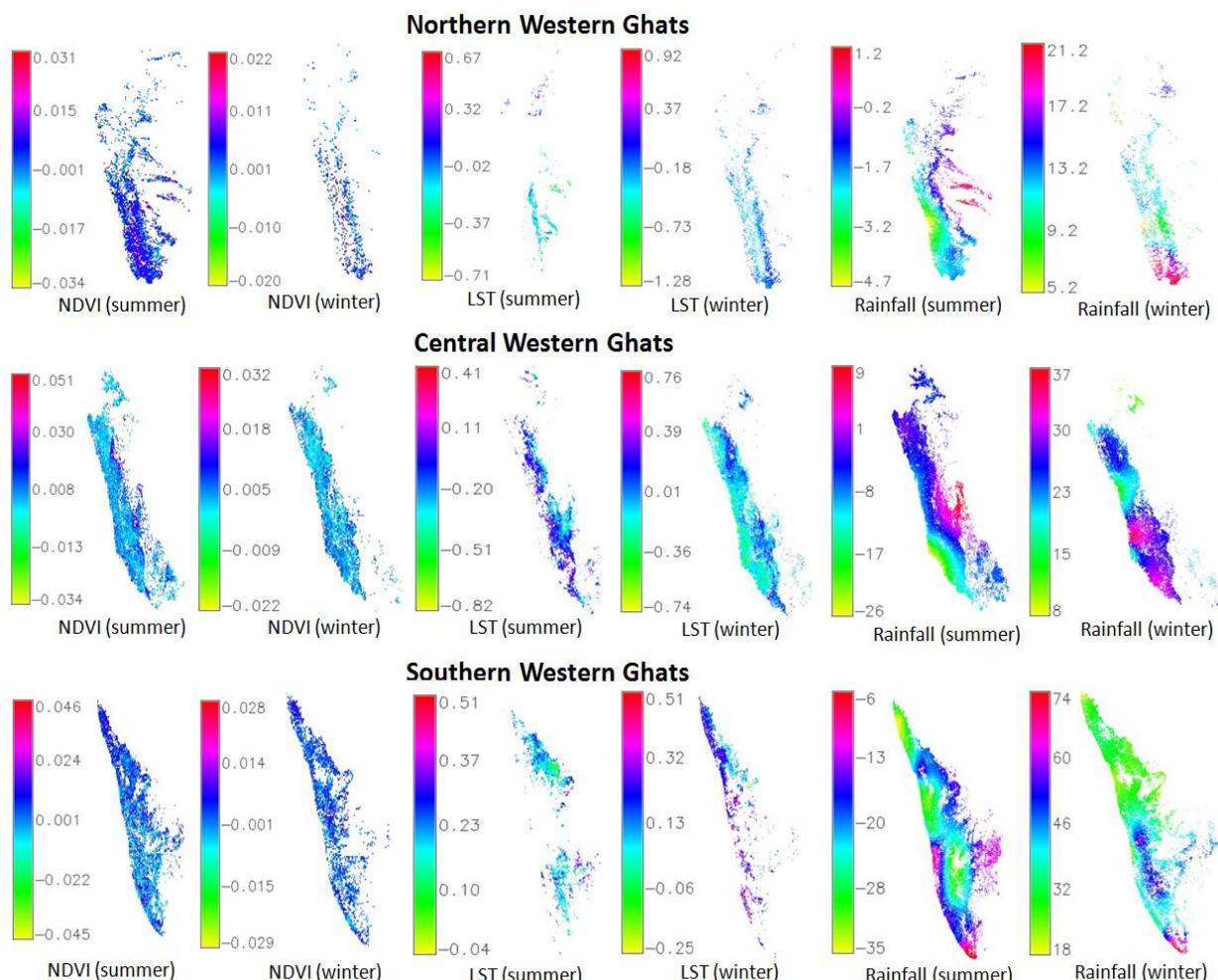
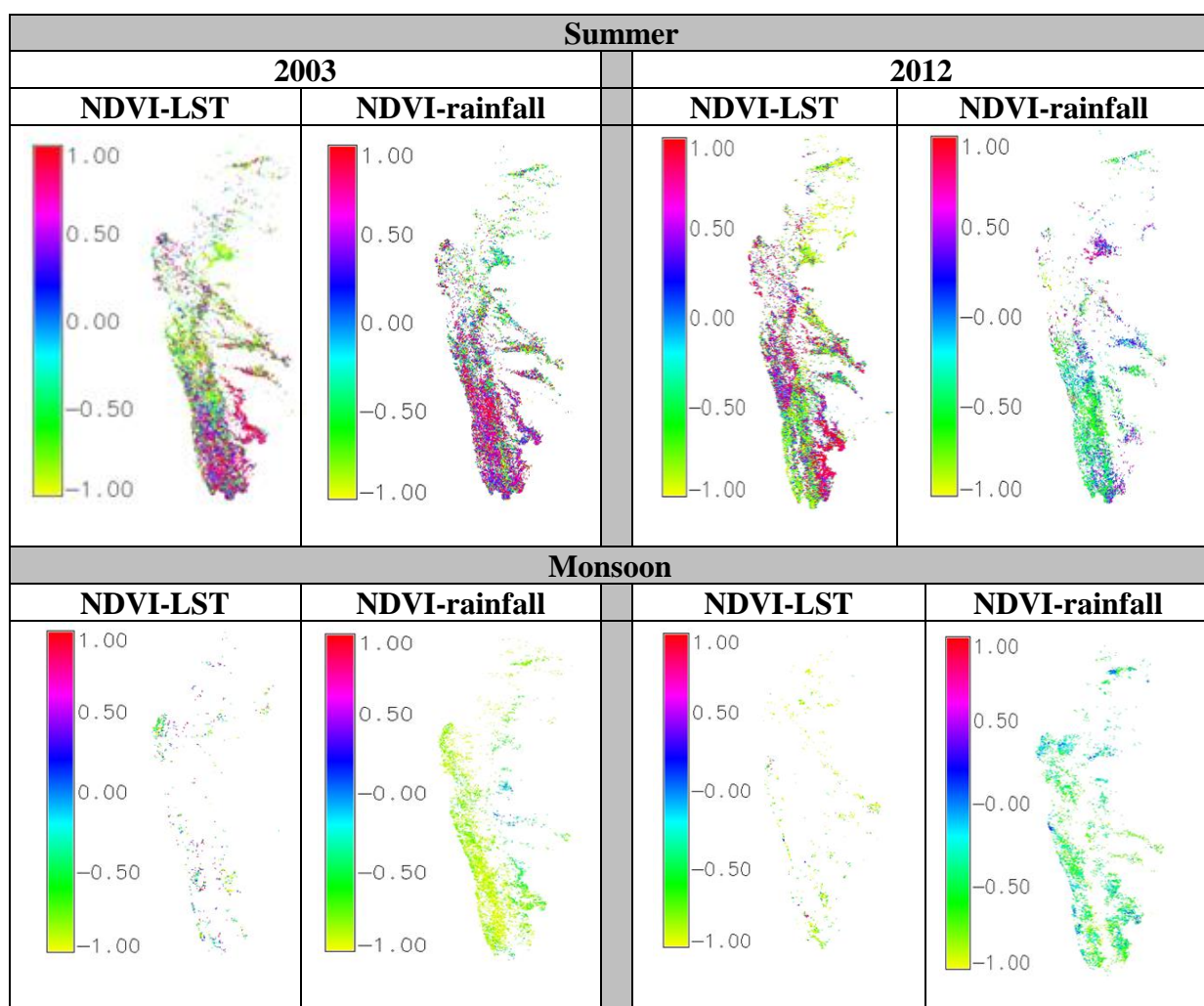


Figure 52: Spatial distribution of trends (rate of change) in summer and winter season for forest NDVI (yr^{-1}), LST ($^{\circ}\text{C yr}^{-1}$) and rainfall (mm yr^{-1}).

A positive rate of change in NDVI (0-0.031 yr^{-1}) in almost 78.83% of the south-western part of northern Western Ghats was observed in summer. In the same region, a downward trend (-0.2 to -4.7 mm yr^{-1}) was observed in rainfall in the summer months in 93% of the area. The pixels that showed moderate increasing trends in NDVI were mainly distributed in the western part of central Western Ghats (0 to 0.051 yr^{-1}) in 72% of the area in summer and (0 to

0.032 yr^{-1}) in winter season in nearly 84% of the area. Central Western Ghats also exhibited 0.3 to 0.1 $^{\circ}\text{C yr}^{-1}$ in summer (see figure 52: LST (summer) in central western Ghats) and -0.3 to 0.3 $^{\circ}\text{C yr}^{-1}$ in winter. The rainfall trend varied with a wide range in both summer and winter. In southern Western Ghats, the NDVI rate of change ranged between -0.015 to 0.02 and -0.01 to 0.01 yr^{-1} in > 70% of the area in summer and winter (see figure 52). LST data had many missing pixels and did not reveal much information. Rainfall varied with a wide range with maximum change happening at -6 mm yr^{-1} in summer and 74 mm yr^{-1} in winter in the southern-most part of the southern Western Ghats.

Figure 53–55 shows pixel to pixel correlation between NDVI of forest and LST, and NDVI of forest and rainfall in summer, monsoon and winter for the three regions of Western Ghats. Summer season showed positive correlation between NDVI–LST and NDVI–rainfall in south-western region in 2003 which showed a decreasing pattern in 2012. In monsoon season, correlation between NDVI–LST was not evident because of lack of data and NDVI–rainfall showed weak positive correlation in both 2003 and 2012. Winter depicted a similar pattern in 2003 and 2012 where correlation between NDVI–LST and NDVI–rainfall did not indicate much change in the decade. NDVI–LST showed low and weak negative correlation and NDVI–rainfall showed high positive correlation between 0.5 towards 0.75 (figure 53).



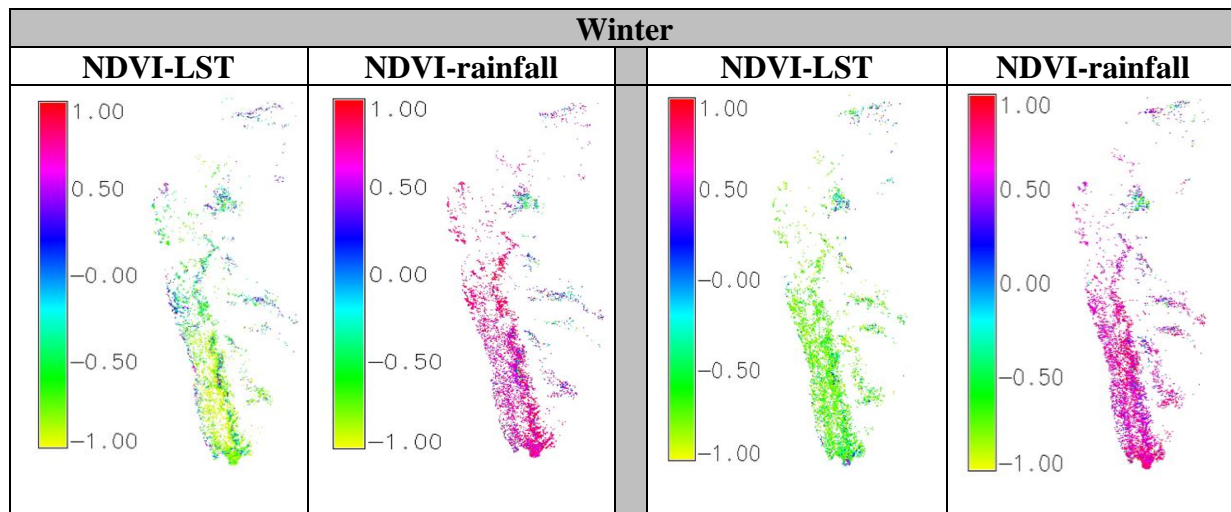
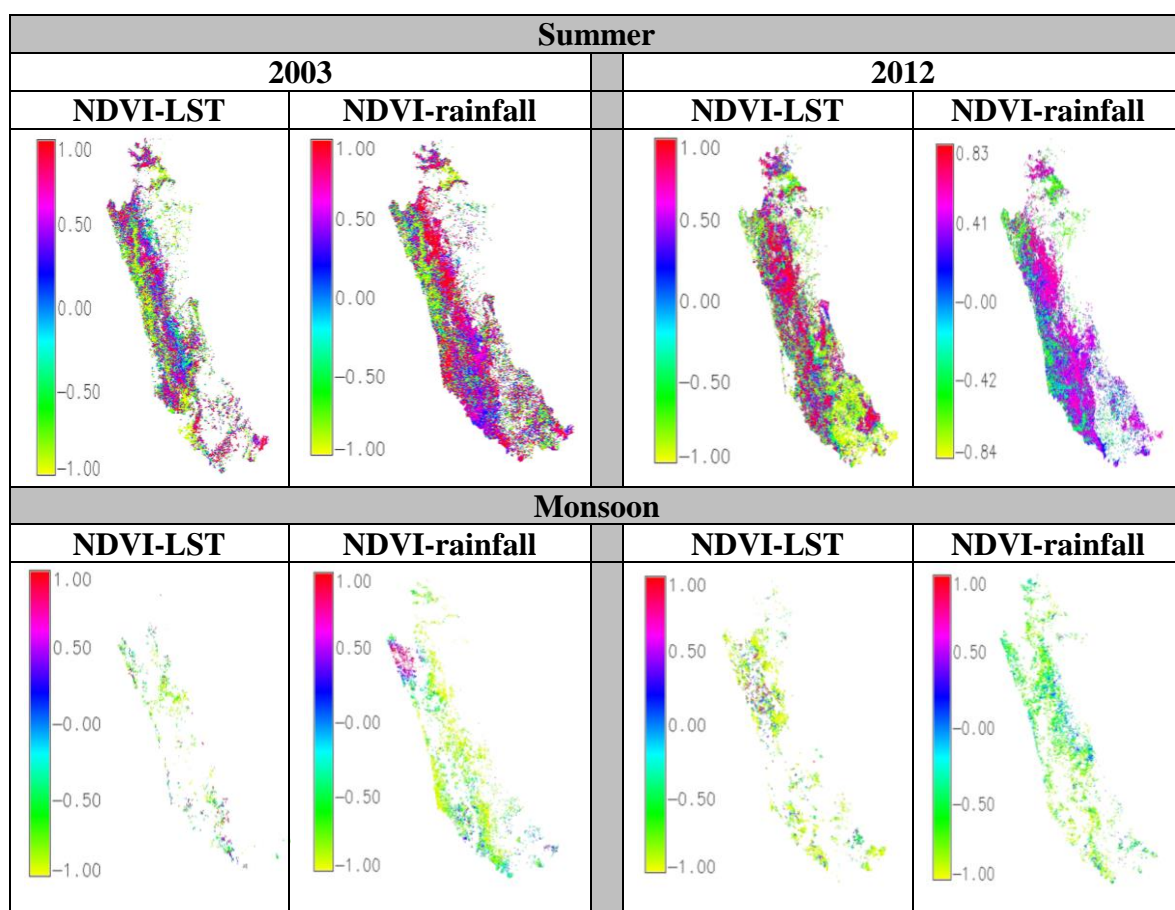


Figure 53: Pixel to pixel correlation between forest NDVI, LST and rainfall for summer, monsoon and winter season for northern Western Ghats.



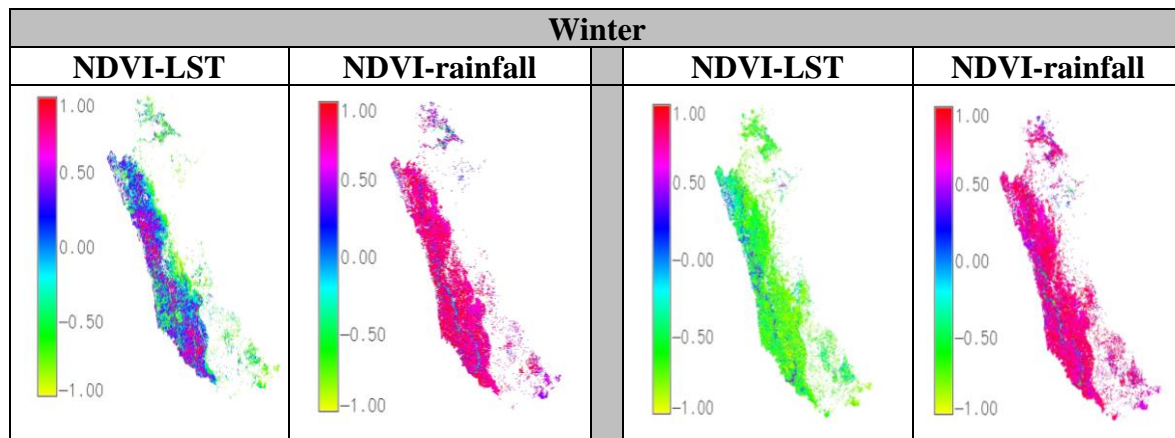
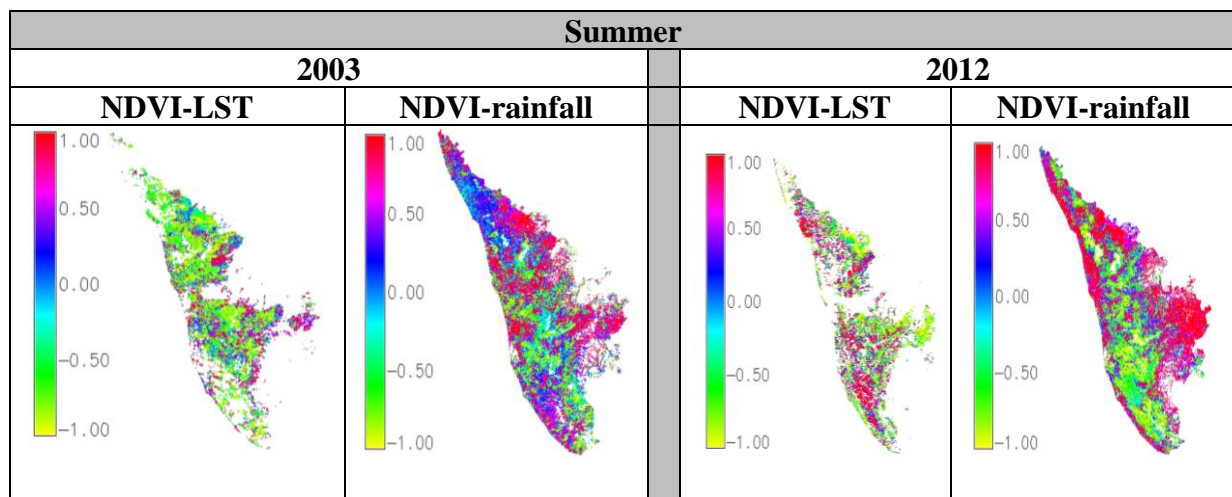


Figure 54: Pixel to pixel correlation between forest NDVI, LST and rainfall for summer, monsoon and winter season for central Western Ghats.

In central Western Ghats, 2003 and 2012 showed similar correlation between NDVI–LST and NDVI–rainfall in summer (figure 54). Monsoon correlation images did not reveal much information due to lack of data, however, they generally showed weak negative to strong negative correlations. In winter, NDVI–LST and NDVI–rainfall showed similar trend as that of northern Western Ghats. NDVI–LST had weak negative correlation and NDVI–rainfall had strong positive correlation in 2003 and 2012.



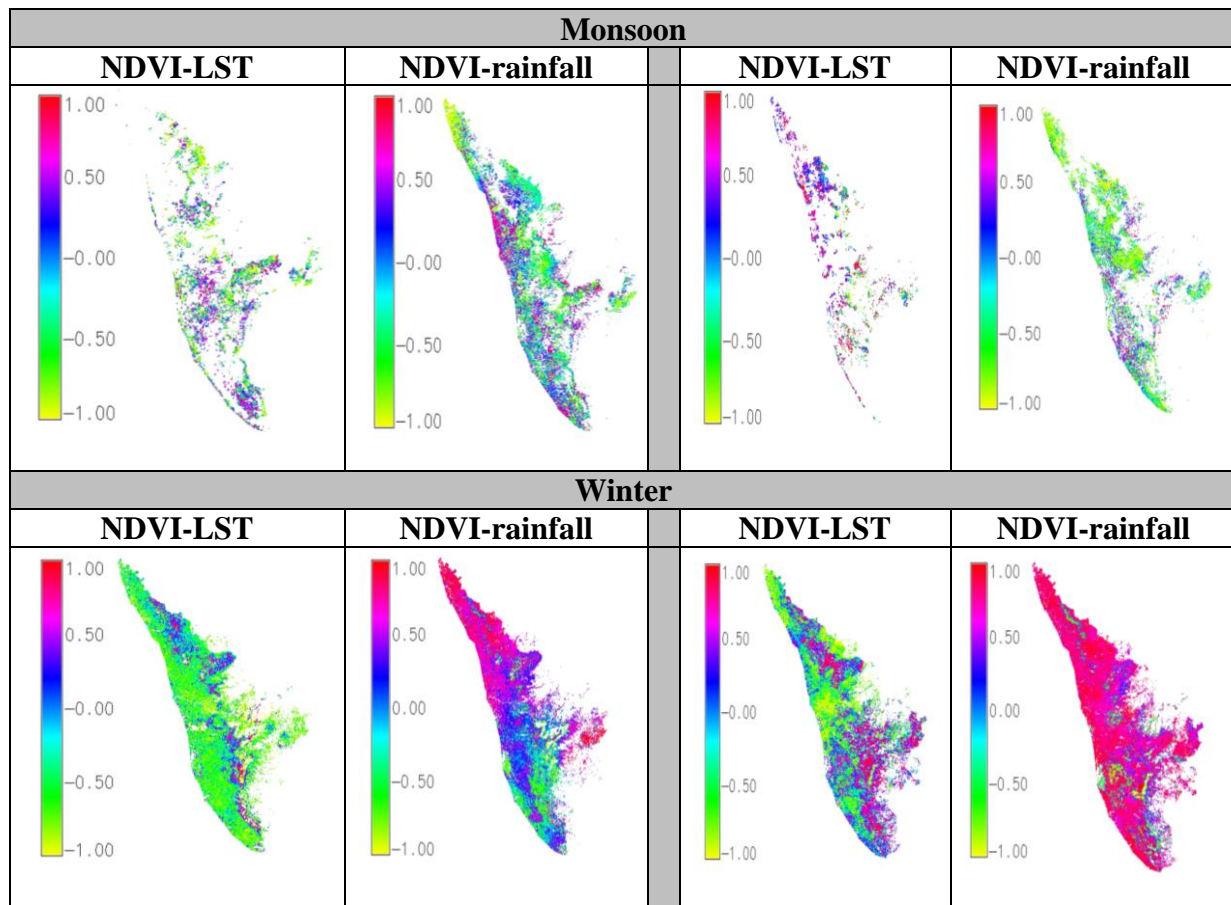


Figure 55: Pixel to pixel correlation between forest NDVI, LST and rainfall for summer, monsoon and winter season for southern Western Ghats.

Southern Western Ghats in general had similar seasonal correlation trends between NDVI–LST and NDVI–rainfall as that of northern and central regions during 2003 and 2012. NDVI–rainfall had more positive correlation in all the three seasons compared to NDVI–LST. Winter showed low to strong negative correlation between NDVI–LST and strong positive correlation between NDVI–rainfall similar to northern and central Western Ghats (figure 55).

6. Is there a varying trend in rainfall pattern as a result of climate change/variability in Western Ghats?

One of the challenges posed by climate change is ascertainment, identification and quantification of trends in rainfall to assist in formulation of adaptation and mitigation measures through appropriate strategies of water resource management (Kampata et al., 2008). Rainfall is one of the key climatic variables that affects spatio-temporal patterns on water availability (De Luis et al., 2000). Therefore, analysis of rainfall trends is important to understand the impacts of climate change for water resource management (Haigh, 2004).

Non-stationary rainfall data in modelling hydrological systems often produce erroneous water resource scenarios (IPCC, 2007). Analysis of trends in rainfall is both temporal and spatial in dimension, so the trends of temporal time-series need to be analysed for homogeneity within the region. An attempt is made here to see if the decadal rainfall pattern in the individual three regions of Western Ghats belong to similar regime, have had any significant trends and if there was a homogeneity in trends among stations. The objective is to determine any intervention on the rainfall time-series and subsequently study the trends in the non-intervened series of monthly rainfall. For this, data from rain gauge stations in the northern, central and southern Western Ghats were used. Rainfall data are sometimes exposed to step or gradual changes (Ndiritu, 2005) due to anthropogenic or natural factors which bring inconsistencies and non-homogeneity in the data. Therefore, data from the individual rain gauge stations need to be assessed for intervention analysis before the trend analysis to confirm if data from individual rainfall stations belong to the same population or climatic regime as explained in the steps below:

- a) Intervention analysis – This was carried out using CUSUM (cumulative summation) technique (Parida et al., 2003) to determine inconsistencies in rainfall data which might have resulted from climate change and/or anthropogenic activities. CUSUM is based on the cumulative sum of the data. If X_1, X_2, \dots, X_n represents n data points, then cumulative sum (S_i) is $S_i = S_{i-1} + (X_i - \bar{X})$ for $i = 1$ to n . The cumulative sum is the cumulative sum of differences between the values and the average (\bar{X}). Since the average is subtracted from each value, the cumulative sum ends at zero i.e. $S_n = 0$. When the series under test is free from any intervention, the plot of S_i versus i normally oscillates around the horizontal axis. A steady decline or rise of this plot suggests the possibility of intervention from the year of observation. Positive slopes indicate a period of above average values of rainfall and a negative slope indicates vice versa. The two series may split by the date of change due to possible intervention and require step change analysis for confirmation of the change.
- b) Step change analysis – Wilcoxon-Mann-Whitney rank-sum test (Helsel and Hirsch, 2002) is a nonparametric test used for testing the difference in median of two subsets of data representing the before and after-event/intervention to analyse any step change. Rank-sum test overcomes the problem of small sample sizes and distribution (Yue et al., 2002). The data are first ranked from smallest to largest and in case of ties (equal data values), the average of rank is used. Next, sum of the ranks of the observations in the smaller group and in the larger group are computed along with the mean and standard deviation of the entire sample. The null hypothesis H_0 is that no change has occurred in the time-series or the two samples come from the same population (i.e. have the same median) is accepted when the computed statistic is less than the value obtained from a normal distribution table at a specific significance level.

- c) Trend analysis – Trend analysis is carried using Mann-Kendall method which is a non-parametric test and can be used to analyse trends of rainfall (Burns et al., 2007; Ndiritu, 2005). A positive value of the test statistic indicates an increasing trend and a negative value indicates a decreasing trend. The null hypothesis H_0 is that there is no trend in the data which is either accepted or rejected depending on the value of the test statistic at a specified significance level.
- d) Test of homogeneity of stations – This is used by combining data from several stations to obtain a single global trend (Helsel and Hirsch, 2002) through Mann-Kendall statistic for each rain gauge station. To test the homogeneity of trends at multiple stations, the homogeneity χ^2 statistic is calculated. The null hypothesis H_0 is that the stations are homogeneous with respect to the trend, and is tested by comparing χ^2 to tables of χ^2 distribution with $p-1$ degrees of freedom, where "p" is the number of rain gauge stations. If it exceeds the critical value for the preselected ' α ' then H_0 is rejected and conclusions are made that different stations exhibit different trends.

10 rain gauge stations were selected in northern, 11 in central and 19 in southern Western Ghats. For each station, monthly rainfall data were collected from 2003 to 2012. Intervention analysis, step change analysis, trend analysis and test of homogeneity were carried out for each station. We present here analysis of 2 random locations from each region. For northern region, CUSUM plots of Mumbai and Goa are shown in figure 56. Figure 57 shows the CUSUM plots for Honavar and Udupi in central, and figure 58 shows CUSUM plots for Kozhikode and Thiruvananthapuram in southern Western Ghats. The monthly rainfall time-series from figure 56 clearly show that for most of the periods the monthly rainfall have been below the long-term mean with an intervention in May, 2005 in northern Western Ghats. For central Western Ghats, Honavar and Udupi shows oscillating patterns with increasing trends in the later part of the decade as shown in figure 57. These two stations (Honavar and Udupi) indicate May, 2007 as the year of intervention. Figure 58 indicates a decreasing pattern with below long-term mean values, and increasing pattern with above long-term mean values in the second half of the decade in southern Western Ghats. Some intervention is seen during April, 2004 in the data.

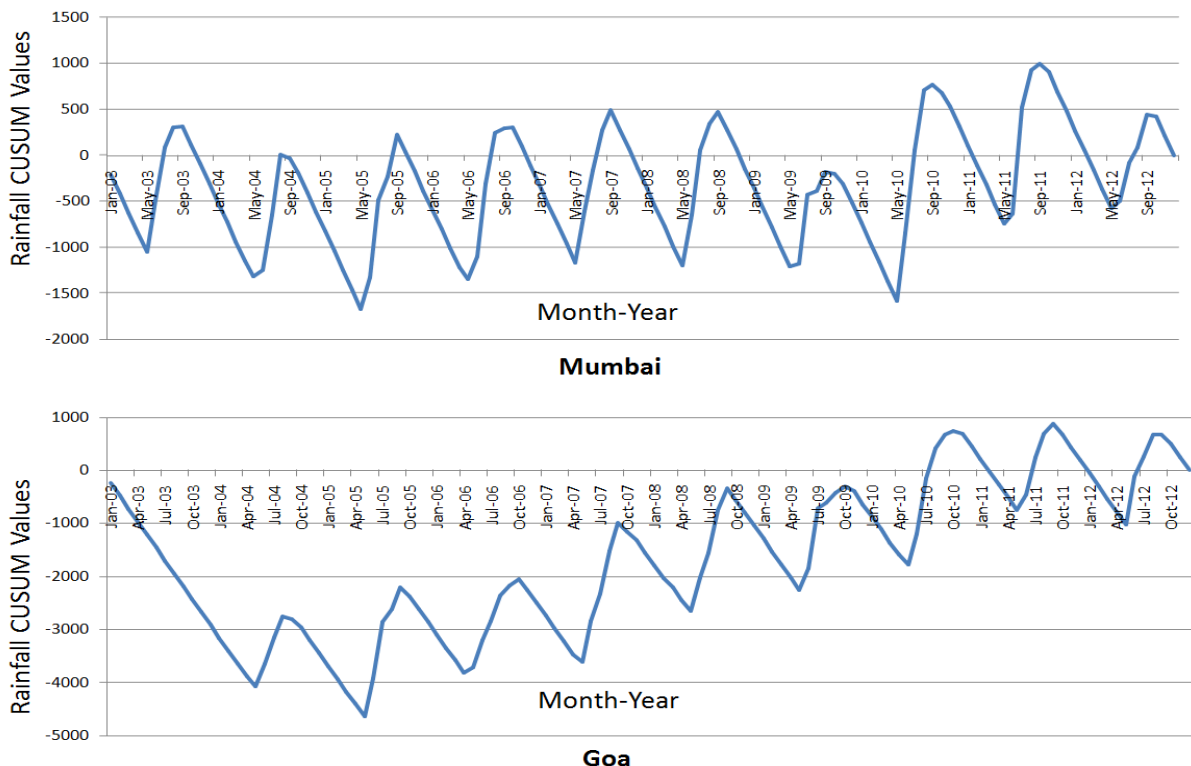


Figure 56: CUSUM plots using observed monthly total rainfall for Mumbai and Goa (January, 2003 to December, 2012).

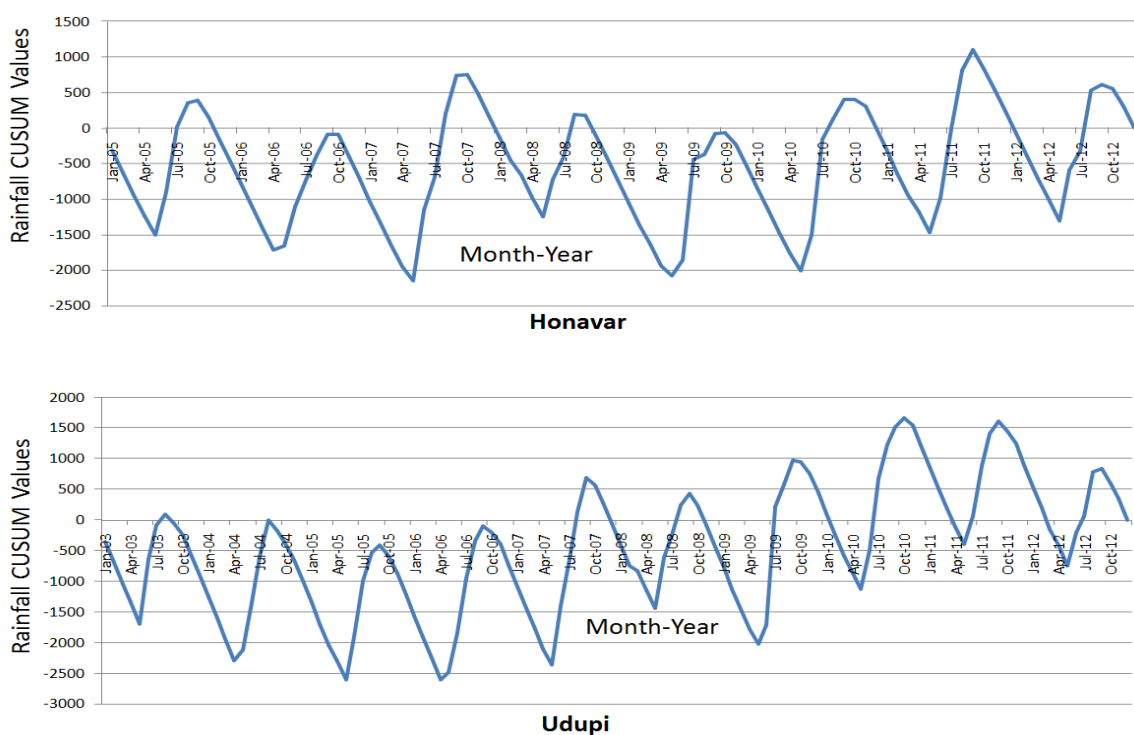


Figure 57: CUSUM plots using observed monthly total rainfall for Honavar and Udupi (January, 2003 to December, 2012).

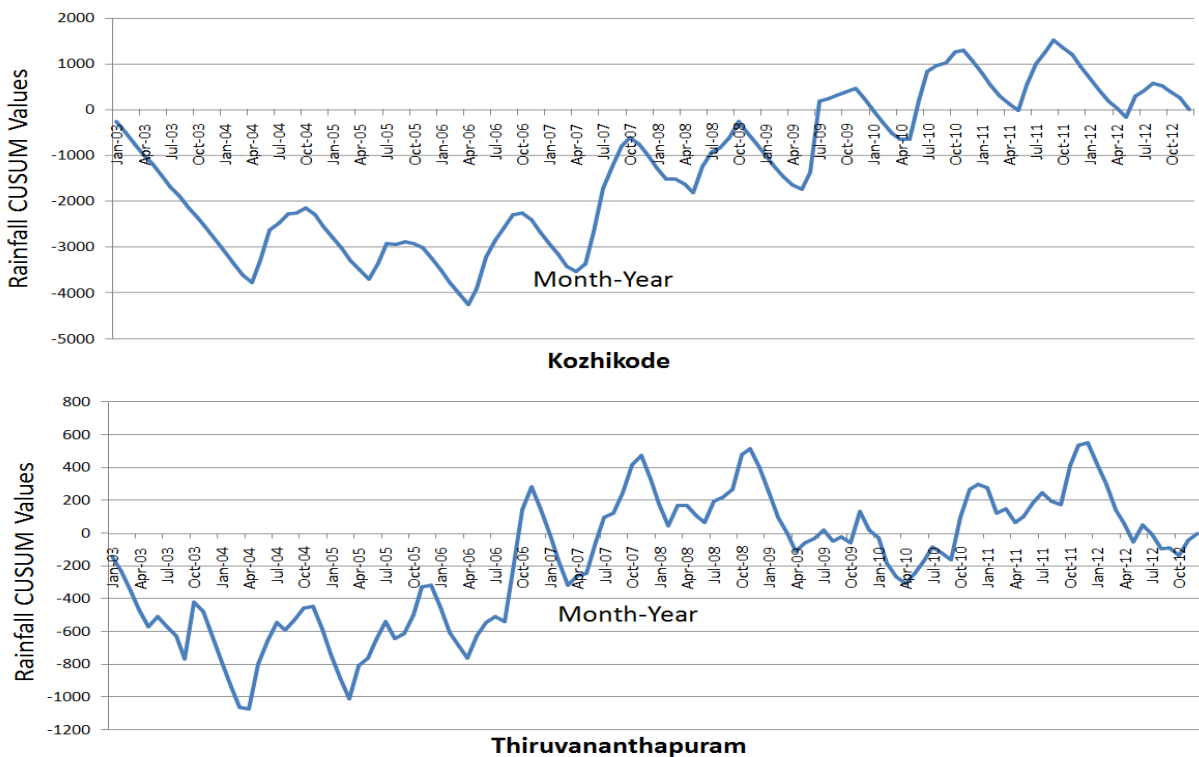


Figure 58: CUSUM plots using observed monthly total rainfall for Kozhikode and Thiruvananthapuram (January, 2003 to December, 2012).

However, to confirm the intervention, the data were subjected to step change analysis. The null hypothesis and alternate hypothesis are stated as below:

H_0 = No change has occurred in the time-series.

H_1 = Change has occurred in the time-series.

At a 0.05 significance level, Wilcoxon-Mann-Whitney rank-sum test showed different results as indicated in table 17.

Table 17: Results of step change analysis using rank sum method

Rain gauge station	Test statistic W	p-value	Result
Mumbai	1330	0.4329	Not significant, Accept H_0
Goa	909	0.0015	Significant, Reject H_0
Honavar	783.5	0.1287	Not significant, Accept H_0
Udupi	1549	0.2286	Not significant, Accept H_0
Kozikode	355	0.0002	Significant, Reject H_0
Thiruvananthapuram	479	0.0064	Significant, Reject H_0

Mumbai data showed that there was no strong evidence against H_0 , hence H_0 was accepted and there was no intervention, while for Goa data, H_0 was rejected in favour of H_1 indicating an intervention. In central Western Ghats, Honavar and Udupi did not show any change in

regime while in the southern Western Ghats, Kozikode and Thiruvananthapuram data showed signs of interventions and revealed that annual rainfall time-series did not belong to the same population.

The trends for each station were investigated using the Mann-Kendall test. The null hypothesis and alternate hypothesis are:

H_0 = There is no trend in the data.

H_1 = There is trend in the data.

At a 0.05 significance level, Mann-Kendall test showed the following results as indicated in table 18.

Table 18: Trend analysis using Mann-Kendall method

Rain gauge station	Kendall's tau statistic	2-sided <i>p</i> -value	Result
Mumbai	-0.0136	0.83717	Not significant Accept H_0
Goa	0.126	0.051248	Not significant Accept H_0
Honavar	0.0435	0.54447	Not significant Accept H_0
Udupi	0.0362	0.56683	Not significant Accept H_0
Kozikode	0.0926	0.13785	Not significant Accept H_0
Thiruvananthapuram	0.0491	0.42853	Not significant Accept H_0

For all the stations, there was no evidence of significant trends (due to lack of strong evidence against H_0), therefore, no trends were observed in Mumbai, Goa, Honavar, Udupi, Kozikode and Thiruvananthapuram rainfall data as the computed statistic were found to be less than the critical value at $\alpha = 0.05$. Rainfall showed a very small increasing trend except in Mumbai, where a small decreasing trend was observed.

For a region wise analysis about the trend at multiple rain gauge stations, the test for homogeneity was applied. It is necessary to investigate whether the monthly rainfall data are serially correlated or not through autocorrelation and partial autocorrelation plots corresponding to the time-series data. In case the monthly data are serially correlated, Mann-Kendall test in conjunction with block bootstrapping can be used to account for the correlation. In this study, it was found that the autocorrelation and partial autocorrelation present in the series were not significant. Using the results from Mann-Kendall calculations from table 18, the homogeneity χ^2 statistic was calculated (Helsel and Hirsch, 2002).

$$\chi^2_{homogeneity} = \chi^2_{total} - \chi^2_{trend}$$

The null hypothesis and alternate hypothesis are:

H_0 = Rain gauge stations are homogeneous with respect to trend.

H_1 = Rain gauge stations are not homogeneous with respect to trend.

Since $\chi^2_{homogeneity}$ was less than the critical value at $\alpha = 0.05$ for all the three regions with $p-1$ degrees of freedom (where "p" is the number of rain gauge stations in each region), it was concluded that there were no sufficient evidence against H_0 , so the individual stations in northern, central and southern Western Ghats had homogeneous trends.

Modelling and forecasting the monthly rainfall time-series: Understanding and predicting rainfall variability helps in planning and decision making process. Analysis of the time-series data is a very powerful tool to reveal the patterns of data and an important aspect is to find a suitable time-series seasonal model for forecasting the amount of rainfall. The analysis is done with two objectives (Harris and Solis, 2003):

- Build a model that fits the data or represents the data well (to find patterns).
- Use the model to forecast.

While the analysis is being carried, we assume the data to follow some pattern along with some outliers (random noise). The data can be smoothed using either moving average or median smoothing or exponential smoothing to remove the outliers or random variations. The method of smoothing is chosen on the basis of data and the level of smoothing required. Moving average is simplest but it does not work well with the data having many outliers, in such cases, median smoothing is more useful. Exponential smoothing is believed to be superior since recent observations in the data are given relatively more weightage in forecasting than the older observations. Most time-series patterns can be described in terms of two basic classes of components: trend and seasonality (Brockwell and Davis, 2002).

- **Trend analysis:** Trend is defined as the long term movement in a time-series without calendar related and irregular effects, and is a reflection of the underlying level. It is the result of influences, for example, population growth, general economic changes, etc. There are no proven automatic techniques to identify trend components in the time-series data. More often, trend is visible from the time-series plots which is usually monotonous in nature, either downward or upward. Time-series data can contain trends which may be either linear or exponential or mixed. If the time-series data contain considerable outliers, then the first step in the process of trend identification is smoothing. In this process, the non-systematic components of individual observations cancel out each other hence making the data free of outliers. They filter out the noise and convert the data into a smooth curve that is relatively unbiased by outliers (Harris and Solis, 2003).

- **Seasonality:** A seasonal pattern exists when a series is influenced by seasonal factors (e.g., the quarter of the year, the month, or day of the week). Seasonality is always of a fixed and known period, therefore, seasonal time-series are also called periodic time-series and represents the repetitive component (Harris and Solis, 2003). A cyclic pattern exists when data exhibit trough and crest that are not of fixed period i.e. if the fluctuations are not of fixed period then they are cyclic; if the period is unchanging and associated with some aspect of the calendar, then the pattern is seasonal. In general, the average length of cycles is longer than the length of a seasonal pattern, and the magnitude of cycles tend to be more variable than the magnitude of seasonal patterns. In short, trend represents long-term change in the level of the series, seasonal factor is the periodic fluctuations of constant length and the random part is the error which is unpredictable in behaviour.

A seasonal time-series consists of a trend component, a seasonal component and an irregular component as its constituents. It assumes the following decomposition model:

$$\begin{aligned} \text{Data} &= \text{Pattern} + \text{Error} \\ &= f(\text{trend}, \text{seasonality}, \text{error}) \end{aligned}$$

So, at any time period 't', the mathematical model for decomposing seasonal data can be approximated as

$$Y_t = f(S_t, T_t, E_t)$$

where,

Y_t = time-series value (actual data) at period t.

S_t = seasonal component at period t.

T_t = trend component at period t.

E_t = irregular component at period t.

Therefore, decomposing a seasonal time-series means separating the time-series into these three components, i.e., estimating these three components. However, the exact functional form of the time-series data depends on the type of decomposition model as briefed below:

- Additive model – An additive model is appropriate if the magnitude of the seasonal fluctuation does not vary with the level of the series.
- Multiplicative model – A multiplicative model is more prevalent with economic series since most seasonal economic series have seasonal variations which increases with the level of the series.

Once the time-series is decomposed, a model can be constructed to analyse and forecast the time-series data. In this study we adopt autoregressive integrated moving average (ARIMA) (Brockwell and Davis, 2002), which is one of the most widely used models in analysing and forecasting time-series data. ARIMA models are defined for stationary time-series, therefore, if the data are non-stationary time-series i.e. when the mean and variance of the data points is not constant over a period of time, the time-series is differenced to obtain a stationary series. ARIMA is then fitted to determine whether AR (Auto Regressive) or MA (Moving Average) terms are needed to correct any autocorrelation that remains in the differenced series. By analysing the autocorrelation function (ACF) and partial autocorrelation function (PACF) plots of the differenced series, the numbers of AR and/or MA terms that are needed can be determined. ACF plot is a bar chart of the coefficients of correlation between a time-series and lags of itself and PACF plot is a plot of the partial correlation coefficients between the series and lags of itself. From this, an ARIMA(p, d, q) model is obtained, where "p" is the value of autocorrelation for the time-series or auto-regression part, "d" is the order of differencing used or trend part and "q" is the partial autocorrelation for the time-series or the moving average part.

- Auto-regressive component (p) – These components represent the memory of the process of previous observations. p in ARIMA(p, d, q) refers to number of auto-regressive components. If it is 1, then the current observation is correlated with its previous observation. If its value is 2, then the observations are correlated with the observations at lag 2.
- Trend component (d) – When time-series data have trend component, then the mean and variance are not constant over time, so it is differentiated once to make the mean constant and d in ARIMA(p, d, q) is set to 1 else the time-series data are differentiated again to make the mean constant and d is set to 2. Differencing is the easiest way to make a non-stationary time-series into stationary time-series. The residual plot and the Normal Q-Q (normal quantile-quantile) plot are generally linear. The Box-Pierce test is used to check the significance of normality of the residual at a specified lag.
- Moving-averages component (q) – These components represent the memory of the process for previous random shocks, i.e., random components in the time-series. q refers to number of auto-regressive components in the ARIMA(p, d, q). If it is 1, then the current observation is correlated with the random shock at lag 1. If its value is 2, then the observations are correlated with the random shocks at lag 2.

ARIMA model includes an explicit statistical model for the irregular component of a time-series that allows non-zero autocorrelations in the irregular component. This feature is not supported by exponential smoothing method, therefore ARIMA model is preferred for forecasting. In this study, the seasonal rainfall time-series is assumed to be of the additive model form since the random fluctuations in the data are roughly constant over time and do not depend on the level of time-series i.e. there is a seasonal variation in the amount of

rainfall per month. Adf (Augmented Dickey-Fuller test) and the pp test (Phillips-Perron Unit Root test) were performed to check for the stationarity. The Dickey-Fuller Z(alpha) was -5.1208, Truncation lag parameter was 1 and *p*-value was 0.000821 indicating that the null hypothesis H_0 : data is stationary was true.

Figure 59 shows the rainfall time-series plot of forest cover for northern, central and southern Western Ghats, all of them highlighting a seasonal component. Figure 60 shows the decomposition of additive time-series into original time-series (top), the estimated trend component (second from top), the estimated seasonal component (third from top), and the irregular component (bottom). The highest seasonal factor is observed in July and August and the lowest is recorded from December through April for each year in northern Western Ghats. The estimated seasonal component shows increasing trend in rainfall from May to August and a decreasing trend from September to April in this region. In central and southern Western Ghats, highest seasonal factor is seen in June and lowest is observed in January–February. Here, the estimated seasonal component shows increasing trend in rainfall from April to June and a decreasing trend from July to March.

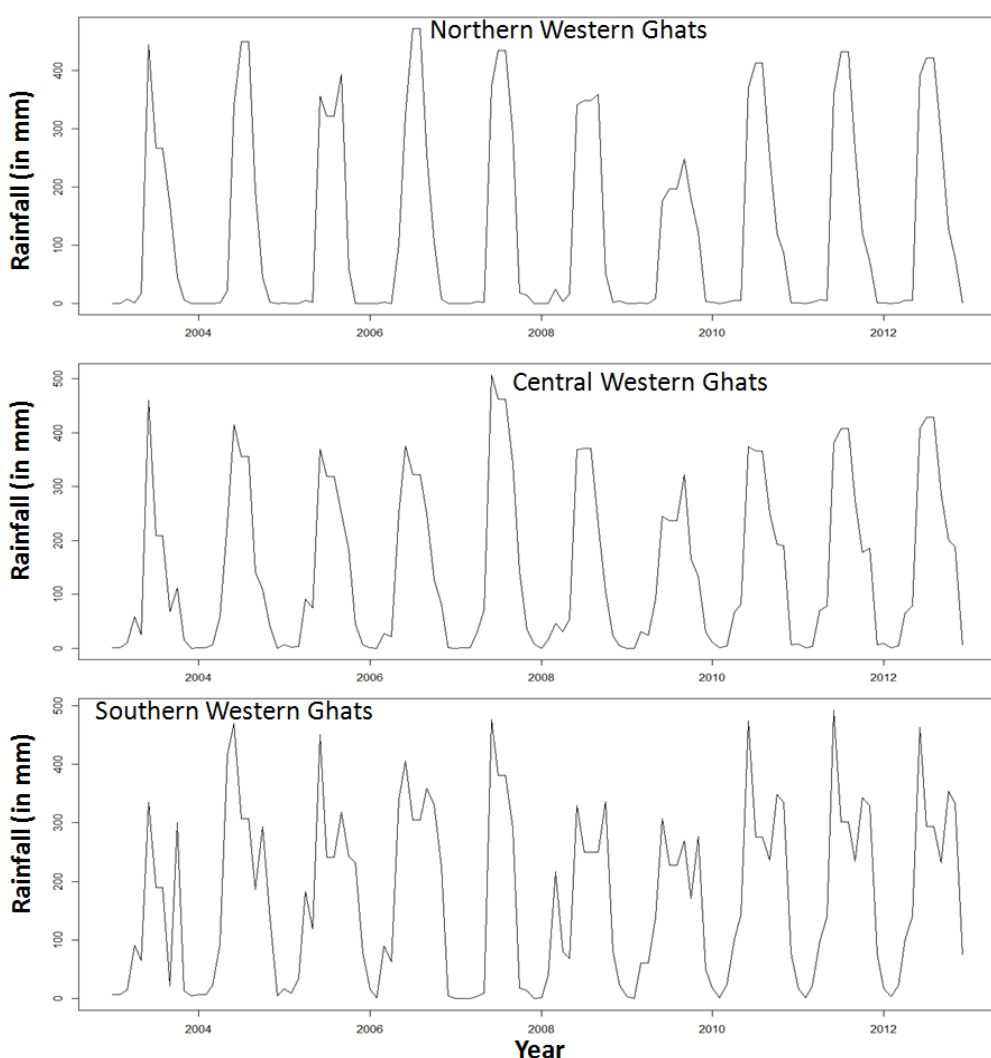


Figure 59: Rainfall time-series plots over dense forest cover.

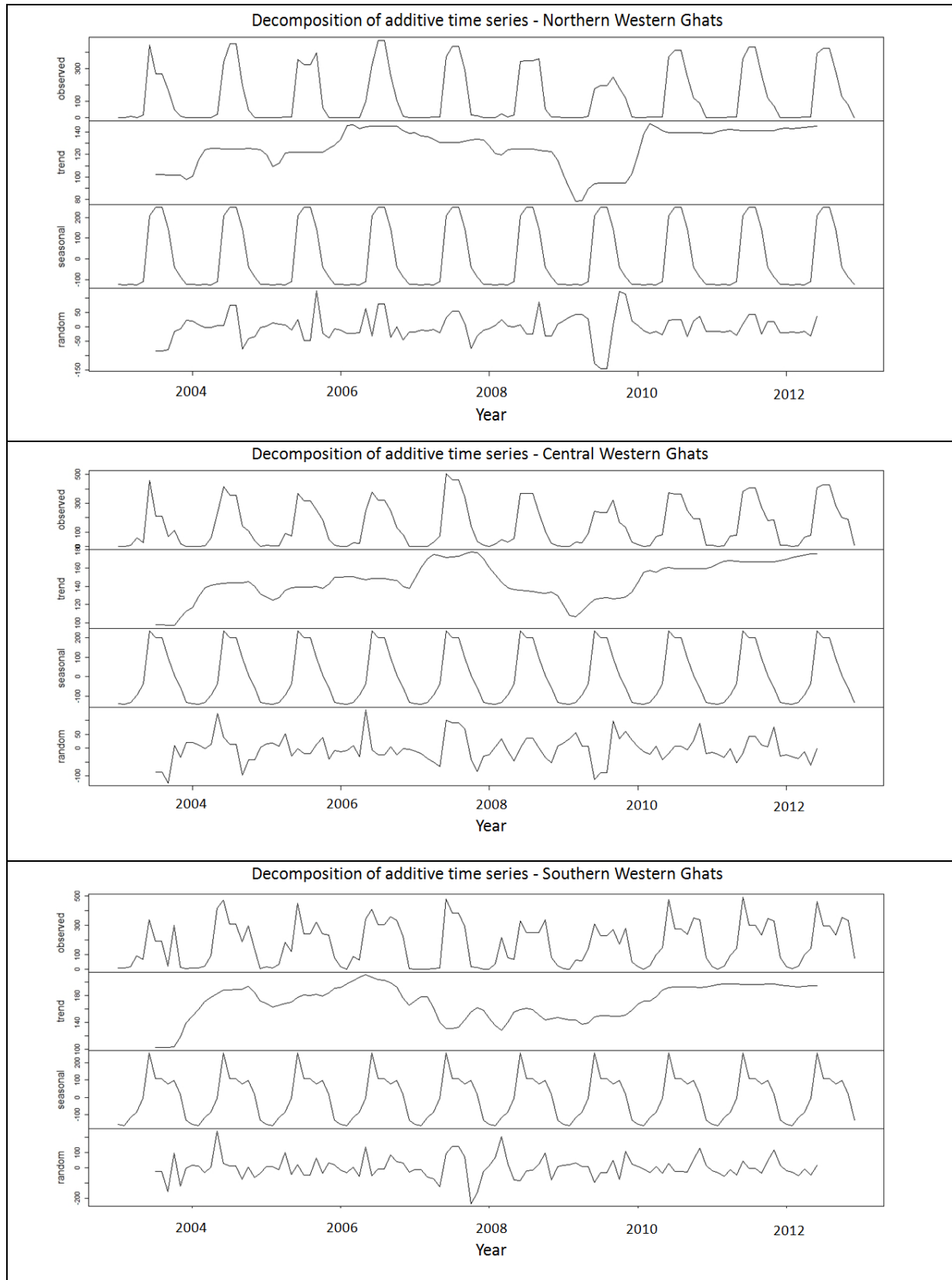


Figure 60: Decomposition of time-series – observed, trend, seasonal and random components over dense forest cover.

ARIMA(0,0,1) was found to be most suitable for northern, and ARIMA(1,0,0) with non-zero mean was adapted for rainfall data pertaining to central and southern Western Ghats. These models were used to make forecasts for future values of the rainfall time-series. Figure 61 shows the forecast plots for the three regions from 2013 to 2020 in blue line, 80% prediction interval as dark grey shaded area, and 95% prediction interval as light grey shaded area. Appendix 3 (table 1–3) details the monthly forecasted rainfall values from 2013 to 2020 for the forest class for northern, central and southern Western Ghats.

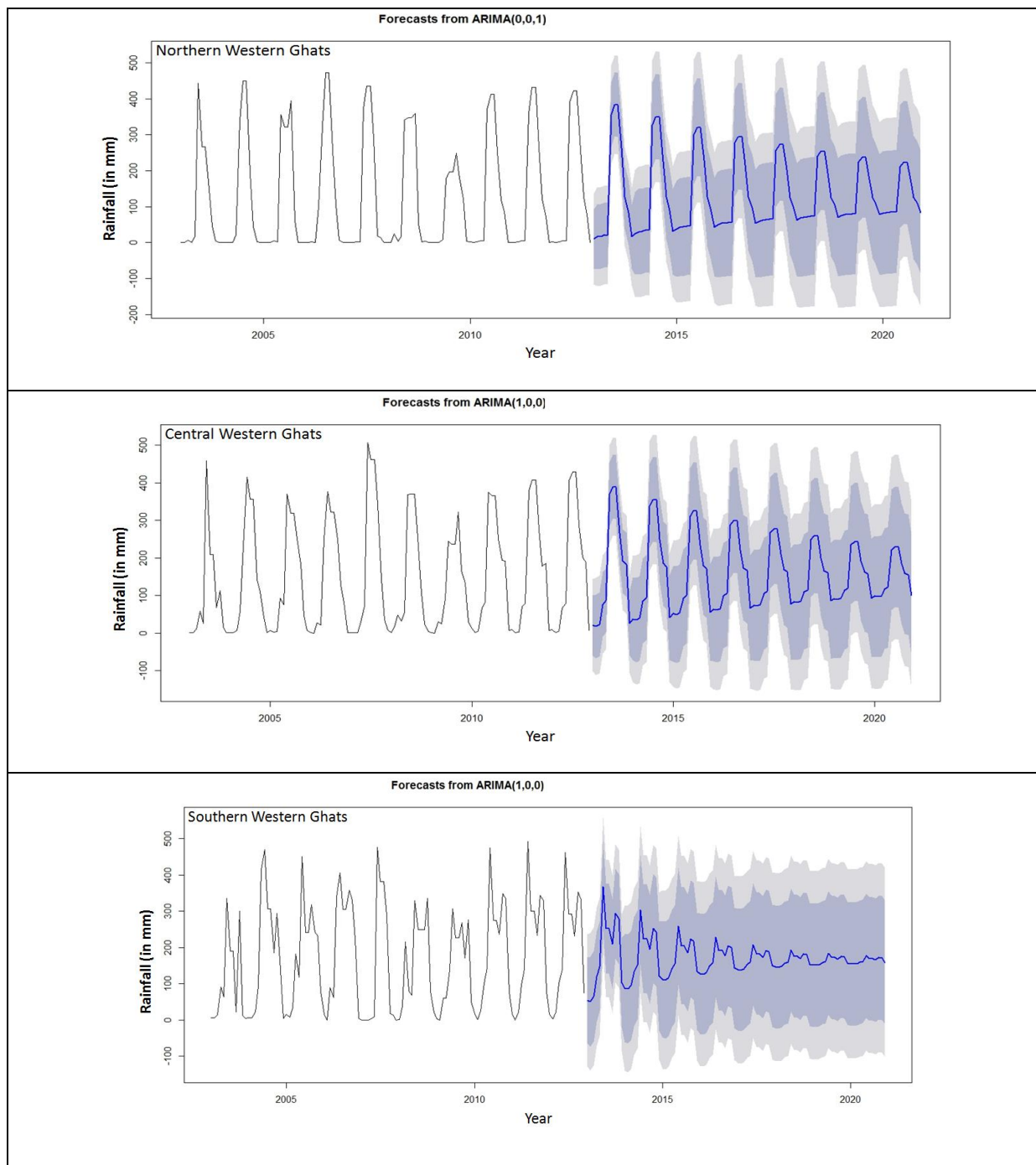


Figure 61: Time-series forecast plots of rainfall over forest cover for the northern, central and southern Western Ghats.

Figure 62 shows the rainfall time-series plots over agriculture/grassland areas for northern, central and southern Western Ghats highlighting a seasonal component. Figure 63 shows decomposition of additive time-series into original (top), estimated trend component, estimated seasonal component, and the irregular component (bottom). The highest and the lowest seasonal factor of rainfall in agriculture/grassland LC was similar to that of forest LC type (i.e. high in July and August and low from December to April) in northern Western Ghats. The estimated seasonal component also showed increasing trend in rainfall from May to August and a decreasing trend from September to April. Even the central and southern Western Ghats indicated similar trends of rainfall in agriculture/grassland areas as that of forest cover i.e. highest seasonal factor was seen in June and lowest was observed in January–February. The estimated seasonal component also showed increasing trend in rainfall from April to June and a decreasing trend from July to March.

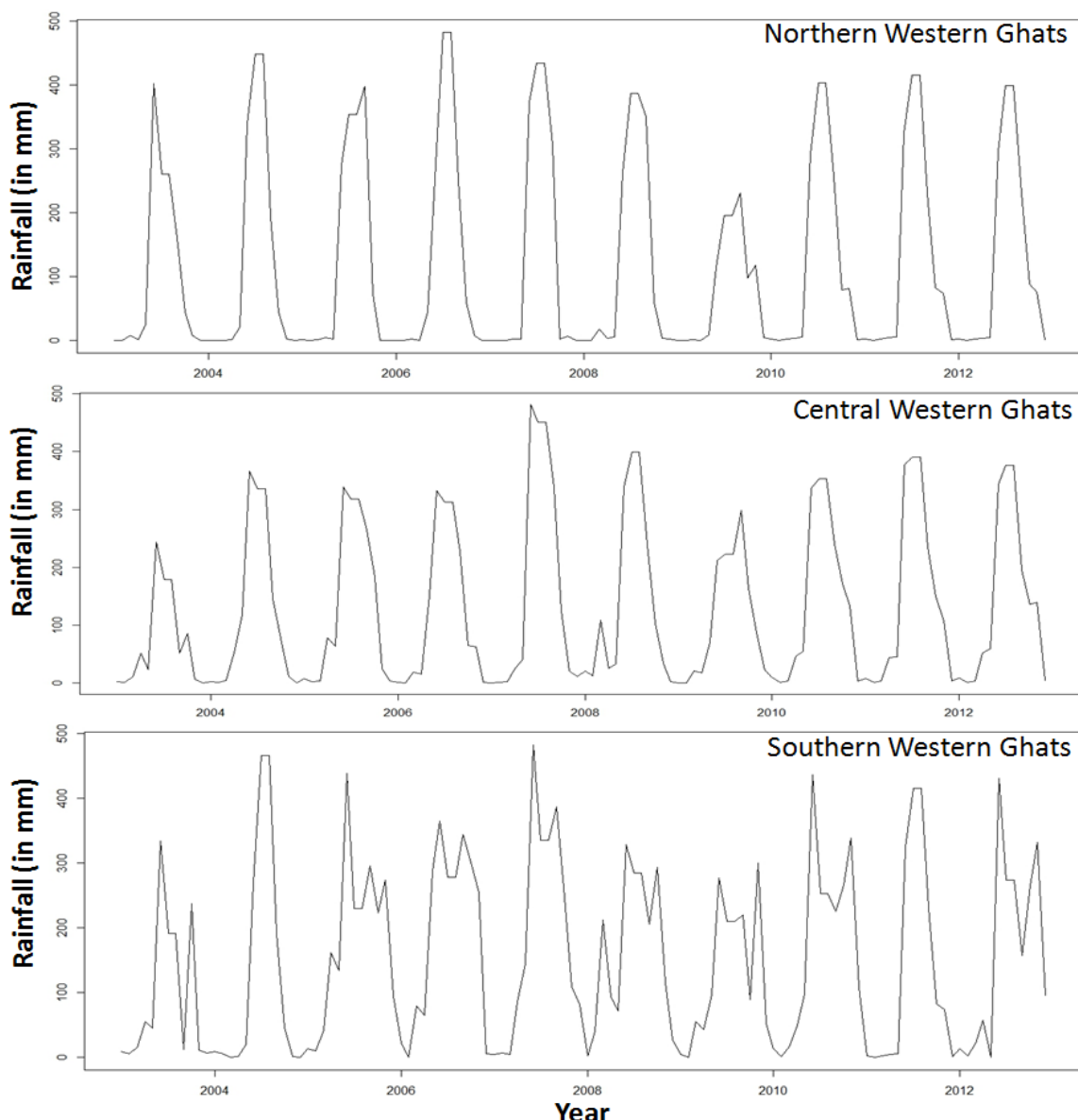


Figure 62: Rainfall time-series plots over agriculture/grassland land cover.

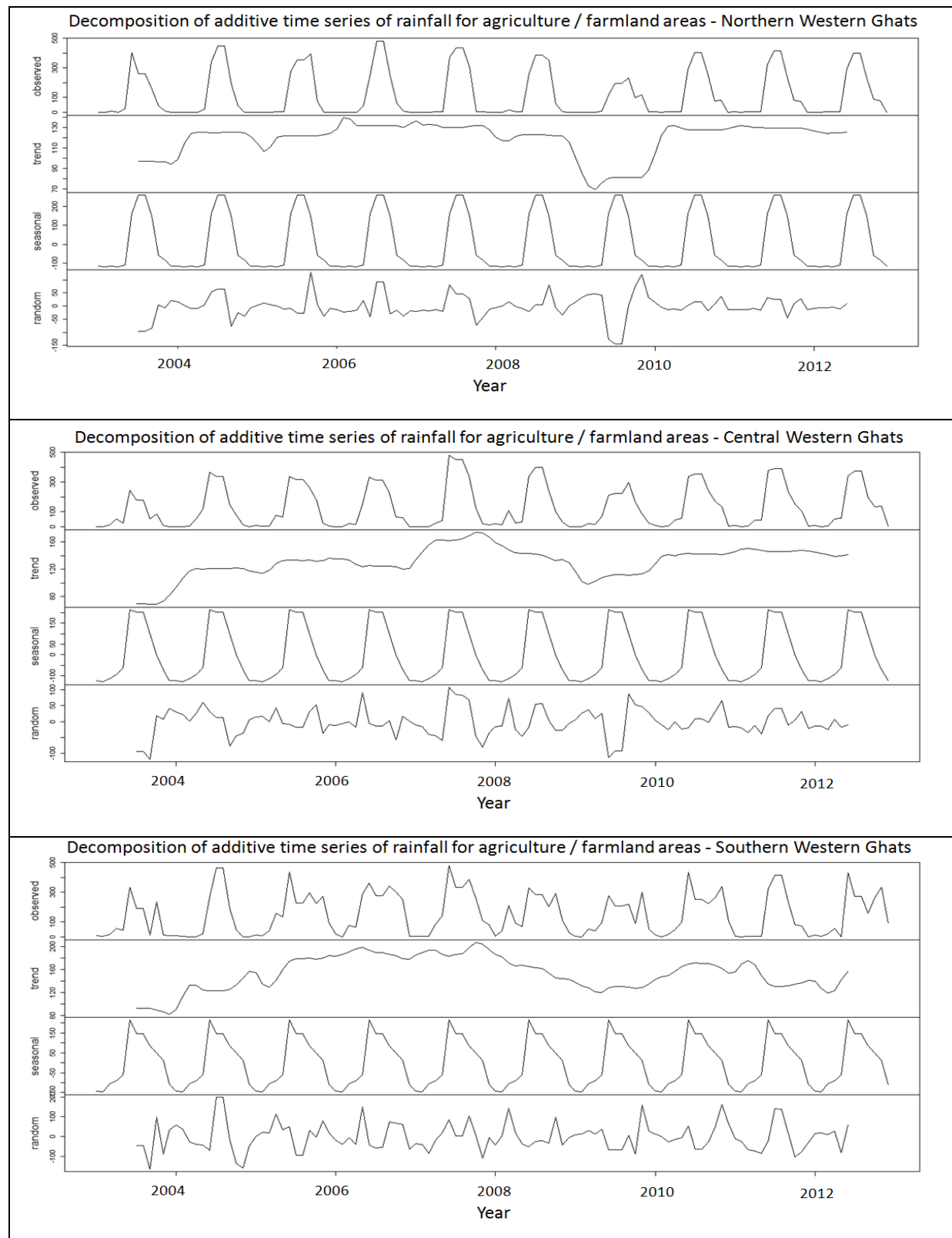


Figure 63: Decomposition of time-series – observed, trend, seasonal and random components of rainfall in agriculture/grassland land cover.

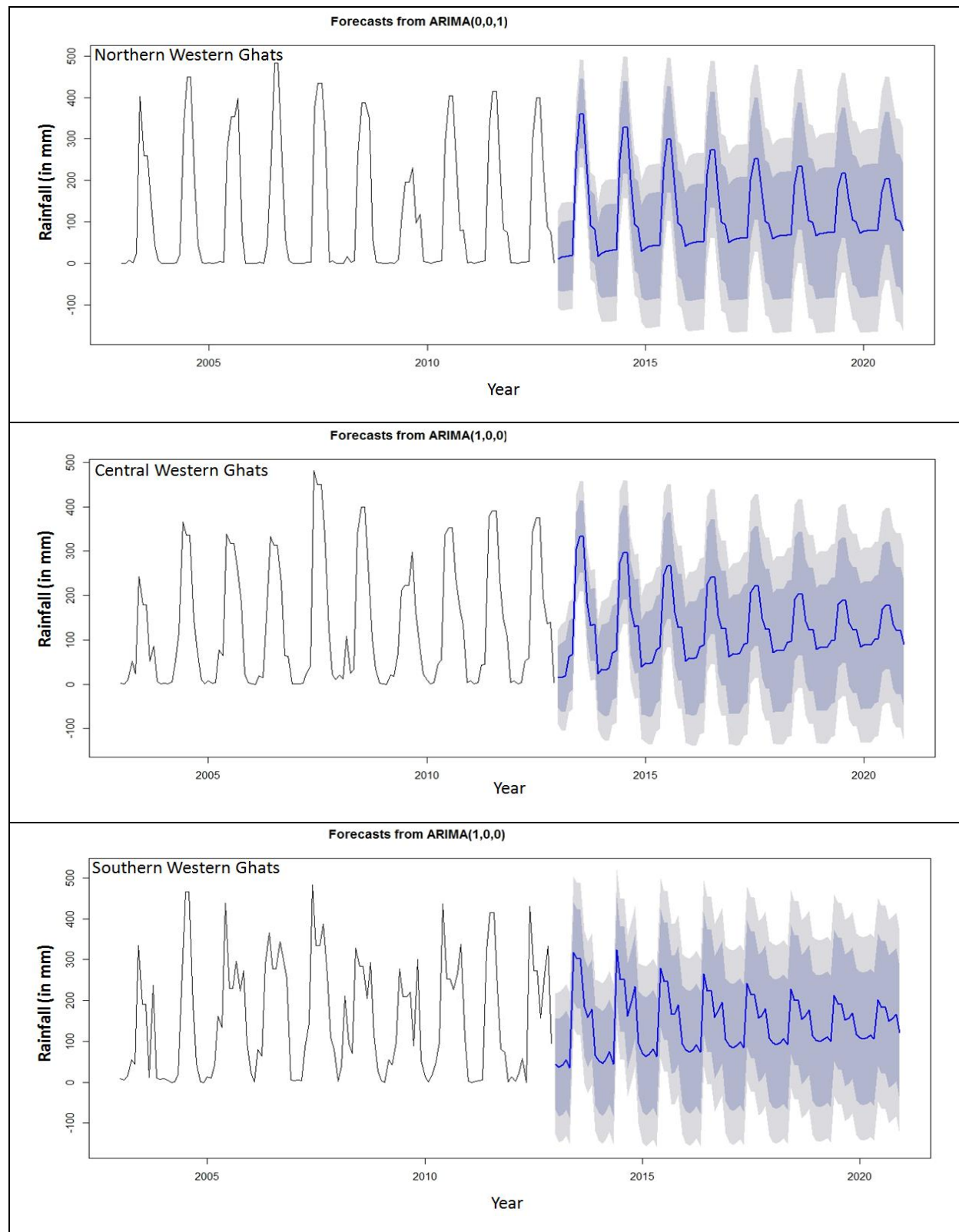


Figure 64: Time-series forecast plots of rainfall in agriculture/grassland areas for the northern, central and southern Western Ghats.

ARIMA(0,0,1) was used for forecasting the rainfall pattern in agricultural/grassland areas in northern Western Ghats, and ARIMA(1,0,0) with non-zero mean was used for rainfall data pertaining to central and southern Western Ghats. Figure 64 shows the forecast plots for the three regions from 2013 to 2020 in blue line, 80% prediction interval as dark grey shaded area, and 95% prediction interval as light grey shaded area. Appendix 3 (table 4–6) details the monthly forecasted rainfall values from 2013 to 2020 in the agricultural/grassland areas for northern, central and southern Western Ghats. In general, we see a decreasing trend in the rainfall pattern over vegetative areas (forest and agricultural/grassland) from 2013 towards 2020 in northern, central and southern Western Ghats.

7. Discussion

Vegetation plays an important role in moderating/regulating climate through the exchange of energy, water vapour and momentum between the land surface and the atmosphere (Wang, 2006). Vegetation also controls atmospheric CO₂ and currently absorbs about one-third of anthropogenic fossil fuel emissions to the atmosphere. The magnitude of the gross flux of carbon taken up annually by photosynthesis is about 15 times the absolute value of fossil fuel emissions (Wang et al., 2011). Thus, even a small change in vegetation photosynthesis could have a large effect on the role of vegetation as a carbon sink. Therefore, understanding how vegetation growth responds to climate change is a critical requirement for projecting future ecosystem dynamics.

NDVI has been effectively used in vegetation dynamics monitoring and the study of vegetation responses to climatic change at different scales during the past few years (e.g., Beck et al., 2006; Tucker et al., 2001; Wang et al., 2003; Zhou et al., 2001). Using RS NDVI data to investigate vegetation changes and relationships between vegetation and climate has acquired abundant achievements.

In this study, usage of time-series NDVI was demonstrated by first deriving LC classes by thresholding method and boxplot analysis. Methods incorporated in this work included the application of an automated MODIS NDVI time-series and reference database for the extraction of LC classes (dense vegetation, agriculture/grassland, soil/settlement and water) to support multi-temporal data analysis based on ground information. These LC maps were then validated using test data collected from ground and by Google Earth time-series images. Also, significant difficulties in evaluating change detection results hold from the inability to adequately characterize outcome accuracies (Khorram et al., 1999). Unlike typical LC classification assessment that requires only single date validation data, change detection validation required data for multiple dates to provide sufficient change (i.e., before and after event) documentation. In particular, the characterization of change omission errors represents an especially difficult challenge (Lunetta et al., 2002b, 2004). Because LC change

(conversion) is a relative occurrence over a large area, it is difficult to derive a robust estimate of change omission errors.

Although MODIS NDVI data for the month of July was not considered in our analysis because of the presence of cloud, MODIS NDVI data processing was conducted to provide a filtered and cleaned (anomalous data removed) uninterrupted data stream to support multi-temporal (phenological) analysis. Total annual NDVI values for each 250 m grid cell within the study area (2003–2012) were compared on an annual basis to identify those cells exhibiting greater than specified threshold values and were labeled as LC conversion areas. Intensive LC activities associated with agricultural crop rotations often confound LC conversion determinations. To summarize, table 19 shows decadal changes in area of LC in Western Ghats. Table 20 shows changes in LST and table 21 highlights the decadal pattern in rainfall.

Table 19: Decadal changes in area of LC in Western Ghats

Class	2003		2012		Decadal changes	
	ha	%	Ha	%	ha	%
Northern Western Ghats						
Dense forest	2340719	23.64	2059516	20.80	281203	2.84
Agriculture/ grassland	7315449	73.88	7536259	76.11	220810	2.23
Settlement/ soil	108282.6	1.09	182789	1.84	74506.4	0.75
Water	138085.2	1.39	123183.9	1.24	14901	0.15
Central Western Ghats						
Dense forest	5073131	53.39	4656546	49.01	416585	4.38
Agriculture/ grassland	4331023	45.58	4741510	49.9	410487	4.32
Settlement/ soil	4751	0.05	49410.4	0.52	44659.4	0.47
Water	93119.6	0.98	56061.8	0.59	37057.8	0.39
Southern Western Ghats						
Dense forest	5897318	78.78	5465387	73.01	431931	5.77
Agriculture/ grassland	1538333	20.55	1976253	26.4	437920	5.85
Settlement/ soil	7485.81	0.1	8982.97	0.12	1497.16	0.02
Water	42669.09	0.57	35183.29	0.47	7485.8	0.1

Table 20: Decadal changes in LST in Western Ghats

Class	LST (°C) ± sd (2003)			LST (°C) ± sd (2012)		
	summer	monsoon	Winter	summer	monsoon	winter
Northern Western Ghats						
Dense forest	28±4	26±2	21±3	29±3	25±2	19±3
Agriculture/ grassland	33±4	29±2	26±3	33±3	29±3	24±4
Central Western Ghats						
Dense forest	28±3	24±2	19±4	26±3	24±2	19±4
Agriculture/ grassland	33±3	27±3	26±4	31±3	27±3	26±4
Southern Western Ghats						
Dense forest	28±2	27±1	26±2	29±2	28±1	27±3
Agriculture/ grassland	29±2	28±2	29±1	28±3	29±2	31±2

Table 21: Decadal changes in rainfall in Western Ghats

Class	2003	2012
	Total rainfall (mm)	Total rainfall (mm)
Northern Western Ghats		
Dense forest	241.51	330.55
Agriculture/grassland	262.81	276.43
Central Western Ghats		
Dense forest	248.26	431.55
Agriculture/grassland	170.67	338.49
Southern Western Ghats		
Dense forest	276.27	503.98
Agriculture/grassland	240.2	432.61

Table 19 shows that dense forest area has considerably decreased by 2.84% (281203 ha), 4.38% (416585 ha), and 5.77% (431931 ha), and agricultural/grassland area has increased by 2.23% (220810 ha), 4.32% (410487 ha) and 5.85% (437920 ha) in the northern, central and southern Western Ghats. There is a marginal increase in settlement/soil area and small decrease in the spatial extent of water bodies in all the three regions (see table 19). Table 20 reveals that temperature in dense forest has always been lesser than in agricultural/grassland areas in all the three seasons. Temperature has a decreasing trend from summer to monsoon to winter except in southern Western Ghats, where winter temperatures were higher. Overall, there has not been much variation in the seasonal temperature during the study period. Total

annual rainfall had an increasing trend from 2003 to 2012 (table 21), but number of rainy days have decreased in southern Western Ghats.

Joint analysis of NDVI and LST showed to be of great significance, since they facilitate the identification of changes in land occupation and surface conditions (Nemani et al., 1993) by differentiating seasonal changes from changes in land occupation (Nemani and Running, 1997). NDVI and LST behaviors have also been proven to be partially correlated (Kaufmann et al., 2003): an increase in NDVI values during summer (greater proportion of vegetation) results in lower LST, while higher NDVI values during winter results in an increase in LST.

Correlation analyses between NDVI and climate variable is a powerful tool for probing ecosystem function response to climate change. The present study combined datasets of NDVI from 2003 to 2012 and climate parameters to analyze year to year variations. In this work we described the spatial relationship between MODIS NDVI, MODIS derived LST and rainfall. We focused on vegetation data to investigate the distribution of LST and rainfall because the existing vegetation distribution is largely controlled by temperature and precipitation pattern. Monthly climatic changes and trends in the 10 years provided a clear illustration of the NDVI trends. Differences in NDVI–temperature and NDVI–precipitation correlations relative to vegetation types such as forest and agriculture/grassland were also comprehensively investigated. This result supports and is of similar magnitude as temporal studies showing increase of NDVI corresponding to increase in growing season temperature over the length of the satellite record. The main outcomes from this study can be summarized in the following points.

- Northern and central Western Ghats showed very similar trends. Dense vegetation/forest area increased in September–October–November and decreased in January–February. This season (August–September–October) corresponds from mid to end of the monsoon that brings heavy showers from the Arabian Sea. Due to this rain, entire Ghat section is full of thick vegetation.
- Agriculture/grassland area is maximum in August–September and December–January and minimum in April–May in both northern and central Western Ghats.
- Southern Western Ghats shows a slightly different pattern with peak dense vegetation between October through April and lowest in August and September. Agriculture crops occupy maximum spatial extent between August to December and shows valleys in the time-series graph between April to June.
- The total dense green area in northern and central Western Ghats are between 30–70% of all the LC classes while dense vegetation constitute around 60–90% of the southern Western Ghats throughout the years of study (2003–2012).
- NDVI values for water tend to increase whenever there is a peak in vegetation across the months and year (in monsoon season) in all the three regions of Western Ghats.

- Image to image correlation coefficient (at 0.01 significance level) between NDVI of forest with LST and rainfall, and NDVI of agriculture/grassland class with LST and rainfall for northern, central and southern Western Ghats were computed that reconfirmed the negative correlation between NDVI and LST in northern and central Western Ghats, and negative to weak positive correlation in southern Western Ghats. Most months showed weak negative to strong positive correlation between NDVI and rainfall during 2003–2012 in northern and central Western Ghats. Southern Western Ghats exhibited strong negative to weak positive correlation between 2003 to 2008 and weak negative to stronger positive correlation between NDVI and rainfall from 2009–12. Correlation between NDVI–LST decreased and NDVI–rainfall increased as one moves from forest to grassland.
- The seasonal analysis revealed that mean NDVI of forest is highest in southern Western Ghats followed by central Western Ghats and least in northern Western Ghats. Mean LST is lowest in central Western Ghats followed by northern Western Ghats. In southern Western Ghats, LST is almost constant (around 27 °C) with least deviation. Total rainfall is minimum in northern Western Ghats and maximum in southern Western Ghats.
- In northern Western Ghats, NDVI and LST show increasing trend and rainfall has a decreasing trend. In summer, rainfall is minimum and static from 2009 onwards. Monsoon temperature increased from 2010 onwards indicating more photosynthetic activity and increased NDVI. Winter temperature has increased and rainfall has decreased but have the maximum NDVI during this season.
- In central Western Ghats, summers are dry and NDVI follows a cyclic pattern with both temperature and rainfall following a decreasing trend. Monsoon has higher LST and rainfall which triggers growing season environment for dense vegetation. Winters are warmer with increasing rainfall trend in the decade.
- Southern Western Ghats has overall higher NDVI, LST and total rainfall among all seasons in the entire Western Ghats. Summer and winter LST have increased, NDVI have been decreasing and rainfall trend has decreased in summer and increased in monsoon and winter during 2003 to 2012.
- Lower NDVI values were observed during March to June and high NDVI values were seen during August to January/February for all the years for both dense vegetation and agriculture in northern Western Ghats.
- In central Western Ghats, NDVI values for green vegetation is higher, the minimum–maximum temperature range is lower i.e. the regions is cooler and the area witnesses higher rainfall compared to northern Western Ghats.
- Southern Western Ghats exhibit higher NDVI values throughout the year for dense vegetation (> 0.55) with maximum NDVI reaching 0.79. The mean temperature

variation is very small (~23 to ~35 °C) throughout the year and rainfall is more during April to October/November.

- Rainfall time-series data in forest and agricultural/grassland areas were modelled and forecasted using ARIMA which indicated a decreasing trend in the rainfall pattern over forest and agricultural/grassland from 2013 towards 2020 in northern, central and southern Western Ghats.

There are also, however, several limitations of deriving LC and phenological information from NDVI. Uncertainties in relating NDVI to vegetation are associated with the effects of atmospheric variations, sensor calibration, and sensor degradation over time (James and Kullari, 1994; Townshend, 1995). Surface heterogeneity also complicates interpretation of NDVI. Due to low NDVI values that result from sparse vegetation as in northern Western Ghats, uncertainties in interpreting NDVI can sometimes increase. Vegetation canopies in such environments do not achieve complete coverage, making NDVI susceptible to the spectral influence of the soil and soil moisture in gaps between vegetation (Peters and Eve, 1995).

This study provided not only the current LC status of the Western Ghats, but also identified both the pattern and nature of changes that have impacted the local temperature and rainfall pattern. The analysis highlighted and confirmed several important MODIS data applications, such as a) potentially substantial cost saving on data procurement and analysis, b) minimization of image registration errors that would have otherwise occurred while using multisensor data that typically limit the overlay of multiple date coverage (post-classification) to support change detection analysis, c) practical methods for large area change detection monitoring (using MODIS data) including significant reduction of inter and intraannual vegetation phenology mediated errors and their assessment.

Though this NDVI based analysis of change in vegetation is a significant contribution to the previous researches conducted in this region, future studies could improve the understanding of climate change effects on vegetation growth in a longer time-series. Future studies will involve the use of HANTS (Harmonic ANalysis of Time Series) algorithm to perform the detection of cloud contaminated pixels. Hants algorithm allows the simultaneous observation of mean value, first harmonic amplitude and phase behaviors in the same image (Julien et al., 2006). New studies can combine process-based ecosystem models and climate models and explore how vegetation growth changes affect the terrestrial carbon cycle and its feedback to the Earth's climate system. This study would undoubtedly help to identify the main factors influencing spatio-temporal patterns in vegetation growth over 10 years.

8. Conclusions

During the last few decades, many regions have experienced major LC transformations, often driven by human activities. Assessing and evaluating these changes require consistent data over time at appropriate scales as provided by remote sensing imagery. Given the availability of small and large-scale observation systems that provide the required long-term records, it is important to understand the specific associated characteristics.

This work constructed monthly NDVI sequences from MODIS data during 2003–2012 covering Western Ghats, India. The data were comprehensively used in the LC change analysis, and correlation analysis between NDVI and climatic parameters. The study confirmed the feasibility of long-term NDVI time-series climate research. NDVI trends were spatially heterogeneous, corresponding with regional climatic characteristics for different seasons. Monthly NDVI trend reflected different spatial patterns for different regions and different LC classes. NDVI had significant correlations with monthly mean temperature and monthly precipitation. The correlation between NDVI and temperature was larger than that between NDVI and precipitation. Overall variation trend in NDVI–LST and NDVI–rainfall within the three regions were calculated to see if those could conceal significant changes in short periods. Monsoon and winter NDVI was more correlated with temperature than with rainfall. A decreasing trend in the rainfall pattern over forest and agricultural/grassland areas were forecasted between 2013 to 2020 in northern, central and southern Western Ghats.

Future study will focus on the type of forest/vegetation and their response to change in climatic parameters. Further investigations will address other land use change phenomena, such as combination of short-term disturbance and gradual land use conversion practices typical for areas in Western Ghats. If land use conversions are targeted, change detection based on multi-seasonal and multi-year image classification would complement trend based approaches. This study makes a strong case for the usage of long-term data repository supporting consistent monitoring of terrestrial ecosystem, irrespective of the strategy followed.

References

- [1.] Aguilar, C., Zinnert, J. C., Polo, M. S., and Young, D. R., 2012. NDVI as an indicator for changes in water availability to woody vegetation. *Ecological Indicators*, vol. 23(2012), pp. 290–300.
- [2.] Angert, A., Biraud, S., Bonfils, C., Henning, C., Buermann, W., Pinzon, J., Tucker, C., and Fung, I., 2005. Drier summers cancel out the CO₂ uptake enhancement induced by warmer springs. *Proceedings of the National Academy of Sciences* vol. 102(31), pp. 10823.
- [3.] Balaghi, R., Tychon, B., Eerens, H. and Jlibene, M., 2008. Empirical regression models using NDVI, rainfall and temperature data for the early prediction of wheat grain yields in Morocco. *International Journal of Applied Earth Observation and Geoinformation*, vol. 10(2008), pp. 438–452.
- [4.] Beck, P. S. A., Atzberger, C., and Hogda, K. A., 2006. Improved monitoring of vegetation dynamics at very high latitudes, a new method using MODIS NDVI. *Remote Sensing of Environment*, vol. 100, pp. 321–336.
- [5.] Braswell, B. H., Schimel, D. S., Linder, E., and Moore, B., 1997. The response of global terrestrial ecosystems to interannual temperature variability. *Science*, vol. 238, pp. 870–872.
- [6.] Brockwell, P. J., and Davis, R. A. 2002. *Introduction to Time Series and Forecasting*, Second Edition, Springer-verlag, New York, Inc.
- [7.] Bruce, L. M., Mathur, A., and Byrd, J. D. Jr., 2006. Denoising and wavelet-based feature extraction of MODIS multi-temporal vegetation signatures. *Geoscience and Remote Sensing*, vol. 43(1), pp. 67–77 (Special Issue on Multi Temporal Imagery Analysis).
- [8.] Burns, D. A., Klaus, J., and McHale, M. R., 2007. Recent climate trends and implications for water resources in the Catskill Mountain region, New York, USA. *Journal of Hydrology*, vol. 336(1-2), pp. 155–170.
- [9.] Byrne, G. F., Crapper, P. F., and Mayo, K. K. 1980. Monitoring land-cover change by principal component analysis of multitemporal Landsat data. *Remote Sensing of Environment*, vol. 10, pp. 175–184.
- [10.] Caminade, C., and Terray, L., 2010. Twentieth century sahel rainfall variability as simulated by the ARPEGE AGCM, and future changes. *Climate Dynamics*, vol. 35, pp. 75–94.
- [11.] Chandran M. D. S., Rao G. R., Gururaja K. V. and Ramachandra T. V., 2010. Ecology of the Swampy Relic Forests of Kathalekan from Central Western Ghats, India. *Bioremediation, Biodiversity and Bioavailability* 4 (Special Issue I), Global Science Books, pp. 54–68.
- [12.] Chuvieco, E., Cocero, D., Riano, D., Martin, P., Martinez-Vega, J., de la Riva d, J., and Pe' rez, F., 2004. Combining NDVI and surface temperature for the estimation of live fuel moisture content in forest fire danger rating. *Remote Sensing of Environment*, vol. 92(2004), pp. 322–331.

[13.] Conservation International, 2005. Hotspots Revisited: Earth's Biologically Richest and Most Endangered Terrestrial Ecoregions, CI, US, pp. 392.

[14.] Crist, E. P. 1985. A TM tasseled cap equivalent transformation for reflectance factor data. *Remote Sensing of Environment*, vol. 17, pp. 301–306.

[15.] De Luis, M., Raventos, J., Gonzalez-Hidalgo, J. C., Sanchez, J. R., and Cortina, J., 2000. Spatial analysis of rainfall trends in the region of Valencia (east Spain). *International Journal of Climatology*, vol. 20(12), pp. 1451–1469.

[16.] Dikshit, K. R., 2001. The Western Ghats: A geomorphic overview. *Memoir Geological Society of India*, vol. 47, pp. 159–183.

[17.] Ellis, E., and Pontius, R., 2010. Land-use and land-cover change. In: *Encyclopedia of Earth*. Eds. Cutler J. Cleveland (Washington, D.C.: Environmental Information Coalition, National Council for Science and the Environment). [First published in the *Encyclopedia of Earth* April 18, 2010; Last revised Date April 18, 2010; Retrieved March 16, 2011.
URL: http://www.eoEarth.org/article/Land-use_and_land-cover_change

[18.] Elvidge, C. D., Miura, T., Jansen, T., Groeneveld, D.P., and Ray, J. 1998. Monitoring trends in wetland vegetation using a Landsat MSS time series. In: *Remote sensing change detection: Environmental monitoring methods and applications* (R. S. Lunetta, and C. D. Elvidge, Editors), Ann Arbor Press, Chelsea, MI, 318 p. + Illustrations, and co-published in Europe by Taylor and Francis, UK.

[19.] Fung, T., and LeDrew, E., 1987. Application of principal component analysis for change detection, *Photogrammetric Engineering and Remote Sensing*, vol. 53(12), pp. 1649–1658.

[20.] Gitelson, A. A., Kaufman, Y. J., and Merzlyak, M. N., 1997. An atmospherically resistant “green” vegetation index (ARGI) for EOS-MODIS. *Remote Sensing Environment*, vol. 58, pp. 289–298.

[21.] Groeneveld, D. P., and Baugh, W. M., 2007. Correcting satellite data to detect vegetation signal for eco-hydrologic analyses. *Journal of Hydrology*, vol. 344, pp. 135–145.

[22.] Gunawardhana, L. N., and Kazama, S., 2012. Using subsurface temperatures to derive the spatial extent of the land use change effect. *Journal of Hydrology*, vol. 460-461, pp. 40–51.

[23.] Haigh, M. J., 2004. Sustainable management of headwater resources: the Nairobi headwater declaration (2002) and beyond. *Asian Journal of Water, Environment and Pollution*, vol. 1(1-2), pp. 17–28.

[24.] Harris, R., and Solis, R. 2003. *Applied Time Series Modelling and Forcasting*, John Wiley & Sons (Asia) Pte. Ltd., India.

[25.] Helsel, D. R., and Hirsch, R. M., 2002. Statistical methods in water resources. United States Geological Survey, pp. 524.

[26.] Herrmann, S. M., Anyamba, A., and Tucker, C. J., 2005. Recent trends in vegetation dynamics in the African Sahel and their relationship to climate. *Global Environmental Change-Human and Policy Dimensions*, vol. 15(4), pp. 394–404.

[27.] Hickler, T., Eklundh, L., Seaquist, J. W., Smith, B., Ardo, J., Olsson, L., Sykes, M. T., and Sjostrom, M., 2005. Precipitation controls Sahel greening trend. *Geophysical Research Letters*, vol. 32(L21415).

[28.] Huber, S., Fensholt, S., and Rasmussen, K., 2011. Water availability as the driver of vegetation dynamics in the African Sahel from 1982 to 2007. *Global and Planetary Change*, vol. 76(2011), pp. 186–195.

[29.] Huete, A. R., Didan, K., Miura, T., Rodriguez, E. P., Gao, X., and Ferreira, L. G., 2002. Overview of the radiometric and biophysical performance of the MODIS vegetation indices. *Remote Sensing Environment*, vol. 83(1–2), pp. 195–213.

[30.] Hulme, M., 2001. Climatic perspectives on Sahelian desiccation: 1973–1998. *Global Environmental Change-Human and Policy Dimensions*, vol. 11(1), pp. 19–29.

[31.] IPCC, 2007. Climate change 2007: the physical science basis. In: Solomon, S., Qin, D., Manning, M., Chen, Z., Marquis, M., Averyt, K. B., Tignor, M., Miller, H. L., (Eds.), *Contribution of Working Group I to the Fourth Assessment Report of the Intergovernmental Panel on Climate Change*, Cambridge University Press, Cambridge, United Kingdom and New York, NY, USA.

[32.] Jackson, R. B., Randerson, J. T., Canadell, J. G., Anderson, R. G., Avissar, R., Baldocchi, D. D., Bonan, G. B., Caldeira, K., Diffenbaugh, N. S., and Field, C. B., 2008. Protecting climate with forests. *Environmental Research Letters*, vol. 3, pp. 044006.

[33.] James, M. J., and Kullari, S., 1994. The pathfinder AVHRR land data set: an improved coarse resolution data set for terrestrial monitoring. *International Journal of Remote Sensing*, vol. 15, pp. 3347–3364.

[34.] Jensen, J. R. 2005. *Introductory digital image processing: A remote sensing perspective*, (3rd Edition). Upper Saddle River, NY: Prentice Hall, pp. 525.

[35.] Jiménez-Muñoz, J. C., Sobrino, J. A., Gillespie, A., Sabol, D., and Gustafson, W. T., 2006. Improved land surface emissivities over agricultural areas using ASTER NDVI. *Remote Sensing of Environment*, vol. 103(2006), pp. 474–487.

[36.] Jin, S. , and Sader, S. A., 2005. MODIS time-series imagery for forest disturbance and quantification of patch effects. *Remote Sensing of Environment*, vol. 99, pp. 462–470.

[37.] Jobbágy, E. G., Sala, O. E., and Paruelo, J. M., 2002. Patterns and controls of primary production in the Patagonian steppe: a remote sensing approach. *Ecology*, vol. 83, pp. 307–319.

[38.] Julien, Y., Sobrino, J. A., and Verhoef, W., 2006. Changes in land surface temperatures and NDVI values over Europe between 1982 and 1999. *Remote Sensing of Environment*, vol. 103(2006), pp. 43–55.

[39.] Justice, C. O., Townshend, J. R. G., Holben, B. N., and Tucker, C. J., 1985. Analysis of the phenology of global vegetation using meteorological satellite data. *International Journal of Remote Sensing*, vol. 6, pp. 1271–1318.

[40.] Justice, C. O., Townshend, J. R. G., and Kalb, V. L. 1991. Representation of vegetation by continental data sets derived from NOAA-AVHRR data. *International Journal of Remote Sensing*, vol. 12(5), pp. 999–1021.

[41.] Kampata, J. M., Parida, B. P., and Moalafhi, D. B., 2008. Trend analysis of rainfall in the headstreams of the Zambezi River Basin in Zambia. *Physics and Chemistry of the Earth*, vol. 33(2008), pp. 621–625.

[42.] Karniel, A., Agam, N., Pinker, R. T., Anderson, M., Imhoff, M. L., Gutman, G. G., Panov, N., and Goldberg, A., 2009. Use of NDVI and Land Surface Temperature for

Drought Assessment: Merits and Limitations. *Journal of climate*, vol. 23, pp. 618–633.

[43.] Kaufmann, R. K., Zhou, L., Myneni, R. B., Tucker, C. J., Slayback, D., Shabanov, N. V., et al., 2003. The effect of vegetation on surface temperature: A statistical analysis of NDVI and climate data. *Geophysical Research Letters*, vol. 30(22), pp. 2147.

[44.] Kaufman, Y. J., and Tanré, D., 1996. Strategy for direct and indirect methods for correcting the aerosol effect on remote sensing: from AVHRR to EOS-MODIS. *Remote Sensing Environment*, vol. 55(1), pp. 65–79.

[45.] Khorram, S. K., Biging, G. S., Chrisman, N. R., Colby, D. R., Congalton, R. G., Dobson, J. E., et al., 1999. Accuracy assessment of remote sensing-derived change detection, American Society for Photogrammetry and Remote Sensing, Monograph Series.1-57083-058-4. pp. 64.

[46.] Kremer, R. G., and Running, S. W., 1993. Community type differentiation using NOAA/AVHRR data within a sagebrush-steppe ecosystem. *Remote Sensing of Environment*, vol. 46, pp. 311–318.

[47.] Li, B., Tao, S., and Dawson, R. W., 2002. Relations between AVHRR NDVI and eco-climatic parameters in China. *International Journal of Remote Sensing*, vol. 23(5), pp. 989–999.

[48.] Li, Z., and Kafatos, M., 2000. Interannual variability of vegetation in United States and its relation to El Niño/southern oscillation. *Remote Sensing of Environment*, vol. 71, pp. 239–247.

[49.] Lillesand, T. M. and Keifer, R. W., 1972, *Remote sensing and image interpretation*, Second Edition : John Wiley and Sons, pp. 721.

[50.] Loveland, T., Gutman, G., Buford, M., Chatterjee, K., Justice, C., Rogers, C., Stokes, B., Thomas, J., Andrasko, K., Aspinall, R., Baldwin, V. C., Fladeland, M., Goebel, J., and Jawson, M., 2003, Land-Use / Land-Cover Change (Chapter 6), In *Strategic Plan for the Climate Change Science Program Final Report*, July 2003.
URL: <http://www.climatescience.gov/Library/stratplan2003/final/default.htm>

[51.] Loveland, T. R., Merchant, J. W., Ohlen, D. O., and Brown, J. F., 1991. Development of a landcover characteristics data base for the conterminous U.S.. *Photogrammetric Engineering and Remote Sensing*, vol. 57(11), 1453–1463.

[52.] Lunetta, R. S., Alvarez, R., Edmonds, C. M., Lyon, J. G., Elvidge, C. D., Bonifaz, R., et al., 2002a. An assessment of NALC/Mexico land-cover mapping results: Implications for assessing landscape change. *International Journal of Remote Sensing*, vol. 23(16), pp. 3129–3148.

[53.] Lunetta, R. S., Ediriwickrema, J., Johnson, D. M., Lyon, J. G., and McKerrow, A., 2002b. Impacts of vegetation dynamics on the identification of land-cover change in a biologically complex community in North Carolina USA. *Remote Sensing of Environment*, vol. 82, pp. 258–270.

[54.] Lunetta, R. S., Johnson, D. M., Lyon, J. G., and Crotwell, J., 2004. Impacts of imagery temporal frequency on land-cover change detection monitoring. *Remote Sensing of Environment*, vol. 89(4), pp. 444–454.

[55.] Lunetta, R. S., Knight, J. F., Ediriwickrema, J., Lyon, J. G., and Worthy, L. D., 2006, Land-cover change detection using multi-temporal MODIS NDVI data. *Remote Sensing of Environment*, vol. 105 (2), pp. 142–154.

[56.] Lyon, J. G., Yuan, D., Lunetta, R. S., and Elvidge, C. D., 1998, A change detection experiment using vegetation indices. *Photogrammetric Engineering and Remote Sensing*, vol. 64(2), pp. 143–150.

[57.] Macleod, R. D., and Congalton, R. G., 1998. A quantitative comparison of change-detection algorithms for monitoring eelgrass from remotely sensed data. *Photogrammetric Engineering and Remote Sensing*, vol. 64(3), pp. 207–216.

[58.] Mao, D., Wang, Z., Luo, L., and Ren, C., 2012. Integrating AVHRR and MODIS data to monitor NDVI changes and their relationships with climatic parameters in Northeast China. *International Journal of Applied Earth Observation and Geoinformation*, vol. 18(2012), pp. 528–536.

[59.] Michener, W. K., and Houhoulis, P. F., Detection of vegetation associated with extensive flooding in a forest ecosystem, 1997. *Photogrammetric Engineering and Remote Sensing*, vol. 63(12), pp. 1363–1374.

[60.] MODIS. (1999). MODIS Vegetation Index (MOD 13): Algorithm Theoretical Basis Document Page 26 of 29 (version 3), (http://modis.gsfc.nasa.gov/data/atbd/atbd_mod13.pdf)

[61.] Myneni, R. B., Keeling, C. D., Tucker, C. J., Asrar, G., and Nemani, R. R., 1997. Increased plant growth in the northern high latitudes from 1981 –1991. *Nature*, vol. 386, pp. 698–701.

[62.] Ndiritu, J. G., 2005. Long-term trends of heavy rainfall in South Africa. *Regional hydrological Impacts of Climate Change- Hydroclimatit Variability*. In: Proceedings of symposium S6 held during seventh IAHS Scientific Assembly at Foz do Iguacu, Brazil, April 2005. IAHS Publ. 296, pp.178–183.

[63.] Nemani, R. R., Keeling, C. D., Hashimoto, H., Jolly, W. M., Piper, S. C., Tucker, C. J., et al., 2003. Climate-driven increases in global terrestrial net primary production from 1982 to 1999. *Science*, vol. 300, pp. 1560–1563.

[64.] Nemani, R., Pierce, L., Running, S., and Goward, S., 1993. Developing satellite derived estimates of surface moisture status. *Journal of Applied Meteorology*, vol. 32, pp. 548–557.

[65.] Nemani, R., and Running, S., 1997. Land cover characterization using multitemporal red, near-IR, and thermal-IR data from NOAA/AVHRR. *Ecological Applications*, vol. 7(1), pp. 79–90.

[66.] Nicholson, S., 2000. Land surface processes and Sahel climate. *Reviews of Geophysics*, vol. 38(1), pp. 117–139.

[67.] Nicholson, S. E., Davenport, M. L., and Malo, A. R., 1990. A comparison of the vegetation response to rainfall in the Sahel and east-Africa, using Normalized Difference Vegetation Index from NOAA AVHRR. *Climatic Change*, vol. 17(2 –3), pp. 209–241.

[68.] Orr, B. J., Casady, G. M., Tuttle, D. G., van Leeuwen, W. J. D., Baker, L. E., McDonald, C. L., et al., 2004. Phenology and trend indicators derived from spatially dynamic bi-weekly satellite imagery to support ecosystem monitoring. *Proceedings of the 5th Conference on Research and Resource Management in Southwestern Deserts — Biodiversity and Management of the Madrean Archipelago II: Connecting Mountain Islands and Desert Sea*. May 11–15, 2004. Tucson (AZ).

[69.] Parida, B. P., Moalfhi, D. B., and Kenabatho, P. K., 2003, Effect of urbanization on runoff coefficient: a case of Notwane catchment in Botswana. In: Proceedings of the International Conference on Water and Environment (WE-2003), Bhopal, 'Watershed Hydrology'. Allied Publishers Pvt. Ltd., pp.123–131.

[70.] Pascal J.P., 1988. Wet Evergreen Forests of the Western Ghats of India: Ecology, Structure, Floristic Composition and Succession, Institut Francais De Pondicherry, Pondicherry, pp. 345.

[71.] Peters, A. J., and Eve, M. D., 1995. Satellite monitoring of desert plant community response to moisture availability. *Environmental Monitoring and Assessment*, vol. 37, pp. 273–287.

[72.] Pettorelli, N., Vik, J. O., Mysterud, A., Gaillard, J. M., Tucker, C. J., and Stenseth, N. C., 2005. Using the satellite-derived NDVI to assess ecological responses to environmental change. *Trends in Ecology and Environment*, vol. 20, pp. 503–510.

[73.] Piao, S., Friedlingstein, P., Ciais, P., Zhou, L., and Chen, A., 2006. Effect of climate and CO₂ changes on the greening of the Northern Hemisphere over the past two decades. *Geophysical Research Letters*, vol. 33(23), pp. L23402.

[74.] Piao, S., Mohammat, A., Fang, J., Cai, Q., and Feng, J., 2006. NDVI-based increase in growth of temperate grasslands and its responses to climate changes in China. *Global Environmental Change*, vol. 16(2006), pp. 340–348.

[75.] Piao, S. L., Fang, J. Y., Zhou, L. M., Guo, Q. H., Mark, H., Ji, W., Li, Y., and Tao, S., 2003. Interannual variations of monthly and seasonal normalized difference vegetation index (NDVI) in China from 1982 to 1999. *Journal of Geophysical Research*, vol. 108(14), pp. 1–12.

[76.] Piao, S. L., Fang, J. Y., Ji, W., Guo, Q. H., Ke, J. H., and Tao, S., 2004. Variation in a satellite-based vegetation index in relation to climate in China. *Journal of Vegetation Science*, vol. 15, pp. 219–226.

[77.] Potter, C. S., and Brooks, V., 1998. Global analysis of empirical relations between annual climate and seasonality of NDVI. *International Journal of Remote Sensing*, vol. 15, pp. 2921–2948.

[78.] Radhakrishna, B. P., 2001. The Western Ghats of the Indian peninsula. *Memoir Geological Society of India*, vol. 47, pp. 133–144

[79.] Ramachandra T. V., and Uttam Kumar, 2009. Land Surface Temperature with Land Cover Dynamics: Multi-Resolution, Spatio-Temporal Data Analysis of Greater Bangalore. *International Journal of Geoinformatics*, vol. 5(3), pp. 43–53.

[80.] Reynolds, M. K., Comiso, J. C., Walker, D. A., and Verbyla, D., 2008. Relationship between satellite-derived land surface temperatures, arctic vegetation types, and NDVI. *Remote Sensing of Environment*, vol. 112(2008), pp. 1884–1894.

[81.] Reed, B. C., 2006. Trend analysis of time-series phenology of north America derived from satellite data. *GIScience & Remote Sensing*, vol. 43(1), pp. 24–38 (Special Issue on Multi Temporal Imagery Analysis).

[82.] Reed, B. C., Brown, J. F., VanderZee, D., Loveland, T. R., Merchant, J. W., and Ohlen, D. O., 1994. Measuring phenological variability from satellite imagery. *Journal of Vegetation Science*, vol. 5, pp. 703–714.

[83.] Ren, J., Chen, Z., Zhou, Q., and Tang, H., 2008. Regional yield estimation for winter wheat with MODIS-NDVI data in Shandong, China. *International Journal of Applied Earth Observation and Geoinformation*, vol. 10(2008), pp. 403–413.

[84.] Richards, J. A., 1984. Thematic mapping from multitemporal image data using the principal components transformation. *Remote Sensing of Environment*, vol. 16, pp. 25–46.

[85.] Sakamoto, T., Yokozawa, M., Toritani, H., Shibayama, M., Ishitsuka, N., and Oho, H., 2005. A crop phenology detection method using time-series MODIS data. *Remote Sensing of Environment*, vol. 96, pp. 366–374.

[86.] Schimel, D. S., House, J. I., Hibbard, K. A., Bousquet, P., Ciais, P., Peylin, P., Braswell, B. H., Apps, M. J., Baker, D., Bondeau, A., Canadell, J., Churkina, G., Cramer, W., Denning, A. S., Field, C. B., Friedlingstein, P., Goodale, C., Heimann, M., Houghton, R. A., Melillo, J. M., Moore, B., Murdiyarso, D., Noble, I., Pacala, S. W., Prentice, I. C., Raupach, M. R., Rayner, P. J., Scholes, R. J., Steffen, W. L., and Wirth, C., 2001. Recent patterns and mechanism of carbon exchange by terrestrial ecosystems. *Nature*, vol. 414, pp. 169–172.

[87.] Schultz, P. A., and Halpert, M. S., 1995. Global correlation of temperature, NDVI and precipitation. *Advance in Space Research*, vol. 13, pp. 277–280.

[88.] Seelan, S. K., Laguette, S., Casady, G. M., and Seielstad, G. A., 2003. Remote sensing applications for precision agriculture: A learning community approach. *Remote Sensing of Environment*, vol. 88(12, 30), pp. 157–169.

[89.] Seaquist, J. W., Hickler, T., Eklundh, L., Ardo, J., and Heumann, B., 2008. Disentangling the effects of climate and people on Sahel vegetation dynamics. *Biogeosciences Discussions*, vol. 5, pp. 3045–3067.

[90.] Singh, A. 1989. Digital change detection techniques using remotely-sensed data. *International Journal of Remote Sensing*, vol. 10(6), pp. 989–1003.

[91.] Song, Y., and Ma, M. G., 2008. Variation of AVHRR NDVI and its relationship with climate in Chinese arid and cold regions. *Journal of Remote Sensing*, vol. 12(3), pp. 499–505.

[92.] Sun, J., Wang, X., Chen, A., Ma, Y., Cui, M., and Piao, S., 2011. NDVI indicated characteristics of vegetation cover change in China's metropolises over the last three decades. *Environmental Monitoring and Assessment*, vol. 179(1–4), pp. 1–14.

[93.] Suzuki, P., Tanaka, S., and Yasunari, T., 2000. Relationships between meridional profiles of satellite-derived vegetation index (NDVI) and climate over Siberia. *International Journal of Climatology*, vol. 20, pp. 55–697.

[94.] Swift, T. L., and Hannon, S. J., 2010. Critical thresholds associated with habitat loss: a review of the concepts, evidence, and applications. *Biological Reviews*, vol. 85(1), pp. 35–53.

[95.] Townshend, J. R. G., 1995. Global data sets for land applications from the advanced very high resolution radiometer. *International Journal of Remote Sensing*, vol. 15, pp. 3319–3332.

[96.] Townshend, J. R. G., and Justice, C. O., 1986. Analysis of the dynamics of African vegetation using the normalized difference vegetation index. *International Journal of Remote Sensing*, vol. 8(8), pp. 1189–1207.

[97.] Tucker, C. J., Newcomb, W. W., Los, S. O., and Prince, S. D., 1991. Mean and inter-year variation of growing-season Normalized Difference Vegetation Index for the Sahel 1981 – 1989. *International Journal of Remote Sensing*, vol. 12 (6), pp. 1133–1135.

[98.] Tucker, C. J., Slayback, D. A., Pinzon, J. E., Los, S. Q., Myneni, R. B., and Taylor, M. G., 2001. Higher northern latitude normalized difference vegetation index and growing season trends from 1982 to 1999. *International Journal of Biometeorology*, vol. 45, pp. 184–190.

[99.] van Leeuwen, W. J. D., Huete, A. R., and Laing, T. W., 1999. MODIS vegetation index compositing approach: a prototype with AVHRR data. *Remote Sensing Environment*, vol. 69(3), pp. 264–280.

[100.] Verhoef, W., Menenti, M., and Azzali, S. 1996. A colour composite of NOAA-VHRR-NDVI based on time series analysis (1981–1992). *International Journal of Remote Sensing*, vol. 17(2), pp. 231–235.

[101.] Wang, J., Rich, P. M., and Price, K. P., 2003. Temporal responses of NDVI to precipitation and temperature in the central Great Plains, USA. *International Journal of Remote Sensing*, vol. 24, pp. 2345–2364.

[102.] Wang, X., Piao, S., Ciais, P., Li, J., Friedlingstein, P., Koven, C., and Chen, A., 2011. Spring temperature change and its implication in the change of vegetation growth in North America from 1982 to 2006. *Proceedings of the National Academy of Sciences*, vol. 108(4), pp. 1240–1245.

[103.] Wang, W. et al., 2006. Feedbacks of vegetation on summertime climate variability over the North American grasslands. Part 1: Statistical analysis. *Earth Interact*, vol. 10 (Paper 17).

[104.] Wardlow, B. D., Egbert, S. L., and Kastens, J. H., 2007. Analysis of timeseries MODIS 250 m vegetation index data for crop classification in the U.S. Central Great Plains. *Remote Sensing Environment*, vol. 108(3), pp. 290–310.

[105.] Weismiller, R. A., Kristof, S. J., Scholz, D. K., Anuta, P. E., and Momin, S. M., 1977. Change detection in coastal zone environments. *Photogrammetric Engineering and Remote Sensing*, vol. 43(12), pp. 1533–1539.

[106.] Willem J. D. van Leeuwen, Orr, B. J., Marsh, S. E., Herrmann, S. M., 2006, Multi-sensor NDVI data continuity: Uncertainties and implications for vegetation monitoring applications. *Remote Sensing of Environment*, vol. 100(2006), pp. 67–81.

[107.] Xiao, X., Boles, S., Liu, J., Zhuang, D., Frolking, S., Li, C., Salas, W., and Moore, B. JIII, 2005. Mapping paddy rice agriculture in southern China using multi-temporal MODIS images. *Remote Sensing Environment*, vol. 95(4), pp. 480–492.

[108.] Yang, G. H., Bao, A. M., Chen, X., Liu, H. L., Huang, Y., and Dai, S. Y., 2009. Study of the vegetation cover change and its driving factors over Xinjiang during 1998–2007. *Journal of Glaciology and Geocryology*, vol. 31(3), pp. 436–445.

[109.] Yang, L., Wylie, B. K., Thieszen, L. L., and Reed, B. C., 1998. An analysis of relationships among climate forcing and time-integrated NDVI of grasslands over the U.S. northern and central great plains. *Remote Sensing of Environment*, vol. 65, pp. 25–37.

[110.] Yang, Y., Yang, L., and Merchant, J. W., 1997. An assessment of AVHRR/NDVI-ecoclimatological relations in Nebraska. USA. *International Journal of Remote Sensing*, vol. 18, pp. 2161–2180.

[111.] Yue, S., Pilon, P., and Cavadias, G., 2002. Power of the Mann-Kendall and Spearman's rho tests detecting monotonic trends in hydrological series. *Journal of Hydrology*, vol. 259, pp. 254–271.

[112.] Zhang, Y., Gao, J., Liu, L., Wang, Z., Ding, M., and Yang, X., 2013. NDVI-based vegetation changes and their responses to climate change from 1982 to 2011: A case study in the Koshi River Basin in the middle Himalayas. *Global and Planetary Change*, vol. 108(2013), pp. 139–148.

[113.] Zhou, L. M., Kaufmann, R. K., Tian, Y., Myneni, R. B., and Tucker, C. J., 2003. Relation between interannual variations in satellite measures of vegetation greenness and climate between 1982 and 1999. *Journal of Geophysical Research*, vol. 108(D1).

[114.] Zhou, L. M., Tucker, C. J., Kaufmann, R. K., Slayback, D., Shabanov, N. V., and Myneni, R. B., 2001. Variations in northern vegetation activity inferred from satellite data of vegetation index during 1981 to 1999. *Journal of Geophysical Research-Atmospheres*, vol. 106(D17), pp. 20069–20083.

[115.] Zhao, M., and Running, S. W., 2010. Drought-induced reduction in global terrestrial net primary production from 2000 through 2009. *Science*, vol. 329(5994), pp. 940.

Appendix 1

Table 1: Mean (μ) \pm standard deviation (σ) of NDVI, LST and rainfall for forest class for northern Western Ghats

Month, Year	NDVI ($\mu \pm \sigma$)	LST ($\mu \pm \sigma$)	rainfall ($\mu \pm \sigma$)	Month, Year	NDVI ($\mu \pm \sigma$)	LST ($\mu \pm \sigma$)	rainfall ($\mu \pm \sigma$)
Jan, 2003	0.59 \pm 0.07	--	0.23 \pm 0.41	Jan, 2004	0.65 \pm 0.1	21.25 \pm 3	0.25 \pm 1
Feb, 2003	0.52 \pm 0.08	--	0.03 \pm 0.04	Feb, 2004	0.54	22.50 \pm 3	0.02
Mar, 2003	0.41 \pm 0.09	25.96 \pm 3.3	7.02 \pm 0.78	Mar, 2004	0.5 \pm 0.16	27.3 \pm 4	0.02
Apr, 2003	0.39 \pm 0.10	29.95 \pm 4	1.18 \pm 2.47	Apr, 2004	0.5 \pm 0.16	28.65 \pm 3	1.04 \pm 2.3
May, 2003	0.4 \pm 0.11	29.02 \pm 4	17.74 \pm 8	May, 2004	0.5 \pm 0.16	29.66 \pm 2	21.17 \pm 1
Jun, 2003	0.4 \pm 0.1	23.31 \pm 5	444 \pm 145	Jun, 2004	0.6 \pm 0.14	28.81 \pm 2	400 \pm 82
Aug, 2003	0.63 \pm 0.09	27.50 \pm 2	266 \pm 72	Aug, 2004	0.6 \pm 0.09	25.76 \pm 1	449 \pm 84
Sep, 2003	0.69 \pm 0.10	25.27 \pm 1	169 \pm 35	Sep, 2004	0.7 \pm 0.11	26.3 \pm 2	194 \pm 15
Oct, 2003	0.68 \pm 0.1	29.43 \pm 2	46.42 \pm 17	Oct, 2004	0.7 \pm 0.11	22.09 \pm 6	44 \pm 16.72
Nov, 2003	0.62 \pm 0.1	--	6.09 \pm 2.65	Nov, 2004	0.7 \pm 0.11	22.64 \pm 3	1.68 \pm 1
Dec, 2003	0.6 \pm 0.1	19.56 \pm 2.83	0.00 \pm 0.01	Dec, 2004	0.66	21.14 \pm 4	0 \pm 0.01

Jan, 2005	0.59 ±0.07	22±3.22	0.7±0.8	Jan, 2006	0.59±0.07	22.5±3.9	0.8±0.0
Feb, 2005	0.53 ±0.08	23±3.06	0.1±0.2	Feb, 2006	0.52±0.08	24.5±3.0	--
Mar, 2005	0.42 ±0.10	28±3.41	0.2±0.4	Mar, 2006	0.41±0.09	25.8±3.2	2.0±2.1
Apr, 2005	0.40 ±0.11	29±4.01	5.0±7.7	Apr, 2006	0.39±0.10	28.9±2.9	0.2±0.4
May, 2005	0.40 ±0.11	30±3.67	2.7±4.4	May, 2006	0.40±0.11	33.3±2.9	101.1±69.3
Jun, 2005	0.44 ±0.13	28±1.99	355.7±62.3	Jun, 2006	0.48±0.14	28.4±1.6	323.3±56.8
Aug, 2005	0.60 ±0.09	27±1.06	321.6±86.6	Aug, 2006	0.60±0.08	26.3±1.8	472.3±55.0
Sep. 2005	0.64 ±0.10	25±1.27	394.1±69.8	Sep. 2006	0.69±0.10	29.0±1.3	256.1±20.2
Oct, 2005	0.68 ±0.10	22±3.42	60.4±32.3	Oct, 2006	0.67±0.10	22.7±3.0	105.5±60.0
Nov, 2005	0.63 ±0.09	23±3.23	0.1±0.4	Nov, 2006	0.63±0.09	24.2±3.9	7.2±6.4
Dec, 2005	0.60 ±0.08	20±3.84	0.0±0.0	Dec, 2006	0.60±0.07	26.7±2.9	--
Jan, 2007	0.59±0.07	26.5±2.8	--	Jan, 2008	0.58±0.07	19.67±3.16	0.03±0.13
Feb, 2007	0.52±0.08	27.4±3.2	--	Feb, 2008	0.52±0.08	24.23±3.13	0.46±0.61
Mar, 2007	0.40±0.08	32.7±2.8	0.0±0.1	Mar, 2008	0.41±0.09	27.49±3.43	24.31±22.3
Apr, 2007	0.40±0.11	35.0±2.7	2.7±2.3	Apr, 2008	0.39±0.10	30.20±4.51	3.17±4.98
May, 2007	0.40±0.11	35.4±2.2	2.2±5.0	May, 2008	0.42±0.12	29.54±3.15	16.54±17.4
Jun, 2007	0.43±0.12	31.2±2.4	372.9±126.8	Jun, 2008	0.40±0.11	30.65±2.97	341±72.4
Aug, 2007	0.62±0.09	26.1±1.7	434.5±88.4	Aug, 2008	0.59±0.08	26.25±1.42	348±106
Sep. 2007	0.68±0.10	29.1±1.9	289.9±47.1	Sep. 2008	0.66±0.10	25.20±1.40	359±62.6
Oct, 2007	0.66±0.10	22.3±2.9	17.9±23.1	Oct, 2008	0.65±0.09	25.94±2.99	52.2±22.4
Nov, 2007	0.62±0.08	24.4±2.8	14.0±13.9	Nov, 2008	0.61±0.08	20.67±3.18	2.31±3.19
Dec, 2007	0.59±0.07	26.5±3.0	0.1±0.0	Dec, 2008	0.60±0.08	24.21±3.51	3.8±2.68
Jan, 2009	0.61±0.08	25.42±3.08	0.02±0.05	Jan, 2010	0.60±0.07	23.1±3.41	1.71±1.7

Feb, 2009	0.54±0.09	22.62±3.13	--	Feb, 2010	0.53±0.08	22.5±5.00	0.36±0.2
Mar, 2009	0.46±0.11	26.95±3.47	1.01±0.83	Mar, 2010	0.41±0.08	28.1±3.77	2.18±1.6
Apr, 2009	0.45±0.11	29.80±4.37	0.41±0.90	Apr, 2010	0.40±0.10	30.6±4.40	5.59±5.9
May, 2009	0.46±0.11	29.57±3.38	8.52±9.03	May, 2010	0.41±0.11	32.6±3.76	5.48±6.8
Jun, 2009	0.48±0.12	28.99±2.41	177±67.4	Jun, 2010	0.44±0.12	29.8±3.20	371±70.8
Aug, 2009	0.62±0.10	28.04±1.07	197±30.65	Aug, 2010	0.63±0.09	27.2±1.39	413±46.01
Sep. 2009	0.74±0.10	25.10±1.92	248±71.89	Sep. 2010	0.68±0.10	28.3±1.76	252±53.6
Oct, 2009	0.73±0.09	23.50±3.81	180±105	Oct, 2010	0.68±0.10	25.8±2.12	119.2±59.6
Nov, 2009	0.64±0.09	26.84±3.19	122±12.06	Nov, 2010	0.65±0.09	25.4±3.37	87.4±19.7
Dec, 2009	0.63±0.09	21.11±3.17	3.21±3.6	Dec, 2010	0.61±0.08	19.7±3.63	0.73±1.2
Jan, 2011	0.59±0.07	21.6±3.4	1.3±1.6	Jan, 2012	0.58±0.06	18.18±2	1.5±2
Feb, 2011	0.53±0.08	22.1±2.9	0.2±0.2	Feb, 2012	0.52±0.07	22.07±3	0.3±0
Mar, 2011	0.41±0.09	27.8±4.0	1.6±2	Mar, 2012	0.42±0.09	25.93±3	1.6±1
Apr, 2011	0.40±0.11	26.4±4.3	6.1±6	Apr, 2012	0.40±0.1	29.45±3	5.7±6
May, 2011	0.42±0.12	31.5±3.0	4.9±4.5	May, 2012	0.41±0.1	30.17±3	5.3±7
Jun, 2011	0.38±0.09	30.6±2.0	359±95	Jun, 2012	0.41±0.1	28.33±3	391.0±84
Aug, 2011	0.62±0.09	24.5±2.4	432±63	Aug, 2012	0.60±0.07	25.66±1	421.8±48
Sep. 2011	0.68±0.10	24.6±1.8	264±139	Sep. 2012	0.67±0.09	24.35±2	284.2±135
Oct, 2011	0.67±0.10	22.2±2.9	121±44.7	Oct, 2012	0.68±0.09	22.93±3	127.8±60
Nov, 2011	0.62±0.09	22.0±3.3	72±22.9	Nov, 2012	0.63±0.08	19.37±2	78.0±26
Dec, 2011	0.60±0.07	20.0±3.0	0.7±0.9	Dec, 2012	0.61±0.09	18.14±3	0.9±1

Table 2: Mean (μ) \pm standard deviation (σ) of NDVI, LST and rainfall for agriculture/grassland class for northern Western Ghats

Month, Year	NDVI ($\mu \pm \sigma$)	LST ($\mu \pm \sigma$)	rainfall ($\mu \pm \sigma$)	Month, Year	NDVI ($\mu \pm \sigma$)	LST ($\mu \pm \sigma$)	rainfall ($\mu \pm \sigma$)
Jan, 2003	0.34 \pm 0.08	--	0.51 \pm 0.74	Jan, 2004	0.35 \pm 0.1	21.25 \pm 3	0.25 \pm 0.5
Feb, 2003	0.3 \pm 0.07	--	0.03 \pm 0.06	Feb, 2004	0.31 \pm 0.1	22.5 \pm 3.1	0.02 \pm 0.1
Mar, 2003	0.24 \pm 0.03	30.77 \pm 3	7.35 \pm 0.94	Mar, 2004	0.24	27.3 \pm 4	0.02
Apr, 2003	0.22 \pm 0.03	34.56 \pm 3	0.61 \pm 1.79	Apr, 2004	0.22	28.7 \pm 3.3	1.04 \pm 2.3
May, 2003	0.22 \pm 0.03	33.75 \pm 3	24.81 \pm 9.9	May, 2004	0.22	29.7 \pm 2.4	21.17 \pm 10
Jun, 2003	0.22	30.06 \pm 5.5	402 \pm 109	Jun, 2004	0.22	28.81 \pm 2	340 \pm 82.3
Aug, 2003	0.37 \pm 0.09	27.95 \pm 2.1	260 \pm 66.6	Aug, 2004	0.34 \pm 0.1	25.76 \pm 1	449 \pm 84
Sep, 2003	0.37 \pm 0.09	27.31 \pm 2	160 \pm 31	Sep, 2004	0.39 \pm 0.1	26.30 \pm 2	193.7 \pm 15
Oct, 2003	0.37 \pm 0.09	32.78 \pm 1.5	43.67 \pm 21	Oct, 2004	0.42 \pm 0.1	22.09 \pm 6	44.42 \pm 17
Nov, 2003	0.37 \pm 0.08	26.5 \pm 3.5	7.18 \pm 2.2	Nov, 2004	0.39 \pm 0.1	22.64 \pm 3	1.68 \pm 1
Dec, 2003	0.36 \pm 0.08	23.54 \pm 3.6	0	Dec, 2004	0.38 \pm 0.1	21.14 \pm 4	0
Jan, 2005	0.36 \pm 0.08	24.93 \pm 3.1	1.21 \pm 1.3	Jan, 2006	0.35 \pm 0.1	26.9 \pm 3.7	0
Feb, 2005	0.31 \pm 0.07	26.7 \pm 3.31	0.24 \pm 0.3	Feb, 2006	0.30 \pm 0.1	28.97 \pm 3	--
Mar, 2005	0.24 \pm 0.03	32.21 \pm 3	0.62 \pm 0.9	Mar, 2006	0.24	29.4 \pm 2.5	2.14 \pm 2
Apr, 2005	0.22 \pm 0.03	33.33 \pm 2.8	4.61 \pm 9	Apr, 2006	0.22	32.66 \pm 2	0.24 \pm 0.7
May, 2005	0.22 \pm 0.03	33.72 \pm 2.3	2.23 \pm 3.8	May, 2006	0.22	34.66 \pm 4	44.51 \pm 4
Jun, 2005	0.22 \pm 0.03	31.71 \pm 2	274 \pm 68.2	Jun, 2006	0.22	30.1 \pm 1.5	252.7 \pm 59
Aug, 2005	0.34 \pm 0.09	27.19 \pm 1	353.6 \pm 77	Aug, 2006	0.34 \pm 0.1	27.05 \pm 2	482.9 \pm 72
Sep, 2005	0.37 \pm 0.09	25.5 \pm 1.6	397.5 \pm 71	Sep, 2006	0.39 \pm 0.1	29.46 \pm 1	250.4 \pm 20
Oct, 2005	0.43 \pm 0.06	27.56 \pm 3	72.28 \pm 36	Oct, 2006	0.43 \pm 0.1	27.65 \pm 3	59.30 \pm 30
Nov, 2005	0.39 \pm 0.07	26.8 \pm 3.44	0.04 \pm 0.15	Nov, 2006	0.40 \pm 0.1	27.31 \pm 3	7.64 \pm 5.2

Dec, 2005	0.37 ± 0.08	24.39 ± 4	0 ± 0.03	Dec, 2006	0.38 ± 0.1	29.8 ± 2.5	--
Jan, 2007	0.36 ± 0.08	26.51 ± 3	--	Jan, 2008	0.35 ± 0.1	23.74 ± 4	0.074
Feb, 2007	0.31 ± 0.01	27.38 ± 3.2	0.17 ± 0.1	Feb, 2008	0.31 ± 0.1	28.23 ± 3	0.3 ± 0.57
Mar, 2007	0.24 ± 0.03	32.72 ± 2.8	0.03 ± 0.13	Mar, 2008	0.24	32.23 ± 3	17.23 ± 20
Apr, 2007	0.22 ± 0.03	35.04 ± 2.7	2.71 ± 2.28	Apr, 2008	0.22	35.84 ± 3	3.61 ± 7
May, 2007	0.22 ± 0.03	35.36 ± 2.2	2.15 ± 5.04	May, 2008	0.22	32.64 ± 2	5.57 ± 9.8
Jun, 2007	0.23 ± 0.03	31.15 ± 2.4	373 ± 127	Jun, 2008	0.22	33.35 ± 2	262.9 ± 80
Aug, 2007	0.36 ± 0.09	26.1 ± 1.67	434.5 ± 89	Aug, 2008	0.32 ± 0.1	27.53 ± 2	387.3 ± 97
Sep, 2007	0.37 ± 0.09	28.93 ± 2	306.9 ± 44	Sep, 2008	0.36 ± 0.1	25.55 ± 2	350.8 ± 67
Oct, 2007	0.40 ± 0.07	26.92 ± 3	2.44 ± 7	Oct, 2008	0.42 ± 0.1	29.73 ± 2	59.05 ± 26
Nov, 2007	0.39 ± 0.07	24.59 ± 5	6.15 ± 5.81	Nov, 2008	0.39 ± 0.1	26.64 ± 3	3.19 ± 4
Dec, 2007	0.36 ± 0.08	29.05 ± 3.1	0.01 ± 0.04	Dec, 2008	0.38 ± 0.1	28.23 ± 4	1.77 ± 2.1
Jan, 2009	0.38 ± 0.08	28.51 ± 2.9	0.03 ± 0.06	Jan, 2010	0.38 ± 0.1	27.04 ± 3	2.36 ± 2.2
Feb, 2009	0.32 ± 0.07	27.48 ± 3.5	--	Feb, 2010	0.32 ± 0.1	26.33 ± 5	0.48 ± 0.4
Mar, 2009	0.24 ± 0.03	31.42 ± 2.9	0.98 ± 0.9	Mar, 2010	0.25	32.73 ± 3	2.71 ± 1.5
Apr, 2009	0.22 ± 0.03	35.12 ± 2.7	0.24 ± 0.62	Apr, 2010	0.23	35.87 ± 3	3.68 ± 6
May, 2009	0.22 ± 0.03	33.69 ± 3	8.65 ± 11	May, 2010	0.22	36.69 ± 2	5.18 ± 2.9
Jun, 2009	0.23 ± 0.03	31.62 ± 2	115 ± 42.3	Jun, 2010	0.22	32.08 ± 2	291.4 ± 76
Aug, 2009	0.37 ± 0.09	28.9 ± 1.4	196 ± 27.2	Aug, 2010	0.37 ± 0.1	27.65 ± 2	403.5 ± 54
Sep, 2009	0.38 ± 0.08	26.26 ± 2.4	231 ± 56.8	Sep, 2010	0.39 ± 0.1	28.4 ± 1.8	257.5 ± 49
Oct, 2009	0.42 ± 0.06	29.75 ± 2.9	97.78 ± 49	Oct, 2010	0.43 ± 0.1	27.7 ± 2.3	78.65 ± 38
Nov, 2009	0.4 ± 0.07	23.96 ± 2	117.7 ± 16	Nov, 2010	0.40 ± 0.1	28.3 ± 1.8	81.08 ± 18
Dec, 2009	0.4 ± 0.08	24.18 ± 2.8	4.59 ± 4.12	Dec, 2010	0.41 ± 0.1	23.9 ± 3.4	0.84 ± 1.1

Jan, 2011	0.39 ± 0.07	25.63 ± 3.5	2.15 ± 2.21	Jan, 2012	0.35 ± 0.1	21.43 ± 3	2 ± 2.09
Feb, 2011	0.32 ± 0.06	25.76 ± 3	0.26 ± 0.31	Feb, 2012	0.31 ± 0.1	26.76 ± 4	0.35 ± 0.3
Mar, 2011	0.25 ± 0.03	32.6 ± 3	2.16 ± 1.61	Mar, 2012	0.24	30.26 ± 3	2.22 ± 1
Apr, 2011	0.23 ± 0.03	31.68 ± 3	4.52 ± 6.04	Apr, 2012	0.22	33.5 ± 2.6	3.61 ± 5.5
May, 2011	0.22 ± 0.03	35.14 ± 2	5.25 ± 3	May, 2012	0.22	33.9 ± 2	4.74 ± 3
Jun, 2011	0.23 ± 0.03	31.81 ± 2.2	324 ± 106	Jun, 2012	0.22	31.96 ± 3	295.3 ± 83
Aug, 2011	0.35 ± 0.09	25.87 ± 2.8	415 ± 72	Aug, 2012	0.34 ± 0.1	26.67 ± 2	398.7 ± 56
Sep. 2011	0.38 ± 0.08	25.82 ± 2.6	231 ± 114	Sep. 2012	0.37 ± 0.1	26.14 ± 3	231 ± 114
Oct, 2011	0.42 ± 0.06	27.45 ± 3	81.94 ± 36	Oct, 2012	0.41 ± 0.1	29.4 ± 2.8	87.95 ± 35
Nov, 2011	0.39 ± 0.07	26.29 ± 3.4	74.11 ± 21	Nov, 2012	0.39 ± 0.1	23.78 ± 3	76.16 ± 19
Dec, 2011	0.37 ± 0.08	24.09 ± 4	0.65 ± 0.98	Dec, 2012	0.37 ± 0.1	23.08 ± 4	0.70 ± 1

Table 3: Mean (μ) \pm standard deviation (σ) of NDVI, LST and rainfall for forest class for central Western Ghats

Month, Year	NDVI ($\mu \pm \sigma$)	LST ($\mu \pm \sigma$)	rainfall ($\mu \pm \sigma$)	Month, Year	NDVI ($\mu \pm \sigma$)	LST ($\mu \pm \sigma$)	rainfall ($\mu \pm \sigma$)
Jan, 2003	0.65 \pm 0.11	--	0.81 \pm 1.26	Jan, 2004	0.58 \pm 0.1	16.57 \pm 4	0.78 \pm 1
Feb, 2003	0.53 \pm 0.15	--	0.66 \pm 1.04	Feb, 2004	0.52 \pm 0.1	21.92 \pm 5	0.67 \pm 1.1
Mar, 2003	0.50 \pm 0.16	25.81 \pm 3.4	10.74 \pm 1	Mar, 2004	0.40 \pm 0.1	23.48 \pm 5	6.37 \pm 5.2
Apr, 2003	0.51 \pm 0.17	26.78 \pm 3.4	58.4 \pm 37	Apr, 2004	0.39 \pm 0.1	27.64 \pm 4	58.83 \pm 38
May, 2003	0.50 \pm 0.16	29.92 \pm 4	25.67 \pm 7	May, 2004	0.40 \pm 0.1	25.70 \pm 2	23.9 \pm 119
Jun, 2003	0.52 \pm 0.12	25.76 \pm 2.9	459 \pm 308	Jun, 2004	0.43 \pm 0.1	26.4 \pm 1.7	415 \pm 87.2
Aug, 2003	0.62 \pm 0.1	24.48 \pm 1.1	209 \pm 115	Aug, 2004	0.61 \pm 0.1	25.2 \pm 1	356 \pm 73
Sep. 2003	0.72 \pm 0.11	23.9 \pm 1.98	67.87 \pm 20	Sep. 2004	0.67 \pm 0.1	22.8 \pm 1.8	142.6 \pm 17
Oct, 2003	0.72 \pm 0.11	21.5 \pm 1.85	112 \pm 46.7	Oct, 2004	0.66 \pm 0.1	17.8 \pm 3.4	108.7 \pm 48
Nov, 2003	0.69 \pm 0.11	--	16.7 \pm 10.3	Nov, 2004	0.62 \pm 0.1	19.3 \pm 5.1	40.5 \pm 32
Dec, 2003	0.67 \pm 0.1	18.23 \pm 3.6	0.43 \pm 0.49	Dec, 2004	0.6 \pm 0.07	19.18 \pm 4	0.40 \pm 0.5
Jan, 2005	0.65 \pm 0.11	21.38 \pm 3	7.27 \pm 4.98	Jan, 2006	0.65 \pm 0.1	22.44 \pm 4	0.83 \pm 1.8
Feb, 2005	0.53 \pm 0.15	23.26 \pm 4.1	2.35 \pm 1.98	Feb, 2006	0.53 \pm 0.2	23.6 \pm 4.8	--
Mar, 2005	0.50 \pm 0.16	26.53 \pm 4.5	3.24 \pm 4.20	Mar, 2006	0.5 \pm 0.16	23.68 \pm 4	27.81 \pm 22
Apr, 2005	0.53 \pm 0.17	24.46 \pm 2.9	91.65 \pm 31	Apr, 2006	0.51 \pm 0.2	29 \pm 3.49	21.68 \pm 19
May, 2005	0.53 \pm 0.17	28.52 \pm 3.7	74.97 \pm 35	May, 2006	0.53 \pm 0.2	29.1 \pm 3	251 \pm 96
Jun, 2005	0.57 \pm 0.14	27.08 \pm 1.8	370 \pm 77	Jun, 2006	0.59 \pm 0.2	27.36 \pm 2	375.8 \pm 74
Aug, 2005	0.61 \pm 0.09	25.95 \pm 1.4	319 \pm 51.6	Aug, 2006	0.62 \pm 0.1	24 \pm 2.27	323 \pm 74.9
Sep. 2005	0.66 \pm 0.11	25.68 \pm 1.6	250.8 \pm 52	Sep. 2006	0.7 \pm 0.11	27.3 \pm 2.6	250 \pm 38
Oct, 2005	0.70 \pm 0.11	25 \pm 2.95	183 \pm 81	Oct, 2006	0.72 \pm 0.1	24.5 \pm 2.6	128 \pm 82
Nov, 2005	0.69 \pm 0.1	23.59 \pm 4	45.32 \pm 45	Nov, 2006	0.7 \pm 0.1	24 \pm 4.2	81.17 \pm 35

Dec, 2005	0.67 ± 0.1	20 ± 3.98	7.49 ± 12	Dec, 2006	0.67 ± 0.1	20.5 ± 3	1.05 ± 1.5
Jan, 2007	0.65 ± 0.1	19.89 ± 3.5	0.1 ± 0.29	Jan, 2008	0.65 ± 0.1	19.4 ± 4.3	0.13 ± 0.4
Feb, 2007	0.53 ± 0.15	23 ± 4.37	0.80 ± 1.3	Feb, 2008	0.53 ± 0.2	22.49 ± 4	16 ± 8.96
Mar, 2007	0.49 ± 0.15	23.2 ± 5.03	1.57 ± 0.64	Mar, 2008	0.52 ± 0.2	27.34 ± 3	146.7 ± 56
Apr, 2007	0.53 ± 0.18	25.79 ± 3.6	28.85 ± 14	Apr, 2008	0.53 ± 0.2	25.2 ± 4.5	31.66 ± 14
May, 2007	0.53 ± 0.17	28.63 ± 3.8	72 ± 25.57	May, 2008	0.54 ± 0.2	26.57 ± 4	54.78 ± 24
Jun, 2007	0.56 ± 0.15	26.62 ± 2	507 ± 114	Jun, 2008	0.57 ± 0.2	25 ± 1.66	368.7 ± 88
Aug, 2007	0.62 ± 0.09	27.28 ± 1.4	462 ± 77.4	Aug, 2008	0.59 ± 0.1	28.58 ± 3	370.3 ± 79
Sep, 2007	0.66 ± 0.11	26.74 ± 1.4	342 ± 52.4	Sep, 2008	0.66 ± 0.1	25 ± 1.47	230 ± 85.6
Oct, 2007	0.70 ± 0.1	25.3 ± 2	143 ± 67	Oct, 2008	0.71 ± 0.1	23.3 ± 2.6	106 ± 65.8
Nov, 2007	0.69 ± 0.11	22 ± 4.3	35.39 ± 16	Nov, 2008	0.68 ± 0.1	20.8 ± 4.7	23.7 ± 19
Dec, 2007	0.67 ± 0.10	25.42 ± 3.8	8.62 ± 16.1	Dec, 2008	0.67 ± 0.1	21 ± 4.65	4.54 ± 5
Jan, 2009	0.64 ± 0.1	21.14 ± 4.2	0.05 ± 0.2	Jan, 2010	0.66 ± 0.1	22 ± 3.98	11.01 ± 3
Feb, 2009	0.52 ± 0.15	24.78 ± 5	--	Feb, 2010	0.53 ± 0.2	22.5 ± 4.4	0.79 ± 0.5
Mar, 2009	0.51 ± 0.1	25.09 ± 4	30.64 ± 17	Mar, 2010	0.49 ± 0.2	23.3 ± 4.4	5.12 ± 3.7
Apr, 2009	0.52 ± 0.16	27.51 ± 3.9	24.8 ± 12.9	Apr, 2010	0.52 ± 0.2	25.65 ± 4	67.50 ± 33
May, 2009	0.52 ± 0.17	27.59 ± 3.7	91 ± 33	May, 2010	0.57 ± 0.2	29.3 ± 3.5	81.92 ± 30
Jun, 2009	0.59 ± 0.15	25.6 ± 1.9	245 ± 63.7	Jun, 2010	0.59 ± 0.2	26.35 ± 3	375 ± 79
Aug, 2009	0.63 ± 0.1	25.7 ± 1.5	237 ± 26	Aug, 2010	0.65 ± 0.1	28.15 ± 2	366 ± 65.6
Sep, 2009	0.7 ± 0.1	24.54 ± 1.6	323 ± 58	Sep, 2010	0.66 ± 0.1	25.5 ± 1.3	251 ± 47
Oct, 2009	0.71 ± 0.1	20.2 ± 3	166 ± 78	Oct, 2010	0.70 ± 0.1	--	193 ± 73
Nov, 2009	0.69 ± 0.1	22.47 ± 4.5	133 ± 43.7	Nov, 2010	0.72 ± 0.1	23.7 ± 4.2	191 ± 56
Dec, 2009	0.67 ± 0.1	22 ± 4.04	29.78 ± 14	Dec, 2010	0.66 ± 0.1	24.7 ± 3.2	7.20 ± 7.4

Jan, 2011	0.64 ± 0.1	24.9 ± 3.3	8.2 ± 2.5	Jan, 2012	0.65 ± 0.1	15.9 ± 3.8	9.21 ± 2.7
Feb, 2011	0.53 ± 0.15	29.76 ± 3.7	1 ± 0.81	Feb, 2012	0.53 ± 0.2	22.8 ± 4.7	0.66 ± 0.6
Mar, 2011	0.49 ± 0.15	24.47 ± 3.8	2.98 ± 3.87	Mar, 2012	0.51 ± 0.2	24.98 ± 3	4.83 ± 4
Apr, 2011	0.53 ± 0.17	21.99 ± 3.5	70.89 ± 33	Apr, 2012	0.52 ± 0.2	26.15 ± 3	66 ± 34
May, 2011	0.57 ± 0.18	26.49 ± 4.5	78 ± 31	May, 2012	0.55 ± 0.2	26.86 ± 4	78 ± 31
Jun, 2011	0.51 ± 0.12	27.8 ± 1.8	380 ± 111	Jun, 2012	0.52 ± 0.1	28 ± 2.4	407 ± 107
Aug, 2011	0.62 ± 0.09	26.2 ± 1.1	408 ± 95.6	Aug, 2012	0.62 ± 0.1	26 ± 1.9	429 ± 87
Sep. 2011	0.63 ± 0.09	20 ± 2.26	275 ± 142	Sep. 2012	0.69 ± 0.1	19.9 ± 2.2	286 ± 110
Oct, 2011	0.71 ± 0.1	21.6 ± 2.05	178 ± 49.6	Oct, 2012	0.71 ± 0.1	22 ± 2.88	201 ± 52
Nov, 2011	0.7 ± 0.10	20.02 ± 4.2	185.65 ± 6	Nov, 2012	0.69 ± 0.1	17.99 ± 5	189 ± 48
Dec, 2011	0.67 ± 0.1	20.3 ± 3.38	6.8 ± 7.02	Dec, 2012	0.67 ± 0.1	19.8 ± 4	6.86 ± 7

Table 4: Mean (μ) \pm standard deviation (σ) of NDVI, LST and rainfall for agriculture/grassland class for central Western Ghats

Month, Year	NDVI ($\mu \pm \sigma$)	LST ($\mu \pm \sigma$)	rainfall ($\mu \pm \sigma$)	Month, Year	NDVI ($\mu \pm \sigma$)	LST ($\mu \pm \sigma$)	rainfall ($\mu \pm \sigma$)
Jan, 2003	0.34 \pm 0.07	--	1.67 \pm 1.76	Jan, 2004	0.34 \pm 0.1	24.24 \pm 4	1.72 \pm 1.8
Feb, 2003	0.27 \pm 0.03	--	0.84 \pm 1.22	Feb, 2004	0.27	29.18 \pm 4	0.84 \pm 1.2
Mar, 2003	0.25 \pm 0.03	31.5 \pm 3.78	11.13 \pm 1.1	Mar, 2004	0.25	31.4 \pm 3.6	4.59 \pm 4.8
Apr, 2003	0.23 \pm 0.02	31.86 \pm 3	51.83 \pm 27	Apr, 2004	0.23	34.5 \pm 3.8	52.85 \pm 27
May, 2003	0.23 \pm 0.03	36 \pm 2	22.7 \pm 6.18	May, 2004	0.23	28.8 \pm 3.4	117 \pm 59
Jun, 2003	0.26 \pm 0.04	30 \pm 4.9	243 \pm 167	Jun, 2004	0.26	28.24 \pm 3	366 \pm 73
Aug, 2003	0.34 \pm 0.09	24.51 \pm 1.2	179 \pm 100	Aug, 2004	0.36 \pm 0.1	25.7 \pm 1.8	336 \pm 74
Sep. 2003	0.35 \pm 0.09	27.29 \pm 2.6	51 \pm 20	Sep. 2004	0.38 \pm 0.1	24.5 \pm 2.4	145.4 \pm 17
Oct, 2003	0.36 \pm 0.08	26.88 \pm 3.5	85.26 \pm 49	Oct, 2004	0.42 \pm 0.1	24 \pm 4.1	76.37 \pm 44
Nov, 2003	0.4 \pm 0.07	26 \pm 3.29	7.08 \pm 7.08	Nov, 2004	0.41 \pm 0.1	28.6 \pm 3.7	11.18 \pm 18
Dec, 2003	0.38 \pm 0.07	24 \pm 3.57	0.39 \pm 0.5	Dec, 2004	0.39 \pm 0.1	24.6 \pm 3.5	0.41 \pm 0.5
Jan, 2005	0.35 \pm 0.07	27.04 \pm 2.8	7.8 \pm 5.4	Jan, 2006	0.37 \pm 0.1	28.1 \pm 3.2	0.82 \pm 2.2
Feb, 2005	0.27 \pm 0.03	30 \pm 3.53	2.2 \pm 2	Feb, 2006	0.27	30.6 \pm 3.5	--
Mar, 2005	0.25 \pm 0.03	33.68 \pm 2.8	3.52 \pm 3.88	Mar, 2006	0.25	30.5 \pm 3.2	18.7 \pm 18
Apr, 2005	0.23 \pm 0.02	28.49 \pm 3.7	77 \pm 20	Apr, 2006	0.23	34.75 \pm 3	15 \pm 11.17
May, 2005	0.23 \pm 0.03	34.96 \pm 2.4	63.7 \pm 21	May, 2006	0.23	34.97 \pm 3	151 \pm 43.1
Jun, 2005	0.26 \pm 0.04	29.85 \pm 3	338.6 \pm 46	Jun, 2006	0.26	29.16 \pm 2	333 \pm 51
Aug, 2005	0.36 \pm 0.08	26.28 \pm 2	318 \pm 51	Aug, 2006	0.35 \pm 0.1	23.92 \pm 2.7	313 \pm 81.6
Sep. 2005	0.37 \pm 0.09	26.05 \pm 1.9	264.3 \pm 58	Sep. 2006	0.38 \pm 0.1	28.21 \pm 3	228 \pm 46.7
Oct, 2005	0.41 \pm 0.07	28.1 \pm 4.27	183 \pm 92	Oct, 2006	0.42 \pm 0.1	29.15 \pm 3	64.9 \pm 50
Nov, 2005	0.43 \pm 0.06	27.94 \pm 4	23.9 \pm 32.1	Nov, 2006	0.42 \pm 0.1	27.8 \pm 2.5	62.9 \pm 31

Dec, 2005	0.41 ± 0.07	25.6 ± 3.9	3.04 ± 7.5	Dec, 2006	0.4 ± 0.07	24.7 ± 2.9	1.03 ± 1.5
Jan, 2007	0.35 ± 0.07	26.08 ± 3.2	0.25 ± 0.5	Jan, 2008	0.37 ± 0.1	26.5 ± 3.6	20.9 ± 4.7
Feb, 2007	0.27 ± 0.03	29.4 ± 2.8	0.96 ± 1.58	Feb, 2008	0.27	28.6 ± 3.6	12.3 ± 10
Mar, 2007	0.25 ± 0.03	31.42 ± 3.1	1.89 ± 0.84	Mar, 2008	0.25	31.7 ± 3.1	108 ± 29
Apr, 2007	0.23 ± 0.03	30.89 ± 3.3	24.14 ± 8.8	Apr, 2008	0.23	31.74 ± 3	25.25 ± 6
May, 2007	0.23 ± 0.03	34.33 ± 2.1	40.06 ± 16	May, 2008	0.23	32.4 ± 3.8	33.17 ± 19
Jun, 2007	0.26 ± 0.04	29.57 ± 3.4	482 ± 61	Jun, 2008	0.27	27.55 ± 3	339 ± 67
Aug, 2007	0.37 ± 0.08	27.43 ± 1.8	450.5 ± 84	Aug, 2008	0.31 ± 0.1	28.78 ± 3	400 ± 84
Sep, 2007	0.37 ± 0.09	26.98 ± 1.6	337.9 ± 50	Sep, 2008	0.37 ± 0.1	25.7 ± 2.2	240 ± 87
Oct, 2007	0.41 ± 0.07	28.08 ± 3	125.3 ± 84	Oct, 2008	0.41 ± 0.1	27.15 ± 4	104 ± 63
Nov, 2007	0.43 ± 0.06	26.94 ± 4.8	21.34 ± 13	Nov, 2008	0.42 ± 0.1	29.37 ± 4	33.86 ± 18
Dec, 2007	0.41 ± 0.06	29.39 ± 3.2	10.85 ± 18	Dec, 2008	0.42 ± 0.1	26 ± 3.8	2.1 ± 3.47
Jan, 2009	0.37 ± 0.06	27.1 ± 3.09	0.13 ± 0.29	Jan, 2010	0.38 ± 0.1	27.1 ± 2.6	9.51 ± 2.7
Feb, 2009	0.27 ± 0.03	31.76 ± 3.2	--	Feb, 2010	0.28	28.2 ± 2.8	0.81 ± 0.5
Mar, 2009	0.25 ± 0.03	31.07 ± 2.7	21 ± 16.6	Mar, 2010	0.26	29.6 ± 2.9	3.83 ± 4
Apr, 2009	0.23 ± 0.03	33.89 ± 3	17.04 ± 8.4	Apr, 2010	0.24	32.05 ± 5	46 ± 31.5
May, 2009	0.23 ± 0.03	34.3 ± 2.6	70.58 ± 21	May, 2010	0.23	35.3 ± 2.3	55 ± 31.6
Jun, 2009	0.27 ± 0.04	28.1 ± 2.9	212 ± 45.6	Jun, 2010	0.27	32.1 ± 3.6	336.7 ± 54
Aug, 2009	0.38 ± 0.08	26.95 ± 2.1	223 ± 31	Aug, 2010	0.38 ± 0.1	28.88 ± 2	353 ± 74
Sep, 2009	0.39 ± 0.1	25.4 ± 2	298.1 ± 56	Sep, 2010	0.38 ± 0.1	26 ± 1.5	240.5 ± 47
Oct, 2009	0.43 ± 0.07	25.9 ± 4.42	163.7 ± 69	Oct, 2010	0.4 ± 0.08	26.1 ± 2.6	171.6 ± 78
Nov, 2009	0.41 ± 0.07	27.3 ± 2.25	86.3 ± 22.1	Nov, 2010	0.42 ± 0.1	28.21 ± 1.8	134 ± 66.5
Dec, 2009	0.42 ± 0.06	27.3 ± 3.19	23.3 ± 10.6	Dec, 2010	0.43 ± 0.1	27.9 ± 2.8	3.77 ± 6.2

Jan, 2011	0.39 ± 0.06	24.9 ± 3.31	8.18 ± 2.5	Jan, 2012	0.36	23.3 ± 3.9	8.27 ± 2.4
Feb, 2011	0.28 ± 0.03	29.76 ± 3.7	1.04 ± 0.81	Feb, 2012	0.27	30.5 ± 3.4	0.67 ± 0.5
Mar, 2011	0.26 ± 0.03	30.34 ± 3	2.98 ± 3.87	Mar, 2012	0.25	28.3 ± 2.7	3.2 ± 3.92
Apr, 2011	0.24 ± 0.03	26.46 ± 3.9	43.6 ± 26.9	Apr, 2012	0.24	29.5 ± 2.7	51.5 ± 33
May, 2011	0.23 ± 0.03	33.3 ± 2.73	44.88 ± 30	May, 2012	0.23	35.47 ± 3	59.1 ± 26
Jun, 2011	0.25 ± 0.05	27.6 ± 2	378 ± 106	Jun, 2012	0.26	31 ± 3.1	343 ± 97
Aug, 2011	0.36 ± 0.09	26.4 ± 1.3	391 ± 108	Aug, 2012	0.35 ± 0.1	25.9 ± 2.1	376 ± 108
Sep. 2011	0.37 ± 0.08	21.6 ± 3.32	235 ± 153	Sep. 2012	0.37 ± 0.1	23.2 ± 3.9	195 ± 115
Oct, 2011	0.4 ± 0.08	24.2 ± 3.3	149 ± 57	Oct, 2012	0.4 ± 0.07	28.1 ± 4.7	1356 ± 35
Nov, 2011	0.42 ± 0.06	27.18 ± 4.4	107 ± 62.8	Nov, 2012	0.42 ± 0.1	24.6 ± 4.4	138.9 ± 51
Dec, 2011	0.41 ± 0.07	25.53 ± 3.7	3.82 ± 6.69	Dec, 2012	0.4 ± 0.06	25.5 ± 3.3	4.1 ± 6.85

Table 5: Mean (μ) \pm standard deviation (σ) of NDVI, LST and rainfall for Forest class for southern Western Ghats

Month, Year	NDVI ($\mu \pm \sigma$)	LST ($\mu \pm \sigma$)	rainfall ($\mu \pm \sigma$)	Month, Year	NDVI ($\mu \pm \sigma$)	LST ($\mu \pm \sigma$)	rainfall ($\mu \pm \sigma$)
Jan, 2003	0.69 \pm 0.1	--	6.6 \pm 2.53	Jan, 2004	0.70 \pm 0.1	26.5 \pm 2.3	6.68 \pm 2.5
Feb, 2003	0.62 \pm 0.16	--	6.66 \pm 5.35	Feb, 2004	0.66 \pm 0.1	28.2 \pm 2.5	6.7 \pm 5.38
Mar, 2003	0.61 \pm 0.17	29 \pm 1.37	14.9 \pm 1.56	Mar, 2004	0.59 \pm 0.2	29.4 \pm 18	22.7 \pm 2.5
Apr, 2003	0.6 \pm 0.18	24.7 \pm 1.8	91.3 \pm 35	Apr, 2004	0.65 \pm 0.1	26.9 \pm 1.5	93.53 \pm 35
May, 2003	0.55 \pm 0.15	30.38 \pm 1.4	64.69 \pm 38	May, 2004	0.66 \pm 0.1	25.2 \pm 1.6	416 \pm 216
Jun, 2003	0.62 \pm 0.16	29.3 \pm 1.6	336 \pm 159	Jun, 2004	0.57 \pm 0.2	25.8 \pm 1.6	470 \pm 75
Aug, 2003	0.69 \pm 0.1	25.73 \pm 1	189.7 \pm 73	Aug, 2004	0.57 \pm 0.2	26.2 \pm 1	307.4 \pm 64
Sep, 2003	0.75 \pm 0.1	25.96 \pm 0.8	21.64 \pm 22	Sep, 2004	0.62 \pm 0.2	26.6 \pm 1.2	186 \pm 26.4
Oct, 2003	0.73 \pm 0.1	26 \pm 1	300 \pm 82	Oct, 2004	0.78 \pm 0.1	26.2 \pm 1.5	294 \pm 81
Nov, 2003	0.74 \pm 0.1	26 \pm 0.7	13.05 \pm 5.7	Nov, 2004	0.79 \pm 0.1	30.9 \pm 1.1	136.9 \pm 41
Dec, 2003	0.7 \pm 0.1	23.6 \pm 1.3	4.07 \pm 5.27	Dec, 2004	0.76 \pm 0.1	28.8 \pm 1.9	4.51 \pm 5.6
Jan, 2005	0.69 \pm 0.10	24.1 \pm 0.96	16.59 \pm 3.6	Jan, 2006	0.69 \pm 0.1	28.9 \pm 1.8	16.23 \pm 14
Feb, 2005	0.62 \pm 0.15	27 \pm 1.98	8.77 \pm 3.71	Feb, 2006	0.61 \pm 0.2	23.62 \pm 1	0.62 \pm 0.7
Mar, 2005	0.6 \pm 0.17	22.85 \pm 1.7	34.32 \pm 19	Mar, 2006	0.61 \pm 0.2	25.9 \pm 1.2	89.46 \pm 37
Apr, 2005	0.63 \pm 0.17	28.4 \pm 1.69	182.9 \pm 67	Apr, 2006	0.58 \pm 0.2	25 \pm 1.3	62.6 \pm 34
May, 2005	0.61 \pm 0.15	28 \pm 1.43	119 \pm 56.5	May, 2006	0.6 \pm 0.16	27.86 \pm 2	340 \pm 131
Jun, 2005	0.61 \pm 0.16	28.5 \pm 1.64	450.4 \pm 45	Jun, 2006	0.65 \pm 0.2	28.4 \pm 1.1	406 \pm 67.6
Aug, 2005	0.68 \pm 0.10	26.38 \pm 0.9	240.9 \pm 48	Aug, 2006	0.68 \pm 0.1	26.6 \pm 1.2	304.8 \pm 39
Sep, 2005	0.7 \pm 0.11	27.87 \pm 1	318.6 \pm 46	Sep, 2006	0.69 \pm 0.1	28.5 \pm 1.3	358.58 \pm 3
Oct, 2005	0.71 \pm 0.11	28.74 \pm 1.1	242.5 \pm 51	Oct, 2006	0.73 \pm 0.1	29.3 \pm 1.2	331 \pm 109
Nov, 2005	0.74 \pm 0.11	28.4 \pm 1.41	232.5 \pm 77	Nov, 2006	0.73 \pm 0.1	28.9 \pm 1.2	224.6 \pm 7

Dec, 2005	0.73 ± 0.09	26.78 ± 1.5	78.98 ± 52	Dec, 2006	0.71 ± 0.1	25.4 ± 1.4	4.86 ± 1.2
Jan, 2007	0.68 ± 0.1	23.42 ± 2.7	--	Jan, 2008	0.69 ± 0.1	22.84 ± 1	1.68 ± 0.8
Feb, 2007	0.6 ± 0.15	23.3 ± 3.47	0.13 ± 0.12	Feb, 2008	0.62 ± 0.2	30 ± 1.8	39.1 ± 7.7
Mar, 2007	0.58 ± 0.17	28.1 ± 3.63	0.05 ± 0.12	Mar, 2008	0.62 ± 0.2	29 ± 1.94	217 ± 58.5
Apr, 2007	0.63 ± 0.17	30.15 ± 4	2.84 ± 2.12	Apr, 2008	0.61 ± 0.2	25.8 ± 1.5	80 ± 48.6
May, 2007	0.61 ± 0.15	31.67 ± 3.3	8.79 ± 15.1	May, 2008	0.6 ± 0.16	28.2 ± 1.9	68.42 ± 25
Jun, 2007	0.62 ± 0.17	28.44 ± 1.8	477 ± 116	Jun, 2008	0.57 ± 0.2	28 ± 1.4	329.8 ± 83
Aug, 2007	0.69 ± 0.1	25.67 ± 1.2	381.7 ± 94	Aug, 2008	0.66 ± 0.1	27.7 ± 1.4	250 ± 76
Sep, 2007	0.7 ± 0.11	29.08 ± 1.9	289.9 ± 47	Sep, 2008	0.69 ± 0.1	27.7 ± 1.4	250 ± 76
Oct, 2007	0.71 ± 0.11	22.28 ± 2.9	17.88 ± 23	Oct, 2008	0.72 ± 0.1	31.41 ± 2	336 ± 77.6
Nov, 2007	0.74 ± 0.11	24.41 ± 2.8	13.99 ± 14	Nov, 2008	0.72 ± 0.1	28.97 ± 1	80.35 ± 56
Dec, 2007	0.72 ± 0.1	26.5 ± 3.03	0.052 ± 0.1	Dec, 2008	0.73 ± 0.1	28.8 ± 1.7	22.99 ± 15
Jan, 2009	0.7 ± 0.09	28.61 ± 2.7	3.84 ± 2.4	Jan, 2010	0.71 ± 0.1	27.4 ± 1.9	18.15 ± 12
Feb, 2009	0.63 ± 0.13	30.1 ± 3.05	--	Feb, 2010	0.63 ± 0.2	27.6 ± 1.9	0.87 ± 0.5
Mar, 2009	0.66 ± 0.13	28.7 ± 2.1	60.7 ± 15.8	Mar, 2010	0.59 ± 0.2	29.6 ± 2.7	25 ± 17.8
Apr, 2009	0.65 ± 0.13	29.61 ± 1.8	60.3 ± 23.7	Apr, 2010	0.59 ± 0.2	24.48 ± 2	101.3 ± 55
May, 2009	0.67 ± 0.13	29.14 ± 2.2	138.7 ± 66	May, 2010	0.62 ± 0.2	25.3 ± 2.5	143.7 ± 69
Jun, 2009	0.7 ± 0.14	29 ± 1.76	307 ± 61.9	Jun, 2010	0.60 ± 0.2	26.7 ± 1.2	474.5 ± 6
Aug, 2009	0.67 ± 0.1	26.5 ± 1.04	227 ± 29	Aug, 2010	0.7 ± 0.1	26.22 ± 1	275.9 ± 44
Sep, 2009	0.74 ± 0.11	26.65 ± 1	269.4 ± 58	Sep, 2010	0.72 ± 0.1	29.89 ± 2	236.7 ± 16
Oct, 2009	0.77 ± 0.08	27.3 ± 1.55	170.7 ± 65	Oct, 2010	0.71 ± 0.1	26.6 ± 1.6	348 ± 135
Nov, 2009	0.77 ± 0.08	30.22 ± 1.5	276.9 ± 25	Nov, 2010	0.73 ± 0.1	29.99 ± 1	335.6 ± 61
Dec, 2009	0.76 ± 0.08	28.9 ± 2.06	49.2 ± 10.7	Dec, 2010	0.75 ± 0.1	30.4 ± 3.7	77.1 ± 56

Jan, 2011	0.7 ± 0.11	28.74 ± 2.6	16.8 ± 12.6	Jan, 2012	0.69 ± 0.1	28.2 ± 2.7	16.6 ± 11
Feb, 2011	0.62 ± 0.15	27.27 ± 3.1	0.71 ± 1.06	Feb, 2012	0.61 ± 0.2	27.16 ± 3	2.88 ± 1
Mar, 2011	0.6 ± 0.16	29.73 ± 3.1	22.9 ± 21.2	Mar, 2012	0.6 ± 0.15	28.8 ± 2	22 ± 16.7
Apr, 2011	0.6 ± 0.17	30.05 ± 2	97.1 ± 54.6	Apr, 2012	0.56 ± 0.2	28.9 ± 1.6	101 ± 62.5
May, 2011	0.63 ± 0.16	26.89 ± 2.9	140.4 ± 68	May, 2012	0.59 ± 0.2	--	--
Jun, 2011	0.59 ± 0.16	27.57 ± 1.6	492 ± 71.1	Jun, 2012	0.56 ± 0.1	28.3 ± 1.9	463.1 ± 7
Aug, 2011	0.68 ± 0.10	25.54 ± 0.9	301.2 ± 55	Aug, 2012	0.68 ± 0.1	26.6 ± 1.2	293.3 ± 55
Sep, 2011	0.65 ± 0.1	28.13 ± 1.1	234.22 ± 9	Sep, 2012	0.72 ± 0.1	26.1 ± 1.1	231.9 ± 67
Oct, 2011	0.72 ± 0.11	29.16 ± 1.4	343.3 ± 99	Oct, 2012	0.73 ± 0.1	30.60 ± 1.5	354.2 ± 94
Nov, 2011	0.74 ± 0.1	28.64 ± 2.1	329 ± 66.3	Nov, 2012	0.74 ± 0.1	27.3 ± 2.3	333 ± 60.6
Dec, 2011	0.73 ± 0.1	29.46 ± 2.4	77.1 ± 57.2	Dec, 2012	0.72 ± 0.1	27.1 ± 2.6	75 ± 58.6

Table 6: Mean (μ) \pm standard deviation (σ) of NDVI, LST and rainfall for agriculture/grassland class for southern Western Ghats

Month, Year	NDVI ($\mu \pm \sigma$)	LST ($\mu \pm \sigma$)	rainfall ($\mu \pm \sigma$)	Month, Year	NDVI ($\mu \pm \sigma$)	LST ($\mu \pm \sigma$)	rainfall ($\mu \pm \sigma$)
Jan, 2003	0.37 \pm 0.06	--	8.67 \pm 1.64	Jan, 2004	0.4 \pm 0.06	30.1 \pm 1.5	8.67 \pm 1.6
Feb, 2003	0.27 \pm 0.03	--	5.04 \pm 3.54	Feb, 2004	0.31 \pm 0.1	32.5 \pm 1.3	4.99 \pm 3
Mar, 2003	0.25 \pm 0.03	30.34 \pm 1.2	15.31 \pm 0.6	Mar, 2004	0.26	32.9 \pm 3.2	0.02
Apr, 2003	0.24 \pm 0.02	27.42 \pm 2.9	55.36 \pm 23	Apr, 2004	0.27 \pm 0.1	33 \pm 2.7	0.58 \pm 1.9
May, 2003	0.23 \pm 0.03	29.45 \pm 1.9	44.93 \pm 24	May, 2004	0.32	31.7 \pm 2.7	19.76 \pm 8.3
Jun, 2003	0.28 \pm 0.04	29.74 \pm 2.7	333.9 \pm 80	Jun, 2004	0.26	30.3 \pm 2.1	269.6 \pm 81
Aug, 2003	0.33 \pm 0.09	26.06 \pm 1.7	191.6 \pm 47	Aug, 2004	0.24	26.4 \pm 1.6	467 \pm 102
Sep, 2003	0.32 \pm 0.09	28.25 \pm 1.7	12.23 \pm 8.5	Sep, 2004	0.25	27.94 \pm 2	191 \pm 15
Oct, 2003	0.34 \pm 0.08	28.6 \pm 2.61	238 \pm 63.2	Oct, 2004	0.44 \pm 0.1	27.3 \pm 5.5	46.4 \pm 21
Nov, 2003	0.4 \pm 0.08	26.25 \pm 0.9	10.6 \pm 2.35	Nov, 2004	0.51 \pm 0.1	28 \pm 3.5	1.57 \pm 1.1
Dec, 2003	0.43 \pm 0.06	25.53 \pm 1	6.98 \pm 6.56	Dec, 2004	0.51 \pm 0.1	25.1 \pm 3.2	0.00
Jan, 2005	0.39 \pm 0.05	25.09 \pm 0.7	13.27 \pm 2.7	Jan, 2006	0.42 \pm 0.1	30.5 \pm 1.8	21.97 \pm 15
Feb, 2005	0.28 \pm 0.03	30.4 \pm 1.21	10.27 \pm 2.7	Feb, 2006	0.29	25.1 \pm 0.7	0.49 \pm 0.7
Mar, 2005	0.25 \pm 0.03	25.77 \pm 1.9	41.66 \pm 10	Mar, 2006	0.26	27.5 \pm 1.2	79.42 \pm 25
Apr, 2005	0.24 \pm 0.03	29.2 \pm 2.59	161 \pm 55.6	Apr, 2006	0.24	24.8 \pm 1.6	64.45 \pm 33
May, 2005	0.23 \pm 0.03	26.89 \pm 1.5	133.8 \pm 61	May, 2006	0.24	26.9 \pm 2.9	288 \pm 118
Jun, 2005	0.28 \pm 0.04	28.13 \pm 1.9	437.9 \pm 44	Jun, 2006	0.28	29.07 \pm 2	364.7 \pm 54
Aug, 2005	0.34 \pm 0.08	28.07 \pm 1.7	229.2 \pm 46	Aug, 2006	0.34 \pm 0.1	29.1 \pm 2.3	277.8 \pm 39
Sep, 2005	0.36 \pm 0.08	28.86 \pm 2	296 \pm 41	Sep, 2006	0.34 \pm 0.1	28.2 \pm 1.8	343.4 \pm 27
Oct, 2005	0.38 \pm 0.08	29.2 \pm 1.58	223.4 \pm 67	Oct, 2006	0.37 \pm 0.1	29.3 \pm 1.6	301 \pm 94
Nov, 2005	0.41 \pm 0.08	29.45 \pm 1.8	273 \pm 48.7	Nov, 2006	0.38 \pm 0.1	28 \pm 1.47	253.8 \pm 58

Dec, 2005	0.43 ± 0.07	27.47 ± 1.2	94.6 ± 46.7	Dec, 2006	0.42 ± 0.1	26.3 ± 1.4	5.48 ± 1.1
Jan, 2007	0.39 ± 0.05	29.7 ± 1.14	4.83 ± 1.93	Jan, 2008	0.41 ± 0.1	24 ± 0.65	2.46 ± 0.6
Feb, 2007	0.28 ± 0.03	31.84 ± 1.3	6.16 ± 0.99	Feb, 2008	0.29	31.5 ± 1.5	39.1 ± 4.5
Mar, 2007	0.25 ± 0.03	28.82 ± 1.3	4.49 ± 2.96	Mar, 2008	0.24	28.39 ± 3	211.8 ± 64
Apr, 2007	0.24 ± 0.03	28.9 ± 2.26	85.24 ± 54	Apr, 2008	0.23	25.56 ± 2	93.43 ± 53
May, 2007	0.23 ± 0.03	20.4 ± 3.25	144 ± 62	May, 2008	0.23	27 ± 2.3	70.93 ± 22
Jun, 2007	0.28 ± 0.04	29.2 ± 2.52	482.6 ± 59	Jun, 2008	0.27	27.5 ± 1.5	328.3 ± 77
Aug, 2007	0.34 ± 0.09	29.03 ± 1.8	335.1 ± 2.7	Aug, 2008	0.35 ± 0.1	27.4 ± 2.1	284.4 ± 35
Sep, 2007	0.36 ± 0.08	28.14 ± 2.1	386.4 ± 35	Sep, 2008	0.38 ± 0.1	28.9 ± 2.4	205.3 ± 80
Oct, 2007	0.38 ± 0.08	28.9 ± 1.5	262 ± 89.6	Oct, 2008	0.37 ± 0.1	30.9 ± 2	293.6 ± 61
Nov, 2007	0.41 ± 0.08	28.43 ± 2.1	108.5 ± 38	Nov, 2008	0.42 ± 0.1	30.2 ± 1.9	114.9 ± 45
Dec, 2007	0.43 ± 0.06	31.57 ± 1.7	81.2 ± 24.5	Dec, 2008	0.43 ± 0.1	30 ± 1.5	27.06 ± 15
Jan, 2009	0.39 ± 0.06	31.93 ± 1.7	4.35 ± 1.88	Jan, 2010	0.39 ± 0.1	29.78 ± 2	13.19 ± 11
Feb, 2009	0.28 ± 0.03	35.1 ± 1.79	--	Feb, 2010	0.29	30.9 ± 1.5	0.83 ± 0.5
Mar, 2009	0.25 ± 0.02	32.23 ± 2	54.7 ± 9.28	Mar, 2010	0.26	34.77 ± 2	16.6 ± 8.3
Apr, 2009	0.24 ± 0.02	30.11 ± 2.6	42.45 ± 18	Apr, 2010	0.24	24.4 ± 4.2	49.7 ± 35
May, 2009	0.25 ± 0.02	30.61 ± 2.8	96.78 ± 42	May, 2010	0.24	26.14 ± 4	98.26 ± 52
Jun, 2009	0.26 ± 0.05	30.1 ± 2.33	277.3 ± 56	Jun, 2010	0.27	26.2 ± 1.8	436.6 ± 48
Aug, 2009	0.38 ± 0.08	27.37 ± 1.9	209.4 ± 27	Aug, 2010	0.34 ± 0.1	26.9 ± 1.7	252.9 ± 34
Sep, 2009	0.38 ± 0.09	27.04 ± 1.5	219.9 ± 54	Sep, 2010	0.33 ± 0.1	29.38 ± 2	225.8 ± 16
Oct, 2009	0.41 ± 0.08	30.43 ± 2	89.5 ± 54.7	Oct, 2010	0.38 ± 0.1	26.84 ± 2	266 ± 124
Nov, 2009	0.42 ± 0.09	30.6 ± 1.69	300 ± 24.6	Nov, 2010	0.38 ± 0.1	29.5 ± 1.5	338.2 ± 54
Dec, 2009	0.44 ± 0.06	30.3 ± 2.42	53.2 ± 12.5	Dec, 2010	0.41 ± 0.1	30.4 ± 1.9	108 ± 62.5

Jan, 2011	0.41 ± 0.05	25.63 ± 3.5	2.15 ± 2.21	Jan, 2012	0.41 ± 0.1	32.1 ± 1.8	13.59 ± 11
Feb, 2011	0.29 ± 0.03	25.76 ± 2.9	0.26 ± 0.31	Feb, 2012	0.29	31.43 ± 2	2.46 ± 1.1
Mar, 2011	0.26 ± 0.02	32.6 ± 3	2.16 ± 1.61	Mar, 2012	0.26	27.15 ± 2	22.35 ± 16
Apr, 2011	0.23 ± 0.03	31.68 3.04	4.52 ± 6	Apr, 2012	0.24	29.74 ± 3	57.67 ± 46
May, 2011	0.24 ± 0.04	35.14 ± 2	5.25 ± 2.9	May, 2012	0.23	--	--
Jun, 2011	0.27 ± 0.04	31.81 ± 2.2	324 ± 106	Jun, 2012	0.28	28.67 ± 2	431 ± 64
Aug, 2011	0.34 ± 0.09	25.87 ± 2.8	415 ± 72	Aug, 2012	0.33 ± 0.1	28.8 ± 2.6	273.3 ± 48
Sep. 2011	0.35 ± 0.09	25.82 ± 2.6	231 ± 114	Sep. 2012	0.33 ± 0.1	27.5 ± 2.4	157.3 ± 56
Oct, 2011	0.36 ± 0.09	27.45 ± 2.9	81.9 ± 35.8	Oct, 2012	0.35 ± 0.1	30.5 ± 2.2	264.6 ± 75
Nov, 2011	0.42 ± 0.07	26.29 ± 3.4	74.11 ± 21	Nov, 2012	0.43 ± 0.1	30.5 ± 2.1	332 ± 46
Dec, 2011	0.43 ± 0.07	24.1 ± 3.49	0.65 ± 0.98	Dec, 2012	0.43 ± 0.1	31.79 ± 2	95.78 ± 48

Appendix 2

Table 1: Image to image Pearson product-moment correlation coefficient (CC) between NDVI of forest class with LST and rainfall for northern Western Ghats

Month, Year	CC (r) (NDVI-LST)	CC (r) (NDVI-rainfall)	Month, Year	CC (r) (NDVI-LST)	CC (r) (NDVI-rainfall)
Jan, 2003	--	-0.09	Jan, 2004	-0.47	-0.11
Feb, 2003	--	-0.06	Feb, 2004	-0.51	-0.04
Mar, 2003	-0.65	0.06	Mar, 2004	-0.59	0.02
Apr, 2003	-0.65	0.3	Apr, 2004	-0.65	0.33
May, 2003	-0.63	-0.19	May, 2004	-0.33	0.16
Jun, 2003	-0.43	-0.12	Jun, 2004	-0.4	0.50
Aug, 2003	-0.17	0.09	Aug, 2004	-0.1	0.06
Sep. 2003	-0.36	-0.05	Sep. 2004	-0.42	0.14
Oct, 2003	-0.73	-0.19	Oct, 2004	-0.49	-0.12
Nov, 2003	-0.5	-0.13	Nov, 2004	-0.54	0.13
Dec, 2003	-0.42	0.17	Dec, 2004	-0.47	0.17

Jan, 2005	-0.41	-0.06	Jan, 2006	-0.44	0.24
Feb, 2005	-0.51	-0.01	Feb, 2006	-0.55	--
Mar, 2005	-0.62	-0.15	Mar, 2006	-0.62	0.18
Apr, 2005	-0.66	0.36	Apr, 2006	-0.64	0.20
May, 2005	-0.69	0.35	May, 2006	-0.19	0.48
Jun, 2005	-0.59	0.47	Jun, 2006	-0.49	0.49
Aug, 2005	-0.09	-0.10	Aug, 2006	-0.08	-0.08
Sep. 2005	-0.16	0.06	Sep. 2006	-0.27	0.28
Oct, 2005	-0.64	-0.06	Oct, 2006	-0.68	0.57
Nov, 2005	-0.56	0.09	Nov, 2006	-0.43	0.11
Dec, 2005	-0.37	0.17	Dec, 2006	-0.47	--
Jan, 2007	-0.4	--	Jan, 2008	-0.43	0.43
Feb, 2007	-0.55	-0.15	Feb, 2008	-0.51	0.51
Mar, 2007	-0.64	0.26	Mar, 2008	-0.65	0.65
Apr, 2007	-0.67	0.16	Apr, 2008	-0.76	0.76
May, 2007	-0.66	0.41	May, 2008	-0.63	0.63
Jun, 2007	-0.35	0.41	Jun, 2008	-0.57	0.57
Aug, 2007	-0.1	-0.17	Aug, 2008	-0.06	-0.06
Sep. 2007	-0.1	-0.02	Sep. 2008	-0.29	-0.29
Oct, 2007	-0.69	0.46	Oct, 2008	-0.61	0.61
Nov, 2007	-0.58	0.36	Nov, 2008	-0.55	0.55
Dec, 2007	-0.33	0.29	Dec, 2008	-0.4	0.4
Jan, 2009	-0.52	--	Jan, 2010	-0.41	0.00
Feb, 2009	-0.67	--	Feb, 2010	-0.32	-0.07
Mar, 2009	-0.67	0.13	Mar, 2010	-0.65	0.98
Apr, 2009	-0.7	0.11	Apr, 2010	-0.72	0.37
May, 2009	-0.63	-0.11	May, 2010	-0.74	0.35
Jun, 2009	-0.39	0.31	Jun, 2010	-0.26	0.43
Aug, 2009	0.01	0.06	Aug, 2010	-0.15	0.15
Sep. 2009	-0.35	0.44	Sep. 2010	-0.24	0.08
Oct, 2009	-0.68	0.41	Oct, 2010	-0.51	0.49
Nov, 2009	-0.34	0.2	Nov, 2010	-0.35	0.23
Dec, 2009	-0.4	-0.07	Dec, 2010	-0.47	0.08

Jan, 2011	-0.41	-0.15	Jan, 2012	-0.41	-0.16
Feb, 2011	-0.54	-0.12	Feb, 2012	-0.54	-0.13
Mar, 2011	-0.66	-0.16	Mar, 2012	-0.66	-0.15
Apr, 2011	-0.73	0.26	Apr, 2012	-0.73	0.26
May, 2011	-0.73	0.27	May, 2012	-0.74	0.28
Jun, 2011	-0.24	0.18	Jun, 2012	-0.24	0.18
Aug, 2011	-0.1	0.08	Aug, 2012	-0.1	0.08
Sep. 2011	-0.29	0.22	Sep. 2012	-0.28	0.24
Oct, 2011	-0.68	0.43	Oct, 2012	-0.65	0.44
Nov, 2011	-0.56	0.07	Nov, 2012	-0.60	0.08
Dec, 2011	-0.38	0.08	Dec, 2012	-0.41	0.09

Table 2: Image to image Pearson product-moment correlation coefficient (CC or r) between NDVI of agriculture/grassland class with LST and rainfall for northern Western Ghats

Month, Year	CC (r) (NDVI-LST)	CC (r) (NDVI-rainfall)	Month, Year	CC (r) (NDVI-LST)	CC (r) (NDVI-rainfall)
Jan, 2003	--	-0.21	Jan, 2004	-0.55	-0.18
Feb, 2003	--	-0.14	Feb, 2004	-0.51	-0.15
Mar, 2003	-0.41	-0.23	Mar, 2004	-0.4	-0.10
Apr, 2003	-0.38	-0.05	Apr, 2004	-0.39	-0.08
May, 2003	-0.31	-0.15	May, 2004	-0.23	-0.03
Jun, 2003	-0.18	0.27	Jun, 2004	-0.1	0.04
Aug, 2003	-0.1	-0.03	Aug, 2004	-0.04	-0.12
Sep. 2003	-0.39	0.33	Sep. 2004	-0.08	0.05
Oct, 2003	-0.55	0.38	Oct, 2004	-0.8	0.05
Nov, 2003	-0.67	-0.26	Nov, 2004	-0.42	-0.04
Dec, 2003	-0.55	0.11	Dec, 2004	-0.43	0.08
Jan, 2005	-0.30	-0.22	Jan, 2006	-0.49	0.09
Feb, 2005	-0.43	-0.21	Feb, 2006	-0.52	--
Mar, 2005	-0.38	-0.19	Mar, 2006	-0.26	-0.05

Apr, 2005	-0.12	-0.13	Apr, 2006	-0.33	-0.13
May, 2005	-0.19	-0.11	May, 2006	-0.22	0.15
Jun, 2005	-0.22	0.17	Jun, 2006	-0.12	0.18
Aug, 2005	-0.44	-0.14	Aug, 2006	-0.05	-0.02
Sep. 2005	0.12	-0.09	Sep. 2006	0.02	0.16
Oct, 2005	-0.16	0.02	Oct, 2006	-0.15	-0.07
Nov, 2005	-0.50	0.03	Nov, 2006	-0.4	-0.13
Dec, 2005	-0.47	0.14	Dec, 2006	-0.41	--
Jan, 2007	-0.4	--	Jan, 2008	-0.42	-0.16
Feb, 2007	-0.4	0.04	Feb, 2008	-0.37	-0.01
Mar, 2007	-0.35	-0.10	Mar, 2008	-0.35	-0.13
Apr, 2007	-0.24	-0.14	Apr, 2008	-0.27	-0.14
May, 2007	-0.19	-0.02	May, 2008	-0.2	-0.01
Jun, 2007	-0.21	0.07	Jun, 2008	-0.18	0.16
Aug, 2007	-0.09	-0.13	Aug, 2008	-0.28	-0.08
Sep. 2007	0.14	-0.15	Sep. 2008	-0.14	-0.10
Oct, 2007	-0.27	0.11	Oct, 2008	-0.08	-0.13
Nov, 2007	-0.41	0.09	Nov, 2008	-0.5	-0.16
Dec, 2007	-0.35	0.16	Dec, 2008	-0.48	0.25
Jan, 2009	-0.28	0	Jan, 2010	-0.36	-0.27
Feb, 2009	-0.66	--	Feb, 2010	-0.24	-0.2
Mar, 2009	-0.46	-0.2	Mar, 2010	-0.28	-0.08
Apr, 2009	-0.38	-0.15	Apr, 2010	-0.24	-0.09
May, 2009	-0.37	0.41	May, 2010	-0.19	-0.19
Jun, 2009	-0.16	0.21	Jun, 2010	-0.13	0.16
Aug, 2009	-0.4	0.33	Aug, 2010	-0.05	-0.09
Sep. 2009	-0.35	-0.05	Sep. 2010	-0.16	-0.12
Oct, 2009	-0.00	-0.08	Oct, 2010	-0.08	-0.10
Nov, 2009	-0.01	0.43	Nov, 2010	-0.04	-0.06
Dec, 2009	-0.5	-0.38	Dec, 2010	-0.42	-0.19
Jan, 2011	-0.47	-0.26	Jan, 2012	-0.47	-0.26
Feb, 2011	-0.47	-0.23	Feb, 2012	-0.5	-0.21
Mar, 2011	-0.29	-0.12	Mar, 2012	-0.34	-0.16

Apr, 2011	-0.20	-0.07	Apr, 2012	-0.23	-0.14
May, 2011	-0.24	-0.16	May, 2012	-0.26	-0.18
Jun, 2011	-0.15	-0.03	Jun, 2012	-0.16	0.15
Aug, 2011	-0.09	0.10	Aug, 2012	-0.22	0.17
Sep. 2011	-0.0	-0.04	Sep. 2012	-0.16	0.08
Oct, 2011	-0.31	0.10	Oct, 2012	-0.22	0.01
Nov, 2011	-0.56	-0.03	Nov, 2012	-0.49	-0.1
Dec, 2011	-0.51	-0.18	Dec, 2012	-0.54	-0.1

Table 3: Image to image Pearson product-moment correlation coefficient (CC or r) between NDVI of forest class with LST and rainfall for central Western Ghats

Month, Year	CC (r) (NDVI-LST)	CC (r) (NDVI-rainfall)	Month, Year	CC (r) (NDVI-LST)	CC (r) (NDVI-rainfall)
Jan, 2003	--	-0.24	Jan, 2004	-0.59	-0.24
Feb, 2003	--	-0.31	Feb, 2004	-0.75	-0.33
Mar, 2003	-0.7	-2	Mar, 2004	-0.84	0.15
Apr, 2003	-0.78	-0.06	Apr, 2004	-0.74	-0.07
May, 2003	-0.75	-0.15	May, 2004	-0.53	0.45
Jun, 2003	-0.29	0.26	Jun, 2004	-0.1	0.20
Aug, 2003	-0.07	0.16	Aug, 2004	-0.03	0.25
Sep. 2003	-0.55	0.24	Sep. 2004	-0.45	-0.11
Oct, 2003	-0.60	-0.05	Oct, 2004	-0.72	0.16
Nov, 2003	-0.65	0.27	Nov, 2004	-0.67	0.34
Dec, 2003	-0.61	0.05	Dec, 2004	-0.56	0.07
Jan, 2005	-0.66	0.04	Jan, 2006	-0.6	-0.07
Feb, 2005	-0.77	0.25	Feb, 2006	-0.77	--
Mar, 2005	-0.83	0.26	Mar, 2006	-0.80	-0.08
Apr, 2005	-0.71	0.24	Apr, 2006	-0.68	-0.08
May, 2005	-0.73	-0.20	May, 2006	-0.74	0.54
Jun, 2005	-0.40	0.32	Jun, 2006	-0.5	0.38
Aug, 2005	-0.10	0.12	Aug, 2006	-0.05	0.08
Sep. 2005	-0.30	0.08	Sep. 2006	-0.33	0.27
Oct, 2005	-0.52	-0.03	Oct, 2006	-0.67	0.45

Nov, 2005	-0.60	0	Nov, 2006	-0.38	0.25
Dec, 2005	-0.48	0	Dec, 2006	-0.39	-0.13
Jan, 2007	-0.61	-0.17	Jan, 2008	-0.72	0.15
Feb, 2007	-0.79	-0.14	Feb, 2008	-0.72	0.33
Mar, 2007	-0.84	-0.05	Mar, 2008	-0.63	0.13
Apr, 2007	-0.73	0.04	Apr, 2008	-0.84	0.11
May, 2007	-0.8	0.31	May, 2008	-0.77	0.17
Jun, 2007	-0.45	0.31	Jun, 2008	-0.45	-0.05
Aug, 2007	-0.14	0.15	Aug, 2008	0.03	-0.18
Sep. 2007	-0.11	0.28	Sep. 2008	-0.30	-0.19
Oct, 2007	-0.59	0.16	Oct, 2008	-0.45	0.03
Nov, 2007	-0.65	0.33	Nov, 2008	-0.58	0
Dec, 2007	-0.55	-0.18	Dec, 2008	-0.51	0
Jan, 2009	-0.62	-0.19	Jan, 2010	-0.65	0.37
Feb, 2009	-0.82	--	Feb, 2010	-0.82	0.07
Mar, 2009	-0.84	0.33	Mar, 2010	-0.83	0.13
Apr, 2009	-0.76	0.16	Apr, 2010	-0.69	0.14
May, 2009	-0.77	0.25	May, 2010	-0.78	0.38
Jun, 2009	-0.47	0.33	Jun, 2010	-0.49	0.32
Aug, 2009	-0.25	0.19	Aug, 2010	-0.25	0.2
Sep. 2009	-0.29	0.39	Sep. 2010	-0.20	0.22
Oct, 2009	-0.68	0.28	Oct, 2010	-0.34	0.28
Nov, 2009	-0.32	0.28	Nov, 2010	-0.38	0.46
Dec, 2009	-0.59	0.30	Dec, 2010	-0.59	0.21
Jan, 2011	-0.68	0.3	Jan, 2012	-0.24	0.0
Feb, 2011	-0.78	-0.2	Feb, 2012	-0.21	0.07
Mar, 2011	-0.82	0.07	Mar, 2012	-0.26	0.27
Apr, 2011	-0.67	0.2	Apr, 2012	-0.29	0.29
May, 2011	-0.83	0.28	May, 2012	-0.07	0.38
Jun, 2011	-0.02	0.05	Jun, 2012	-0.10	0
Aug, 2011	-0.16	0.08	Aug, 2012	-0.4	-0.03
Sep. 2011	-0.15	0.12	Sep. 2012	-0.05	-0.04
Oct, 2011	-0.5	0.37	Oct, 2012	0.02	-0.11

Nov, 2011	-0.59	0.33	Nov, 2012	-0.34	0.36
Dec, 2011	-0.5	0.08	Dec, 2012	-0.42	0.20

Table 4: Image to image Pearson product-moment correlation coefficient (CC or r) between NDVI of agriculture/grassland class with LST and rainfall for central Western Ghats

Month, Year	CC (r) (NDVI-LST)	CC (r) (NDVI-rainfall)	Month, Year	CC (r) (NDVI-LST)	CC (r) (NDVI-rainfall)
Jan, 2003	--	0.04	Jan, 2004	-0.45	0.08
Feb, 2003	--	0.13	Feb, 2004	-0.29	0.16
Mar, 2003	-0.21	0.18	Mar, 2004	-0.24	0.21
Apr, 2003	-0.21	0.26	Apr, 2004	-0.23	0.28
May, 2003	-0.17	-0.01	May, 2004	-0.39	0.16
Jun, 2003	-0.45	0.23	Jun, 2004	-0.35	0.03
Aug, 2003	-0.06	0.12	Aug, 2004	-0.14	-0.17
Sep. 2003	-0.08	-0.08	Sep. 2004	0.07	0.02
Oct, 2003	-0.48	0.37	Oct, 2004	-0.16	0.13
Nov, 2003	-0.39	0.35	Nov, 2004	-0.19	0.04
Dec, 2003	-0.41	0.03	Dec, 2004	-0.41	-0.11
Jan, 2005	-0.54	0.17	Jan, 2006	-0.37	0.11
Feb, 2005	-0.36	0.24	Feb, 2006	-0.35	--
Mar, 2005	-0.24	0.16	Mar, 2006	-0.18	0.23
Apr, 2005	-0.38	0.26	Apr, 2006	-0.16	0.24
May, 2005	-0.13	0.32	May, 2006	-0.22	0.25
Jun, 2005	-0.12	0.10	Jun, 2006	-0.15	0.1
Aug, 2005	-0.07	-0.16	Aug, 2006	-0.37	0.11
Sep. 2005	-0.32	-0.21	Sep. 2006	-0.15	-0.03
Oct, 2005	-0.4	-0.04	Oct, 2006	-0.2	-0.06
Nov, 2005	-0.40	0.21	Nov, 2006	-0.00	0.00
Dec, 2005	-0.59	0.21	Dec, 2006	-0.35	0.2
Jan, 2007	-0.4	0.05	Jan, 2008	-0.36	0.15
Feb, 2007	-0.27	0.15	Feb, 2008	-0.26	0.33
Mar, 2007	-0.24	0.14	Mar, 2008	-0.11	0.13

Apr, 2007	-0.27	0.33	Apr, 2008	-0.09	0.11
May, 2007	-0.22	0.30	May, 2008	-0.02	0.17
Jun, 2007	-0.32	-0.02	Jun, 2008	-0.31	-0.05
Aug, 2007	-0.03	-0.15	Aug, 2008	-0.29	-0.18
Sep. 2007	-0.08	-0.18	Sep. 2008	-0.71	-0.19
Oct, 2007	-0.11	-0.09	Oct, 2008	-0.1	0.03
Nov, 2007	-0.24	0.09	Nov, 2008	-0.28	0
Dec, 2007	-0.31	0.16	Dec, 2008	-0.26	0
Jan, 2009	-0.31	0.04	Jan, 2010	-0.23	0.13
Feb, 2009	-0.29	--	Feb, 2010	-0.02	0.12
Mar, 2009	-0.24	0.24	Mar, 2010	-0.2	0.24
Apr, 2009	-0.22	0.31	Apr, 2010	-0.27	0.29
May, 2009	-0.18	0.11	May, 2010	-0.09	0.33
Jun, 2009	-0.28	0.07	Jun, 2010	-0.03	-0.07
Aug, 2009	-0.2	0.09	Aug, 2010	-0.1	-0.17
Sep. 2009	-0.04	-0.2	Sep. 2010	-0.01	-0.1
Oct, 2009	-0.05	-0.13	Oct, 2010	-0.11	-0.16
Nov, 2009	-0.12	0.18	Nov, 2010	-0.16	-0.18
Dec, 2009	-0.2	0.16	Dec, 2010	-0.10	0.06
Jan, 2011	-0.25	0.08	Jan, 2012	-0.44	0.1
Feb, 2011	-0.21	0.07	Feb, 2012	-0.27	0.2
Mar, 2011	-0.26	0.27	Mar, 2012	-0.24	0.3
Apr, 2011	-0.3	0.29	Apr, 2012	-0.21	0.3
May, 2011	-0.07	0.38	May, 2012	-0.15	0.4
Jun, 2011	-0.10	0	Jun, 2012	-0.26	0.16
Aug, 2011	-0.7	-0.03	Aug, 2012	0.08	0.06
Sep. 2011	-0.05	-0.04	Sep. 2012	-0.2	0.04
Oct, 2011	0.02	-0.11	Oct, 2012	-0.4	0.21
Nov, 2011	-0.34	0.36	Nov, 2012	-0.31	0.32
Dec, 2011	-0.42	0.2	Dec, 2012	-0.3	0.1

Table 5: Image to image Pearson product-moment correlation coefficient (CC or r) between NDVI of forest class with LST and rainfall for southern Western Ghats

Month, Year	CC (r) (NDVI-LST)	CC (r) (NDVI-rainfall)	Month, Year	CC (r) (NDVI-LST)	CC (r) (NDVI-rainfall)
Jan, 2003	--	-0.06	Jan, 2004	-0.52	0.03
Feb, 2003	--	0.17	Feb, 2004	-0.57	0.20
Mar, 2003	-0.42	-0.06	Mar, 2004	-0.77	0.28
Apr, 2003	-0.66	-0.55	Apr, 2004	-0.52	0.54
May, 2003	-0.19	0.41	May, 2004	-0.39	0.36
Jun, 2003	-0.28	-0.09	Jun, 2004	-0.05	0.05
Aug, 2003	-0.18	-0.07	Aug, 2004	0.11	0.05
Sep. 2003	-0.38	0.11	Sep. 2004	-0.31	-0.03
Oct, 2003	-0.24	0.22	Oct, 2004	-0.44	0.17
Nov, 2003	-0.42	0.16	Nov, 2004	-0.20	0.04
Dec, 2003	-0.58	-0.13	Dec, 2004	-0.35	-0.08
Jan, 2005	-0.47	0.26	Jan, 2006	-0.13	0.02
Feb, 2005	-0.74	-0.21	Feb, 2006	0.16	0.03
Mar, 2005	-0.7	-0.11	Mar, 2006	0.13	0.08
Apr, 2005	-0.67	0.31	Apr, 2006	0.21	-0.24
May, 2005	-0.37	0.13	May, 2006	0.27	-0.4
Jun, 2005	-0.37	0.32	Jun, 2006	0.29	-0.26
Aug, 2005	-0.28	-0.06	Aug, 2006	-0.3	0.17
Sep. 2005	-0.24	0.07	Sep. 2006	0.14	0.04
Oct, 2005	-0.42	-0.04	Oct, 2006	0.22	-0.18
Nov, 2005	-0.47	-0.21	Nov, 2006	0.22	0.06
Dec, 2005	-0.37	-0.12	Dec, 2006	0.19	0.01
Jan, 2007	-0.49	-0.26	Jan, 2008	-0.57	-0.43
Feb, 2007	-0.7	0.08	Feb, 2008	-0.5	-0.51
Mar, 2007	-0.64	0.33	Mar, 2008	-0.11	-0.65
Apr, 2007	-0.52	0.46	Apr, 2008	-0.67	-0.76
May, 2007	-0.52	0.48	May, 2008	-0.59	-0.63
Jun, 2007	-0.35	0.44	Jun, 2008	-0.33	-0.57
Aug, 2007	-0.35	0.04	Aug, 2008	-0.30	-0.06
Sep. 2007	-0.24	0.12	Sep. 2008	-0.32	-0.29

Oct, 2007	-0.29	0.23	Oct, 2008	0.02	-0.61
Nov, 2007	-0.56	0.1	Nov, 2008	-0.49	-0.55
Dec, 2007	-0.47	-0.38	Dec, 2008	-0.42	-0.4
Jan, 2009	-0.31	0.35	Jan, 2010	-0.43	-0.11
Feb, 2009	-0.56	--	Feb, 2010	-0.73	0.15
Mar, 2009	-0.71	-0.01	Mar, 2010	-0.79	0.3
Apr, 2009	-0.44	0.34	Apr, 2010	-0.36	0.58
May, 2009	-0.55	-0.09	May, 2010	-0.57	0.48
Jun, 2009	-0.16	0.23	Jun, 2010	-0.23	0.34
Aug, 2009	0.09	0.00	Aug, 2010	-0.15	-0.11
Sep. 2009	-0.14	-0.07	Sep. 2010	-0.1	-0.04
Oct, 2009	-0.27	0.22	Oct, 2010	-0.33	0.26
Nov, 2009	-0.13	-0.09	Nov, 2010	-0.2	-0.03
Dec, 2009	-0.30	0.32	Dec, 2010	-0.55	-0.19
Jan, 2011	-0.59	0.16	Jan, 2012	-0.58	0.16
Feb, 2011	-0.74	0.19	Feb, 2012	-0.68	0.2
Mar, 2011	-0.76	0.42	Mar, 2012	-0.58	0.15
Apr, 2011	-0.44	0.52	Apr, 2012	-0.47	0.5
May, 2011	-0.81	0.41	May, 2012	-0.17	0.33
Jun, 2011	-0.29	0.23	Jun, 2012	-0.43	0.23
Aug, 2011	-0.05	-0.04	Aug, 2012	-0.18	0.00
Sep. 2011	-0.18	-0.09	Sep. 2012	-0.32	0.19
Oct, 2011	-0.28	0.34	Oct, 2012	-0.05	0.24
Nov, 2011	-0.53	-0.07	Nov, 2012	-0.73	-0.04
Dec, 2011	-0.46	-0.16	Dec, 2012	-0.62	-0.21

Table 6: Image to image Pearson product-moment correlation coefficient (CC or r) between NDVI of agriculture/grassland class with LST and rainfall for southern Western Ghats

Month, Year	CC (r) (NDVI-LST)	CC (r) (NDVI-rainfall)	Month, Year	CC (r) (NDVI-LST)	CC (r) (NDVI-rainfall)
Jan, 2003	--	0.13	Jan, 2004	-0.37	0.01
Feb, 2003	--	-0.25	Feb, 2004	-0.47	0.19
Mar, 2003	-0.08	0.17	Mar, 2004	-0.20	0.05
Apr, 2003	0.00	-0.02	Apr, 2004	-0.06	0.17
May, 2003	0.19	-0.15	May, 2004	-0.10	0.01
Jun, 2003	0.23	0.1	Jun, 2004	0.13	-0.15
Aug, 2003	0.07	0.04	Aug, 2004	-0.06	-0.02
Sep. 2003	-0.43	0.06	Sep. 2004	0.14	-0.03
Oct, 2003	-0.36	0.11	Oct, 2004	-0.22	0.14
Nov, 2003	0.33	0.01	Nov, 2004	0.22	0.11
Dec, 2003	-0.11	-0.02	Dec, 2004	-0.13	0.05
Jan, 2005	-0.07	0.03	Jan, 2006	-0.13	0.02
Feb, 2005	-0.17	0.14	Feb, 2006	0.16	0.03
Mar, 2005	0.08	0.08	Mar, 2006	0.13	0.08
Apr, 2005	0.39	-0.3	Apr, 2006	0.21	-0.24
May, 2005	0.18	-0.06	May, 2006	0.27	-0.40
Jun, 2005	0.23	-0.31	Jun, 2006	0.29	-0.26
Aug, 2005	-0.33	0.18	Aug, 2006	-0.3	0.17
Sep. 2005	-0.05	0.09	Sep. 2006	0.14	0.04
Oct, 2005	-0.09	0.14	Oct, 2006	0.22	-0.18
Nov, 2005	0.26	-0.04	Nov, 2006	0.22	0.06
Dec, 2005	0.13	-0.03	Dec, 2006	0.19	0.01
Jan, 2007	-0.15	0.20	Jan, 2008	-0.11	0.17
Feb, 2007	-0.13	0.00	Feb, 2008	0.19	-0.00
Mar, 2007	0.00	0.03	Mar, 2008	0.21	-0.05
Apr, 2007	0.31	0.32	Apr, 2008	0.34	-0.19
May, 2007	0.19	-0.14	May, 2008	0.31	-0.01
Jun, 2007	0.34	-0.3	Jun, 2008	0.30	-0.29
Aug, 2007	-0.31	0.23	Aug, 2008	0.17	-0.09

Sep. 2007	-0.38	0.04	Sep. 2008	0.04	-0.02
Oct, 2007	0.02	-0.04	Oct, 2008	0.11	-0.11
Nov, 2007	0.32	-0.16	Nov, 2008	0.31	0.10
Dec, 2007	0.14	0.22	Dec, 2008	0.12	-0.12
Jan, 2009	-0.37	0.22	Jan, 2010	0.12	-0.09
Feb, 2009	-0.07	0.00	Feb, 2010	0.07	0.15
Mar, 2009	0.07	0.12	Mar, 2010	0.00	0.01
Apr, 2009	0.31	0.28	Apr, 2010	0.29	-0.24
May, 2009	0.05	0.49	May, 2010	0.3	-0.32
Jun, 2009	0.17	-0.17	Jun, 2010	0.23	-0.16
Aug, 2009	-0.03	-0.04	Aug, 2010	0.00	0.14
Sep. 2009	0.16	-0.18	Sep. 2010	0.16	0.06
Oct, 2009	0.41	-0.29	Oct, 2010	0.28	-0.16
Nov, 2009	0.04	0.39	Nov, 2010	0.23	0.03
Dec, 2009	0.16	-0.09	Dec, 2010	0.26	0.00
Jan, 2011	0.04	-0.1	Jan, 2012	0.00	0.00
Feb, 2011	0.19	-0.05	Feb, 2012	0.00	0.03
Mar, 2011	0.11	-0.13	Mar, 2012	0.24	-0.09
Apr, 2011	0.24	-0.18	Apr, 2012	0.32	0.28
May, 2011	0.27	0.24	May, 2012	0.13	0.24
Jun, 2011	0.2	-0.3	Jun, 2012	0.37	-0.16
Aug, 2011	0.00	0.23	Aug, 2012	0.41	0.15
Sep. 2011	0.00	0.18	Sep. 2012	0.15	0.26
Oct, 2011	0.17	-0.03	Oct, 2012	0.22	0.08
Nov, 2011	0.04	-0.05	Nov, 2012	0.26	-0.05
Dec, 2011	--	--	Dec, 2012	-0.11	0.1

Appendix 3

Table 1: Forecast for monthly rainfall in forest area from 2013 to 2020 for northern Western Ghats.

Month-Year	Forecast	Low 95%	High 95%	Month-Year	Forecast	Low 95%	High 95%
Jan-2013	10.90	-115.75	137.54	Jan-2017	59.53	-179.37	298.43
Feb-2013	16.45	-120.53	153.42	Feb-2017	62.71	-178.05	303.47
Mar-2013	17.64	-119.33	154.61	Mar-2017	63.39	-177.37	304.15
Apr-2013	21.15	-115.82	158.13	Apr-2017	65.40	-175.36	306.17
May-2013	20.82	-116.15	157.79	May-2017	65.21	-175.55	305.97
Jun-2013	356.32	219.35	493.29	Jun-2017	257.26	16.49	498.02
Jul-2013	383.16	246.19	520.13	Jul-2017	272.62	31.86	513.38
Aug-2013	383.16	246.19	520.13	Aug-2017	272.62	31.86	513.38
Sep-2013	263.39	126.41	400.36	Sep-2017	204.06	-36.70	444.82
Oct-2013	127.41	-9.56	264.38	Oct-2017	126.23	-114.53	366.99
Nov-2013	84.05	-52.92	221.02	Nov-2017	101.41	-139.35	342.17
Dec-2013	16.99	-119.99	153.96	Dec-2017	63.02	-177.74	303.78
Jan-2014	25.70	-150.07	201.48	Jan-2018	68.01	-180.87	316.89
Feb-2014	30.53	-151.00	212.07	Feb-2018	70.77	-179.46	321.00
Mar-2014	31.57	-149.97	213.11	Mar-2018	71.37	-178.87	321.60
Apr-2014	34.63	-146.91	216.16	Apr-2018	73.12	-177.12	323.35
May-2014	34.34	-147.20	215.87	May-2018	72.95	-177.28	323.18
Jun-2014	326.16	144.62	507.70	Jun-2018	239.99	-10.24	490.22
Jul-2014	349.50	167.97	531.04	Jul-2018	253.35	3.12	503.59
Aug-2014	349.50	167.97	531.04	Aug-2018	253.35	3.12	503.59
Sep-2014	245.32	63.79	426.86	Sep-2018	193.72	-56.51	443.95
Oct-2014	127.05	-54.48	308.59	Oct-2018	126.02	-124.21	376.25
Nov-2014	89.33	-92.20	270.87	Nov-2018	104.43	-145.80	354.66
Dec-2014	31.00	-150.53	212.54	Dec-2018	71.04	-179.19	321.27
Jan-2015	38.58	-166.69	243.85	Jan-2019	75.38	-180.79	331.55
Feb-2015	42.78	-166.25	251.81	Feb-2019	77.78	-179.38	334.95
Mar-2015	43.69	-165.35	252.72	Mar-2019	78.30	-178.87	335.47
Apr-2015	46.34	-162.69	255.38	Apr-2019	79.82	-177.34	336.99
May-2015	46.09	-162.94	255.12	May-2019	79.68	-177.49	336.85
Jun-2015	299.92	90.89	508.96	Jun-2019	224.97	-32.19	482.14
Jul-2015	320.23	111.20	529.26	Jul-2019	236.60	-20.57	493.76
Aug-2015	320.23	111.20	529.26	Aug-2019	236.60	-20.57	493.76
Sep-2015	229.61	20.58	438.64	Sep-2019	184.73	-72.44	441.89
Oct-2015	126.74	-82.29	335.77	Oct-2019	125.84	-131.33	383.01
Nov-2015	93.93	-115.10	302.96	Nov-2019	107.06	-150.11	364.23
Dec-2015	43.19	-165.84	252.22	Dec-2019	78.02	-179.15	335.19

Jan-2016	49.79	-175.25	274.82	Jan-2020	81.79	-179.76	343.35
Feb-2016	53.44	-174.20	281.08	Feb-2020	83.88	-178.41	346.18
Mar-2016	54.22	-173.41	281.86	Mar-2020	84.33	-177.96	346.63
Apr-2016	56.54	-171.10	284.18	Apr-2020	85.66	-176.63	347.95
May-2016	56.32	-171.32	283.96	May-2020	85.53	-176.76	347.82
Jun-2016	277.10	49.47	504.74	Jun-2020	211.91	-50.38	474.20
Jul-2016	294.76	67.13	522.40	Jul-2020	222.02	-40.27	484.31
Aug-2016	294.76	67.13	522.40	Aug-2020	222.02	-40.27	484.31
Sep-2016	215.95	-11.69	443.58	Sep-2020	176.90	-85.39	439.20
Oct-2016	126.47	-101.17	354.10	Oct-2020	125.68	-136.61	387.98
Nov-2016	97.93	-129.71	325.57	Nov-2020	109.35	-152.94	371.64
Dec-2016	53.79	-173.84	281.43	Dec-2020	84.09	-178.21	346.38

Table 2: Forecast for monthly rainfall in forest area from 2013 to 2020 for central Western Ghats.

Month-Year	Forecast	Low 95%	High 95%	Month-Year	Forecast	Low 95%	High 95%
Jan-2013	20.73	-101.45	142.92	Jan-2017	74.23	-151.36	299.82
Feb-2013	17.57	-112.21	147.34	Feb-2017	72.48	-154.40	299.36
Mar-2013	22.67	-108.04	153.38	Mar-2017	75.30	-151.74	302.34
Apr-2013	76.04	-54.79	206.87	Apr-2017	104.78	-122.28	331.84
May-2013	86.54	-44.31	217.39	May-2017	110.58	-116.48	337.65
Jun-2013	369.75	238.90	500.60	Jun-2017	267.03	39.96	494.10
Jul-2013	388.81	257.96	519.66	Jul-2017	277.56	50.49	504.63
Aug-2013	388.82	257.97	519.67	Aug-2017	277.56	50.49	504.63
Sep-2013	266.27	135.42	397.12	Sep-2017	209.87	-17.20	436.93
Oct-2013	192.19	61.34	323.04	Oct-2017	168.94	-58.13	396.01
Nov-2013	182.10	51.25	312.95	Nov-2017	163.37	-63.70	390.44
Dec-2013	25.25	-105.60	156.10	Dec-2017	76.73	-150.34	303.79
Jan-2014	37.21	-130.77	205.20	Jan-2018	83.33	-151.07	317.74
Feb-2014	34.48	-137.67	206.64	Feb-2018	81.83	-153.50	317.15
Mar-2014	38.88	-133.80	211.57	Mar-2018	84.26	-151.19	319.70
Apr-2014	84.89	-87.86	257.64	Apr-2018	109.67	-125.79	345.13
May-2014	93.95	-78.81	266.71	May-2018	114.67	-120.79	350.14
Jun-2014	338.10	165.34	510.87	Jun-2018	249.55	14.08	485.01
Jul-2014	354.54	181.77	527.30	Jul-2018	258.63	23.16	494.09
Aug-2014	354.54	181.78	527.31	Aug-2018	258.63	23.17	494.09
Sep-2014	248.89	76.13	421.66	Sep-2018	200.27	-35.20	435.73
Oct-2014	185.03	12.26	357.79	Oct-2018	164.99	-70.48	400.45
Nov-2014	176.33	3.57	349.10	Nov-2018	160.18	-75.28	395.65
Dec-2014	41.11	-131.65	213.87	Dec-2018	85.49	-149.98	320.95
Jan-2015	51.42	-143.76	246.60	Jan-2019	91.18	-149.57	331.93

Feb-2015	49.07	-148.80	246.93	Feb-2019	89.88	-151.53	331.30
Mar-2015	52.86	-145.35	251.06	Mar-2019	91.98	-149.53	333.48
Apr-2015	92.53	-105.72	290.77	Apr-2019	113.89	-127.62	355.40
May-2015	100.33	-97.92	298.59	May-2019	118.20	-123.31	359.71
Jun-2015	310.82	112.57	509.08	Jun-2019	234.48	-7.04	475.99
Jul-2015	324.99	126.74	523.25	Jul-2019	242.30	0.79	483.82
Aug-2015	325.00	126.74	523.25	Aug-2019	242.31	0.79	483.82
Sep-2015	233.91	35.66	432.17	Sep-2019	191.99	-49.52	433.51
Oct-2015	178.85	-19.40	377.11	Oct-2019	161.58	-79.94	403.09
Nov-2015	171.36	-26.90	369.61	Nov-2019	157.44	-84.08	398.95
Dec-2015	54.78	-143.48	253.03	Dec-2019	93.04	-148.48	334.55
Jan-2016	63.67	-149.49	276.82	Jan-2020	97.95	-147.41	343.30
Feb-2016	61.64	-153.35	276.63	Feb-2020	96.83	-149.02	342.67
Mar-2016	64.91	-150.31	280.13	Mar-2020	98.63	-147.27	344.54
Apr-2016	99.11	-116.14	314.36	Apr-2020	117.52	-128.39	363.44
May-2016	105.84	-109.42	321.09	May-2020	121.24	-124.67	367.16
Jun-2016	287.30	72.05	502.56	Jun-2020	221.49	-24.43	467.40
Jul-2016	299.52	84.26	514.77	Jul-2020	228.23	-17.68	474.15
Aug-2016	299.52	84.27	514.78	Aug-2020	228.24	-17.68	474.15
Sep-2016	221.00	5.74	436.25	Sep-2020	184.86	-61.06	430.77
Oct-2016	173.53	-41.72	388.79	Oct-2020	158.64	-87.28	404.55
Nov-2016	167.07	-48.19	382.32	Nov-2020	155.07	-90.85	400.98
Dec-2016	66.56	-148.69	281.82	Dec-2020	99.55	-146.37	345.46

Table 3: Forecast for monthly rainfall in forest area from 2013 to 2020 for southern Western Ghats.

Month-Year	Forecast	Low 95%	High 95%	Month-Year	Forecast	Low 95%	High 95%
Jan-2013	54.40	-127.75	236.55	Jan-2017	138.85	-118.78	396.49
Feb-2013	50.84	-138.47	240.14	Feb-2017	138.07	-119.82	395.96
Mar-2013	65.64	-124.23	255.51	Mar-2017	141.34	-116.57	399.25
Apr-2013	120.12	-69.79	310.03	Apr-2017	153.39	-104.53	411.30
May-2013	147.39	-42.52	337.31	May-2017	159.42	-98.50	417.33
Jun-2013	368.69	178.77	558.60	Jun-2017	208.35	-49.56	466.26
Jul-2013	252.30	62.39	442.22	Jul-2017	182.61	-75.30	440.53
Aug-2013	252.31	62.39	442.22	Aug-2017	182.62	-75.30	440.53
Sep-2013	210.16	20.24	400.08	Sep-2017	173.30	-84.62	431.21

Oct-2013	294.03	104.12	483.95	Oct-2017	191.84	-66.07	449.75
Nov-2013	279.57	89.65	469.49	Nov-2017	188.64	-69.27	446.56
Dec-2013	102.77	-87.14	292.69	Dec-2017	149.55	-108.36	407.46
Jan-2014	88.48	-138.83	315.79	Jan-2018	146.39	-113.00	405.78
Feb-2014	86.03	-144.01	316.08	Feb-2018	145.85	-113.66	405.35
Mar-2014	96.18	-134.08	326.45	Mar-2018	148.09	-111.42	407.61
Apr-2014	133.54	-96.74	363.82	Apr-2018	156.35	-103.16	415.87
May-2014	152.24	-78.04	382.52	May-2018	160.49	-99.03	420.00
Jun-2014	303.99	73.71	534.27	Jun-2018	194.04	-65.47	453.56
Jul-2014	224.19	-6.09	454.47	Jul-2018	176.40	-83.12	435.91
Aug-2014	224.19	-6.09	454.47	Aug-2018	176.40	-83.12	435.91
Sep-2014	195.29	-34.99	425.57	Sep-2018	170.01	-89.51	429.52
Oct-2014	252.80	22.52	483.08	Oct-2018	182.72	-76.79	442.24
Nov-2014	242.88	12.60	473.16	Nov-2018	180.53	-78.98	440.05
Dec-2014	121.65	-108.63	351.93	Dec-2018	153.72	-105.79	413.24
Jan-2015	111.84	-133.85	357.54	Jan-2019	151.56	-108.65	411.76
Feb-2015	110.17	-136.72	357.05	Feb-2019	151.18	-109.08	411.45
Mar-2015	117.13	-129.85	364.11	Mar-2019	152.72	-107.54	412.99
Apr-2015	142.75	-104.24	389.74	Apr-2019	158.39	-101.88	418.65
May-2015	155.57	-91.42	402.56	May-2019	161.22	-99.04	421.49
Jun-2015	259.63	12.64	506.62	Jun-2019	184.24	-76.03	444.50
Jul-2015	204.90	-42.09	451.90	Jul-2019	172.13	-88.13	432.40
Aug-2015	204.91	-42.09	451.90	Aug-2019	172.13	-88.13	432.40
Sep-2015	185.09	-61.90	432.08	Sep-2019	167.75	-92.51	428.02
Oct-2015	224.53	-22.46	471.52	Oct-2019	176.47	-83.79	436.74
Nov-2015	217.73	-29.27	464.72	Nov-2019	174.97	-85.30	435.23
Dec-2015	134.59	-112.40	381.58	Dec-2019	156.59	-103.68	416.85

Jan-2016	127.87	-126.01	381.74	Jan-2020	155.10	-105.49	415.69
Feb-2016	126.72	-127.71	381.14	Feb-2020	154.84	-105.77	415.46
Mar-2016	131.49	-122.98	385.96	Mar-2020	155.90	-104.72	416.52
Apr-2016	149.06	-105.41	403.53	Apr-2020	159.78	-100.83	420.40
May-2016	157.85	-96.62	412.32	May-2020	161.73	-98.89	422.35
Jun-2016	229.21	-25.26	483.68	Jun-2020	177.51	-83.11	438.13
Jul-2016	191.68	-62.79	446.15	Jul-2020	169.21	-91.41	429.83
Aug-2016	191.68	-62.79	446.15	Aug-2020	169.21	-91.41	429.83
Sep-2016	178.09	-76.38	432.56	Sep-2020	166.20	-94.41	426.82
Oct-2016	205.14	-49.33	459.61	Oct-2020	172.19	-88.43	432.80
Nov-2016	200.47	-54.00	454.94	Nov-2020	171.15	-89.46	431.77
Dec-2016	143.46	-111.01	397.93	Dec-2020	158.55	-102.07	419.16

Table 4: Forecast for monthly rainfall in agricultural/grassland area from 2013 to 2020 for northern Western Ghats.

Month-Year	Forecast	Low 95%	High 95%	Month-Year	Forecast	Low 95%	High 95%
Jan-2013	10.51	-106.73	127.74	Jan-2017	56.11	-167.45	279.67
Feb-2013	15.70	-113.63	145.02	Feb-2017	59.02	-166.62	284.67
Mar-2013	17.31	-112.01	146.63	Mar-2017	59.93	-165.72	285.58
Apr-2013	18.51	-110.81	147.83	Apr-2017	60.60	-165.04	286.25
May-2013	19.50	-109.82	148.82	May-2017	61.15	-164.49	286.80
Jun-2013	270.96	141.64	400.28	Jun-2017	202.20	-23.45	427.85
Jul-2013	360.45	231.13	489.77	Jul-2017	252.40	26.75	478.04
Aug-2013	360.45	231.13	489.77	Aug-2017	252.40	26.75	478.04
Sep-2013	214.83	85.51	344.15	Sep-2017	170.72	-54.93	396.36
Oct-2013	91.51	-37.81	220.83	Oct-2017	101.54	-124.10	327.19

Nov-2013	81.30	-48.02	210.62	Nov-2017	95.82	-129.83	321.47
Dec-2013	16.00	-113.32	145.32	Dec-2017	59.19	-166.45	284.84
Jan-2014	24.49	-139.88	188.86	Jan-2018	63.95	-168.76	296.67
Feb-2014	28.98	-142.05	200.00	Feb-2018	66.47	-167.75	300.69
Mar-2014	30.38	-140.65	201.40	Mar-2018	67.26	-166.96	301.47
Apr-2014	31.41	-139.61	202.44	Apr-2018	67.84	-166.38	302.05
May-2014	32.27	-138.76	203.29	May-2018	68.32	-165.90	302.53
Jun-2014	249.88	78.86	420.91	Jun-2018	190.38	-43.84	424.60
Jul-2014	327.33	156.31	498.35	Jul-2018	233.82	-0.40	468.03
Aug-2014	327.33	156.31	498.35	Aug-2018	233.82	-0.40	468.03
Sep-2014	201.31	30.28	372.33	Sep-2018	163.13	-71.08	397.35
Oct-2014	94.58	-76.44	265.61	Oct-2018	103.27	-130.95	337.49
Nov-2014	85.75	-85.27	256.77	Nov-2018	98.32	-135.90	332.53
Dec-2014	29.24	-141.78	200.26	Dec-2018	66.62	-167.60	300.83
Jan-2015	36.58	-155.66	228.83	Jan-2019	70.74	-168.60	310.08
Feb-2015	40.47	-156.08	237.01	Feb-2019	72.92	-167.52	313.35
Mar-2015	41.68	-154.86	238.22	Mar-2019	73.60	-166.84	314.03
Apr-2015	42.58	-153.97	239.12	Apr-2019	74.10	-166.33	314.53
May-2015	43.32	-153.23	239.86	May-2019	74.51	-165.92	314.95
Jun-2015	231.64	35.10	428.19	Jun-2019	180.15	-60.28	420.58
Jul-2015	298.67	102.12	495.21	Jul-2019	217.74	-22.69	458.18
Aug-2015	298.67	102.12	495.21	Aug-2019	217.74	-22.69	458.18
Sep-2015	189.61	-6.94	386.15	Sep-2019	156.57	-83.86	397.00
Oct-2015	97.25	-99.30	293.79	Oct-2019	104.76	-135.67	345.20
Nov-2015	89.60	-106.94	286.15	Nov-2019	100.48	-139.96	340.91
Dec-2015	40.70	-155.85	237.24	Dec-2019	73.05	-167.39	313.48

Jan-2016	47.05	-163.67	257.77	Jan-2020	76.61	-167.57	320.79
Feb-2016	50.41	-163.26	264.08	Feb-2020	78.50	-166.49	323.48
Mar-2016	51.46	-162.21	265.13	Mar-2020	79.08	-165.90	324.07
Apr-2016	52.24	-161.43	265.91	Apr-2020	79.52	-165.47	324.51
May-2016	52.88	-160.79	266.55	May-2020	79.88	-165.11	324.87
Jun-2016	215.86	2.19	429.53	Jun-2020	171.30	-73.69	416.28
Jul-2016	273.86	60.19	487.53	Jul-2020	203.83	-41.16	448.82
Aug-2016	273.86	60.19	487.53	Aug-2020	203.83	-41.16	448.82
Sep-2016	179.48	-34.19	393.15	Sep-2020	150.89	-94.10	395.88
Oct-2016	99.55	-114.12	313.22	Oct-2020	106.06	-138.93	351.04
Nov-2016	92.94	-120.73	306.61	Nov-2020	102.35	-142.64	347.33
Dec-2016	50.61	-163.06	264.28	Dec-2020	78.61	-166.38	323.59

Table 5: Forecast for monthly rainfall in agricultural/grassland area from 2013 to 2020 for central Western Ghats.

Month-Year	Forecast	Low 95%	High 95%	Month-Year	Forecast	Low 95%	High 95%
Jan-2013	16.56	-89.57	122.69	Jan-2017	68.09	-136.23	272.41
Feb-2013	14.82	-105.04	134.68	Feb-2017	67.25	-138.84	273.34
Mar-2013	19.33	-104.04	142.70	Mar-2017	69.43	-137.14	276.00
Apr-2013	60.88	-63.44	185.20	Apr-2017	89.51	-117.19	296.22
May-2013	67.85	-56.73	192.43	May-2017	92.88	-113.86	299.62
Jun-2013	304.95	180.30	429.60	Jun-2017	207.47	0.72	414.23
Jul-2013	332.77	208.09	457.44	Jul-2017	220.92	14.16	427.67
Aug-2013	332.86	208.18	457.54	Aug-2017	220.96	14.21	427.72
Sep-2013	182.12	57.44	306.80	Sep-2017	148.11	-58.65	354.87
Oct-2013	132.53	7.85	257.21	Oct-2017	124.14	-82.61	330.90
Nov-2013	135.14	10.46	259.82	Nov-2017	125.40	-81.35	332.16
Dec-2013	22.74	-101.94	147.42	Dec-2017	71.08	-135.68	277.83
Jan-2014	33.13	-119.79	186.05	Jan-2018	76.10	-135.04	287.24
Feb-2014	31.68	-128.14	191.50	Feb-2018	75.40	-136.93	287.73
Mar-2014	35.44	-126.23	197.11	Mar-2018	77.22	-135.44	289.87
Apr-2014	70.09	-92.09	232.27	Apr-2018	93.96	-118.78	306.71
May-2014	75.90	-86.41	238.22	May-2018	96.77	-116.00	309.54
Jun-2014	273.59	111.24	435.95	Jun-2018	192.32	-20.46	405.09
Jul-2014	296.79	134.42	459.15	Jul-2018	203.53	-9.25	416.31
Aug-2014	296.87	134.50	459.23	Aug-2018	203.57	-9.21	416.34
Sep-2014	171.18	8.81	333.55	Sep-2018	142.82	-69.96	355.60
Oct-2014	129.83	-32.53	292.20	Oct-2018	122.84	-89.94	335.62
Nov-2014	132.01	-30.36	294.38	Nov-2018	123.89	-88.89	336.67

Dec-2014	38.29	-124.08	200.66	Dec-2018	78.59	-134.19	291.37
Jan-2015	46.95	-131.41	225.32	Jan-2019	82.78	-132.97	298.53
Feb-2015	45.75	-136.78	228.27	Feb-2019	82.20	-134.36	298.76
Mar-2015	48.88	-134.77	232.53	Mar-2019	83.71	-133.07	300.50
Apr-2015	77.77	-106.19	261.73	Apr-2019	97.67	-119.17	314.52
May-2015	82.61	-101.43	266.66	May-2019	100.02	-116.85	316.88
Jun-2015	247.45	63.38	431.52	Jun-2019	179.68	-37.18	396.55
Jul-2015	266.79	82.71	450.86	Jul-2019	189.03	-27.84	405.90
Aug-2015	266.85	82.78	450.93	Aug-2019	189.06	-27.81	405.93
Sep-2015	162.06	-22.02	346.14	Sep-2019	138.41	-78.46	355.28
Oct-2015	127.58	-56.49	311.66	Oct-2019	121.75	-95.12	338.62
Nov-2015	129.40	-54.68	313.47	Nov-2019	122.63	-94.24	339.49
Dec-2015	51.25	-132.82	235.33	Dec-2019	84.86	-132.01	301.73
Jan-2016	58.48	-135.62	252.57	Jan-2020	88.35	-130.55	307.25
Feb-2016	57.47	-139.29	254.24	Feb-2020	87.86	-131.59	307.32
Mar-2016	60.09	-137.41	257.58	Mar-2020	89.13	-130.48	308.73
Apr-2016	84.17	-113.52	281.87	Apr-2020	100.77	-118.88	320.42
May-2016	88.21	-109.54	285.96	May-2020	102.72	-116.94	322.38
Jun-2016	225.65	27.89	423.41	Jun-2020	169.15	-50.52	388.81
Jul-2016	241.77	44.00	439.54	Jul-2020	176.94	-42.73	396.60
Aug-2016	241.83	44.06	439.60	Aug-2020	176.97	-42.70	396.63
Sep-2016	154.45	-43.32	352.22	Sep-2020	134.74	-84.93	354.40
Oct-2016	125.71	-72.06	323.48	Oct-2020	120.84	-98.82	340.51
Nov-2016	127.22	-70.55	324.99	Nov-2020	121.57	-98.09	341.24
Dec-2016	62.06	-135.71	259.83	Dec-2020	90.08	-129.58	309.75

Table 6: Forecast for monthly rainfall in agricultural/grassland area from 2013 to 2020 for southern Western Ghats.

Month-Year	Forecast	Low 95%	High 95%	Month-Year	Forecast	Low 95%	High 95%
Jan-2013	44.81	-126.97	216.59	Jan-2017	89.35	-147.09	325.78
Feb-2013	35.99	-147.68	219.65	Feb-2017	84.77	-152.71	322.25
Mar-2013	42.10	-143.20	227.41	Mar-2017	89.64	-147.99	327.27
Apr-2013	54.74	-130.79	240.28	Apr-2017	98.91	-138.74	336.56
May-2013	34.83	-150.74	220.40	May-2017	84.03	-153.62	321.68
Jun-2013	317.98	132.40	503.55	Jun-2017	241.21	3.55	478.86
Jul-2013	301.60	116.02	487.17	Jul-2017	213.55	-24.11	451.20
Aug-2013	301.59	116.01	487.16	Aug-2017	213.54	-24.11	451.19
Sep-2013	184.08	-1.50	369.65	Sep-2017	157.11	-80.55	394.76
Oct-2013	158.64	-26.94	344.21	Oct-2017	163.40	-74.26	401.05
Nov-2013	178.84	-6.74	364.41	Nov-2017	179.78	-57.87	417.43
Dec-2013	65.96	-119.61	251.54	Dec-2017	108.08	-129.58	345.73
Jan-2014	53.73	-141.17	248.63	Jan-2018	96.76	-145.00	338.53
Feb-2014	46.00	-150.20	242.19	Feb-2018	92.88	-149.47	335.23
Mar-2014	56.47	-139.92	252.85	Mar-2018	97.32	-145.11	339.75
Apr-2014	75.68	-120.73	272.09	Apr-2018	105.67	-136.78	348.11
May-2014	44.56	-151.85	240.97	May-2018	92.23	-150.22	334.67
Jun-2014	323.75	127.34	520.17	Jun-2018	227.38	-15.07	469.82
Jul-2014	251.82	55.41	448.24	Jul-2018	200.47	-41.98	442.91
Aug-2014	251.82	55.41	448.23	Aug-2018	200.46	-41.98	442.91
Sep-2014	162.38	-34.04	358.79	Sep-2018	153.42	-89.02	395.87
Oct-2014	198.60	2.19	395.02	Oct-2018	162.26	-80.18	404.71
Nov-2014	234.05	37.64	430.47	Nov-2018	177.22	-65.22	419.67

Dec-2014	95.58	-100.84	291.99	Dec-2018	114.04	-128.40	356.49
Jan-2015	69.93	-147.30	287.16	Jan-2019	103.55	-142.18	349.29
Feb-2015	63.55	-156.50	283.59	Feb-2019	100.29	-145.92	346.49
Mar-2015	69.74	-150.71	290.19	Mar-2019	103.87	-142.40	350.15
Apr-2015	81.71	-138.79	302.22	Apr-2019	110.66	-135.62	356.94
May-2015	62.56	-157.96	283.07	May-2019	99.75	-146.53	346.03
Jun-2015	278.28	57.76	498.79	Jun-2019	212.62	-33.67	458.90
Jul-2015	246.46	25.94	466.97	Jul-2019	191.67	-54.61	437.95
Aug-2015	246.45	25.93	466.97	Aug-2019	191.67	-54.62	437.95
Sep-2015	166.09	-54.43	386.61	Sep-2019	151.66	-94.63	397.94
Oct-2015	167.97	-52.55	388.48	Oct-2019	157.37	-88.92	403.65
Nov-2015	188.74	-31.78	409.26	Nov-2019	169.43	-76.85	415.72
Dec-2015	93.33	-127.19	313.84	Dec-2019	117.41	-128.87	363.70
Jan-2016	79.29	-148.52	307.11	Jan-2020	109.02	-139.40	357.45
Feb-2016	73.83	-155.00	302.67	Feb-2020	106.26	-142.47	354.99
Mar-2016	80.38	-148.60	309.36	Mar-2020	109.37	-139.40	358.14
Apr-2016	92.60	-136.40	321.60	Apr-2020	115.23	-133.55	364.01
May-2016	72.89	-156.12	301.89	May-2020	105.80	-142.98	354.58
Jun-2016	264.93	35.92	493.94	Jun-2020	201.69	-47.09	450.47
Jul-2016	223.69	-5.31	452.70	Jul-2020	183.13	-65.65	431.91
Aug-2016	223.69	-5.32	452.70	Aug-2020	183.13	-65.65	431.91
Sep-2016	158.26	-70.74	387.27	Sep-2020	149.50	-99.28	398.28
Oct-2016	174.13	-54.88	403.14	Oct-2020	155.19	-93.59	403.97
Nov-2016	196.22	-32.79	425.22	Nov-2020	165.66	-83.13	414.44
Dec-2016	104.98	-124.03	333.99	Dec-2020	121.09	-127.69	369.87

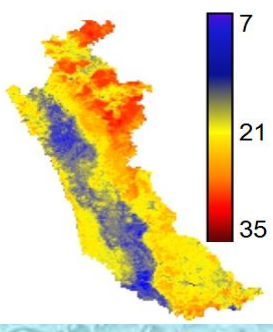
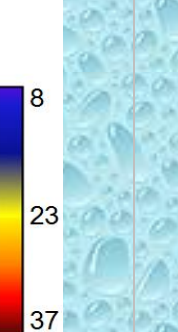
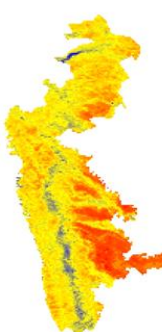
Sahyadri Conservation Series: 53, ETR 100

Northern Western Ghats

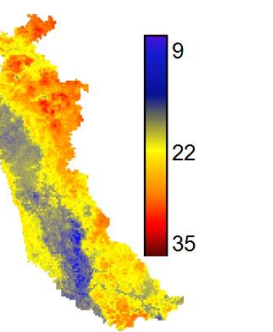
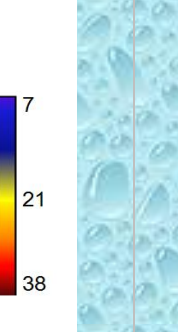
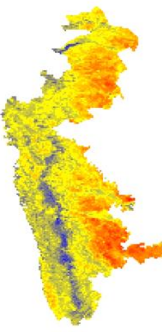
Central Western Ghats

Southern Western Ghats

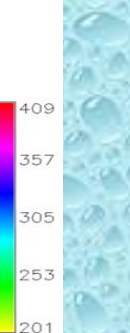
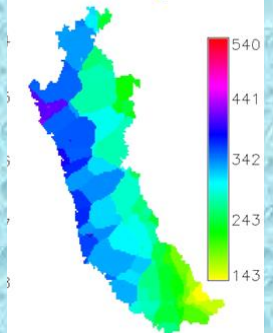
Land Surface Temperature during January 2003



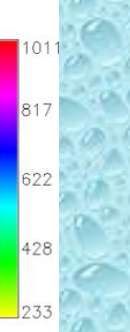
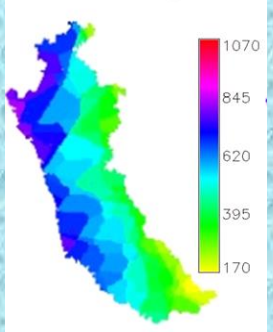
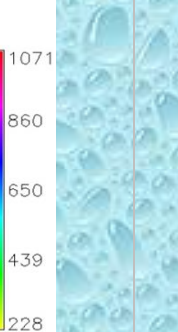
Land Surface Temperature during December 2012



Precipitation during July 2003



Precipitation during July 2012



Indian Institute of Science
Bangalore-560012

**ENERGY AND WETLANDS RESEARCH GROUP
CENTRE FOR ECOLOGICAL SCIENCES**

NEW BIOSCIENCE BUILDING, III FLOOR, E-WING, LAB: TE15

Indian Institute of Science, Telephone : 91-80-22933099/22933503(Ext:107)/23600985

Fax : 91-80-23601428/23600085/23600683[CES-TVR]

Email : cestvr@ces.iisc.ernet.in, energy@ces.iisc.ernet.in

Web: <http://ces.iisc.ernet.in/energy>, <http://ces.iisc.ernet.in/biodiversity>

Open Source GIS: <http://ces.iisc.ernet.in/grass>